Acid-base balance in ageing and age-related disease

Eliano Martins dos Santos

A thesis submitted in partial fulfilment of the requirements for the degree of

Doctor of Philosophy

February 2023

Imperial College London
Institute of Clinical Sciences

Medical Research Council
London Institute of Medical Sciences

Statement of Originality

The work presented here is entirely my own. Any collaborations or contributions by others are clearly acknowledged and/or referenced accordingly throughout the text.

This work was funded by the Medical Research Council (MRC) and was carried out in the Redox Metabolism group at the MRC London Institute of Medical Sciences, under the supervision of Dr Helena Cochemé.

Copyright Declaration

The copyright of this thesis rests with the author. Unless otherwise indicated, its contents are licensed under a Creative Commons Attribution Non-Commercial 4.0 International Licence (CC BY-NC).

Under this licence, you may copy and redistribute the material in any medium or format. You may also create and distribute modified versions of the work. This is on the condition that you credit the author and do not use it, or any derivative works, for a commercial purpose.

When reusing or sharing this work, ensure you make the licence terms clear to others by naming the licence and linking to the licence text. Where a work has been adapted, you should indicate that the work has been changed and describe those changes. Please seek permission from the copyright holder for uses of this work that are not included in this licence or permitted under UK Copyright Law.

Abstract

Ageing is a major risk factor for debilitating conditions. Interventions that target ageing hallmarks prevent disease and extend healthy lifespan in model organisms. To translate interventions into clinical practice, efficient targets need to be conserved and convergent. One essential chemical property for normal physiology that affects different aspects of ageing is pH, yet little is known about the role of acid-base balance in ageing and age-related disease. Here, extracellular pH homeostasis is proposed to be a novel hallmark of ageing. *Drosophila* is used as the model given its simple fluid compartmentalisation and short lifespan.

In flies, systemic acidification is shown to occur with age and to correlate with mortality rate, independently of strain, sex and diet. This correlates with insufficient acid excretion and to downregulation of genes proposed to be important for acid-base regulation in the fly excretory tract. Interventions that induce haemolymph acidification in independent ways shorten survival. With age, flies also become more sensitive to acidotic stress. Conversely, increasing haemolymph pH pharmacologically extends fly lifespan.

Acid-base imbalance promotes age- and diet-related lithiasis in fly tubules. Overnutrition through added sugar shortens fly survival independently of classically associated metabolic defects, such as insulin resistance. This study suggests fluid homeostasis, particularly acid-base balance, is a major determinant of health. Future research should further dissect the causes of age-related acidification and its impact on the pathophysiology of chronic diseases. Maintaining acid-base balance may be a preventive medicine strategy to promote a healthy lifespan.

Acknowledgements

This document is older than its years. It compiles the work I made at the London Institute of Medical Sciences (LMS) but contains ideas I developed years prior over my academic path. I acknowledge everyone who contributed to it directly and indirectly throughout the years.

Back when I went to college in my hometown, part of the curriculum was to develop a final-year project about any topic within science. I persuaded three friends to make a short documentary about ageing. Part of that documentary involved interviewing people around town about their willingness to take an anti-ageing pill if it were to be developed. To my surprise, the vast majority of the cohort we interviewed would decline that offer, and the main reasons for that were: 1) that ageing is a natural process; 2) that they were looking forward to retiring and enjoying their last years of life; and 3) that they would not want to live a longer life sick and stuck in a bed. Thus, I will begin this thesis by briefly deconstructing this romantic idea of natural ageing and arguing that treating ageing can be the most effective way to avoid an extended period of life sick and stuck in a bed.

As part of the research for the documentary, we reached out to an ageing scientist, Prof. Henrique Almeida, who took an afternoon out of his busy schedule and drove to a small town to have an informal meeting with four college students to talk about ageing research. What seemed like a given then, that a professor would spare time to discuss his research with us, looks like an immense gesture looking back. A gesture that had a significant impact on my career as I now write my doctoral thesis on ageing and inspires me to do science outreach as part of my job as a researcher.

Still during the research for the documentary, I came across a website that was to me an outstanding primer for ageing research (senescence.info). That website had a section on how to become a biogerontologist and further inspired me to follow that path. In search of career advice, as I was applying for university, I decided to contact the website developer. Prof. João Pedro de Magalhães not only gave advice then but also later on as I was applying for doctoral programmes, which, in retrospect, seems also incredibly generous and for which I am grateful.

I ended up going to medical school but tried to still have one foot in fundamental sciences. Dr Paula Videira and her then-PhD student Mariana Silva introduced me to the lab in my first month. That was probably what kept me in medical school at the time as I struggled to find interest in descriptive anatomy. As I was finishing my degree,

Dr Silvia Conde took me into her research group as a volunteer and allowed me to explore my ideas. Her lab works on how chemoreceptors affect metabolic disease, and I was interested in exploring how chemoreceptors change with age. And even though I was focused on cellular senescence then, this is when I started wondering about the potential role of acid-base balance in ageing, as one of its regulators seemed to become dysfunctional with age. I thank Silvia Conde and her research group, with a special mention to Joana Sacramento and Bernardete Melo, the then-PhD students who helped me develop in the lab.

After finishing medical school, during my clinical foundation year, I applied for doctoral programmes where I could do fundamental research on ageing. I was lucky to be offered the position in the Redox Metabolism lab which allowed me to perform the research presented here. I want to acknowledge everyone who I worked with for the past 4 years: Andrea Foley, for all her essential help throughout – from making vast amounts of food, taking care of experimental flies in my absence, to spending whole afternoons collecting haemolymph with me – and, on top of that, for giving advice and always keeping the morale up in the lab; Claudia Lennicke, not just for her help with molecular biology techniques that eluded me (i.e., most of them) and for being the person who most challenged my ideas and pushed me to do better, but also for being present and a supporting friend in crucial moments; Alec Vincent, Paul Middleton and Daniel Pap for helpful debates, support in the lab and the occasional beer; Marcela Buricova for her encouragement and for her essential help at the start of the project, from collecting haemolymph to discussing ideas; and, finally, Helena Cochemé, my supervisor, for allowing me to explore my curiosity in acid-base balance from the start, for giving me the opportunity to attend and present at multiple conferences, and for her continuous support, not just technical but also financial and personal, especially for the times when she did not have to – her support was crucial for me to go back and perform the experiments I needed to conclude this thesis. I also thank Helena for the feedback and help in improving this document.

Here, I also want to acknowledge everyone at the LMS who supported me during these last years: the cohort of students I started with for their encouragement and for bringing more fun into these years; the student committee students, with a special mention to the ones who helped me create *Otoscope*, a science podcast series; members of neighbour labs, for creating a good work environment, with a special mention to Laura Camplese for her support and positive energy and to Siamak

Redhai for allowing me to use fly lines he generated; and my assessors, Prof. Filipe Cabreiro and Dr Susumu Hirabayashi, for their appraisals and feedback at key points.

Throughout these four years, London became my home and I want to thank Carla Costa for taking me into her family and easing me into the city for the first couple of years, as well as the reliable Saturday tennis group at Chiswick House & Gardens for being there since week one. My friends' support from my other two hometowns was crucial before and during this time. From the ones who made an ageing documentary with me back in college, to the ones that backed my decision to pursue a doctoral degree instead of a medical specialty, and the ones that gave me encouragement and positive affirmations during these past years. I thank them all, but want to particularly mention a few: Ana Cláudia Paiva, Ana Rafaela Coelho, Ana Isabel Alves, Ana Viana, Andreia Vinhas, Beatriz Porteiro, Filipa Vila Nova, Inês Nunes, Inês Santos, Joana Ribeiro, João Afonso Carvalho, João Lucas, Mafalda Gonçalves, Miguel Roxo, Pedro Vasques, Sofia Cruz and, last but not least – perhaps most, Tiago Moreira.

London feels especially like home now because it is the city where I made my best discovery: my partner, James Wilson-Rhead. His love and encouragement saw me through the challenges these last couple of years and were vital for this document to come into being. I feel the luckiest in the world for having him in my life and the thought of having more time with him brings the extra motivation to extend our lives.

Finally, I want to end the acknowledgements where it all started and thank my family, particularly my parents, Gustavo Correia and Rosa Costa, my sister Flávia, my aunt Daniela and my uncle Ilídio. My parents were both unable to progress beyond primary school but they worked very hard to give my sister and me the opportunities they did not have. My father, in particular, always fomented my curiosity and allowed me to pursue my goals and attend university, even when it meant working more than 12 hours a day, 6 days a week. He always believed in me, and I know he would be proud of my path. He is and will always be the co-author of any work I produce.

Table of Contents

Statement of Originality 1
Copyright Declaration 1
Abstract 2
Acknowledgements 3
List of Figures 11
List of Tables 13
Abbreviations 14

Chapter 1. Introduction: Ageing and acid-base balance 16

1.1. Ageing as a target for preventive medicine 16

1.2. Defining ageing and its mechanisms 18
1.2.1. The hallmarks of ageing 18
1.2.2. Entropy and a deeper reductionist view on ageing 20

1.3. Acid-base homeostasis in ageing 21
1.3.1. Introduction to acid-base chemistry 21
1.3.2. Acid base physiology 23
1.3.3. Acid-base homeostasis in aged fluids 23
1.3.4. Acid-base balance interactions with ageing mechanisms 24

1.4. *Drosophila melanogaster* as a model for acid-base in ageing 26

1.5. Hypothesis: acid-base is a hallmark of ageing 30

Chapter 2. Materials and methods 31

2.1. Fly maintenance and genetics 31
2.1.1. General fly maintenance 31
2.1.2. Fly media 31
2.1.3. Fly strains and modulation of gene expression 33
2.1.4. Complete list of fly genotypes 40

2.2. Fly behavioural & functional assays 41
2.2.1. Survival 41
2.2.2. Fecundity 41
2.2.3. Feeding and drinking 41
2.2.4. Respirometry 42
2.2.5. Malpighian tubules deposit scoring 43

2.3. Fly sample collection 43
2.3.1. Freezing flies 43
2.3.2. Excretory system dissections 44
2.3.3. Larval haemolymph collection 44
2.3.4. Adult haemolymph collection 44
2.4. pH measurements 45
2.4.1. Haemolymph pH 45
2.4.2. Excreta pH 49
2.5. Molecular biology methods 50
2.5.1. Primer design 50
2.5.2. Fly genomic DNA extraction 50
2.5.3. Polymerase chain reaction 50
2.5.4. DNA gel electrophoresis 51
2.5.5. RNA extraction, purification and cDNA synthesis 51
2.5.6. Primer validation for quantitative PCR 52
2.5.7. Quantitative PCR 53
2.5.8. Protein quantification 53
2.6. Enzymatic assays 53
2.6.1. Carbonic anhydrase activity 53
2.7. Mass-spectrometry-based methods 55
2.7.1. Haemolymph proteomics 55
2.7.2. Haemolymph metabolomics 56
2.8. Statistics and data analysis 57
Chapter 3. Correlation of extracellular pH with survival 58
3.1. Introduction 58
3.2. Extracellular fluid pH during *Drosophila* ageing 58
3.2.1. Age-dependent acidification is independent of sex or strain 58
3.2.2. Age effect of acidification occurs in different diets 62
3.3. Correlation of age-related pH changes with mortality rate 63
3.3.1. Effect of environmental temperature on pH and survival 64
3.3.2. Age-dependent acidification in long-lived genetic model 66
3.4. Key messages and interpretation 68

Chapter 4. Pharmacological modulation of acid-base balance in Drosophila *70*

4.1. Introduction **70**

4.2. Modelling chronic metabolic acidosis in *Drosophila* **70**

4.2.1. Ethylene glycol-induced acidosis shortens fly survival 71

4.2.2. EG-induced acidosis is independent of tubule function 72

4.2.3. Acidosis resistance decreases with age 75

4.2.4. Acetazolamide does not effectively induce acidosis in flies 76

4.3. Chemically preventing age-related haemolymph acidification **78**

4.3.1. Low-dose alkalotic compounds do not consistently alter survival 78

4.3.2. High-dose alkalotic compounds alter resistance to acidotic stress 82

4.3.3. High-dose $NaHCO_3$ extends fly lifespan, even from middle-age 85

4.4. Key messages and interpretation **89**

Chapter 5. Extracellular buffers and proteome in ageing *91*

5.1. Introduction **91**

5.2. Extracellular buffering **91**

5.2.1. The carbonic acid - bicarbonate buffer 91

5.2.2. Carbonic anhydrases 92

5.3. Carbonic anhydrases in *Drosophila* **93**

5.3.1. Carbonic anhydrase activity in whole fly homogenates 93

5.3.2. Carbonic anhydrase activity in fly haemolymph 96

5.3.3. Carbonic anhydrase 1 is present in fly haemolymph 98

5.3.4. Changes in *CAH1* gene expression and survival 100

5.3.5. Ubiquitous CAH1 overexpression lowers metabolic rate and fecundity 103

5.4. Fly haemolymph proteome changes with age **104**

5.4.1. Functional analysis of proteome changes with age 106

5.4.2. Exploring the role of v-ATPase changes in haemocytes 108

5.5. Key messages and interpretation **109**

Chapter 6. Excretory regulation of acid-base balance *112*

6.1. Introduction **112**

6.1.1. *Drosophila* excretory system 112

6.1.2. Fly excretory system in acid-base regulation 115

6.2. Acid excretion capacity with age in *Drosophila* 116

6.3. Genetic modulation of acid excretion and survival 117

6.3.1. Expression of CAs in fly tubules with age 118

6.3.2. Tubule-specific expression of CA genes and survival 120

6.3.3. Expression of v-ATPase subunits in fly tubules with age 122

6.3.4. Tubule-specific expression of v-ATPase subunit genes and survival 126

6.3.5. Expression of chloride channels in fly tubules with age 128

6.3.6. Tubule-specific pHCl-2 gene expression and survival 131

6.4. Key messages and interpretation 133

Chapter 7. Acid-base imbalance, metabolism and diet-related disease 137

7.1. Introduction 137

7.2. Metabolic production of acids with age and mortality 138

7.2.1. *Drosophila* metabolic rate with age 138

7.2.2. Fly haemolymph metabolome changes with age 139

7.2.3. The potential role of microbiota changes with age 143

7.3. Diet-induced acid-base imbalance and age-related disease 144

7.3.1. Fly tubule lithiasis as an age- and diet-related disease 145

7.3.2. Excess sugar causes tubule lithiasis in flies 145

7.3.3. Excess sugar leads to increased acid excretion 149

7.3.4. Dietary yeast as a driver of uric acid crystallisation 151

7.3.5. Yeast concentration does not alter systemic acid-base balance 152

7.3.6. Tubule lithiasis can be uncoupled from survival 154

7.3.7. The role of excess fat in tubule lithiasis 157

7.3.8. Excess fat-related lithogenic factors 158

7.4. Key messages and interpretation 163

Chapter 8. Global perspective and future directions 166

8.1. Loss of acid-base balance as a hallmark of *Drosophila* ageing 166

8.1.1. Extracellular acidification occurs during ageing 166

8.1.2. Factors that promote acidification shorten survival 169

8.1.3. Factors that prevent acidification extend survival 170

8.1.4. Limitations of survival as a readout for ageing 172

8.2. Acid-base imbalance as a promoter of age-related disease 173

8.2.1. Overnutrition can induce age-related disease through pH imbalance 173
8.2.2. Acid-base and hallmarks of ageing may interact to cause disease 175

8.3. Outlook and future directions 176

References 182

Appendix 1. List of peptides resulting from trypsin digestion of CAs/v-ATPase subunits 220
Appendix 2. Summary of haemolymph proteomics (written by Alex Montoya) 253
Appendix 3. Publications arising from this thesis 255

List of figures

Figure 1.1. Approaches to health in old age: disease- and ageing-focused models 17
Figure 1.2. The hallmarks of ageing 19
Figure 1.3. *Drosophila* life cycle 27
Figure 1.4. Comparison of human and fly bodily fluids compartments 28
Figure 1.5. Comparison of human and fly internal organ anatomy 29
Figure 2.1. Experimental population set-up 31
Figure 2.2. The GAL4/UAS expression system 34
Figure 2.3. Recombination of CAH1 KK line 36
Figure 2.4. Validation of VDRC UAS-RNAi lines 36
Figure 2.5. Generation of novel UAS lines 38
Figure 2.6. Validation of novel UAS lines 39
Figure 2.7. FlyPAD 42
Figure 2.8. Tubule deposits scoring 43
Figure 2.9. Larval haemolymph collection 44
Figure 2.10. Adult haemolymph collection 45
Figure 2.11. The effect of different standard solutions on pH measurements 46
Figure 2.12. Factors that alter absolute pH values 47
Figure 2.13. Bromothymol blue spectrophotometric pH measurements 48
Figure 2.14. Analysis of excreta number and pH 50
Figure 2.15. Primer validation 52
Figure 2.16. Optimization of carbonic anhydrase activity assay 54
Figure 3.1. Age-related haemolymph acidification in w^{Dah} flies 59
Figure 3.2. Age-related haemolymph acidification in w^{1118} flies 60
Figure 3.3. Age-related haemolymph acidification in Ore^{R} flies 61
Figure 3.4. Age-related haemolymph acidification is diet-independent 62
Figure 3.5. Effect of higher temperature on survival and pH 63
Figure 3.6. Effect of lower temperature on survival and pH 66
Figure 3.7. Long-lived mutant shows slower rates of haemolymph pH decline 67
Figure 4.1. Ethylene glycol causes acidosis and shortens survival in flies 72
Figure 4.2. Ethylene glycol does not impair acid excretion in flies 74
Figure 4.3. Resistance to acidotic stress declines with age 76
Figure 4.4. Effect of acetazolamide on haemolymph pH and survival in flies 77
Figure 4.5. Effect of low-dose $NaHCO_3$ on the survival of w^{Dah} flies 79
Figure 4.6. Effect of low-dose $NaHCO_3$ on the survival of w^{1118} flies 80
Figure 4.7. Effect of low-dose tris base on the survival of w^{Dah} flies 80
Figure 4.8. Effect of low-dose tris citrate on the survival of w^{Dah} flies 81

Figure 4.9. Effect of high-dose NaHCO3 on acidotic stress resistance 82
Figure 4.10. Effect of high-dose Tris base on acidotic stress resistance 83
Figure 4.11. Alkalotic compounds rescue EG-induced haemolymph acidification 84
Figure 4.12. Effect of high-dose tris base on the survival of w^{Dah} flies 86
Figure 4.13. Effect of high-dose $NaHCO_3$ on the survival of w^{Dah} flies 87
Figure 4.14. Effect of Na^+-matched medium pH on survival 88
Figure 5.1. CA activity in whole fly lysate 95
Figure 6.1. Fly excretory system and proteins of interest 112
Figure 6.2. General physiology, cell composition and function of the fly excretory tract 113
Figure 6.3. Functional assessment of the fly excretory tract with age 117
Figure 6.4. CA distribution and changes in gene expression with age 119
Figure 6.5. Acidotic stress resistance upon changes in expression of CAH1 and CAH2 120
Figure 6.6. Lifespan of flies overexpressing CAH1 or CAH2 122
Figure 6.7. *VhaSFD* and *Mitf* distribution and changes in gene expression with age 123
Figure 6.8. Distribution and changes in gene expression of other v-ATPase subunits 125
Figure 6.9. Acidotic stress resistance upon changes in *VhaSFD* expression 126
Figure 6.10. Acidotic stress resistance upon knockdown of other v-ATPase subunits 127
Figure 6.11. Lifespan of flies overexpressing *VhaSFD* 128
Figure 6.12. *pHCl-2* and *Ndae1* distribution and changes in gene expression with age 130
Figure 6.13. Acidotic stress resistance upon changes in *pHCl-2* expression 132
Figure 6.14. Lifespan of flies overexpressing pHCl-2 133
Figure 7.1. Fly metabolic rate with age 139
Figure 7.2. Metabolomics data normalisation and ANOVA significant hits. 140
Figure 7.3. Sample correlation heatmap and principal components analysis 141
Figure 7.4. Hierarchical clustering and functional analysis of significant hits 142
Figure 7.5. Impact of microbiota-related intervention on haemolymph pH 144
Figure 7.6. HS depletes extracellular volume and shortens fly survival in a water-dependent manner 146
Figure 7.7. Flies raised on a HS diet are thirstier 147
Figure 7.8. HS causes uric acid lithiasis in fly tubules 148
Figure 7.9. Haemolymph pH of flies raised on a HS diet 149
Figure 7.10. HS causes excretory tract acidification 150
Figure 7.11. Water rescue in HS diets is yeast-dependent 152
Figure 7.12. Haemolymph pH under HY and methionine diets 153
Figure 7.13. Calcium oxalate stones uncouple survival from lithiasis 155
Figure 7.14. Effect of allantoin and potassium citrate on fly survival 156
Figure 7.15. High fat diet causes tubule lithiasis in flies 158

Figure 7.16. High fat diet causes thirst to the same degree as a high sugar diet 159
Figure 7.17. High fat diet increases fly mortality under starvation 160
Figure 7.18. Respirometry of flies raised under a high fat diet 161
Figure 7.19. Haemolymph pH of flies raised on high fat diets 162
Figure 7.20. The effect of knockdown of acid-excreting proteins on HF-related lithiasis 163
Figure 8.1. Acid-base balance as a convergent target for ageing interventions 177

List of tables

Table 1. List of chemical compounds added to fly media 32
Table 2. Embryo genotypes and insertion site of UAS lines constructs 39
Table 3. Complete list of the fly lines used in this study 40
Table 4. List of fly carbonic anhydrases 94
Supplementary table 1. List of primers for genomic DNA PCR and Sanger sequencing 178
Supplementary table 2. Tris-HCl (50 mM) buffer solution composition 179
Supplementary table 3. Sorensen's phosphate (100 mM) buffer solution composition 180
Supplementary table 4. List of primers used in this study for qPCR 181

Abbreviations

A-	anion
ACN	acetonitrile
act5c	*actin 5c*
Acz	acetazolamide
AMPK	AMP-activated protein kinase
ANOVA	analysis of variance
AP	allopurinol
A_{TOT}	total weak acids and respective anions
ATP	adenosine triphosphate
BSA	bovine serum albumin
CA	carbonic anhydrase (enzyme)
CAH	*carbonic anhydrase* (*Drosophila* gene)
cDNA	complementary DNA
Cl^-	chloride ion
da	*daughterless*
dILP	*Drosophila* insulin-like peptide
DMSO	dimethyl sulfoxide
EG	ethylene glycol
FA	formic acid
FDR	false discovery rate
GC-MS	gas chromatography-mass spectrometry
GH	growth hormone
H^+	proton
H_2CO_3	carbonic acid
HA	weak acid
HCO_3^-	bicarbonate
HF	high fat
HL	haemolymph
HY	high yeast
Hml	*hemolectin*
HS	high sugar
IGF-1	insulin like growth factor 1
IIS	insulin/IGF signalling
K^+	potassium ion
K_A	acid dissociation constant
K_B	base dissociation constant

LC-MS	liquid chromatography-mass spectrometry
Na^+	sodium ion
$NaHCO_3^-$	sodium bicarbonate
NaOx	sodium oxalate
NEAP	net endogenous acid production
OH-	hydroxide ion
PBS	phosphate-buffered saline
PCA	principal component analysis
PCR	polymerase chain reaction
PEPCK	phosphoenolpyruvate carboxykinase
qPCR	quantitative polymerase chain reaction
ROS	reactive oxygen species
RQ	respiratory quotient
RT	room temperature
RNAi	RNA interference
SID	strong ion difference
SYA	sugar-yeast-agar medium (standard control diet)
TBST	Tris-buffered saline, Tween-20
TORC1	target of rapamycin complex 1
UAS	upstream activation sequence
uro	*urate oxidase*
w^{1118}	*white 1118* (isogenic control strain)
w^{Dah}	*white Dahomey* (outbred background strain)

Chapter 1. Introduction: Ageing and acid-base balance

Ageing is the main risk factor for chronic diseases and geriatric syndromes (Hayflick, 2021; Inouye et al., 2007; Niccoli & Partridge, 2012; Rae et al., 2010). The increasing prevalence of these conditions is a serious public health challenge which will continue to grow in complexity as populations age (Kontis et al., 2017; United Nations, 2019). Age-related conditions are responsible for significant healthcare costs and can lead to dependence on caregivers, which may become unsustainable from an economic and societal standpoint (European Commission, 2020; Scott et al., 2021). Understanding and preventing the mechanisms through which ageing impacts health is thus an emerging and urgent scientific quest.

1.1. Ageing as a target for preventive medicine

Major advances in modern medicine that significantly improved human health and increased life expectancy arose from preventive approaches, such as immunisation against infectious diseases and public health campaigns (Partridge et al., 2018). In geriatric medicine, personalised prevention is already part of clinical practice. For example, death from cardiovascular events (e.g., stroke, heart attack) is pharmacologically prevented by treating risk factors such as hypercholesterolemia and hypertension in the population at risk. The development of other age-related diseases, such as type-2 diabetes and certain types of cancer, is similarly delayed through dietary programmes and the cessation of smoking (Burns, 2000; Everitt et al., 2006; Stewart et al., 2017).

Geroscience proposes targeting a more comprehensive risk factor - ageing itself (Figure 1.1). If prevalent and limiting population survival, treating or preventing an individual disease can increase human life expectancy. This is the current disease-focused approach to health. Survival after a specific time is often the primary outcome of clinical trials testing new therapies for age-related diseases. However, the added years resulting from disease-focused treatments do not necessarily correlate with improved quality of life (Wang et al., 2020) because ageing simultaneously affects the function of multiple organs and promotes the development of other diseases. Ageing also causes geriatric syndromes, such as frailty, which further contribute to disease burden and reduced quality of life in the elderly (Inouye et al., 2007).

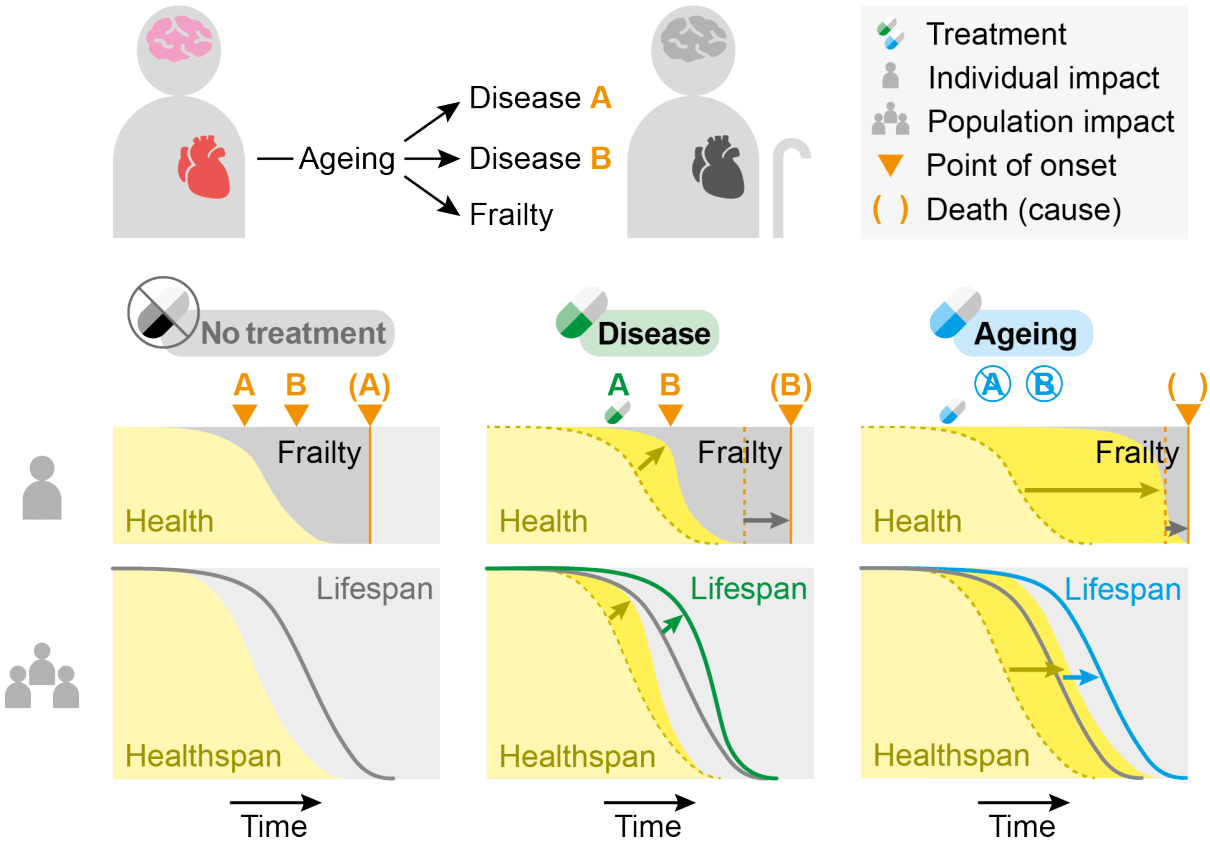


Figure 1.1. Approaches to health in old age: disease- and ageing-focused models. In this theoretical representation, ageing is the major risk factor for prevalent diseases 'A' and 'B' and causes frailty. Left untreated or treated symptomatically, a typical individual in this population will develop diseases 'A' and 'B' and die of complications related to disease 'A' in this scenario. Ageing combined with these diseases will result in a certain period of frailty. At a population level, the life expectancy or median lifespan will be limited by the prevalent disease 'A', and health span will be determined by the burden of diseases 'A', 'B' and ageing. In the disease-centred approach to health in old age, the ideal scenario of curing or preventing disease 'A' will increase both health- and lifespan at an individual and populational level, but the period of frailty is unlikely to change due to the burden of other untreated age-related diseases – here represented by disease 'B' – and ageing itself. In the ageing-centred approach to health in old age, the ideal scenario of slowing or preventing ageing will similarly increase both health- and lifespan at an individual and populational level by preventing or delaying the development of diseases 'A' and 'B' and necessarily decrease the period of frailty.

Geriatric syndromes are associated with higher mortality and poorer clinical outcomes (Keeble et al., 2019) and result in severe healthcare costs. An illustrative syndrome is the risk of falling. Falls are one of the leading causes of hospital admission

in the elderly (Galet et al., 2018). Like other geriatric syndromes, falls result from multiple ageing-related factors, including deteriorating muscle strength, loss of balance, and impaired vision. This demonstrates the challenge of managing these conditions with a disease-focused approach. Instead, targeting fundamental ageing processes has the potential to decrease the incidence of both age-related diseases and geriatric syndromes, extending human life with added years of health. Indeed, interventions that target ageing-related processes improve healthspan in a range of animal models (Fontana et al., 2010; Partridge et al., 2020).

1.2. Defining ageing and its mechanisms

Although seemingly simple, defining ageing is still one of the major challenges of geroscience. Semantic discrepancies can determine the primary outcomes of ageing research, limit reproducibility across studies, and hinder the translation of findings into clinical practice. Here, ageing is broadly defined as the gradual loss of function and homeostatic resilience that increases the mortality rate over time.

Ageing is a complex trait. Theories have been postulated over the years to explain it and, each with their own shortcomings, have contributed to different understandings of age-related processes (Jin, 2010). All theories come from a primary dichotomy: ageing is either seen as a programmed or a stochastic process. Programmed ageing theories propose that age-related changes occur due to the evolutionary benefits of a limited lifespan. Stochastic ageing theories postulate that ageing occurs due to the absence of natural selection for somatic maintenance post-reproduction in the face of entropy-driven damage (da Costa et al., 2016). To tackle the problem on various fronts, several classifications have been made to categorise either the theories of ageing or phenomena that correlate with it (De Grey et al., 2002; López-Otín et al., 2013, 2023; Medvedev, 1990). The most prominent example is the stochastic classification of ageing as hallmarks (Figure 1.2), first proposed a decade ago and recently updated (López-Otín et al., 2013, 2023).

1.2.1. The hallmarks of ageing

The current factors defined as hallmarks of ageing are subclassified as primary, antagonistic and integrative. The primary hallmarks reflect molecular damage that progressively accumulates with time: genomic instability, telomere attrition, epigenetic

alterations, loss of proteostasis, and disabled macroautophagy. The antagonistic hallmarks reflect responses to that damage and are examples of antagonistic pleiotropy (i.e., promote successful reproduction but have deleterious effects post-reproduction): deregulated nutrient-sensing, mitochondrial dysfunction and cellular senescence. The integrative hallmarks occur after the exhaustion of mechanisms that compensate for the accumulated damage inflicted by the primary and antagonistic hallmarks: stem cell exhaustion, altered intercellular communication, chronic inflammation, and dysbiosis (Figure 1.2).

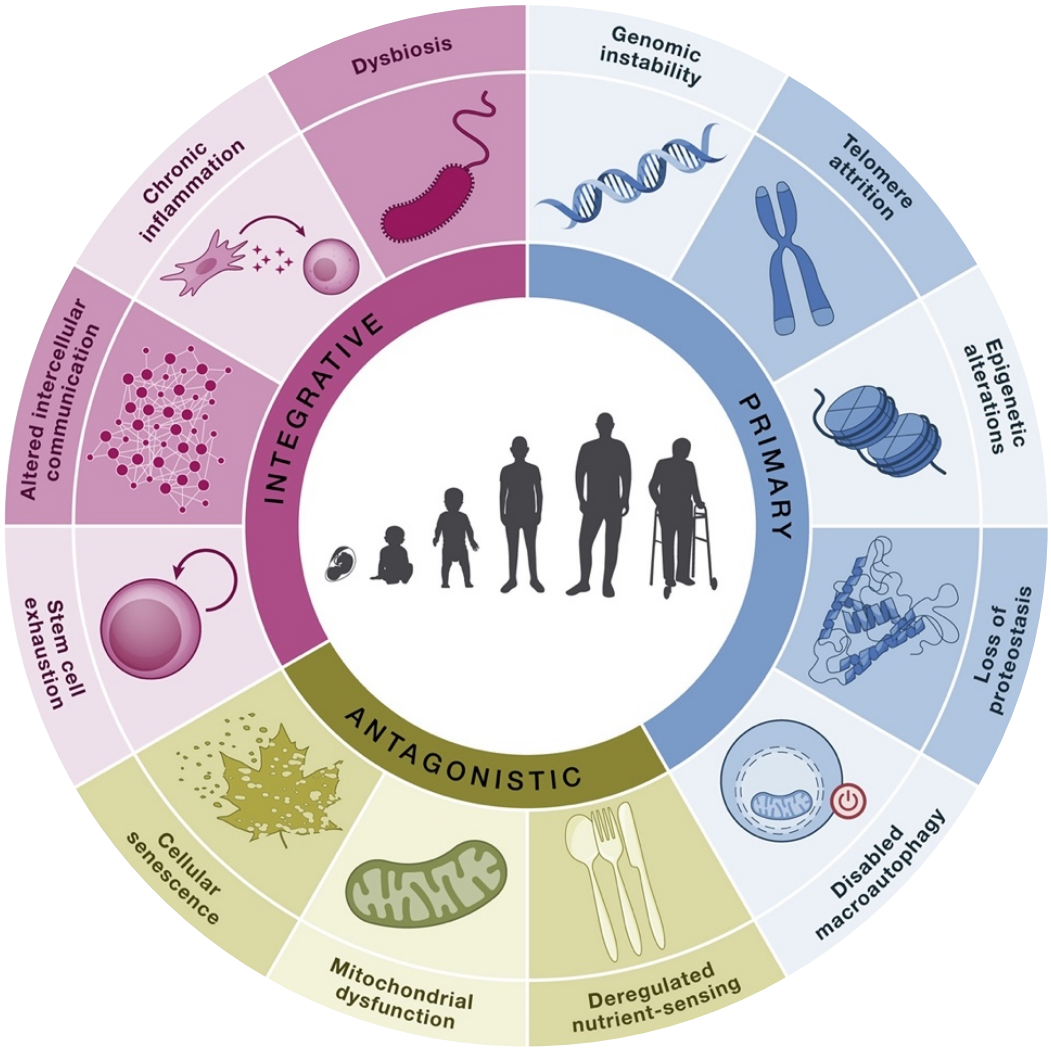


Figure 1.2. The hallmarks of ageing. This scheme compiles the proposed 12 hallmarks of ageing: genomic instability, telomere attrition, epigenetic alterations, loss of proteostasis, disabled macroautophagy, deregulated nutrient-sensing, mitochondrial dysfunction, cellular senescence, stem cell exhaustion, altered intercellular communication, chronic inflammation, and dysbiosis. These hallmarks are categorised into primary, antagonistic, and integrative. (Reprinted from López-Otín et al., 2023)

By definition, these 12 factors: 1) manifest during normal ageing; 2) accelerate ageing when experimentally aggravated; and 3) retard ageing when experimentally ameliorated (López-Otín et al., 2013, 2023). Longevity is commonly used as the readout for ageing, and longevity-based studies are the pillars of this classification, but functional outcomes are also considered (López-Otín et al., 2023).

These hallmarks interact and are interdependent. From an interventional perspective, it is crucial to find common targets either upstream or downstream of these processes to create potent strategies that prevent the effects of ageing on health.

1.2.2. Entropy and a deeper reductionist view on ageing

As a stochastic ageing classification, the hallmarks are seen as a result of entropy-driven damage, particularly affecting the primary hallmarks argued to be the cause of ageing. This argument is based on the second law of thermodynamics, which states that the total entropy of a system either increases or remains constant in any spontaneous process; it never decreases.

The second law of thermodynamics may not apply to biology, much less to ageing. On the evolutionary scale, biological systems tend to become more organised through selection. Besides, entropy applies to closed thermodynamic systems. On an individual scale, living organisms are open systems that obtain energy from natural substrates, which they use to maintain or increase order through maintenance and repair, violating the entropy law. With ageing, the ability to obtain or use energy can be lost. This loss allows damage to accumulate, suggesting it is upstream of the primary hallmarks as a potential cause of ageing. Therefore, metabolic dysfunction may cause ageing, and consistent with this idea, metabolism is one of the major determinants of longevity (López-Otín et al., 2016). The primary hallmarks of ageing can also cause metabolic dysfunction and thus create a positive feedback loop that accelerates ageing. However, the initial damage likely comes from the mishandling of energy.

Another reason the primary hallmarks are often seen as causative is that they occur at the lowest strata of organisation of an organism from all considered in the review by López-Otín et al., 2023, molecules. Despite its limitations, the reductionist method of dissecting biological systems into their constituent parts has effectively

explained the chemical basis of living processes (Regenmortel, 2004). Taking biology's reductionist view a level further, the behaviour of sub-atomical particles may alter metabolism and thus cause the primary hallmarks of ageing.

There are different sub-atomical scales, but here I focus on the dimension of protons and electrons. Both protons and electrons alter the structure and function of molecules. In the context of ageing, electrons have thoroughly been studied as an integral part of the free radical theory of ageing. This theory proposed that free oxygen radicals (i.e., species with an unpaired electron) cause damage to macromolecules which accumulate and impair cells until organs stop functioning (Gerschman et al., 1954; Harman, 1956). However, the original theory has been questioned by examples of lifespan extension despite increased oxidative stress and restructured to argue that: 1) reactive oxygen species (ROS) are needed for signalling and normal cellular function, and 2) with overproduction of ROS during the life course, these signalling pathways are disrupted or overactive and cause ageing (Afanas'ev, 2010). Importantly, redox signalling is vital for metabolic pathways related to ageing (Lennicke & Cochemé, 2020), and their disruption may ultimately cause a loss of energy for somatic maintenance.

Relative to electrons, protons have received very little attention in the context of ageing, even though their presence in solution alters redox reactions and is essential for effectively all living processes. The concentration of protons in a solution is determined by its acid-base balance. Here, I introduce acid-base balance and hypothesise its loss as a hallmark of ageing, and one of its fundamental causes.

1.3. Acid-base homeostasis in ageing

1.3.1. Introduction to acid-base chemistry

The concentration of protons (H^+) in an aqueous solution is determined by the balance of acids and bases in that solution. Acids can generally be defined as molecules that dissociate and generate a H^+ in solution, and bases as molecules that associate with a H^+. The concentration of protons in body fluids is extremely low (e.g., $4x10^{-8}$ Eq/L in arterial blood), so it is commonly expressed as pH, where:

$$pH = - \log [H^+]$$

Despite their low concentration, protons have a very high charge density, resulting in very large electric field gradients in their neighbourhoods, impacting the

molecules therein. For example, they can affect the strength of hydrogen bonds, which are essential to determine macromolecular structure and configuration (Kellum & Elbers, 2009). This can significantly impact the activity of enzymes and thus effectively all biological processes.

$[H^+]$ is determined by the dissociation of water, the constant (K_W) of which is influenced by factors such as temperature and ionic strength. A solution is neutral when $[H^+] = [OH^-]$, acid when $[H^+] > [OH^-]$ and basic when $[H^+] < [OH^-]$, independently of $[H^+]$ itself (and thus pH). For example, the pH of neutral pure water at human body temperature (37ºC) is 6.8. This demonstrates that factors such as temperature can alter biological function, such as enzyme activity, through pH, independently of solution neutrality. This is something to consider when the effects of temperature on pH and mortality rate are presented later (Section 3.3.1).

Solution neutrality is altered by electrolyte composition. Depending on whether they fully or partly dissociate in biological solutions, electrolytes can be classified as strong or weak, respectively. The effect of dissociated strong ions (e.g., Na^+, Cl^-) on $[H^+]$ is entirely dependent on their collective net charge, called strong ion difference (SID). Conversely, the effect of weak ions on $[H^+]$ depends on the dissociation constants (K_A for acids, K_B for bases) of their respective electrolytes. Weak electrolytes function as buffers in solution, as their dissociation maintains $[H^+]$ in a specific range. In body fluids, weak electrolytes are usually acids. Weak acids (HA) dissociate into H^+ and their respective anion (A^-). The combined concentration of weak acids and their dissociated anions ($[A_{TOT}]$), i.e., the concentration of buffers, was proposed to be another independent variable determining solution pH (Kellum & Elbers, 2009).

The main buffering system in most multicellular organisms is the carbonic acid–bicarbonate system (see Section 5.2.1). Carbon dioxide (CO_2) is the major end-product of metabolism. It dissolves in water depending on the gas solubility coefficient, which is also temperature-dependent. In solution, CO_2 reacts with water to form carbonic acid, H_2CO_3. This reaction is slow and only physiologically relevant when catalysed by carbonic anhydrases (CAs), as explored later (Section 5.2.2). H_2CO_3 then dissociates into bicarbonate (HCO_3^-) and H^+. The following equation represents this equilibrium:

$$CO_2 + 2H_2O \rightleftharpoons H_2CO_3 \rightleftharpoons HCO_3^- + H^+$$

1.3.2. Acid base physiology

There are two main perspectives on how acid-base balance is regulated in biological systems: 1) the descriptive view, primarily based on HCO_3^- regulation, and 2) the quantitative view, based on SID, $[A_{TOT}]$ and the partial pressure of CO_2 (Kellum, 2005). Both perspectives have shortcomings (Kurtz et al., 2008). Because these variables are interdependent, both views are quantitatively identical and efforts to reconcile them tend to accept both as true. The descriptive view can be seen as useful to simplify the classification of clinical acid-base disorders, and the quantitative view as more suitable for understanding them and generating mechanistic hypotheses (Kellum, 2005). Here, I attempt to formulate hypotheses and interpret results in light of both.

Due to its impact on biological function, pH is tightly regulated in all compartments of bodily fluids. The intracellular compartment has a higher $[H^+]$ than extracellular fluids, particularly the blood. Even within cells, $[H^+]$ differs in each organelle (Casey et al., 2010). Here, I focus on the regulation of extracellular pH as a representation of systemic acid-base status.

The normal blood pH ranges from 7.35 to 7.45, and small fluctuations can significantly impact physiology (Kraut and Madias, 2010). Upon the addition of acids or bases to the blood, different mechanisms act to counteract pH changes: 1) buffering by different equilibria, but primarily the carbonic acid-bicarbonate system; 2) respiratory response, regulated by peripheral and central chemoreceptors; 3) renal control of the net acid excretion; and 4) regulation from other organs of pH-determining variables, such as the gastrointestinal tract (DiBartola, 2012). In comparison, interstitial and intracellular fluids have fewer immediate response mechanisms and ultimately depend on systemic compensation.

1.3.3. Acid-base homeostasis in aged fluids

As an essential part of normal physiology and a tightly regulated property, pH would be expected to remain constant throughout life. However, sub-clinical changes in blood pH were found to occur in humans (Frassetto et al., 1996). These seemingly small changes likely reflect a more profound acid-base imbalance with age, given that all regulatory mechanisms must be overwhelmed or dysfunctional. Besides, in fluids with fewer regulatory levels, such as intracellular and interstitial fluids, age-related

changes in acid-base balance may be even more significant and have critical local consequences. For example, increased heterogeneity in organ perfusion with age, through loss of microcirculation, may cause pockets of hypoxia and acidity that escape systemic compensation as the joint venous outflows buffer the low pH of those regions.

Interstitial fluid is less accessible from a sample collection standpoint, so its acid-base physiology and how it might change with age at the tissue level are unexplored. From the few studies measuring interstitial fluid pH, it is clear that different tissues are bathed by fluids with specific pH values. For example, interpleuritic fluid has a basic pH of ~7.6 (Zocchi, 2002), while cerebrospinal fluid has a pH of ~7.3 (Siesjö, 1972) and lymph nodes show an acidic pH ranging from 6.2 to 6.8 (Estrella et al., 2019). No data is available on how pH in these fluids changes with age.

Some pH regulatory elements, such as the tubular portion of kidneys, change structurally and lose function over time (Denic et al., 2016). This is pointed out as one reason for the loss of acid-base balance in the blood with age (Frassetto et al., 1996) and is explored in Chapter 6. This would suggest that acid-base imbalance is a consequence of kidney ageing rather than a cause. However, a factor that affects kidney function and may act as a primary cause of acidification is the net endogenous acid production, directly related to diet, which is explored in CChapter 7.

1.3.4. Acid-base balance interactions with ageing mechanisms

Extracellular pH imbalance is associated with multiple hallmarks of ageing, but the evidence is sparse and the mechanisms understudied. Extracellular acidity can induce genomic instability, often regarded as a cause of ageing (López-Otín et al., 2023). Several mammalian cell types, including human, cultured in low pH (~6.5-7.2 range) media have lower capacity to repair DNA damage (DNA adducts, mutations and double-strand breaks with associated histone H2AX phosphorylation) induced by different methods (ultraviolet irradiation, benzo[a]pyrene and bleomycin treatments) compared to cells in higher pH (~7.4-7.8) (Massonneau et al., 2018; Shi et al., 2017; Xiao et al., 2003; Yuan et al., 2000). DNA damage in acidic conditions can be induced in a topoisomerase II-mediated manner (Xiao et al., 2003).

Loss of acid-base balance impairs proteostasis. By directly impacting protein stability through changes in intramolecular electrostatic interactions and hydrogen bonds, low pH can cause protein misfolding or unfolding that induce targeted

degradation, as observed in rat muscle (Mitch et al., 1994). Protein degradation upon metabolic acidosis leads to sarcopenia (Graham et al., 1996; Reaich et al., 1993), a common clinical manifestation of ageing. Macroautophagy is inhibited by an acidic extracellular fluid in rat cardiomyocytes (Zhao et al., 2016), which suggests acidosis may simultaneously contribute to the accumulation of defective organelles, proteins and other macromolecules in susceptible tissues (Shirakabe et al., 2016).

Acidosis is related to increased inflammation and impaired function of both innate and adaptive immune cells (Erra Díaz et al., 2018; Lardner, 2001). Low-grade inflammation is a common feature of ageing, and accumulation of senescent cells in aged tissues is thought to be a contributing factor through secretion of specific pro-inflammatory factors (López-Otín et al., 2023). Senescent cells have lower intracellular pH compared to proliferating cells, a susceptible trait explored in recent searches for senolytic compounds (Johmura et al., 2021; Triana-Martínez et al., 2019). Intracellular pH decreases in these cells upon lysosomal membrane damage (Johmura et al., 2021). The potential role of acidity in initiating senescence is underexplored, but a recent report correlates exposure to extracellular acidity with induction of senescence markers in melanoma cells (Böhme & Bosserhoff, 2020). Another factor suggested to add to age-related inflammation is dysbiosis, particularly of the intestinal microbiota (López-Otín et al., 2023). Environmental pH alters the intestinal microbiota species composition and production of essential metabolites (Duncan et al., 2009; Firrman et al., 2022), but whether these changes contribute to age-related dysbiosis is unknown.

The most characterised interaction between pH and ageing hallmarks relates to nutrient signalling pathways, particularly glucose homeostasis. At a physiological level, chronic acidaemia is known to impair glucose tolerance in humans and, if present from childhood, can cause growth defects, which resolve when acidaemia is treated (Kraut & Madias, 2010). Besides, acute acidosis is associated with resistance to the action of insulin (Kraut & Madias, 2010). These effects link dysregulation of pH homeostasis to insulin and growth hormone-insulin like growth factor 1 (GH-IGF-1) signalling, the most conserved longevity-modulating pathway across species (López-Otín et al., 2016). At a cellular level, pH is proposed to act as a second messenger for nutrient signalling, affecting and being affected by different components of nutrient-sensing pathways (Deprez et al., 2018). For example, in multiple cell lines, decreasing the extracellular pH reduces the phosphorylation of the target of rapamycin complex 1 (TORC1) substrate S6 kinase (Balgi et al., 2011; Walton et al., 2018). This inhibition

disrupts the cellular circadian clock (Walton et al., 2018). While inhibition of TORC1 is seen as a pro-longevity strategy (Bitto et al., 2016; Castillo-Quan et al., 2015; Mannick et al., 2018), chronic inhibition may be deleterious through disruption of circadian rhythms or tissue-specific effects. For example, T cells require mTORC1 for differentiation and activation of effector cells, which is blunted by acidic media (Walton et al., 2018). In another report showing altered nutrient signalling upon exposure to acidic extracellular fluid, myocytes exposed to low pH were shown to have lower protein kinase B (Akt) and AMP-activated protein kinase (AMPK) phosphorylation (Genders et al., 2019). This report also links low extracellular pH with mitochondrial dysfunction (Deprez et al., 2018; Genders et al., 2019), another feature of ageing.

Beyond the hallmarks, acid-base balance also regulates klotho levels. Klotho is an essential protein for the regulation of phosphate, increasing its renal excretion in response to FGF23 (Frassetto & Sebastian, 2019a). *klotho* knockout mice have metabolic acidosis, growth defects, accelerated ageing-like phenotypes and a short lifespan (Kuro-o et al., 1997). Treating these mice with sodium bicarbonate restores acid-base balance and, despite not preventing growth defects, extends their lifespan (Leibrock et al., 2016). Conversely, overexpression of *klotho* in mice also makes them live longer, independently of sex (Kurosu et al., 2005).

Regardless of upstream causality, these examples demonstrate how pH can be relevant for longevity research by interacting with the currently described hallmarks of ageing and other longevity-relevant processes.

1.4. *Drosophila melanogaster* as a model for acid-base in ageing

To fully comprehend how extracellular acid-base can alter organ function, beyond blood, interstitial fluids would need to be analysed as their pH can have organ-specific effects. Obtaining interstitial fluid from humans is still challenging (Wiig & Swartz, 2012). Even testing lymph collected from the thoracic duct, the convergent point before the lymphatic fluid joins the circulatory system, would have limitations. This would require a surgical procedure in healthy volunteers, with complex ethics. To manipulate and assess the consequences of extracellular pH on ageing, mammalian models such as mice would not be ideal either due to their relatively long lifespan (~2-3 years under standard laboratory conditions).

Here, I use *Drosophila melanogaster* (hereafter referred to as *Drosophila* or fly) as the model to study the impact of acid-base balance on ageing. Due to its comparatively short lifespan (~2-3 months under standard laboratory conditions) and strong evolutionary conservation of longevity-modulating pathways, the fly is a widely used model in ageing research (Piper & Partridge, 2018). It is estimated that ~75% of disease-related genes in humans have functional orthologues in the fly (Reiter et al., 2001). Besides, the fly also has a much faster life cycle than rodents (Figure 1.3) which allows cohorts of hundreds of flies to be produced in ~10 days at 25ºC. Lifespan experiments with flies benefit from the ability to have large group sizes and the scope to test a higher number of conditions and interventions compared to mammals which are more restricted from an ethical and financial perspective. Other advantages include the existence of powerful genetic tools, including tractable expression systems, a wide range of tools for tissue-specific modulation of gene expression, and publicly available genome-wide RNAi libraries (see Chapter 2).

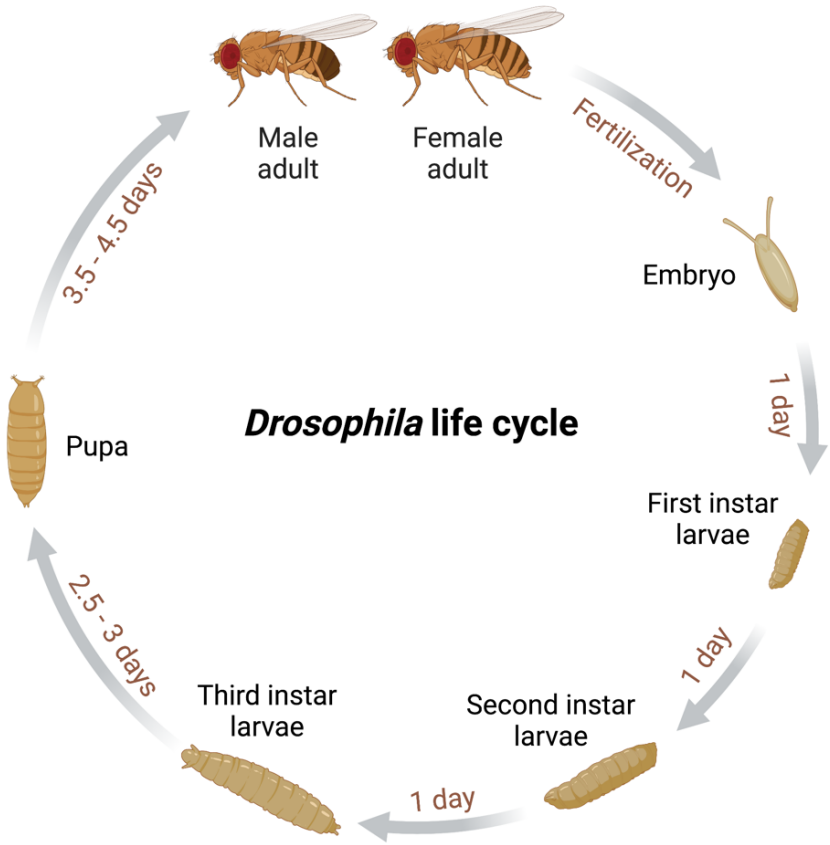


Figure 1.3. *Drosophila* life cycle. The fly life cycle is divided into four stages: embryo, larvae, pupa, and adult. The time length of the stages is approximate for flies raised at 25ºC and is shown in days. (Designed with BioRender.com)

As one of the most prevalent occurrences across life, ageing is expected to happen through analogous processes and manifest in invertebrates via shared pathways. Indeed, many pioneering discoveries in the ageing field were initially made in flies and subsequently shown to be evolutionarily conserved in mammals (Piper & Partridge, 2018). The *Drosophila* model is also historically important in discovering and characterising compounds that modulate longevity. According to the DrugAge database, there are >500 compounds potentially modulating lifespan (Barardo et al., 2017), and >100 of those have been tested in the fly.

Drosophila shows phenotypical signs of ageing that correlate to manifestations of the hallmarks of ageing (Piper & Partridge, 2018). These include changes in behaviour (reduced feeding, courtship and exploration, increased sleep fragmentation), decreased physical activity (impaired negative geotaxis, reduced voluntary flying and walking), altered neuronal function (impaired learning and memory), reduced reproductive capacity (reduced egg laying, decreased sperm and accessory fluid production), loss of stress resistance, decreased immune capacity, progressive intestinal dysplasia and reduced barrier function, and compromised cardiac function (Piper & Partridge, 2018).

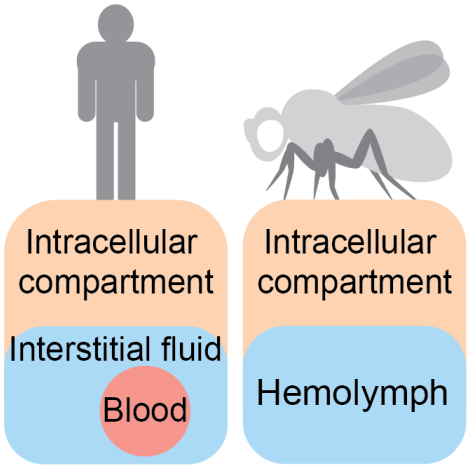


Figure 1.4. Comparison of human and fly bodily fluids compartments. This scheme represents the compartmentalisation of fluids in humans and flies. The main difference is the existence of an intravascular space in humans. In flies, the haemolymph bathes all organs, and the orchestrated activity of several tissues (mainly the dorsal vessel) drives its circulation.

To assess the role of extracellular pH homeostasis on physiology and ageing, *Drosophila* has the significant advantage of having an open circulatory system (Rotstein & Paululat, 2016), with a single extracellular fluid compartment, the haemolymph, bathing all organs (Figure 1.4). This makes it a simplified model to manipulate and understand the effects of extracellular pH variation on health and survival. Flies have complex organs that perform similar functions to their mammalian counterparts (Figure 1.5), including an excretory tract that contains Malpighian tubules functionally comparable to kidney tubules (Ugur et al., 2016). Despite the anatomical and physiological differences, the fly regulates systemic acid-base through similar mechanisms to humans: 1) buffers, predominantly the carbonic acid–bicarbonate equilibria (see Section 5.2); 2) excretory system, composed of similar transport proteins and ion channels (see Section 6.1.1); and 3) metabolic production of acids (see Section 7.2), with conserved metabolic pathways. These mechanisms will be introduced at the start of each respective chapter.

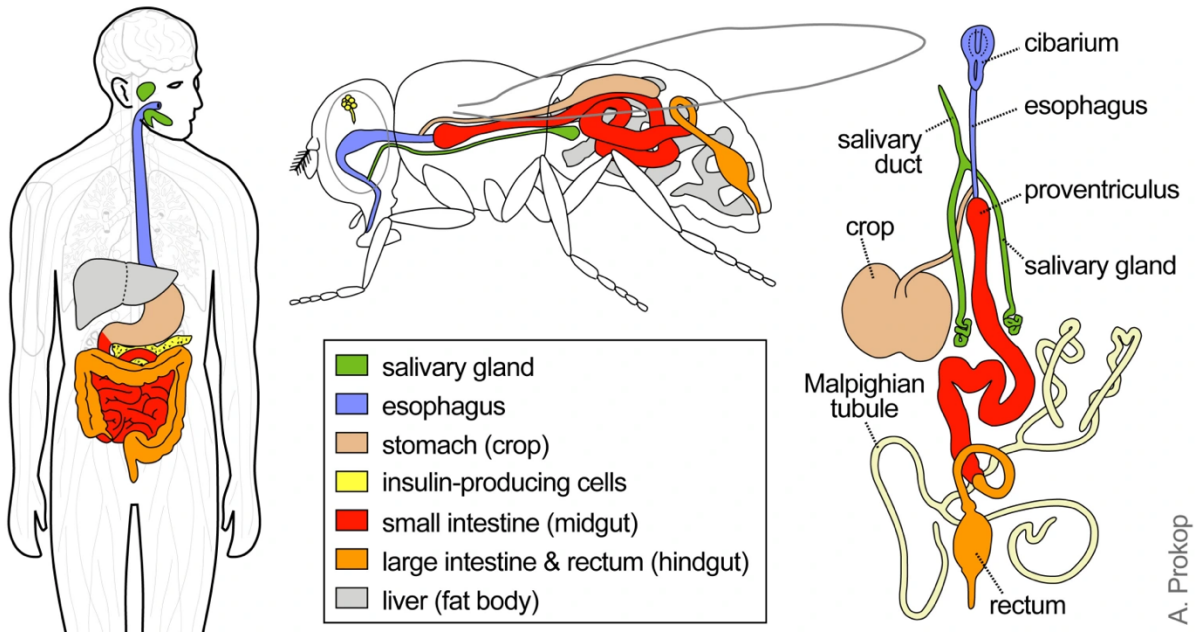


Figure 1.5. Comparison of human and fly internal organ anatomy. The excretory tract is composed of the two pairs of Malpighian tubules, the hindgut and the rectum. Malpighian tubules insert into the fly intestine above the hindgut. (Designed by Andreas Prokop; reprinted from droso4schools.wordpress.com/organs)

1.5. Hypothesis: acid-base is a hallmark of ageing

Here, I propose that loss of acid-base homeostasis is a novel hallmark of ageing, which translates into the following testable hypotheses:

1. Systemic acidification occurs during normal ageing
2. Factors promoting acidification accelerate ageing
3. Factors preventing acidification delay ageing

In this study, I focus on the extracellular fluid as a representation of systemic acid-base balance while recognising that intracellular pH regulation will have a critical role in ageing (Osanai et al., 2018). The idea that loss of acid-base balance towards acidification with ageing can promote chronic disease has been proposed before and gained some new interest recently (DiNicolantonio & O'Keefe, 2021; Frassetto et al., 2020; Frassetto & Sebastian, 2019a; Vormann & Goedecke, 2002). This work attempts to test the principle that systemic acid-base balance is lost with age and that it impacts survival. It also explores the role of acid-base balance as a dietary factor that promotes age-related disease.

Chapter 2. Materials and methods

2.1. Fly maintenance and genetics

2.1.1. General fly maintenance

Flies were kept in an incubator or room with controlled humidity (65%) and temperature on a light-dark cycle of 12 h each. Stock flies were maintained at 18°C, while experiments were performed at 25°C unless otherwise stated.

To get synchronised experimental cohorts, parental flies were put into cages with apple juice-agar plates supplemented with live yeast paste (Figure 2.1). After 24 h, eggs were collected by rinsing the plates with phosphate-buffered saline (PBS, 140 mM NaCl, 10 mM phosphate buffer, 3 mM KCl, pH 7.4 at 25°C, Sigma 524650) into 15 mL falcon tubes, allowed to settle by gravity, and washed once in PBS solution. Flies were reared at constant density by pipetting 16 μL of egg suspension using a wide-bore tip, giving ~300 eggs per bottle.

After 10 days (Figure 1.3), newly eclosed adults were transferred onto fresh sugar-yeast-agar (SYA) medium without anaesthesia and kept as a mixed population for 2 days to mature and mate. Flies were then sorted using a light microscope by sex and genotype under mild CO_2 anaesthesia into experimental vials at 15 or 20 flies per vial (depending on sex and purpose of the experiment). Flies were provided fresh media every ~2-4 days.

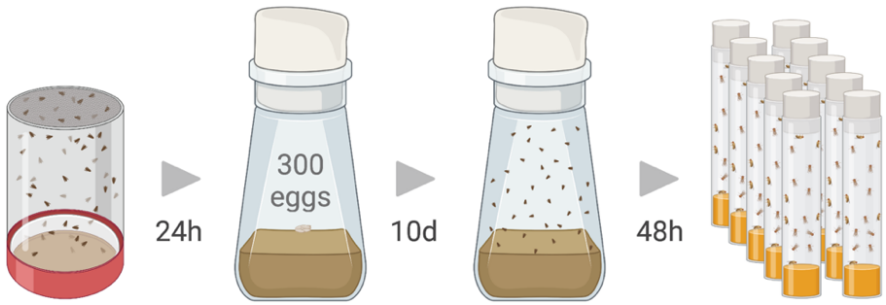


Figure 2.1. Experimental population set-up. Scheme of the method and timeline to set up adult experimental cohorts. (Designed with BioRender.com)

2.1.2. Fly media

Flies were fed a standard SYA medium consisting of 5% (weight/volume, hereafter w/v) sucrose (granulated sugar), 10% (w/v) Brewer's yeast (903312, MP Biomedicals)

and 1.5% (w/v) agar (Sigma A7002), supplemented with 3% (volume/volume, v/v) nipagin (10% w/v in 95% ethanol; H5501, Sigma) and 0.3% (v/v) propionic acid (P1386, Sigma) as preservatives, added once the food had cooled down to <60ºC. Media was dispensed at ~5-7 mL into narrow plastic vials or ~50 mL into 250 mL plastic bottles and allowed to set at room temperature (RT) before being stored at 4°C.

Apple juice-agar plates for cages were composed of 25% (v/v) apple juice, 2.3% (w/v) glucose, 2.3% (w/v) agar and 1.5% (v/v) nipagin.

2.1.2.1. Nutritional variations

To test interactions between diet and ageing as risk factors for disease (see Chapter 7), the standard SYA medium was altered to have different sugar and/or yeast percentages. High-sugar food (HS) was 20% (w/v) sucrose, high-yeast (HY) food was 25% (w/v) yeast, low-yeast (LY) food was 5% (w/v) yeast and high-fat (HF) food was SYA supplemented with 15% (w/v) of either lard or hydrogenated coconut oil. For starvation assays, flies were maintained on 1.5% (w/v) agar-only media. To supply the flies with an additional water source when required, 20 µL filter tips containing 1.5% (w/v) agar were inserted into the food vials.

Compound	Concentration range	Solvent	CAS number
Acetazolamide	0.001 – 5 mM	DMSO	59-66-5
Allantoin	0.01 – 10 mM	Water	97-59-6
Allopurinol	0.1 – 1 mM	Water	315-30-0
Ethylene glycol	0.5 – 5% v/v	n/a	107-21-1
Potassium citrate	0.01 – 1 mM	Water	6100-05-6
Sodium bicarbonate	1 – 100 mM	Water	144-55-8
Sodium oxalate	0.001 – 1% w/v	Water	62-76-0
Streptomycin	0.4 – 3.2 mM	Water	3810-74-0
Tris base	1 – 100 mM	Water	77-86-1
Tris citrate	1 – 25 mM	Water	68-04-2

Table 1. List of chemical compounds added to fly media. n/a – non-applicable.

2.1.2.1. Added drugs or chemicals

As a tool to modulate acid-base balance, drugs or chemicals were supplemented to standard media (see Chapter 4) once cooled down to <60ºC. Where drugs needed to be diluted in dimethyl sulfoxide (DMSO), the same volume of DMSO was added to the

control medium. All the compounds, concentrations, type of solution used for dilution, and their Chemical Abstracts Service registry (CAS) numbers are listed in Table 1.

2.1.2.2. Chemically-defined medium

To modulate specific dietary components (amino acids, cholesterol) or to increase the bioavailability of a chemical/drug, a chemically-defined (holidic) medium with an amino acid profile similar to yeast was used (Piper et al., 2014).

2.1.3. Fly strains and modulation of gene expression

For most experiments, the *white Dahomey* (w^{Dah}) strain of *Drosophila melanogaster* was used as the outbred wild-type background (Broughton et al., 2005). Additional experiments were performed in the isogenic control line w^{1118} and the wild-type *Oregon-R*. Mutant fly lines were backcrossed into the w^{Dah} or w^{1118} strain background for ~7 or 3 generations, respectively. Backcrossing is a process by which the genetic background of mutant flies is matched by a series of crosses to flies of a control background. Specific characteristics (e.g., eye colour) mark the presence of the desired genetic construct and are used to select flies containing that sequence. After sufficient generations, almost all other genetic background becomes the same due to meiotic recombination (Piper & Partridge, 2016).

2.1.3.1. The GAL4/UAS gene expression modulation system

To alter the expression of target genes, I used the GAL4/UAS gene expression system (Brand & Perrimon, 1993; Hales et al., 2015; Southall et al., 2008). Inserting the yeast (*Saccaromyces cerevisiae*) GAL4 gene, which encodes the transcriptional activator protein GAL4, under a promoter of a specific gene allows GAL4 to be expressed in the same tissue as that specific gene. GAL4 can then bind to an upstream activation sequence (UAS) to induce the transcription of the target gene preceded by that sequence (Figure 2.2). This allows spatial control of the target gene expression to match that of the gene under whose promoter GAL4 sits. This expression system is only active when both components are present, allowing stock lines with only the GAL4 gene (hereafter called drivers) or the UAS sequence (UAS lines) where gene expression is unaltered.

Before setting up a cross, unmated female flies are collected after eclosion. Unmated females have specific identifiable traits: lighter colour and an abdominal dark

spot (the meconium - remains of their last meal before pupation). To set up a cross, unmated female/male flies of a driver line are crossed with unmated females/males of a UAS line. Flies from each line are also crossed with wild-type flies of the same background (+) to serve as controls for insertional mutagenesis. For example, to precisely modulate the expression of gene *A* in the tissue *B* of flies, a driver where the GAL4 gene is under the promoter of a gene expressed solely in tissue *B* is crossed to a UAS line for gene A. Crossing each line to wild-type flies of the same background results in progeny expressing both of the components or each individually, represented as 1) *B*-GAL4 > UAS-*A*, 2) + > UAS-*A* and 3) *B*-GAL4 > +, where 1 is the experimental progeny, and 2/3 are the controls.

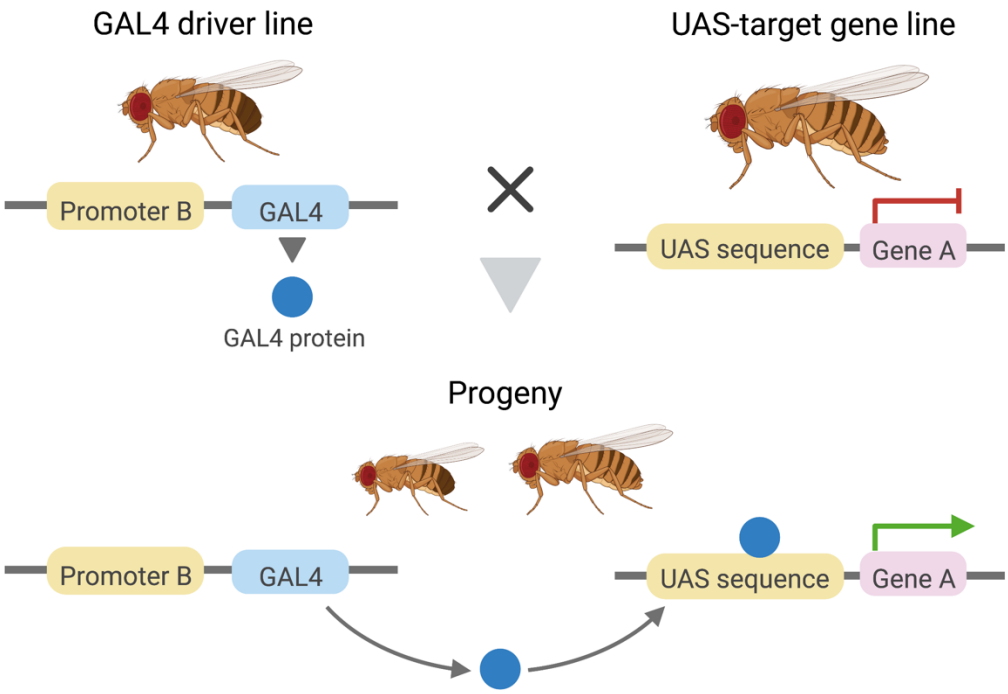


Figure 2.2. The GAL4/UAS expression system. Example of a cross between a male from a driver line to an unmated female from a UAS line. The resulting progeny expresses gene A in the tissues where promoter-related gene B is normally expressed. (Adapted from "*Drosophila GAL4/UAS System*", by BioRender.com, 2023)

The UAS line can be a reporter (e.g., GFP), an overexpressor construct, or an RNA interference (RNAi) knockdown transgene. RNA interference occurs when the endogenous mRNA of the target gene is targeted by a complementary hairpin double stranded RNA and degraded.

2.1.3.2. Drosophila gene knockdown libraries and validation

Both drivers and UAS-RNAi lines are publicly available in stock centres such as the Bloomington Drosophila Stock Center (https://bdsc.indiana.edu) and the Vienna Drosophila Resource Center (VDRC; https://stockcenter.vdrc.at). For this project, UAS-RNAi lines were ordered from the VDRC, which has two main collections, the GD and the KK libraries. In the GD library, UAS-RNAi constructs are inserted into random sites by germline transformation of an isogenic w^{1118} host using a hyper-active P-element transposase (Dietzl et al., 2007). All insertions are molecularly validated and mapped to a specific chromosome, and the isogenic w^{1118} background is retained throughout.

In the KK library, instead of random insertion, UAS-RNAi constructs are carried in a vector and inserted into a specific landing site by targeted recombination. This process allows consistent expression levels of UAS-RNAi constructs and avoids the potential, unpredictable disruption of host genes that can happen with random P-element-based insertion. However, one gene (*tiptop*) can be disrupted depending on which of the two potential landing sites the construct was inserted into (Vissers et al., 2016). Briefly, the KK library was designed to insert constructs at the 40D locus of chromosome 2L, but most constructs were unintentionally inserted at the 30B locus of the same chromosome. Insertion at the 40D site is upstream of the *tiptop* gene, which can cause growth problems, including specific eye and wing phenotypes (Figure 2.3b), while the 30B landing site is not predicted to disrupt host gene expression. Since *tiptop* disruption may affect fly survival, lines with a predicted 40D insertion were avoided.

For the CAH1 gene, only a single RNAi line was available at the VDRC, which has the construct inserted into both the 30B and 40D landing sites. After crossing the UAS-CAH1-RNAi line to a ubiquitous driver (daGAL4), although the target gene was knocked down (Figure 2.3a), the flies had the expected eye and wing phenotype characteristic of *tiptop* disruption. A clean 30B-only line was generated by separating the two landing sites by meiotic recombination. The original line was crossed into w^{1118} unmated females, and the progeny was then sorted by eye colour into white, gradient-eyed, dark red and bright red. By multiplex PCR as described (Vissers et al., 2016), I found that white-eyed flies lost both constructs, dark red-eyed had constructs on both landing sites, gradient-eyed had the 40D landing site occupied only, and the bright red-eyed the 30B only (Figure 2.3c). The selected 30B line was backcrossed into w^{1118} for 2 additional generations before establishing a homozygous stock.

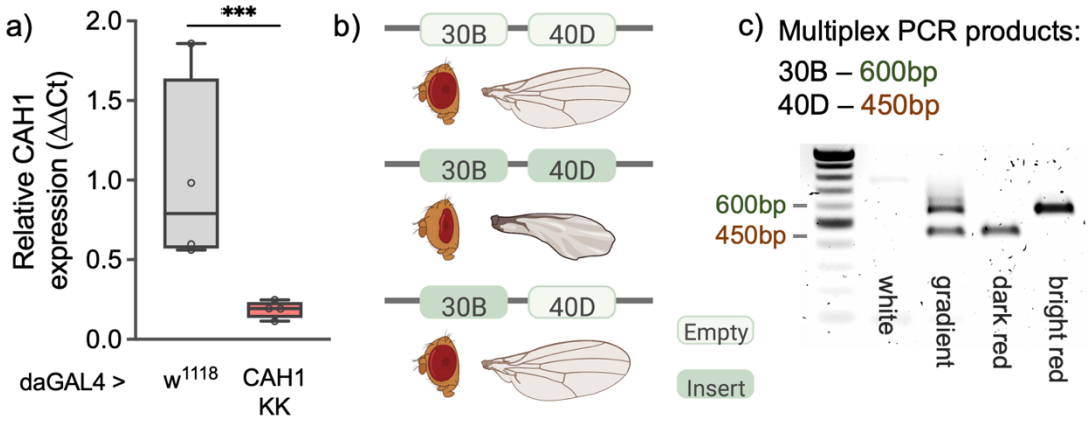


Figure 2.3. Recombination of CAH1 KK line: a) Gene expression of the target gene in the original VDRC line is decreased when ubiquitously driven (qPCR analysed with ΔΔCT method; n=4 biological replicates; statistical significance determined by unpaired t-test; ***, p<0.001); b) Illustration of fly phenotypes depending on the occupancy of the 30B and 40D landing sites (designed with BioRender.com); c) Representative multiplex PCR for the occupancy of the 30B (600bp) and 40D (450bp) landing sites of flies with different eye phenotypes.

Unmated females from a ubiquitous driver (daGAL4) were crossed to males of each UAS-RNAi line ordered from VDRC. As a control, unmated daGAL4 females were crossed to males of the same background (w^{1118}) with no UAS construct. The final cleaned-up UAS-CAH1-RNAi line and the UAS-CAH2-RNAi line resulted in the knock-down of the target gene (Figure 2.4a and 2.4b, respectively), measured by quantitative PCR (qPCR, see Section 2.5.7).

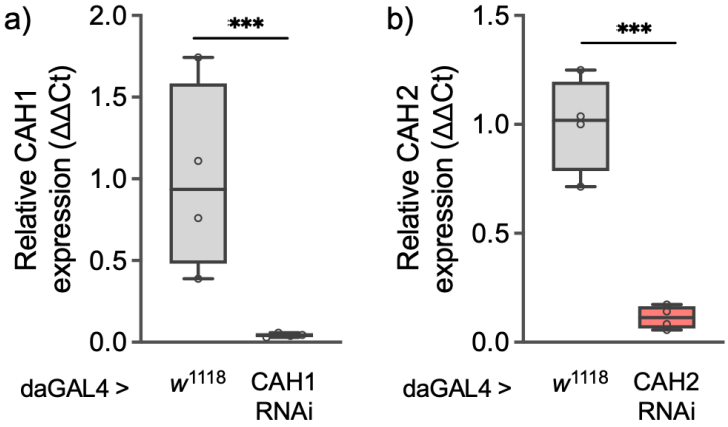


Figure 2.4. Validation of VDRC UAS-RNAi lines. Both the expression of a) *CAH1* and b) *CAH2* is decreased when their respective UAS-RNAi construct is ubiquitously driven; qPCRs analysed with ΔΔCT method; n=4 biological replicates; statistical significance determined by unpaired t-test; ***, p<0.001.

Eggs with the genes Vha55 and VhaSFD ubiquitously knocked down did not develop. These genes are translated into subunits of the v-ATPase which is essential in multiple signalling pathways and biological processes, including development (Mo et al., 2020; Pamarthy et al., 2018; Vaccari et al., 2010). Given that the control flies developed and eclosed normally, I inferred from the lethality that these lines resulted in the expected knock down of the target genes, although the effect size was not tested.

2.1.3.3. Generation of UAS-target gene lines

Unlike gene knockdown lines, UAS lines that result in the overexpression of genes are less readily available. To test my hypotheses, I needed lines overexpressing *CAH1*, *CAH2*, *VhaSFD* and *pHCl-2*. The UAS-pHCl-2 line was a generous gift from Irene Miguel-Aliaga (Redhai et al., 2020). I generated UAS lines for the other genes.

To do that, separate transformation vectors were ordered for each gene containing constructs with the UAS, Flag and hemagglutinin tags, attB site and the target gene in their sequence. These plasmids were obtained from the *Drosophila* Genomics Resource Center (DGRC) and originated from the Berkeley *Drosophila* Genome Project Tagged ORF Collection. The clones were processed following the DGRC protocol (McKillip & Klueg, 2006) and the transformation protocol for the cells I used (Stellar™ Competent Cells, Takara Bio), after determining the transformation efficiency of a test sample in those cells. In short, competent cells were transformed with the clones, which contained a gene that when integrated made them resistant to either ampicillin or chloramphenicol (Figure 2.5a). Those cells were placed in low or high density onto plates filled with lysogeny broth supplemented with ampicillin or chloramphenicol, respectively. From the transformed colonies that grew after overnight incubation, 5 were picked per condition and expanded. DNA was extracted from those expanded colonies using a commercial kit (Plasmid Midi Kit, QIAGEN), following its protocol (Figure 2.5b). The extracted plasmids were resuspended in pure water instead of the recommended buffers to increase the viability of embryos after the injection of the plasmids.

To confirm that the extracted plasmids contained the correct original sequence, plasmids were sent to a company (Genewiz) that performed Sanger sequencing using the primer recommended by DGRC (UAS_HSP_UP, Supplementary Table 1). After confirming the sequence, I sent the plasmids to another company (BestGene) for

injection, generation and identification of transformants (Figure 2.5c). Each construct was injected into embryos of different fly strains containing attP landing sites in different positions of their genome and PhiC31. PhiC31 integrates the sequence with the UAS and the target gene into that specific position (Bateman et al., 2006). Table 2 contains the genotype of the embryo strains into which each construct containing the target genes was inserted and the respective site of integration. Those different locations with a resulting light orange-eye phenotype were selected to make potential crosses or recombination of different lines more efficient.

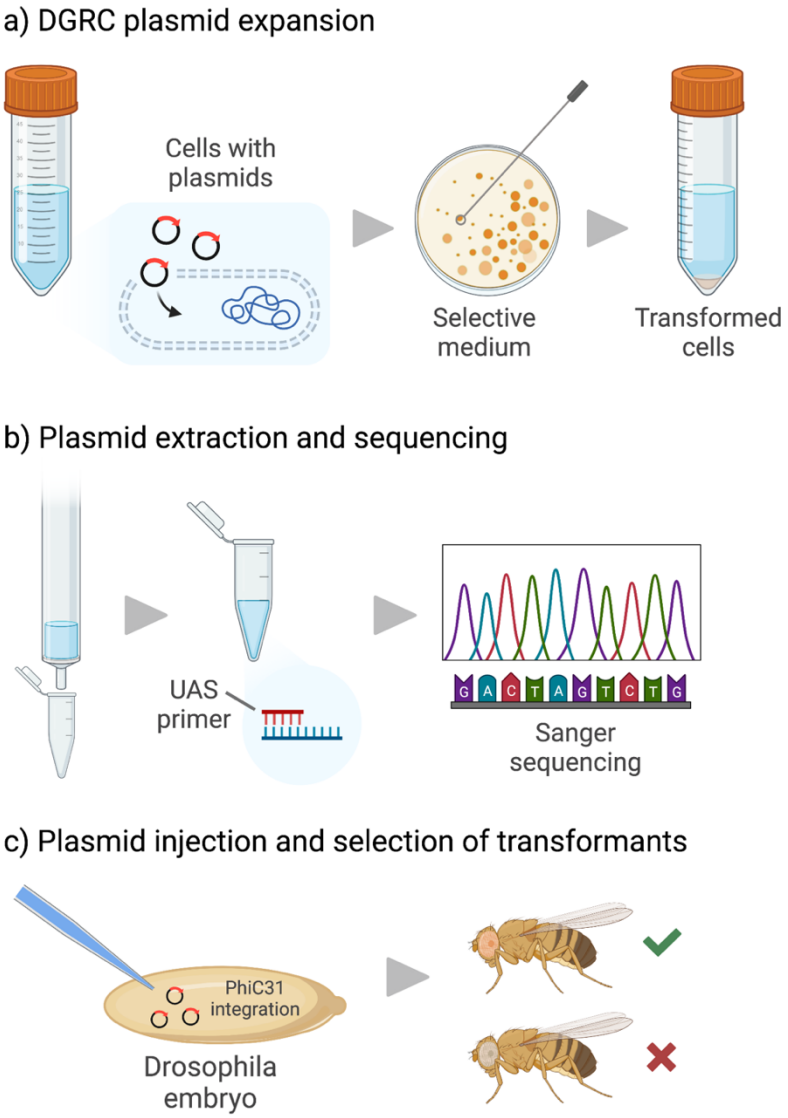


Figure 2.5. Generation of novel UAS lines. Illustration of the steps taken to generate novel UAS lines: a) expansion of DGRC plasmids; b) plasmid extraction and Sanger sequencing; and c) plasmid injection into embryos and selection of transformants based on eye colour. (Designed with BioRender.com)

Target gene	Embryo genotype	Chromosome	CytoSite
CAH1	PBac{yellow[+]-attP-9A}VK00028	3R	92F1
CAH2	PBac{yellow[+]-attP-9A}VK00022	2R	57F5
VhaSFD	PBac{yellow[+]-attP-3B}VK00031	3L	62E1

Table 2. Embryo genotypes and insertion site of UAS lines constructs. Different chromosomal locations were selected to facilitate potential crosses and recombinations.

After injection, the company selected and backcrossed transformants for each line into the *yw* strain for 2 generations and sent me the progeny of the second cross. I crossed males of each line with w^{1118} unmated females and selected non-yellow males from the progeny to discard the *y* mutation. Each line was then backcrossed for 3 generations into the lab w^{1118} stock and a final cross was made to keep homozygote stocks by selecting for dark orange- or red-eyed flies.

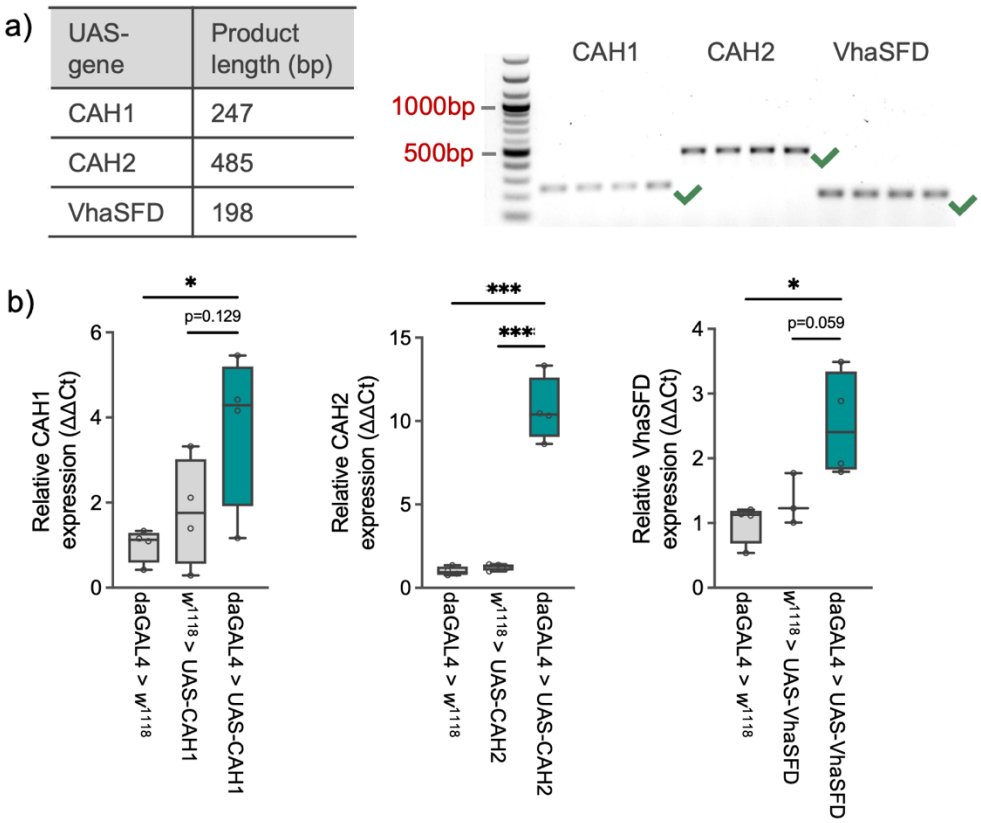


Figure 2.6. Validation of novel UAS lines: a) The presence of each UAS construct confirmed by PCR, b) Overexpression of each target gene when driven ubiquitously (qPCRs analysed with ΔΔCT method; n=4 biological replicates; statistical significance determined by ANOVA with Tukey correction for multiple testing; *, p<0.05; ***, p<0.001)

PCR confirmed the presence of the UAS-target gene construct (Figure 2.6a) in the selected flies (designed primers shown in Supplementary Table 1). Higher gene expression of the target gene was confirmed by qPCR after crossing each UAS line to the ubiquitous daGAL4 driver and to w^{1118} controls (Figure 2.6b).

2.1.4. Complete list of fly genotypes

All the fly lines used in this project are listed here, with their genotype, the abbreviation used throughout this document to refer to them and their origin.

	Genotype	Abbreviation	Origin
Control background	w^{Dah}	w^{Dah}	Broughton et al., 2005
	w^{1118}	w^{1118}	Bjedov et al., 2010
	Ore^{R}	Ore^{R}	Gut Signalling and Metabolism lab, LMS
Drivers	w^{1118};;daGAL4	daGAL4	Wodarz et al., 1995
	w^{1118};uroGAL4;	uroGAL4	Terhzaz et al., 2010
	w^{1118};;byn-GAL4/TM6Sb	bynGAL4	Bangi et al., 2016
	w^{1118};;P{HmlΔ-GAL4}3,P{UAS-2xeGFP}AH3/MKRS	HmlGAL4	Bloomington #30142
UAS-RNAi lines	w^{1118};P{KK108727}VIE-260B/CyO;	UAS-CAH1-RNAi	VDRC #104429
	w^{1118};;P{GD2438}v8357	UAS-CAH2-RNAi	VDRC #8357
	w^{1118};P{KK106835}VIE-260B;	UAS-pHCl2-RNAi	Redhai et al., 2020
	w^{1118};P{GD10564}v25985;	UAS-Vha13-RNAi	VDRC #25986
	w^{1118};;P{GD10617}v46563	UAS-Vha44-RNAi	VDRC #46563
	w^{1118};;P{GD9363}v46553/TM3	UAS-Vha55-RNAi	VDRC #46553
	w^{1118};P{GD8795}v47471;	UAS-VhaSFD-RNAi	VDRC #47471
UAS lines	w^{1118};;UAS-CAH1	UAS-CAH1	Present work
	w^{1118};UAS-CAH2;	UAS-CAH2	
	w^{1118};;UAS-VhaSFD	UAS-VhaSFD	
	w^{1118};UAS-pHCl2/CyO;	UAS-pHCl2	Redhai et al., 2020
	w^{Dah};;Δdilp2-3,5	Δdilp2-3,5	Grönke et al., 2010

Table 3. Complete list of the fly lines used in this study

The haemocyte-specific HmlGAL4 driver was kindly provided by Marc Dionne, Imperial College London. The UAS-pHCl2 overexpressor line and UAS-RNAi lines against Vha13, Vha44 and pHCl2 were generously gifted from Irene Miguel-Aliaga, MRC London Institute of Medical Sciences. The w^{Dah}, w^{1118} and $\Delta dilp2\text{-}3,5$ strains were originally received from Linda Partridge, University College London.

2.2. Fly behavioural & functional assays

2.2.1. Survival

Experimental flies were set up and maintained as described above. Deaths and censors (i.e., flies killed or lost during transfer) were scored every 2-3 days as the flies were transferred into vials with fresh media. During the transfer, dead flies were removed from vials, as carrying them over is reported to shorten the survival of the remaining (Chakraborty et al., 2019).

In survival experiments under stress conditions (acidotic stress, starvation), deaths were scored more frequently, up to twice a day. Dead flies were removed every 2-3 days as flies were transferred onto fresh food. Typically, 140 to 150 flies were set up per condition for all survival experiments.

2.2.2. Fecundity

Fecundity was quantified by counting the total number of eggs 7-day-old flies laid over 24 h in experimental vials. The number of eggs was divided by the number of flies to get the mean fecundity per fly.

2.2.3. Feeding and drinking

2.2.3.1. Automated proboscis extension detection

Feeding was assessed using a fly proboscis and activity detector (FlyPAD) automated system (Itskov et al., 2014). Individual flies were placed (unanaesthetised, using a pooter) in small arenas with two channels: one to serve as a reference and another with solid media at the centre over an electrode. Whenever the flies ate, they stood over another electrode close to the food and completed a circuit between the two electrodes (Figure 2.7). The change in capacitance between the two electrodes was detected, and from this, the number of times they touched the food (number of sips) and for how long were inferred.

This behaviour was recorded for up to 2 h, at about 25°C. Media was freshly prepared to prevent drying out. Previously prepared SYA/starvation medium was melted by microwaving it, and the food was poured into a petri dish until the height of the FlyPAD arenas. When the food was set, a cylinder with the diameter of the central electrode was transferred (using a cut tip) into the centre of the arena.

The data was collected using the Bonsai software and analysed with Mathworks, a MatLab package, as originally described (Itskov et al., 2014).

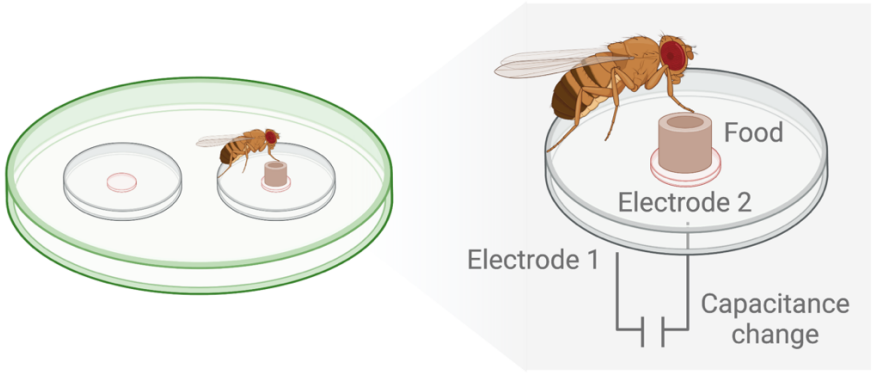


Figure 2.7. FlyPAD. Representation of a single FlyPAD arena. Flies touching both electrodes simultaneously close a circuit and the change in capacitance is measured. (Designed with BioRender.com)

2.2.4. Respirometry

To measure the metabolic rate of flies, i.e. the amount of oxygen consumed or carbon dioxide produced per minute, a high-resolution insect respirometry system developed by Sable Systems was used as previously described (Lighton, 2008; Lighton & Schilman, 2007). Groups of either 3 female or 5 male unanaesthetised flies were put into respirometry chambers. Each chamber had a food source in a loose plastic cuvette cap, made by melting previously prepared medium and pouring it into the cap. The reference chamber (with no flies) had the same food source in it.

This respirometry system measures changes in gas (oxygen, carbon dioxide and water vapour) partial pressures over a period of time that counts as a cycle (in this set-up, 48 min). These changes result in a peak from the baseline gas partial pressure and can be analysed as the area under the curve. Data was typically recorded over 24 hours using the ExpeData software provided by Sable Systems. The same software can be used to analyse the data, but the macro needed for data analysis was not provided at the time of writing. The respirometry data presented in this document is

descriptive and displayed as a typical recording of a 48 min cycle, where each column containing 2 peaks: oxygen consumption and carbon dioxide production. Each column represents an independent group of flies.

2.2.5. Malpighian tubules deposit scoring

The excretory system was dissected from flies by pulling their rectal pad on 10 mM PBS. The tubules were scored according to the percentages of stones within each tubule from 0 to 4, in which: 0 is a clear tubule, 1 is a tubule with <25% stones, 2 is a tubule with 25-50% stones, 3 is a tubule with 50-75% stones and 4 is a tubule with >75% stones (Figure 2.8).

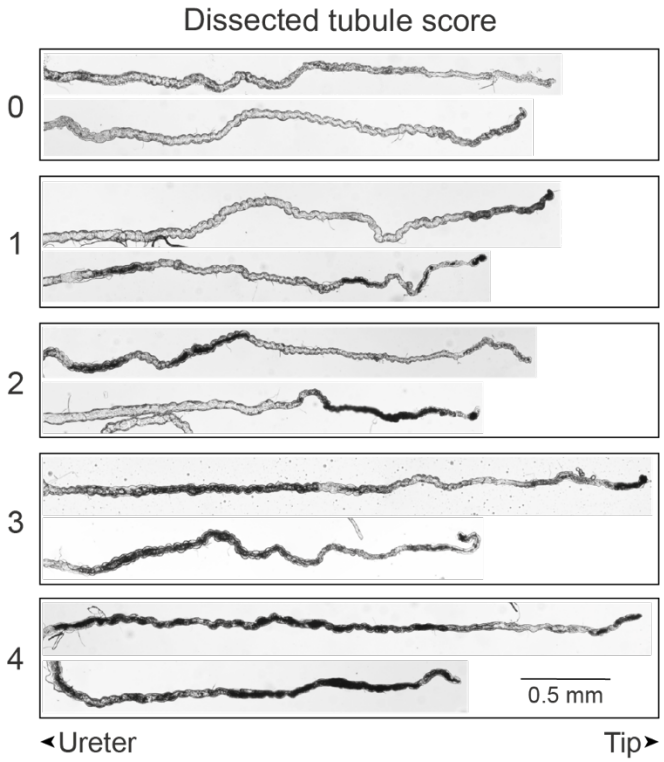


Figure 2.8. Tubule deposits scoring. 0, clear tubule; 1, <25% stones; 2, 25-50% stones; 3, 50-75% stones; and 4, >75% stones. (Reprinted from van Dam et al., 2020)

2.3. Fly sample collection

2.3.1. Freezing flies

Flies were transferred directly from vials with media into 1.5- or 2-mL tubes on dry ice using a dry ice-chilled funnel and stored at -80°C. Typically, I froze the flies from approximately 2 to 4 pm to minimise circadian variation on subsequent experiments.

2.3.2. Excretory system dissections

The excretory system (Malpighian tubules, hindgut and rectal ampulla) was dissected from ice-cold-anaesthetised flies by pulling their intestine from the rectal pad on an RNA stabilisation solution (RNAlater). The intestine was cut above the insertion of the Malpighian tubules, and the dissected tissue was transferred into 1.5 mL tube on dry ice (15 excretory systems per tube). Frozen samples were stored at -80°C.

2.3.3. Larval haemolymph collection

To collect haemolymph from *Drosophila* 3rd instar larvae, a brush was used to pick larvae from bottles and transfer groups of 10 into cell strainers (Figure 2.9). Each sieve was placed into a petri dish with 10 mM PBS to immerse the larvae for about 15 s to clean their cuticle. After drying the larvae with a tissue, I transferred them into a 0.5 mL tube with tweezers, piercing their mouth to create a hole for the haemolymph to be drained from. These 0.5 mL tubes had been cut with a razor blade 3-4 mm at the bottom so that when placed into a 1.5 mL tube and spun for 10 s in a benchtop centrifuge, clear haemolymph was drained. Haemolymph was snap-frozen in liquid nitrogen and kept on dry ice during the collection process.

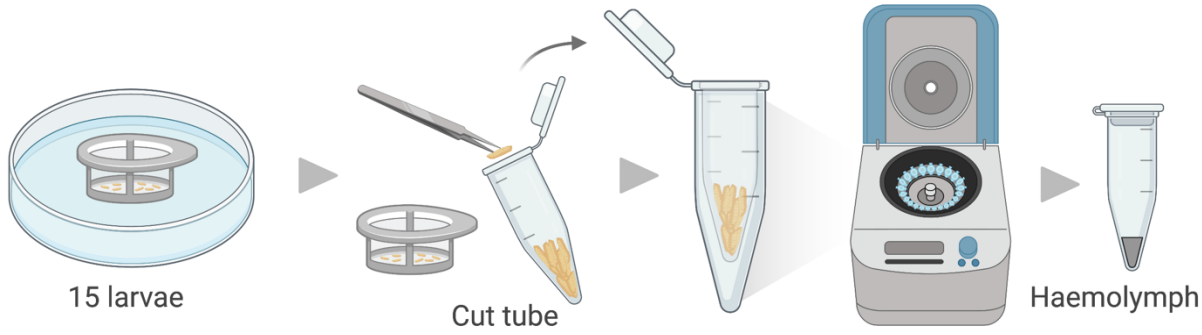


Figure 2.9. Larval haemolymph collection. Illustration of the steps required for larval haemolymph extraction. (Designed with BioRender.com)

2.3.4. Adult haemolymph collection

To extract haemolymph from adult flies, live cohorts of 12 or 15 flies (if female or male, respectively) were decapitated under ice anaesthesia using a scalpel blade (Figure 2.10). The bodies were placed upside down into 200 µL pipette tips within a 1.5 mL tube and gently centrifuged for 15 min at 1,500 x g, 4ºC to drain the haemolymph. The tube was then snap-frozen in liquid nitrogen and kept on dry ice during the collection

process before being stored at -80°C until required. Samples which were not clear (i.e. cloudy or containing eggs) were discarded.

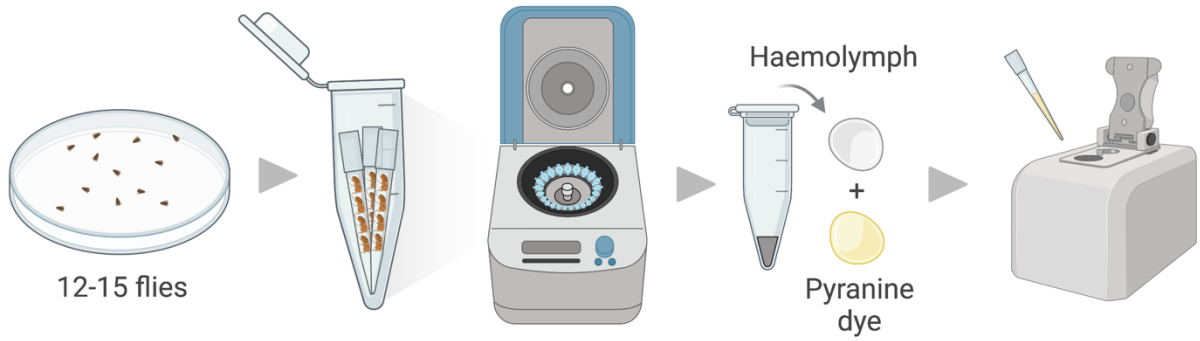


Figure 2.10. Adult haemolymph collection. Illustration of the steps required for adult fly haemolymph extraction. (Designed with BioRender.com)

2.4. pH measurements

2.4.1. Haemolymph pH

2.4.1.1. Pyranine dye

The main method to measure haemolymph pH was based on the spectrophotometric profile of the pH-sensitive cell-impermeable pyranine dye. The gold standard method for measuring hydrogen ion activity in a solution is the pH meter, which measures the difference in electrical potential between the electrode dipped in the experimental solution and an electrode in a reference solution. However, the low haemolymph volumes make it technically challenging to measure pH with this method.

Instead, I adapted and optimised a published pH-dye-based protocol (Ghosh & O'Connor, 2014). In short, to obtain the pH of a haemolymph sample, 1 µL of the pH-sensitive dye pyranine (2.4 mM in water; H1529, Sigma) was mixed with 1 µL of haemolymph (Figure 2.10). The absorbance ratio of pyranine's protonated and deprotonated peaks was measured by spectrophotometry using the Nanodrop One (Thermo Scientific). These peaks were respectively at 405 and 450 nm with automated baseline correction (Figure 2.11c) or 425 and 484 nm without (Figure 2.11a).

To obtain an approximate value of sample pH, 1 µL of pyranine was mixed with 1 µL of 50 mM Tris-HCl solutions of different pH, ranging between 6.6 and 7.8. A standard curve was obtained, plotted as a second-degree polynomial equation with pH on the y-axis and the absorption ratio on the x-axis (Figures 2.11b,d-f). The Henderson-Hasselbalch Calculator (https://www.cytographica.com/lab/HHTris.html)

was used to prepare the solutions in that pH range (Supplementary Table 2). The pH of each solution was confirmed using a pH meter.

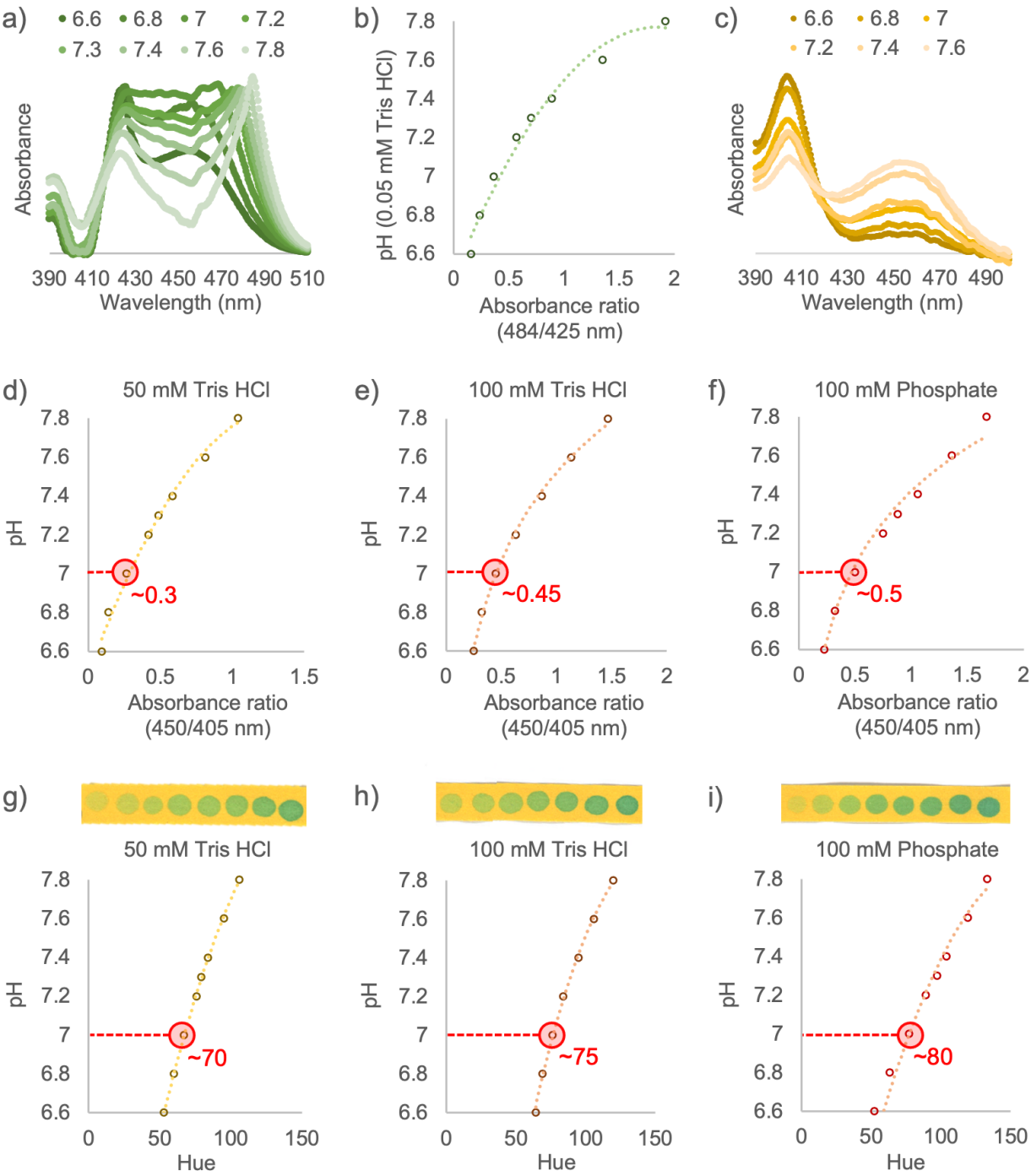


Figure 2.11. The effect of different standard solutions on pH measurements. pH-dependent absorbance peaks a) with and c) without baseline correction. Standard curves of pH depending on absorbance ratio of b) uncorrected and corrected d-f) baseline peaks. Standard curve shift depending on which solutions were used for pH standards using both d-f) the pyranine dye or g-i) the pH paper method, exemplified by different absorbance ratios and hues for pH 7.

During the optimisation process, 100 mM Tris-HCl and 100 mM phosphate solutions (Supplementary Table 3) were also used in the same pH range. Depending on which standard curve was used to compare the absorption ratio of the sample to, different absolute pH values were obtained (Figures 2.11d-f). This seems to be dependent on the molarity of the standard pH solutions, as this is the factor that differs between the standard curve from Figure 2.11d and the one from Figure 2.11e. Consistent with this hypothesis, phosphate-based standard pH solutions with the same molarity have more comparable ratios. While this effect could result from a higher dilutional effect of solutions with lower molarity when mixed with the pyranine dye solution, that is unlikely given that the same shift of the standard curve was seen when an alternative method which does not consist of mixing solutions, the pH paper, was used (Figure 2.11g-i).

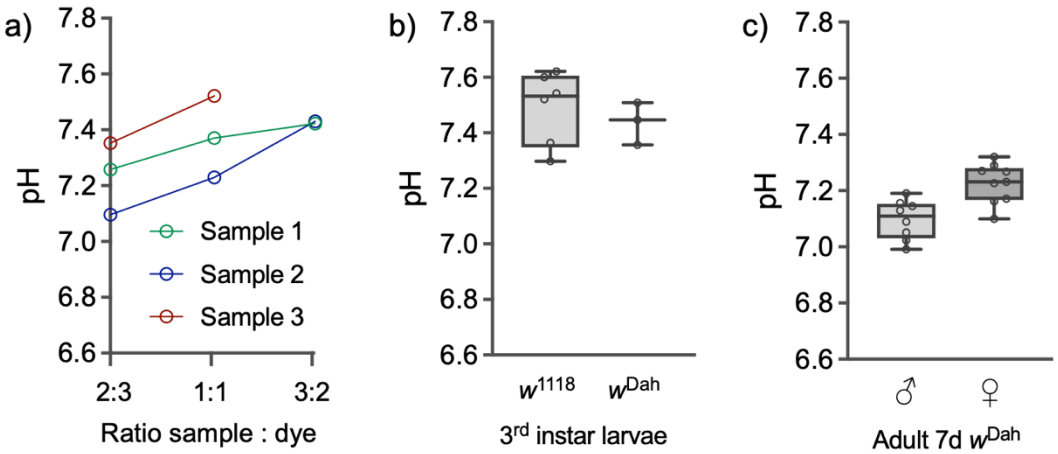


Figure 2.12. Factors that alter absolute pH values: a) The dilution of haemolymph samples may alter measured pH; b) Larval haemolymph pH of different strains; c) Example of measured haemolymph pH of adult 7-day-old flies of both sexes.

Other factors besides solution molarity may affect both methods. The ideal experimental standard curve, fly haemolymph with a range of different pH, is technically not possible. Artificial fly haemolymph can be prepared and has been used before in *Drosophila* heart studies (Vogler & Ocorr, 2009), but its composition does not replicate all haemolymph components which can affect either pH or the pyranine dye spectrophotometric profile. Different sample to pyranine dye solution ratios can also affect absolute pH values, with lower ratios resulting in increased sample dilution and lower pH values (Figure 2.12a).

I ultimately decided to use the 50 mM Tris-HCl standard curve to obtain the absolute pH values, as this was previously described (Ghosh & O'Connor, 2014) and because the chloride molarity of those solutions is more comparable to that of fly haemolymph (Singleton & Woodruff, 1994). I used a 1:1 ratio for all conditions. Using this standard curve, pH values for 3rd instar larvae haemolymph were in the range of 7.4-7.5 (Figure 2.12b), similarly to published data (Ghosh & O'Connor, 2014), and pH was about 7.1 for control 7-day old male flies and 7.2 for female flies (Figure 2.12c). From the sample pH values calculated from the 50 mM Tris-HCl standard curve, pH differences relative to the mean of the experimental control condition were calculated and pH data hereafter is presented as these relative differences which are more relevant for this work.

2.4.1.2. Bromothymol blue dye

During the optimisation process of obtaining accurate haemolymph pH based on the spectrophotometric profile of a pH-sensitive dye, I developed a second colorimetric assay using bromothymol blue, based on the same rationale.

The advantage of bromothymol blue was that this dye would allow more precise measurements of pH values at a lower range (6.0 to 7.6). This would have been useful given that the absolute pH values obtained for adult haemolymph were in the lower range of the pH standard curves with the pyranine dye, under which measurements become less precise.

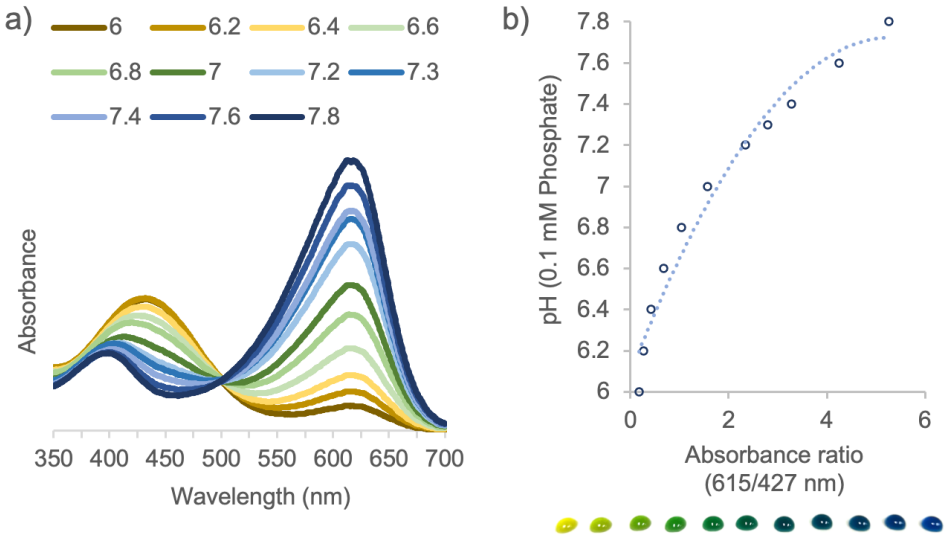


Figure 2.13. Bromothymol blue spectrophotometric pH measurements: a) pH-dependent absorbance peaks; b) Standard curve of pH depending on the 615/427 nm absorbance ratio.

The absorbance of bromothymol blue dye when mixed with pH-controlled 100 mM phosphate solutions (1:1 ratio) was measured. From this, a ratio between the protonated (427 nm) and deprotonated (615 nm) peaks was obtained (Figure 2.13a) to create a standard curve, plotted as a second-degree polynomial equation with pH on the y axis and absorption ratio on the x axis (Figure 2.13b).

When I tried to measure the pH of haemolymph samples, all (both larval and adult) turned yellow and out of the range of the standard curve (pH <6), so I abandoned this method. This may happen because the original bromothymol blue solution had a higher dilutional effect than pyranine, acidifying the haemolymph values to pH below 6, the dye entered the intracellular compartment whose pH is lower or because other factors in the haemolymph interact with the dye.

2.4.1.3. pH paper

pH paper (range 5.5-9.0; 1095640003, Merck) was used as an independent measure of pH during the optimisation of the dye-based approach, as shown above. To analyse the pH, the paper was scanned right after pipetting pH-controlled solutions into it and the image processing software FIJI (ImageJ) was used to obtain the hue of each drop with the colour histogram tool. Standard curves for these solutions were obtained to calculate sample pH (Figures 2.11g-i). This method was also used to measure absolute values of haemolymph independently during the optimisation process and to confirm relative differences of key experiments.

2.4.2. Excreta pH

2.4.2.1. Poo plates

To measure excreta pH, groups of 5 flies were transferred without anaesthesia to a Petri dish containing a 1/4 wedge of SYA medium supplemented with the pH-sensitive dyes bromophenol blue (0.5% w/v; B0126, Sigma) or bromocresol purple (0.5% w/v; 114375, Sigma) (Cognigni et al., 2011). SYA medium was made without propionic acid and pH was adjusted to 4.0 or 5.6, respectively. The flies were kept in the dishes for 24 h at 25ºC.

The plate lids were scanned and the excreta was analysed using the T.U.R.D. software, version 0.8 (Wayland et al., 2014), with the following settings: block size 25, offset 5, minimum size 35, maximum size 3500, shape circle, size 3, and circularity

threshold 0.70. Excreta with hue above 300 (end of blue) and below 30 (end of yellow) were excluded.

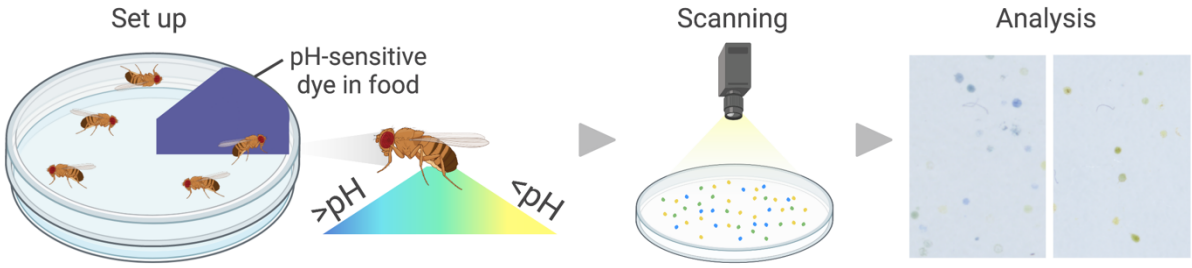


Figure 2.14. Analysis of excreta number and pH. Illustration of method to analyse adult fly excreta pH. Flies are transferred to Petri dishes and maintained there over 24 h with pH-sensitive dye-supplemented food. The plate lids are scanned and excreta is analysed to obtain number and hue, representative images on the right. (Designed with BioRender.com)

2.5. Molecular biology methods

2.5.1. Primer design

Primers were designed using the Primer-BLAST tool (ncbi.nlm.nih.gov/tools/primer-blast). Primers were designed for qPCR so that they would span exon-exon junctions and were specific for the gene but not for any specific isoform of that gene. List of primers used in this work can be found in Supplementary Table 4.

2.5.2. Fly genomic DNA extraction

Single flies were homogenised by placing them in individual wells of a 96-well plate and mashing them mechanically for about 10 s with a pipette tip filled with squishing buffer, expelled afterwards. This buffer (pH 8.2) was composed of 10 mM Tris-HCl, 1 mM EDTA, 25 mM NaCl and 200 µg/mL proteinase K (Gloor et al., 1993). The fly homogenates were then incubated at 37ºC for 1 h followed by 10 min at 95ºC to inactivate the proteinase K. Extracts were stored at 4ºC until required.

2.5.3. Polymerase chain reaction

PCR was performed with either Q5® High-Fidelity DNA Polymerase kit (M0492L, New England BioLabs) or with the JumpStart™ Taq DNA polymerase (Sigma-Aldrich) and separate nucleotides. Thermal cycling parameters for the Q5 polymerase: initial denaturation for 1 min at 98ºC; 35 cycles of denaturation for 10 s at 98ºC, annealing

for 30 s at 59ºC, and extension for 30 s at 72ºC. Cycling parameters for the JumpStart polymerase: initial denaturation for 1 min at 94ºC; 35 cycles of denaturation for 30 s at 94ºC, annealing for 30 s at 60ºC, and extension for 1 min at 72ºC.

2.5.4. DNA gel electrophoresis

To perform DNA electrophoresis, ethidium bromide (0.002% w/v) agarose (1.5% w/v, A9539, Sigma-Aldrich) gels in TAE buffer (40 mM Tris, 20 mM acetic acid, 1 mM EDTA, prepared by the LMS core facility) were prepared. A 1 kb DNA ladder (N0468S, NEB) was loaded in the first well and 5 µl of DNA was mixed with 1 µL of 6x DNA loading dye (R0611, Thermo Scientific) before loading into the wells. Electrophoresis was typically run at 80-100 V for ~1 h, and imaged in a UV transilluminator chamber (Syngene InGenius).

2.5.5. RNA extraction, purification and cDNA synthesis

RNA was extracted from either 5 frozen whole flies or 15 frozen dissected excretory tracts. To do that, the samples were placed into Ribolyser tubes with 1 ml of TRIzol and homogenised in a tissue homogeniser (Precellys 24, Bertin Instruments). After a 5 min incubation at room temperature (RT), 200 µL of chloroform was added and mixed in a vortex for 15 s. Samples were incubated at RT for another 2 min and centrifuged for 15 min, at 16,650 g, 4ºC. From the resulting upper aqueous phase, 0.5 mL were transferred to a 1.5 mL tube with 0.5 mL isopropanol and gently mixed by inversion. At this point, samples were left at RT for ~15 min and then transferred to a -20ºC freezer to improve the yield. Usually the day after, I proceeded with the purifying steps of the protocol. The samples were centrifuged for 15 min at 16,650 g, 4ºC, and the resulting gel-like pellets containing the RNA were washed in 500 µL of 70% ethanol (v/v in diethyl pyrocarbonate-treated water) after removal of supernatant. The samples were then centrifuged again for 5 min, at 16,650 g, 4 ºC and washed 2 additional times. After the last wash, the pellets were left to dry until translucent, redissolved in RNAse-free water and incubated at 60ºC for 10 min.

RNA concentration in each sample and the presence of potential contaminants were determined using the NanoDrop One. Samples were then DNAse-treated before cDNA synthesis. To do that, 3 µg of RNA from each sample were mixed in a solution composed of 10% (v/v) 10-fold DNAse buffer (AM2222, Invitrogen) and 5% (v/v) of a

DNAse solution (AM2222, Invitrogen) and incubated for 30 min at 37ºC in the thermocycler. DNAse was then inactivated by the addition of 50 mM EDTA to the solution (4.5 mM final concentration) and an incubation at 75ºC for 10 min.

To synthesise cDNA from each sample, 1 µg of DNAse-treated RNA was mixed in a solution made of 5% (v/v) reverse transcriptase (iScript, Bio-Rad) solution and 20% (v/v) 5-fold iScript buffer (Bio-Rad). The solutions were placed in a thermocycler with the following program: priming for 5 min at 25ºC, reverse transcription for 20 min at 46ºC, reverse transcriptase inactivation for 1 min at 95ºC. From each solution, 5 µL were mixed together to have an undiluted solution for the qPCR standard curve. The rest of each solution was then diluted 1:4 and kept at -20ºC until needed.

2.5.6. Primer validation for quantitative PCR

To validate the specificity of the primers to the target gene, PCRs and DNA gel electrophoresis were performed for each primer using cDNA from whole w^{Dah} female flies. A primer pair was considered specific for a target gene if only one band at the expected product length was seen (Figure 2.15).

Primer pair	Product length (bp)
CAH1	487
CAH2	257
CAH3	146
CAH9	358
Vha13	129
Vha44	463
Vha55	131
Vha55_2	274
VhaSFD	446
PMCA	487
pHCl-2	376
Ndae1	363
Uro	369



Figure 2.15. Primer validation. Expected product length and gel electrophoresis for each primer pair. Initial Vha55 primer pair was unspecific and a new one (Vha55_2) was designed.

2.5.7. Quantitative PCR

Solutions were made for primers standard curves by serially diluting 1:2 (in ultrapure water) undiluted cDNA mixed from all experimental conditions. In a 384-well plate, I added 10 µL solutions composed of 50% (v/v) iTaq SYBR™ Green Master Mix (Thermo Scientific) containing the iTaq DNA polymerase, 2.5% (v/v) of each primer pair 10 µM solution and 10% (v/v) diluted cDNA. Amplification curves of the fluorescent product were measured using the QuantStudio™ 7 Flex Real-Time PCR System (Thermo Scientific). The threshold cycle (Ct) was determined for each sample. Because this cycle is proportional to the initial target gene cDNA concentration, it was used to compare the relative amount of target gene cDNA compared to a housekeeper gene.

The results are the mean of 2 technical replicates. For analysis, I used the delta-delta Ct method (Livak & Schmittgen, 2001). Expression values were normalised to the housekeeper primer pairs whose expression was not expected to be altered by the experimental conditions, either RPL32 or Actin (Supplementary Table 4). The relative difference was normalised to the mean relative difference of the control condition.

2.5.8. Protein quantification

Protein samples for proteomics and enzymatic assays were quantified using the BCA protein assay. 20 µL of the samples and bovine serum albumin standard solutions (2.5 mg/mL, serially diluted) were loaded in duplicate into the wells of a 96-well plate. 200 µL of a 50:1 mixture of reagents A and B of the BCA kit (Pierce 23225) was added to each well. The plate was left to incubate at 37°C for 30 min, and absorbance was measured at 562 nm in the plate reader (FLUOstar Omega, BMG LABTECH).

2.6. Enzymatic assays

2.6.1. Carbonic anhydrase activity

To measure the activity of carbonic anhydrases (CAs) in the fly, an esterase activity-based method was used. Given the limited sample volume for haemolymph samples, alternative methods for direct measure of carbon dioxide hydration are not technically feasible.

A commercial kit was first used to measure the CA activity in fly haemolymph (ab284550, abcam). Given the lack of inhibition by the inhibitor included in the kit (20

mM acetazolamide) and the absence of information regarding the other components, I set up the method from scratch.

For the assay, I used a 25 mM HEPES 66 mM Na_2SO_4 buffer (pH 7.6) which has been used to measure CA activity before (Tu et al., 1986). With this buffer, a 2 mM nitrophenol solution was made and used to plot a standard curve (Figure 2.16a).

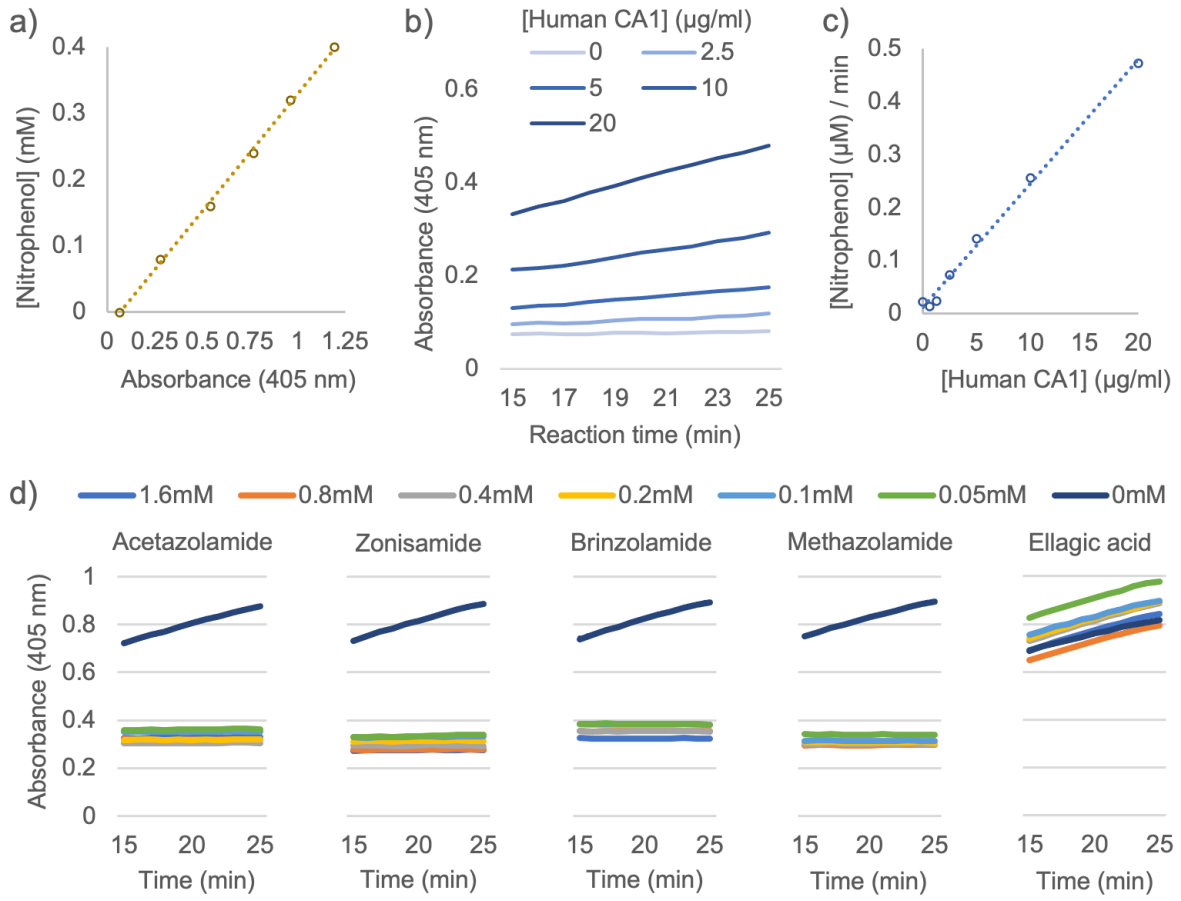


Figure 2.16. Optimization of carbonic anhydrase activity assay: a) nitrophenol standard curve, absorbance at 405 nm on the x axis, nitrophenol concentration on the y axis; b) nitrophenol production (absorbance at 405 nm) over time in the linear range dependent on the concentration of a positive control (human CA1); c) rate of nitrophenol production is linearly dependent on concentration of human CA1; d) the effect of different inhibitors on nitrophenol production over time in the linear range.

To set up an assay, the wells of a 96-well plate were filled with either 5 µL of sample, positive control (isolated CA) or buffer (for background control), with or without 2 µL of inhibitor, and made up to 95 µL. Solutions were mixed for 15 min at RT in a microplate shaker and then 5 µL of freshly made nitrophenyl acetate was added. The

substrate was dissolved in methanol and kept at -20ºC as a 32 mM stock which was diluted 1:4 right before the experiment in assay buffer. Absorbance at 405 nm was measured in kinetic mode typically for 60 min in the plate reader (FLUOstar Omega, BMG LABTECH). To analyse the results, 2 time points in the linear range of the plot were chosen and the difference of absorbance over time was calculated. Enzyme activity was calculated against the nitrophenol standard curve to give the rate of nitrophenol production per min.

I used left-over positive control (presumably isolated CA) from the commercial kit to test the effect of altering the pH of assay buffer or the addition of zinc chloride on nitrophenol production but neither increased it. Using isolated human CA1 from erythrocytes (CAS 9001-03-0, Merck) diluted in assay buffer (1 mg/mL), I tested the enzyme concentration dependence of nitrophenol production to validate the assay (Figure 2.16b). The rate of nitrophenol production was linearly correlated with the enzyme concentration (Figure 2.16c).

With this setting, the effectiveness of different CA inhibitors was measured at different concentrations (Figure 2.16d). I selected these inhibitors because they are predicted to inhibit the CA isoforms most similar to the fly CA isoforms 1 and 2 with different potency and specificity (searched in gene2function.org and drugbank.com). All selected sulfonamide derivatives (acetazolamide, zonisamide, brinzolamide and methazolamide) completely inhibited the reaction even at the lowest concentration. Ellagic acid, an expected CA inhibitor from a different drug class, did not significantly inhibit the reaction.

2.7. Mass-spectrometry-based methods

2.7.1. Haemolymph proteomics

To analyse the proteome of adult fly haemolymph, an *in-silico* digestion of the peptides from carbonic anhydrase isoforms and v-type ATPase subunits was made to decide on which enzyme to use for protein digestion. Digestion with trypsin was predicted to provide unique peptides for each of the protein isoforms (Appendix 1), and so trypsin was used for digestion during sample processing for liquid chromatography-mass spectrometry (LC-MS).

Haemolymph samples were processed by the LMS Mass Spectrometry Facility. In summary, after protein denaturation, sequential reduction and alkylation, and trypsin

digestion, samples were analysed by LC-MS using an Ultimate 3000 RSLC nano liquid chromatography system (Thermo Scientific) coupled to a Q-Exactive HFX mass spectrometer (Thermo Scientific) via an EASY spray source (Thermo Scientific). Acquired data was processed using the MaxQuant (Tyanova et al., 2016) software platform (v1.6.10.43). Peptide spectrum matches and protein identification were done by searching against the Uniprot (A. Bateman et al., 2023) *Drosophila* melanogaster reference protein database. Quality-control analysis was done by Alex Montoya from the facility. See Appendix 2 for further details on sample processing, LC-MS sample analysis and the upstream data analysis (database searching and protein quantification) written by Alex Montoya.

2.7.2. Haemolymph metabolomics

To perform metabolomics, metabolites were extracted from haemolymph samples. To do that, 200 µL of methanol were added to 2 µL of haemolymph, and the solution was sonicated in an ultrasonic bath for 10 min and 400 µL of chloroform was added. After vortexing each sample for 30 s, 150 µL of water were added, mixed again for 30 s and the samples were centrifuged for 15 min at 21,000 g. 200 µL of supernatant was then transferred to a vial with a glass insert and dried down using a vacuum concentrator (Savant SpeedVac, Thermo Scientific). Pooled quality controls were created by pooling equal aliquots of each sample to assess technical replicate reproducibility.

Extracted metabolite samples were then processed by Joao Mokochinski and analysed by gas chromatography-mass spectrometry (GC-MS) in the LMS Mass Spectrometry Facility. GC-MS analysis was performed with an Agilent 5977B gas chromatograph/mass selective detector and an Agilent 7693A automatic liquid sampler. Dried samples were suspended and incubated for 1h at 30ºC in a solution of O-methoxylamine hydrochloride in pyridine. N-methyl-N-trimethylsilyltrifluoracetamide was added, followed by a 30 min incubation at 37ºC with shaking. After derivatisation, samples were injected into the gas chromatograph inlet in the split mode with the inlet temperature held at 250ºC, 10:1 split ratio. The gas chromatograph had an initial temperature of 60ºC for 1 min, followed by a 10ºC/min rise to 325ºC and a hold of 2 min. A 30m Agilent Zorbax DB-5MS with a 10m Duraguard capillary column were used for chromatographic separation. Helium was the carrier gas at a rate of 1 mL/min. Data was collected using the MassHunter software (Agilent). Metabolites were identified

and their peak area was recorded using MassHunter Quant. Metabolite identity was established using the Fiehn library. Data was normalized to the sample mass. Statistical analysis was performed using MetaboAnalyst 5.0 (Pang et al., 2021).

2.8. Statistics and data analysis

Survival curves were analysed by Log-Rank test in Microsoft Excel using a custom macro. Other experiments were analysed by either unpaired t-test or one-way ANOVA with Tukey's correction for multiple comparison depending on whether two or more groups were compared, respectively. Data were plotted and analysed using GraphPad Prism 9 and Microsoft Excel software. Significance of probability values: non-significant (ns) if $p>0.05$; * if $p<0.05$; ** if $p<0.01$; *** if $p<0.001$.

Parametrical comparison of 2 groups was made by t-test. Parametric comparison of three or more groups was made by one-way ANOVA with multiple comparisons with Tukey post-hoc correction. Downstream proteomics and metabolomics analysis is described in the respective results chapters.

Chapter 3. Correlation of extracellular pH with survival

3.1. Introduction

The significance of acid-base balance in the context of ageing has been underexplored experimentally, despite suggestions that its imbalance may drive age-related diseases in humans (DiNicolantonio & O'Keefe, 2021; Frassetto et al., 2020; Frassetto & Sebastian, 2019a; Vormann & Goedecke, 2002). Besides subclinical changes in humans (Frassetto & Sebastian, 1996), descriptive studies have shown systemic acidification with age in rats and flies (Massie et al., 1981).

The reported pH changes with age in flies were measured in groups of whole flies homogenised and diluted in 10 mL of water (Massie et al., 1981). The dilution of 50 flies in such a comparably large volume of water does not allow accurate pH measurements. What is measured is how much the homogenised fly components alter the pH of water by changing its SID and weak electrolyte content. Aside from the confounding role of intracellular pH, the total weight, protein and ionic content of flies may change with age, altering the pH of water more or less when diluted.

In this study, I focus specifically on measuring extracellular pH as a readout for systemic acid-base balance. The first step to test the hypothesis that extracellular fluid acid-base imbalance is a hallmark of ageing in flies was to assess if the concentration of H^+ varies with age. In this chapter, I also explore how haemolymph pH changes throughout lifespan in response to established interventions known to modulate fly mortality rate.

3.2. Extracellular fluid pH during *Drosophila* ageing

3.2.1. Age-dependent acidification is independent of sex or strain

Having established a method to measure haemolymph pH using the pyranine dye (see Section 2.4.1.1), I followed the lifespan of wild-type *white Dahomey* (w^{Dah}) flies raised at 25°C on standard sugar-yeast-agar (SYA) medium and collected their haemolymph at different timepoints. For most experiments, samples were extracted at 7, 28 and 56 days which represent young, middle-aged and old flies, respectively. Samples from flies of intermediate ages (14, 42 days) were collected for key experiments to account for age-specific variability and to have a more complete view on age-related changes.

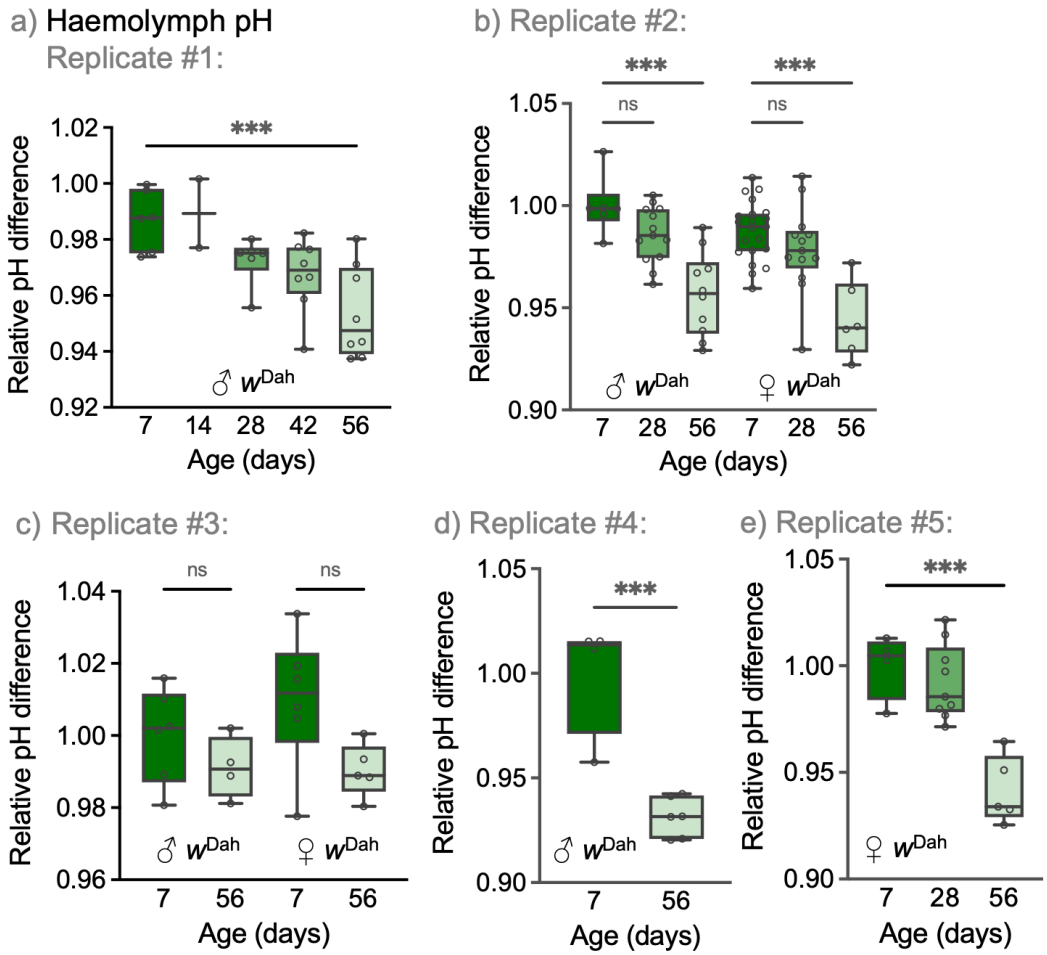


Figure 3.1. Age-related haemolymph acidification in w^{Dah} flies. Haemolymph was extracted from cohorts of 12 flies (females) or 15 flies (males), and the pH measured spectrophotometrically using the pyranine dye at different ages. Data are shown for 5 independent biological experiments (with n=2-22 replicates per condition). Statistical significance was determined by ANOVA with Tukey correction for multiple comparisons (a,b,c,e) or unpaired t-test (d). n/s, $p>0.05$; ***, $p<0.001$.

As hypothesised, fly haemolymph becomes significantly more acidic with age (Figure 3.1a). This age-related acidification is sex-independent (Figures 3.1a-e). Although ageing has sex-specific manifestations (Austad & Fischer, 2016), the fundamental processes that drive those changes are likely to be sex-independent given the ubiquitous nature of ageing. The age-dependent pH change varies between experiments, but typically old flies (day 56) have a relative 5% lower pH compared to day 7 (Figures 3.2a-e).

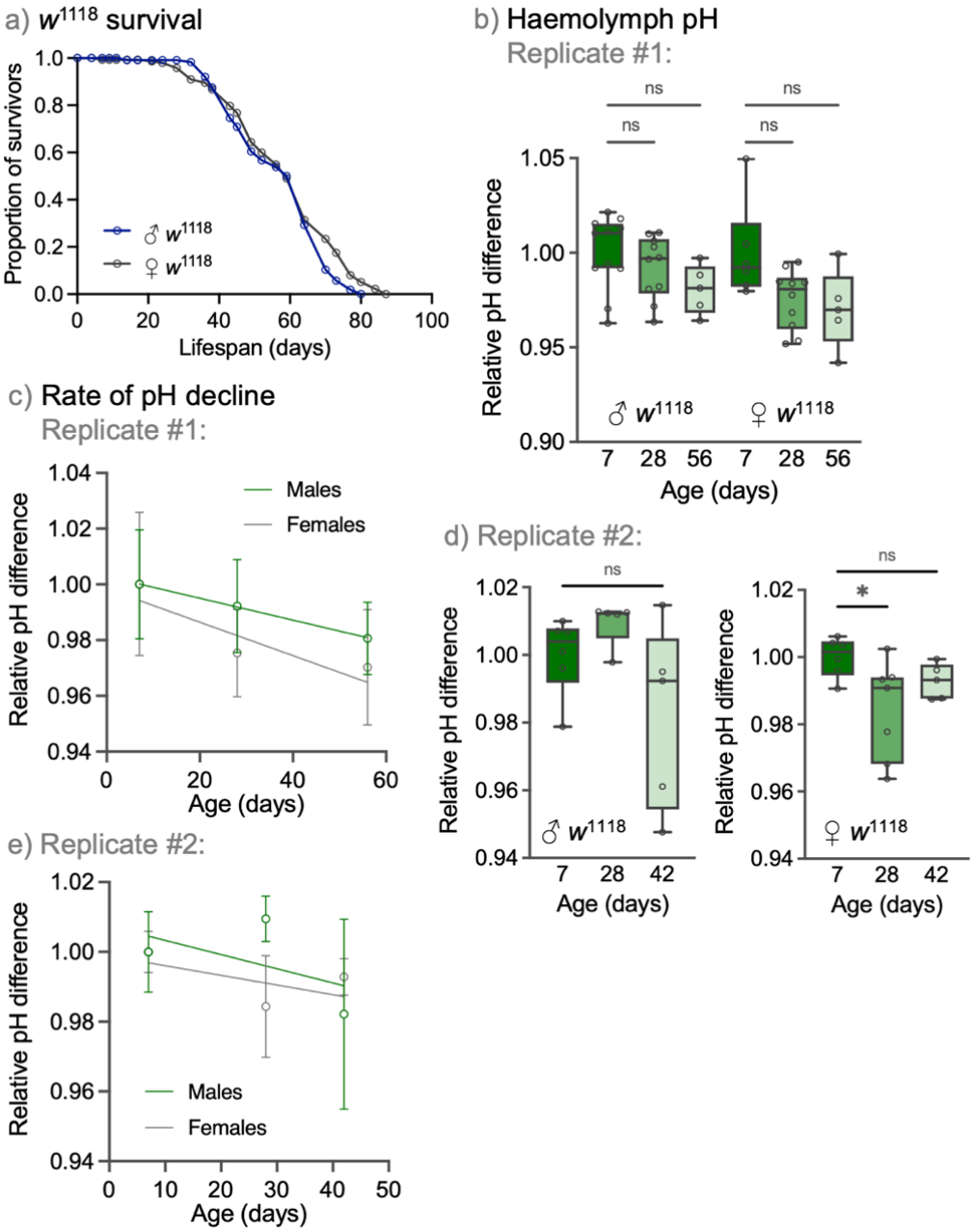


Figure 3.2. Age-related haemolymph acidification in *w*^{1118} flies: a) Typical lifespan curves of *w*^{1118} flies, n=150 for females and n=140 for males; b-e) Haemolymph pH in *w*^{1118} flies measured with age by the pyranine method. Data are shown for 2 independent biological experiments (n=5-11 replicates per condition). Statistical significance was determined by ANOVA with Tukey correction for multiple comparisons (b,d) or simple linear regression (c,e). n/s, p>0.05; *, p<0.05.

Next, to confirm the validity of my findings, I tested if the same acidification was seen in different fly strains. A similar trend of age-related acidification was observed in the isogenic strain *w*^{1118}, which is frequently used as a control line in *Drosophila*

experiments (Figures 3.2b-e). Although the difference was not statistically significant, this is likely explained due to high biological variability, and a low n number. However, when plotted as the relative difference of pH over time, the slope of the trend of pH decline is significantly non-zero, i.e., the slope is a value other than the value specified by the null hypothesis (0) (Figure 3.2c).

Both the w^{Dah} and w^{1118} strains have a mutation in the *white* gene. This gene encodes a transporter protein that transports pigment precursors into the eye (causing a white-eyed phenotype in its absence), as well as other ageing-relevant metabolites, including tetrahydrofolate whose regulation by *white* is involved in ageing-induced intestinal stem cell proliferation (Mackenzie et al., 1999; Sasaki et al., 2021). To ensure haemolymph acidification was not a consequence of the *white* mutation and therefore w^{Dah}- or w^{1118}-background specific, I confirmed that acidification occurs in both males and females of the wild-type (red-eyed) strain, *Oregon-R*, at the same timepoints of their lifespan (Figure 3.3). Observed sex differences in lifespan (Figure 3.3a) are commonly seen and expected, but are variable and strain specific (Hoffman et al., 2021). Indeed, they are not observed in our w^{1118} flies (Figure 3.2a). This variation likely reflects differences in adaptation to specific lab conditions, such as food.

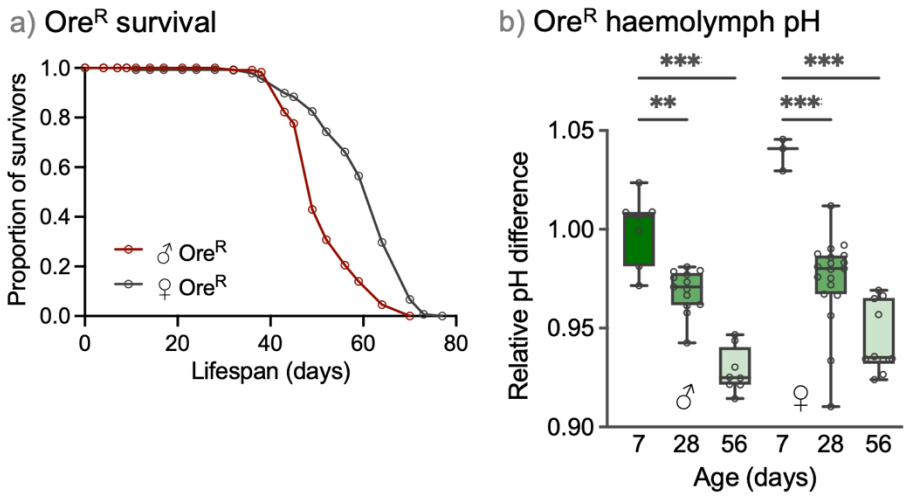


Figure 3.3. Age-related haemolymph acidification in *Ore^R* flies. a) Typical lifespan curves of *Ore^R* flies, n=150 for females and n=140 for males; b) Haemolymph pH in *Ore^R* flies measured with age by the pyranine method (n=3-19 replicates per condition). Statistical significance was determined by ANOVA with Tukey correction for multiple comparisons. **, p<0.01; ***, p<0.001.

3.2.2. Age effect of acidification occurs in different diets

To test if the age-related acidification is a consequence of a specific factor in our control yeast-based diet, the haemolymph pH of w^{Dah} flies raised on a chemically defined medium was measured (Piper et al., 2014). Flies have similar lifespans on both diets (Figures 3.4a-b) and when raised on a defined medium, they lay even more eggs, which is an indication that they are healthy under those conditions (Figure 3.4c). Haemolymph was collected at the same timepoints as above and acidification was observed (Figure 3.4).

Although dietary components may interact with ageing to accelerate or decelerate this process (*see Chapter* 7), loss of acid-base balance with age occurs in all the dietary variations I tested.

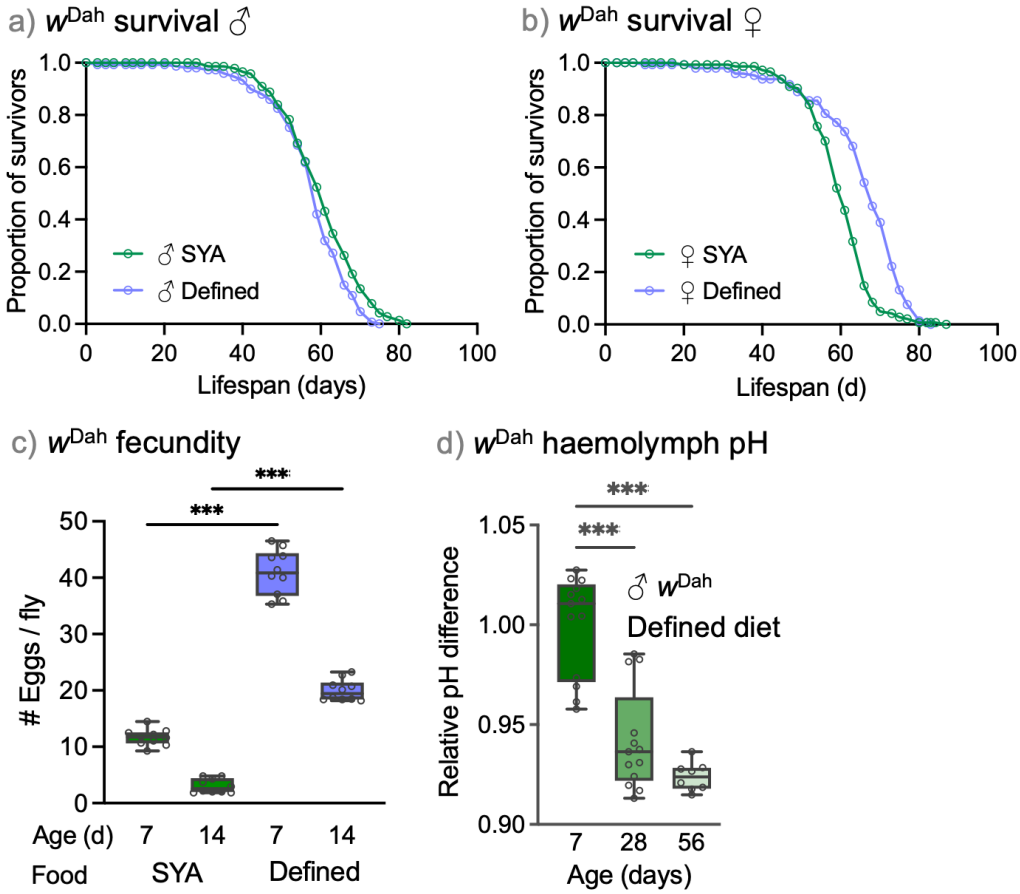


Figure 3.4. Age-related haemolymph acidification is diet-independent. Typical lifespan curves of a) male and b) female w^{Dah} flies raised on a defined diet, n=150 for females and n=140 for males; c) Egg laying over 24 h of flies raised on SYA and defined media, at 7 and 14 days (n=10 groups of 15 female w^{Dah} flies); d) Haemolymph pH in w^{Dah} flies with age measured by the pyranine method (n=8-13 replicates per condition). Statistical significance was determined by ANOVA with Tukey correction for multiple comparisons. ***, p<0.001.

3.3. Correlation of age-related pH changes with mortality rate

Mortality rate is more ageing-specific than survival (Ebeling et al., 2021; Gems et al., 2002). To check whether extracellular acidification is a process that inherently occurs with ageing, I set up flies under conditions that are known to alter their survival and mortality rate, and correlated these changes to the rate of haemolymph acidification.

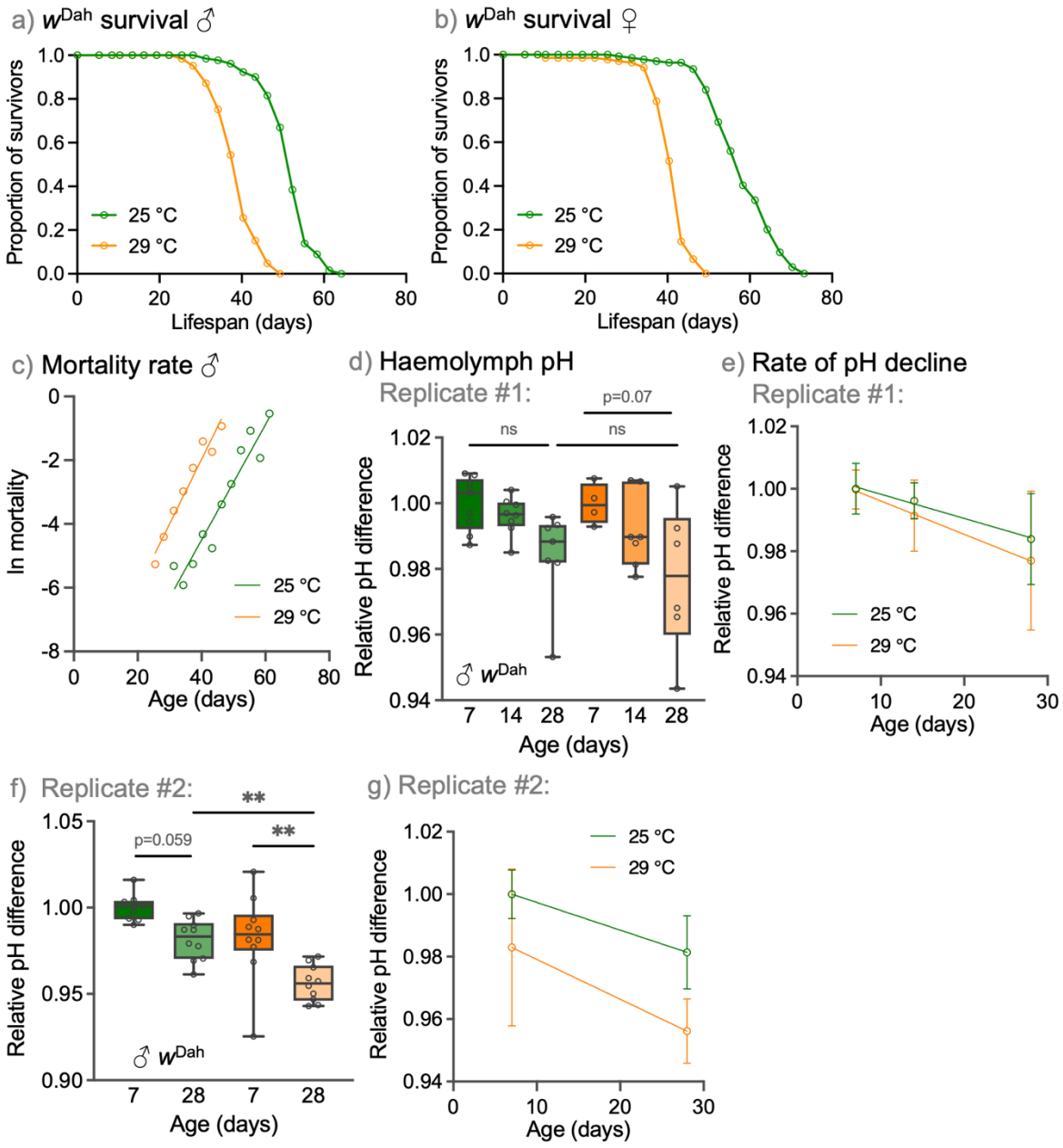


Figure 3.5. Effect of higher temperature on survival and pH. Typical lifespan curves of a) male and b) female *w*^{Dah} flies raised in 25 and 29°C, n=150 for females and n=140 for males; c) Mortality rate of male *w*^{Dah} flies raised in 25 and 29°C, n=140; d-g) Haemolymph pH in male *w*^{Dah} flies measured with age by the pyranine method. Data are shown for 2 independent

biological experiments (n=4-10 replicates per condition). Statistical significance was determined by ANOVA with Tukey correction for multiple comparisons (d,f) or simple linear regression (e,g). n/s, $p>0.05$; **, $p<0.01$.

3.3.1. Effect of environmental temperature on pH and survival

Flies are ectotherms, i.e., they are unable to regulate their body temperature by internal mechanisms, so their body temperature is determined by their environment. Altering the environmental temperature in which adult flies are kept in determines their mortality rate (Mair et al., 2003; Miquel et al., 1976). Control flies are usually kept at 25°C. When raised at a higher environmental temperature of 29°C, their lifespan is significantly shorter (Figures 3.5a-b), and conversely, when raised at a lower temperature of 18°C, they live significantly longer, independently of their sex (Figures 3.6a-b).

Since pH is directly influenced by temperature (Reijenga et al., 2013) and, like lifespan, inversely correlated with it, I tested whether a direct effect of temperature on haemolymph pH could explain the changes in survival. If the temperature effect was indeed direct, pH would be expected to stay lower at higher temperatures and higher at lower temperatures throughout the fly lifespan.

Haemolymph was collected from age-matched male flies at those three temperatures. Despite trending to be lower at 29°C compared to 25°C in control flies, haemolymph pH further decreases with age (Figures 3.5d,f) in the higher temperature. The rate of decline tends to be faster too (Figures 3.5e,g), at 29°C. This correlates with shortened survival, although the mortality rate of male flies unexpectedly did not significantly change with temperature (Figure 3.5c).

To test if a lower temperature had the opposite effect, haemolymph was collected from flies raised at 18°C at the same timepoints as flies raised at 25°C. Indeed, lower temperature tends to slow down the rate of haemolymph acidification at timepoints with lower mortality rate (Figures 3.6e,g). However, haemolymph pH eventually declines as the mortality rate increases at later ages to levels comparable to old flies raised at 25°C (Figure 3.6d,f,h). This suggests that the temperature effect on haemolymph pH is indirect, i.e., (patho)physiological. The effect may be related to decreased metabolic production of acid, compatible with the slowdown of fly metabolism at lower temperatures (Carvalho et al., 2017; Mołoń et al., 2020), or

prevention against other effects of ageing on tubule function, preserving the ability to excrete acid for longer.

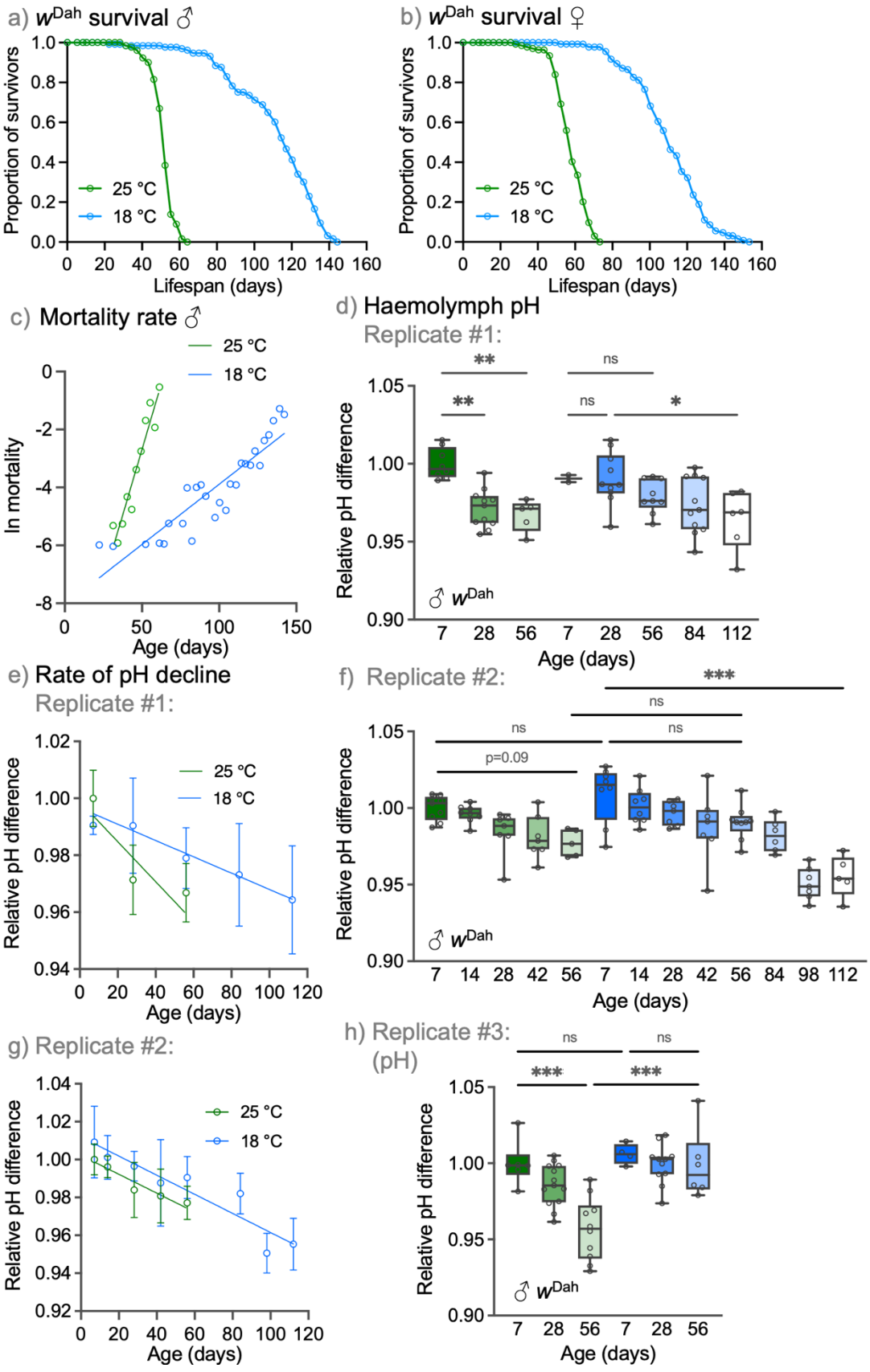


Figure 3.6. Effect of lower temperature on survival and pH. Typical lifespan curves of a) male and b) female w^{Dah} flies raised in 25 and 18°C, n=150 for females and n=140 for males; c) Mortality rate of male w^{Dah} flies raised in 25 and 18°C, n=140; d-h) Haemolymph pH in male w^{Dah} flies measured with age by the pyranine method. Data are shown for 3 independent biological experiments (n=2-13 replicates per condition). Statistical significance was determined by ANOVA with Tukey correction for multiple comparisons (d,f,h) or simple linear regression (e,g). n/s, $p>0.05$; *, $p<0.05$; **, $p<0.01$; ***, $p<0.001$.

3.3.2. Age-dependent acidification in long-lived genetic model

To further explore the correlation between mortality rate and haemolymph acidification beyond the effects of temperature, the mortality rate of flies was altered genetically. Altering the expression of specific genes has shown to be sufficient to extend fly lifespan (Piper & Partridge, 2018). Here, the long-lived *Δdilp2-3,5* mutant was used to check if its lower mortality rate also correlated with a lower rate of haemolymph acidification.

Drosophila has 7 insulin-like peptides (dILPs) that are the ligands for the sole fly insulin receptor and activate the *Drosophila* insulin/IGF signalling (IIS) pathway (Grönke et al., 2010). The dILPs 2, 3 and 5 are expressed in the fly brain median neurosecretory cells. Both ablating these cells or deleting these genes extends the lifespan of female flies (Grönke et al., 2010). This is consistent with the observation that reduced activity of the IIS pathway can extend the lifespan of multiple organisms, from yeast to mammals (Grönke et al., 2010).

After confirming that these mutants are long-lived and have a slower mortality rate compared to background-matched control flies (Figures 3.7a-c), I collected haemolymph at different timepoints throughout their lifespans and measured its pH. Although acidification still occurs with ageing in these mutants (Figure 3.7d), the rate of pH decline is slower (Figure 3.7e). This result suggests again a correlation between mortality rate and rate of pH decline.

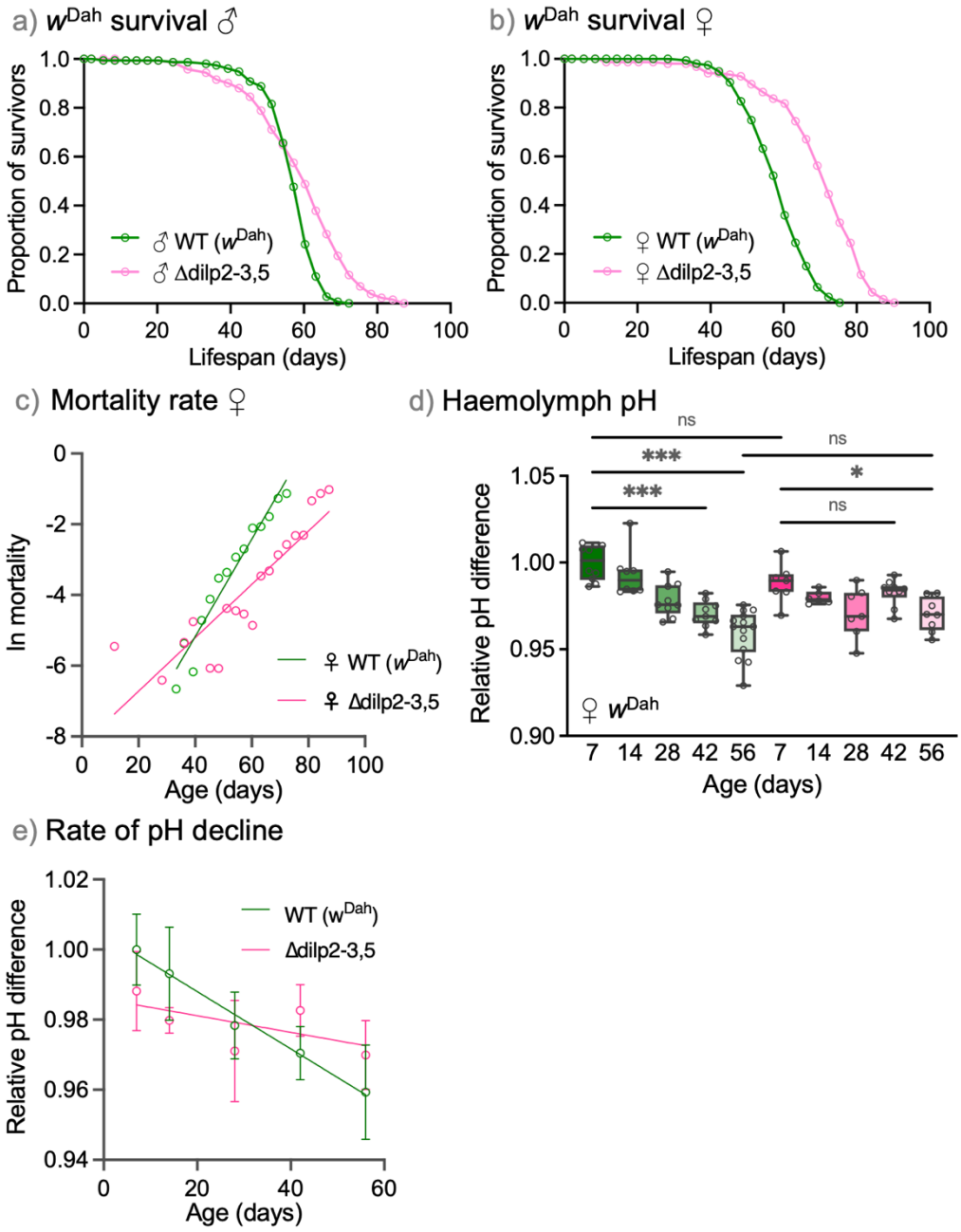


Figure 3.7. Long-lived mutant shows slower rates of haemolymph pH decline. Typical lifespan curves of a) male and b) female *Δdilp2-3*,5 (with w^{Dah} genetic background) and *w^{Dah}* flies, n=150 for females and n=140 for males; c) Mortality rate of female *Δdilp2-3*,5 and *w^{Dah}* flies, n=140; d-e) Haemolymph pH in female *Δdilp2-3*,5 and *w^{Dah}* flies measured with age by the pyranine method (n=2-13 replicates per condition). Statistical significance was determined by ANOVA with Tukey correction for multiple comparisons (d) or simple linear regression (e). n/s, p>0.05; *, p<0.05; ***, p<0.001.

3.4. Key messages and interpretation

In this chapter, the hypothesis that systemic loss of acid-base balance occurs with age in flies was tested. Three main messages can be taken from the results:

- Fly haemolymph [H^+] increases with age, independently of sex, strain or diet
- The temperature effect on haemolymph pH is indirect, i.e., physiological
- The rate of acidification correlates with mortality rate

To further strengthen these conclusions, it would be interesting to measure the acid-base status of flies under other unrelated conditions that alter their survival. These could include other genetic, dietary and pharmacological interventions. *Drosophila* has been used as a tool to validate drug targets for healthy lifespan. According to the DrugAge database, more than 150 compounds have been shown to extend fly lifespan (Barardo et al., 2017). The most significant effect observed to date has been from the triple combination of the clinically-approved drugs rapamycin (also known as sirolimus), lithium and trametinib, which extends fly survival by ~50% (Castillo-Quan et al., 2019). Assessing the acid-base balance of flies treated with drugs with distinct mechanisms of action over their lifespan would be a first step towards using the rate of acidification as a predictor for the success of potential life-extending interventions.

The next step to test whether mortality rate and biological age can be predicted at an individual level by measuring changes in haemolymph pH would be to perform longitudinal studies. These are not technically possible in this model organism since haemolymph collection is only feasible upon killing the flies. Having an internal pH-tracker and imaging flies could circumvent that issue, but would also require external interventions, such as a considerable period of CO_2 anaesthesia, which could artefactually affect pH and negatively impact their survival. Therefore, it would be interesting to explore pH homeostasis in other models where its tracking could be possible at an individual level in live animals throughout their lifespan with minimal intervention. One example would be the worm *C. elegans*, by whole body imaging. There are genetically encoded reporter worms with the pH-sensitive GFP pHluorin attached to an integrin facing towards the extracellular space, the worm pseudocoelom (Pfeiffer et al., 2008). Besides, isolation of extracellular fluid from worms is technically possible (Banse & Hunter, 2012) and can be used to validate imaging results. If the extracellular fluid of worms also became more acidic with age, we could then follow a

genetically heterogeneous population, split and categorise worms mid-life into groups of different extracellular pH, and check whether the groups with higher pH mid-life would live longer.

The observations that loss of pH homeostasis occurs independently of sex, strain and diet, and that both temperature and genetic interventions alter mortality rate and acid-base through seemingly unrelated mechanisms suggests that haemolymph acidification may be either: 1) a common consequence of ageing, independently of what the cause of acidification may be; or 2) a cause of ageing whose consequences are ameliorated by different interventions. Whether it is a convergent or divergent mechanism, respectively, acid-base imbalance may therefore be itself a target for intervention. In the following chapters I will explore how intervening directly on haemolymph pH can impact survival and explore potential causes.

Chapter 4. Pharmacological modulation of acid-base balance in *Drosophila*

4.1. Introduction

Given the loss of extracellular acid-base balance with age, I aimed to modulate the pH of fly haemolymph pharmacologically. These drugs could serve as tools to understand what makes a fly resistant to acidotic stress and to directly test the impact of altering haemolymph pH on fly survival.

4.2. Modelling chronic metabolic acidosis in *Drosophila*

As shown in the previous chapter, the fly haemolymph acidifies with ageing and this correlates with survival. To test if extracellular acidification can limit fly lifespan, I set out to model chronic metabolic acidosis in flies by further acidifying their haemolymph pharmacologically. Metabolic acidosis can be caused by either increasing acid production or decreasing acid excretion. To induce those effects in flies, either ethylene glycol or acetazolamide were added to their food, respectively.

Inducing metabolic, rather than respiratory, acidosis is more likely to emulate the underlying causes of haemolymph acidification in flies, and to model the chronic, mild blood acidification seen in humans (Frassetto et al., 1996). The meta-analysis that shows acid-base imbalance with age in human blood also suggests this acidification is metabolic in origin rather than respiratory, as both bicarbonate and partial pressure of CO_2 decrease with age (Frassetto et al., 1996).

In flies, age-related acidification is also likely to be metabolic rather than respiratory in origin. As insects, flies have an open respiratory system with a network of vessels (trachea) where gases are exchanged directly with tissues independently of the circulation of extracellular fluid. As CO_2 can freely cross cellular membranes to equal its partial pressure on both sides, it is unlikely to accumulate systemically and cause acidosis in the CO_2-controlled environment the flies are raised in.

The tracheal system could deteriorate with ageing compromising gas exchange. In larvae and young flies, tracheal branching exhibits plasticity, particularly in response to oxygen in the environment and nutritional status (Henry & Harrison, 2004; Linneweber et al., 2014), which may be lost with age. Besides, despite being an open network, the entry of air is regulated by spiracles, valve-like structures important

for minimising water loss (Lehmann, 2001). Loss of spiracle function may occur with age, but there is currently no experimental evidence for this in the literature.

If gas exchange becomes compromised with age, metabolic rate would be expected to change when assessed by respirometry. Reports on fly metabolic rate with age based on CO_2 production in males are conflicting, one study showing a low rate from early adulthood (Khazaeli et al., 2005) and another reporting no difference with age (Promislow & Haselkorn, 2002). As presented later (Figure 7.1), metabolic rate, assessed by both CO_2 production and O_2 consumption, was unaltered with age in w^{Dah} males. Conversely, although metabolic rate may decline in female w^{Dah} flies, the sex difference can be attributed to the lower metabolic demand for egg laying as it decreases with age, rather than tracheal dysfunction. Here, the working hypothesis is that the acidification is metabolic in origin.

4.2.1. Ethylene glycol-induced acidosis shortens fly survival

To model metabolic acidosis caused by increased acid production, varying percentages (v/v) of ethylene glycol (EG) were added to control medium.

EG causes acute metabolic acidosis in humans (Kraut & Madias, 2010; Liamis et al., 2010). It is metabolised into glycolaldehyde by alcohol dehydrogenase before being converted by aldehyde dehydrogenases into glycolic acid, the main acid causing the acidosis (Green et al., 2005). Being a precursor, EG does not alter food pH, which means that its potential effect on the fly acid-base status depend on its metabolism.

Young flies were fed EG from d2 of adulthood at a range of concentrations (0.05-5% v/v), and haemolymph was collected after 7 days. I found that haemolymph pH decreased upon EG treatment in a concentration-dependent manner (Figure 4.1a-c). The highest dose (5%) killed the flies before the haemolymph collection timepoint, but 2.5% caused a drop in haemolymph pH of ~5% after 7 days, comparable to the drop in haemolymph pH in old flies compared to young.

This effect of EG was seen in different diets. In addition to SYA, I also tested a EG treatment using a chemically defined medium. Lower doses of EG are sufficient to cause haemolymph acidification using a defined medium, as expected since the defined medium results in higher bioavailability of compounds (Piper et al., 2014). In accordance with the hypothesis that acidosis affects survival, the lifespan of flies fed the same range of EG concentrations is shortened in a concentration-dependent

manner (Figure 4.1d-e). This effect is strain-independent (Figure 4.1d-e) and is even more pronounced in females (Figure 4.3b), which is likely due to the established higher food consumption by female flies (Wong et al., 2009).

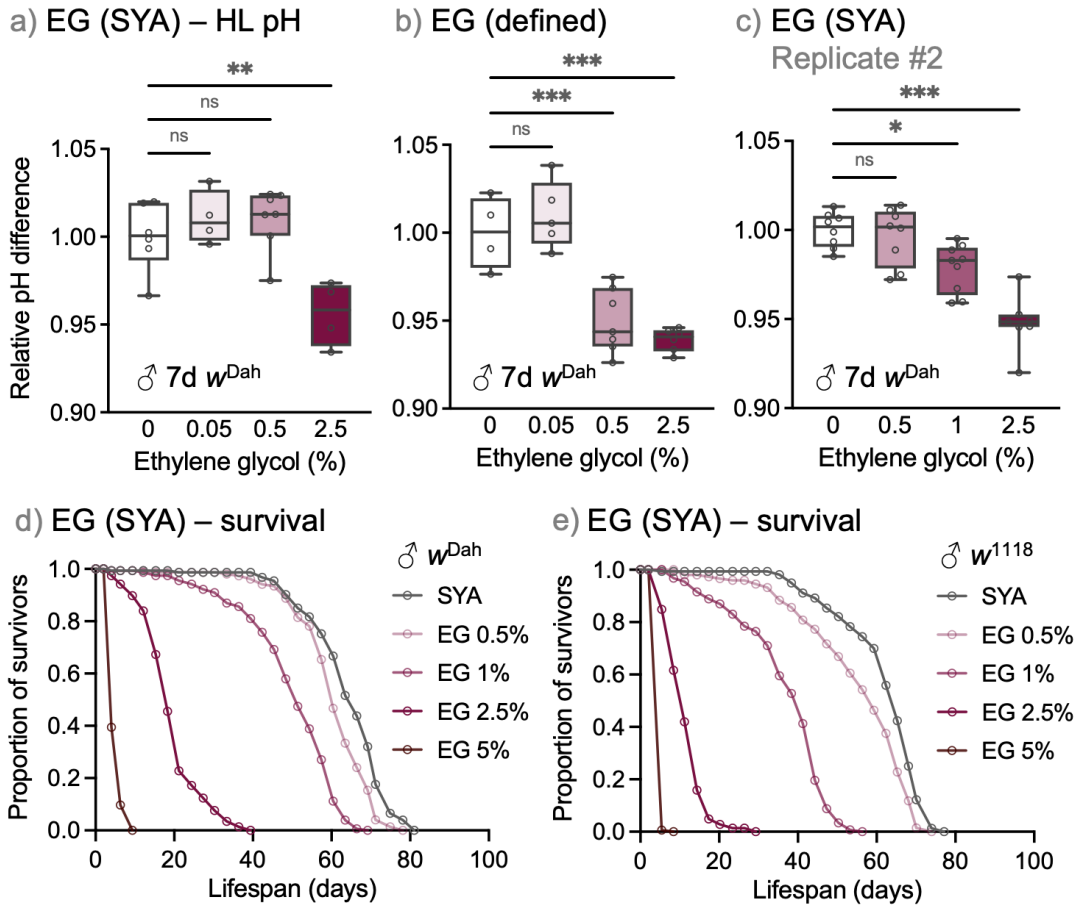


Figure 4.1. Ethylene glycol causes acidosis and shortens survival in flies. Haemolymph pH was measured using the pyranine method in w^{Dah} male flies after 7 days of dietary treatment with a range of EG doses. Experiments were performed on SYA (a,c) or chemically defined medium (b). Data are box-plots of n=4-9 replicates per condition. Statistical analysis was based on ANOVA with Tukey correction for multiple comparisons. ns, p>0.05; *, p<0.05; **, p<0.01; ***, p<0.001. Survival curves of w^{Dah} (d) and w^{1118} (e) male flies treated with EG from d2 of adulthood, n=140 flies per condition.

4.2.2. EG-induced acidosis is independent of tubule function

Glycolic acid can be metabolised into oxalic acid. Because of its low pK_a, oxalic acid almost fully dissociates at physiological pH into oxalate and H^+. Oxalate is filtered by the kidney where it can bind to calcium and crystalise to cause lithiasis. Indeed, patients often have oxalate crystals in their urine after EG poisoning (Liamis et al.,

2010). EG is commonly used to model calcium oxalate nephrolithiasis in mammals (Green et al., 2005). As the kidneys are the major regulators of systemic acid-base balance, acute tubular damage caused by calcium oxalate crystals might contribute to the metabolic acidosis associated with EG.

In flies, EG has also been used as a model of tubule lithiasis (Chen et al., 2011). EG is reported to cause deposits of calcium oxalate crystals in the Malpighian tubules, the fly equivalent of renal tubules. This effect is dose-dependent (up to 1% EG) and independent of sex (Chen et al., 2011). The same study shows a dose-dependent shortening of fly survival which can be partially rescued by the addition of potassium citrate to the medium, attributed to the prevention of crystal formation. However, potassium citrate increases base load, and its effect on survival can be due to its influence on acid-base balance. Indeed, 1% (w/v) of potassium citrate rescued survival but did not prevent crystals from forming (Chen et al., 2011).

Besides acid production, tubule dysfunction caused by lithiasis could therefore be a contributing factor to the acidosis induced by feeding flies 2.5% EG. Surprisingly, however, I did not see any crystal formation in male tubules after 7 or 14 days of 2.5% EG feeding, when they already have significantly lower haemolymph pH (score of 0 in n=20 dissected w^{Dah} male flies of each age). This discrepancy may be related to: 1) strain-specific susceptibilities to calcium oxalate crystal formation or rates of metabolic conversion of glycolic acid into oxalic acid; 2) the timing of crystal formation, as the cited report quantified crystals at 3 weeks of age; 3) diet-related factors, although comparisons are limited because the concentration of medium components is not reported in the publication (Chen et al., 2011); or 4) the dose of EG. Likely, the difference lies in a combination of these factors. The report tests a range of doses up to 1%. Lower doses may not be sufficient to cause acidosis depending on the fly medium. This would allow time for glycolic acid to be metabolised and for calcium oxalate crystals to form, contrary to a higher dose (here, 2.5%) which may kill the flies from acidosis before crystals can be formed. Supporting this hypothesis, a different group showed that providing a low dose (0.75%) of EG in drinking water to rats caused hyperoxaluria but not metabolic acidosis in rats (Green et al., 2005).

As discussed in Chapter 7, flies raised on SYA form crystals in their tubules with ageing but these may be composed of uric acid from excretion of excess nitrogen, contrary to the reported EG-induced crystals. EG-induced acidification could promote the deposition of uric acid crystals in fly tubules under protein-rich diets, such as SYA.

However, besides the absence of crystals in the tubules at the timepoints tested, addition of 1 mM allopurinol, a xanthine oxidase inhibitor that lowers uric acid levels, to the medium did not rescue the fly survival under acidotic stress (Figure 4.2a).

To further exclude that excretory dysfunction was the cause of acidosis independently of crystal deposition, I analysed the number and pH of fly deposits by adding a pH-sensitive dye to the medium. Flies fed 2.5% EG have a higher number of deposits (Figure 4.2b) with a lower pH (Figure 4.2c-d). This suggests that the excretory tract is still efficiently excreting acid, but the rate of acid excretion is overwhelmed by the rate of metabolic conversion of EG into acid, causing acidosis.

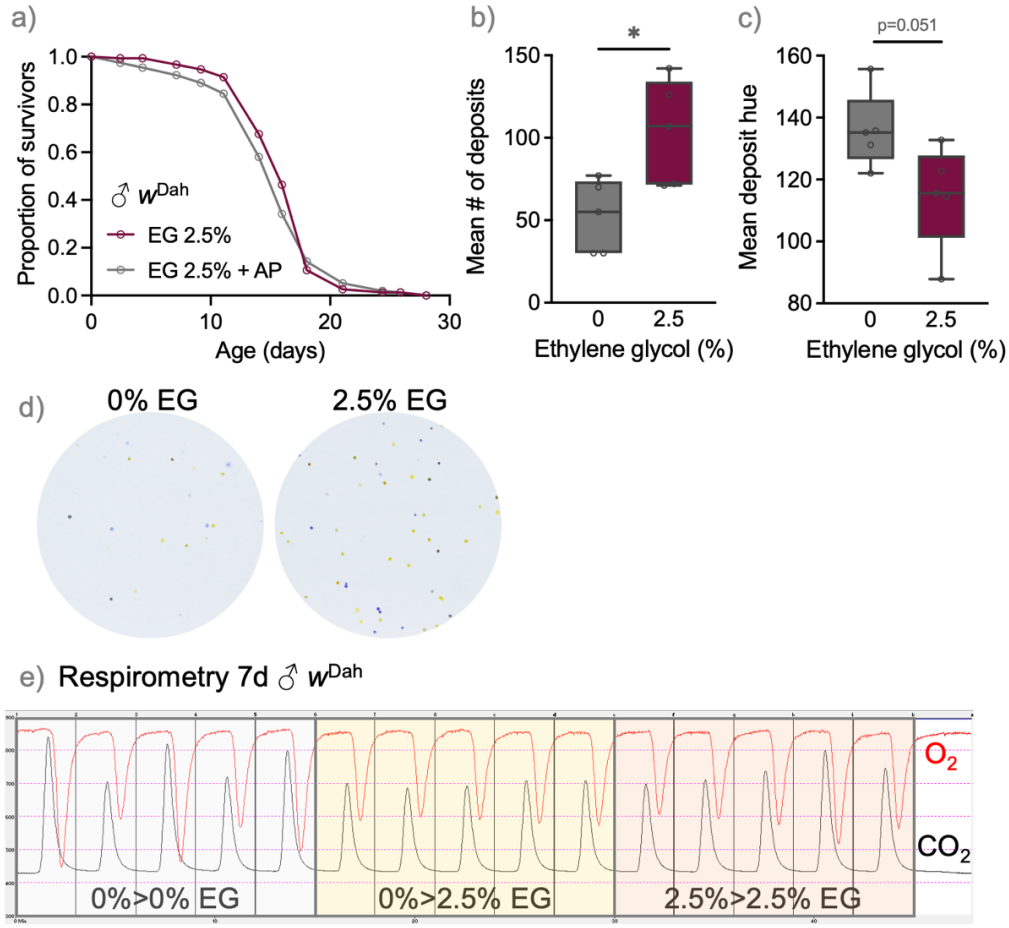


Figure 4.2. Ethylene glycol does not impair acid excretion in flies. Survival curves (a) of w^{Dah} male flies treated with EG ± 1 mM allopurinol from d2 of adulthood, n=140 flies per condition. Poo plates analysis of mean deposit number (b) or hue (c) of w^{Dah} flies after 7 days of 2.5% EG treatment, n=5 plates with 5 flies each, and representative plate lid scans (d). Statistical analysis was based on unpaired t-test; *, $p<0.05$. Representative graph of O_2/CO_2 respirometry (e) of w^{Dah} male flies after 7 days of 2.5% EG treatment (red box), acute exposure (yellow box) or 7 days in control medium (white box); each box contains five columns that correspond to 5 replicates (n=5 flies each) of measured O_2/CO_2 peaks after a 48 min cycle.

As a way of further excreting excess metabolic acid acutely, flies could intracellularly convert it into CO_2 and release it via the tracheal system as a form of respiratory compensation despite the absence of lungs. To explore this idea, flies were assessed by respirometry after 7 days of EG exposure or acute exposure to EG after 7 days of control feeding, compared to flies fed a control diet throughout. EG-treated flies appear to have lower metabolic rates both after 7 days and after acute transfer to EG-containing food (Figure 4.2e). It was previously reported that exposing myocytes to low pH decreases basal and maximal mitochondrial respiratory capacity (Genders et al., 2019). This might be a side-effect of acidosis or a compensatory mechanism to decrease the production of other metabolic acids. Interestingly, EG-treated flies for 7 days seem to be able to excrete excess CO_2 since the respiratory quotient (RQ, ratio of CO_2 produced to O_2 consumed) appears to be higher than 1, compared to flies under a control diet whose RQ is ~1 as expected.

To model haemolymph acidification in subsequent assays and to use EG as a screening tool to test fly sensitivity to acidosis, I chose to use the 2.5% concentration in SYA as it causes acidification to levels compared with the effect of ageing by increased acid production (not tubule dysfunction) and decreases survival enough to interpret it as an acidotic stress assay.

4.2.3. Acidosis resistance decreases with age

Despite partially responding to 2.5% EG-induced acidosis by increasing acid excretion, flies treated from 2-days of adulthood have a shorter lifespan. As haemolymph acidifies with age in flies under control conditions (see Chapter 1), their ability to respond to an acidotic stress may be compromised with age.

To test this hypothesis, flies of different ages (2, 7, 14, 28 and 42 days old) were fed medium supplemented with 2.5% EG and their survival was measured. Indeed, the older the flies are, the more sensitive they become to acidotic stress, and this effect is sex-independent (Figure 4.3a-b). This occurs despite the observation that flies eat less as they age (Wong et al., 2009), suggesting even lower intake of EG is sufficient to cause acidosis-related mortality at older ages.

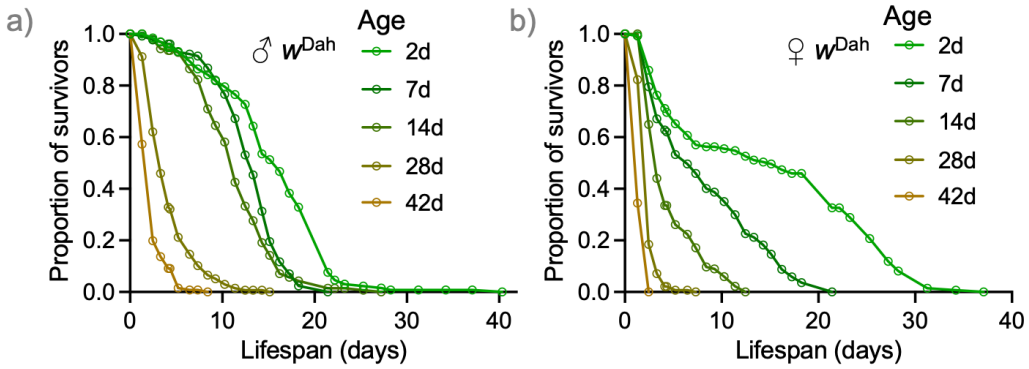


Figure 4.3. Resistance to acidotic stress declines with age. Survival curves of w^{Dah} male (a) and female (b) flies fed 2.5% EG starting at different ages, n=140 flies per condition.

4.2.4. Acetazolamide does not effectively induce acidosis in flies

To induce acidosis by blocking effective acid excretion independently of production, fly food was supplemented with varying concentrations of acetazolamide (Acz). Acz is a sulfonamide, which inhibits carbonic anhydrases and is another known cause of metabolic acidosis in humans (Liamis et al., 2010). As discussed in more detail in the following chapters, Acz causes acidosis in humans by inhibiting the carbonic anhydrases in the kidney that are necessary for effective reabsorption of HCO_3^- (Kraut & Madias, 2010) and excretion of chloride (decreasing serum [SID]).

Like humans, flies express carbonic anhydrases in their tubules (see Chapter 6) where they presumably contribute to tubular acid-base regulation. Physiologically, the mechanism will necessarily be different to humans given the fly excretory tract does not filter haemolymph, as discussed later. It may instead be related to active acid excretion similarly to their necessary role in excreting acid in the acidic region of the fly midgut (Overend et al., 2016).

Acz was reported to inhibit carbonic anhydrase activity and to extend fly lifespan (Massie et al., 1981). Carbonic anhydrase activity in whole male fly homogenates is also reported to decrease with age, although the trend is variable and seems to be stable in old (44 days) age (Massie et al., 1981). In the same study, Acz is reported to decrease the activity of carbonic anhydrases in 7-day-old flies, yet it only partially inhibited the activity of the enzymes in middle and old age in a non-dose-dependent manner (Massie et al., 1981). Importantly, the effect of inhibiting the enzyme on acid-base homeostasis was not tested in this study.

Here, the same concentrations of Acz (100 and 500 μM) were fed to flies in control (SYA) medium. This had no effect on haemolymph pH or survival (Figure 4.4a-

b). The difference compared to what was previously published might be strain- or diet-dependent. I then used the defined medium which increases drug bioavailability and still saw no effect at the concentrations used in the report (Figure 4.4a). Only much higher concentrations of Acz on a defined medium were able to acidify the fly haemolymph (Figure 4.4a).

The effect of Acz on the activity of fly carbonic anhydrase isoforms is discussed further in the next chapter. Due to the high doses needed to be delivered in a defined medium to cause haemolymph acidification, using this drug would be an inefficient way to model acute acidosis as a screening tool, and was abandoned for that purpose.

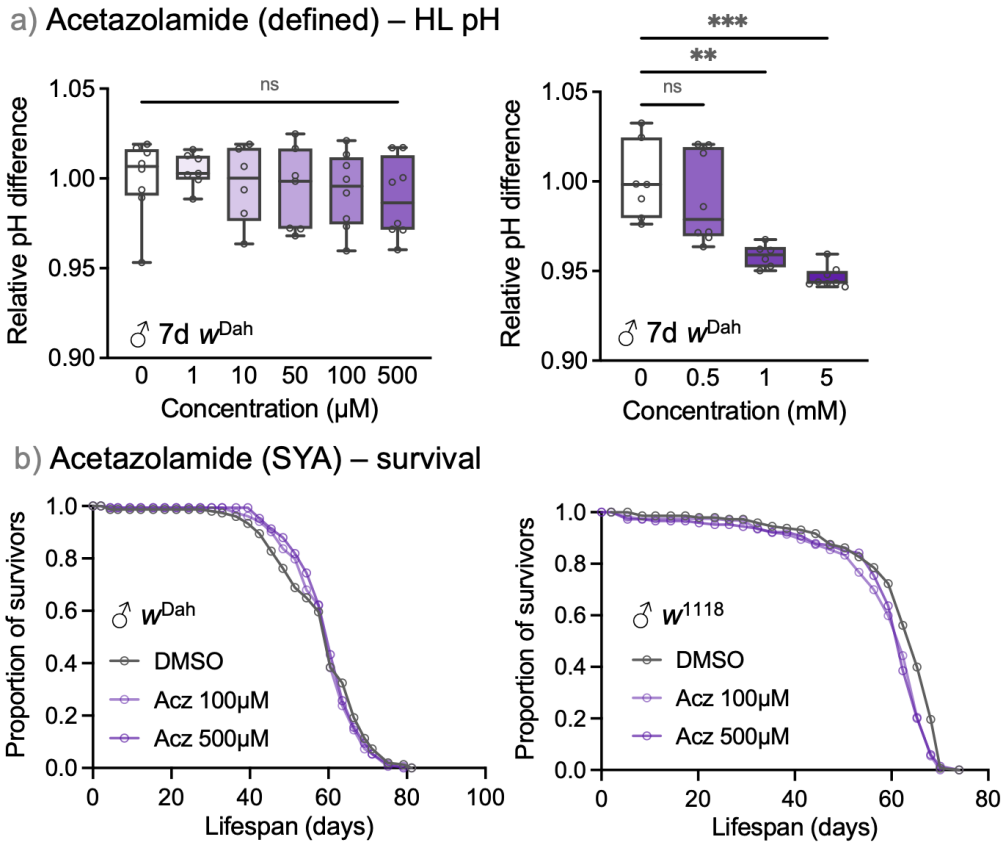


Figure 4.4. Effect of acetazolamide on haemolymph pH and survival in flies. Haemolymph pH (a) was measured using the pyranine method in w^{Dah} male flies after 7 days of dietary treatment with a range of Acz doses on a chemically defined medium. Data are box-plots of n=6-8 replicates per condition. Statistical analysis was based on ANOVA with Tukey correction for multiple comparisons. ns, p>0.05; **, p<0.01; ***, p<0.001. Survival curves (b) of w^{Dah} and w^{1118} male flies treated with 100-500 µM Acz or 0.5% DMSO control from d2 of adulthood, n=140 flies per condition.

4.3. Chemically preventing age-related haemolymph acidification

After establishing that chronic acidotic stress decreases fly survival, I next aimed to supplement the fly medium with compounds potentially capable of counteracting the age-related acidification to assess whether they would alter survival.

In humans, metabolic acidosis is primarily treated by identifying and addressing its underlying cause (Kraut & Madias, 2010). However, alkalotic treatment can be an option to rapidly re-establish acid-base balance in cases of either severe acidaemia or less severe acidaemia associated with acute kidney injury (Jaber et al., 2018). The most studied option is sodium bicarbonate ($NaHCO_3$), but other drugs such as tromethamine (Tris base) have been used for that purpose (Kraut & Madias, 2010).

These compounds act as bases in different ways and their precise mechanisms of action depend on which view on acid-base balance you adopt (see Section 1.3.2). By the descriptive bicarbonate-based view, $NaHCO_3$ is alkalotic by directly increasing the numerator of the bicarbonate/carbonic acid fraction in the Henderson-Hasselbalch equation. In Stewart's quantitative view, $NaHCO_3$ increases pH by the addition of sodium, raising [SID], while bicarbonate plays no direct role and can lead to acute intracellular acidosis if given rapidly or in high doses due to increased PCO_2. Tris base has a similar mechanism in both views. Its amide group associates with H^+ to form Tris-NH_3^+ and the reaction is CO_2 consuming by shifting the bicarbonate buffer equation to increase CO_2 hydration transiently. Besides, to Stewart's view, this introduces a weak base (Tris-NH_3^+) as an independent variable, B_{TOT}, with a significant positive charge that changes the electrical neutrality equation. All fluid equilibria, such as water and weak acid dissociations, are altered as a result and increase pH.

Because of their substantially different properties, I selected both these chemicals to assess their impact on acid-base balance and survival in flies.

4.3.1. Low-dose alkalotic compounds do not consistently alter survival

Both $NaHCO_3$ and Tris base have previously been used to buffer fly food in order to assess how different buffering compounds affected survival (Massie et al., 1981). Both of them extended fly lifespan, $NaHCO_3$ at 30 mM and Tris base at 1 mM, which would be in line with the idea that preventing acidification over time with these chemicals can impact survival and may therefore slow down ageing or the development of age-related disease in flies.

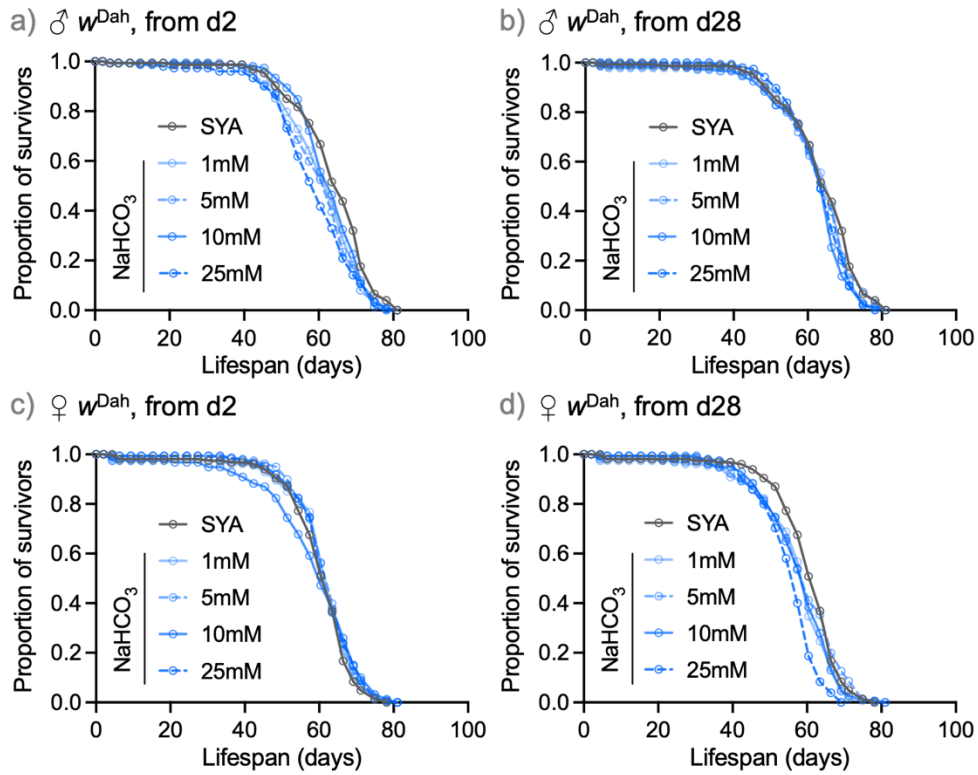


Figure 4.5. Effect of low-dose $NaHCO_3$ on the survival of w^{Dah} flies. Survival curves of w^{Dah} male (a,b) and female (c,d) flies fed a range of $NaHCO_3$ concentrations starting at either d2 (a,c) or d28 (b,d), n=140 flies per condition.

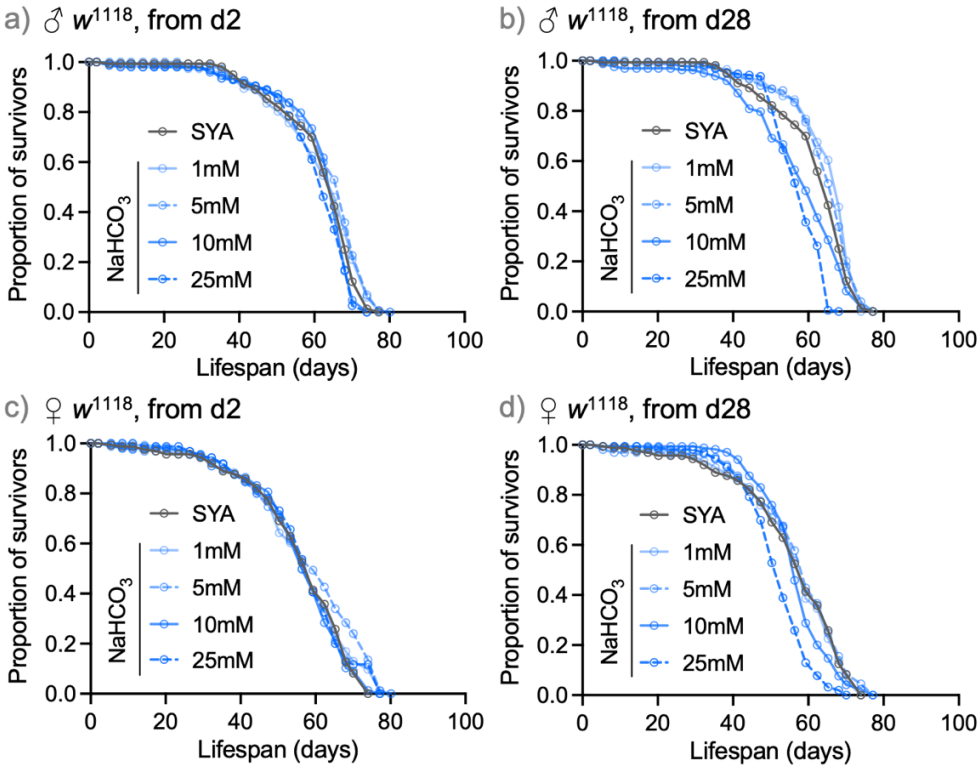


Figure 4.6. Effect of low-dose $NaHCO_3$ on the survival of w^{1118} flies. Survival curves of w^{1118} male (a,b) and female (c,d) flies fed a range of $NaHCO_3$ concentrations starting at either d2 (a,c) or d28 (b,d), n=140 flies per condition.

To test if this would be replicated in our conditions and fly strains (w^{Dah} and w^{1118}), fly medium was supplemented with a range of $NaHCO_3$ concentrations that was comparable to the ones used in that study. Surprisingly, no significant effect on survival was seen in either of the strains, in either males or females (Figures 4.5 and 4.6). Additionally, supplementing $NaHCO_3$ later in life (from 28 days), when a certain degree of acidification has already occurred, also did not have an effect on fly survival, in neither male or female flies.

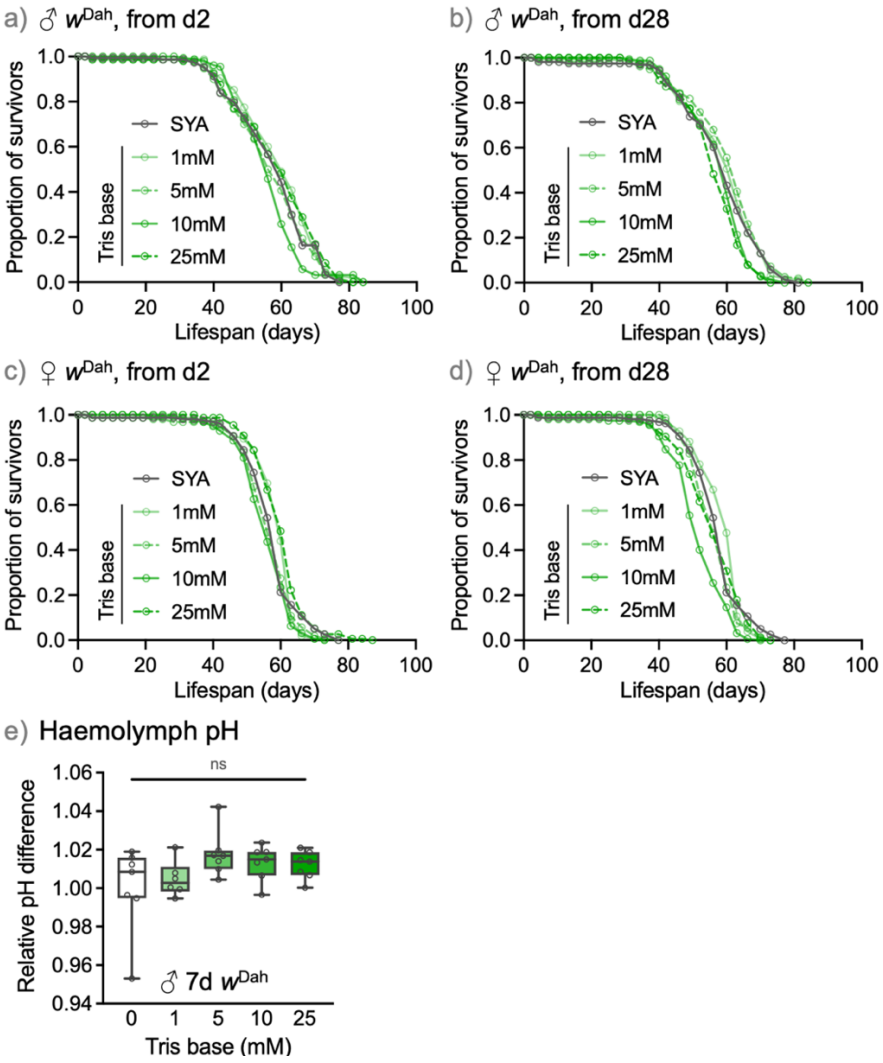


Figure 4.7. Effect of low-dose tris base on the survival of w^{Dah} flies. Survival curves of w^{Dah} male (a,b) and female (c,d) flies fed a range of Tris base concentrations starting at either d2 (a,c) or d28 (b,d), n=140 flies per condition. Haemolymph pH (e) was measured using the

pyranine method in w^{Dah} male flies after 7 days of dietary treatment with a range of Tris base doses on SYA. Data are box-plots of n=6-7 replicates per condition. Statistical analysis was based on ANOVA with Tukey correction for multiple comparisons. ns, p>0.05.

Similarly, no significant effect on survival occurred after administration of Tris base at the concentrations previously reported to extend fly lifespan (Massie et al., 1981). This again was independent of sex and whether the drug was provided from a young or older age (Figure 4.7a-d). Tris base also had no impact at these doses on the haemolymph pH of young flies (Figure 4.7e), although perhaps expected since young flies still have a high haemolymph pH, no further alkalotic effect was observed. Because Tris base can have negative gastrointestinal effects, I tried Tris citrate at the same concentration range. Tris citrate was shown to be more palatable and tolerable when given orally to dogs, while also having an alkalinising effect (Nahas et al., 1964). However, similarly to the other compounds, Tris citrate did not alter fly survival from either early or late in life and in either sex (Figure 4.8).

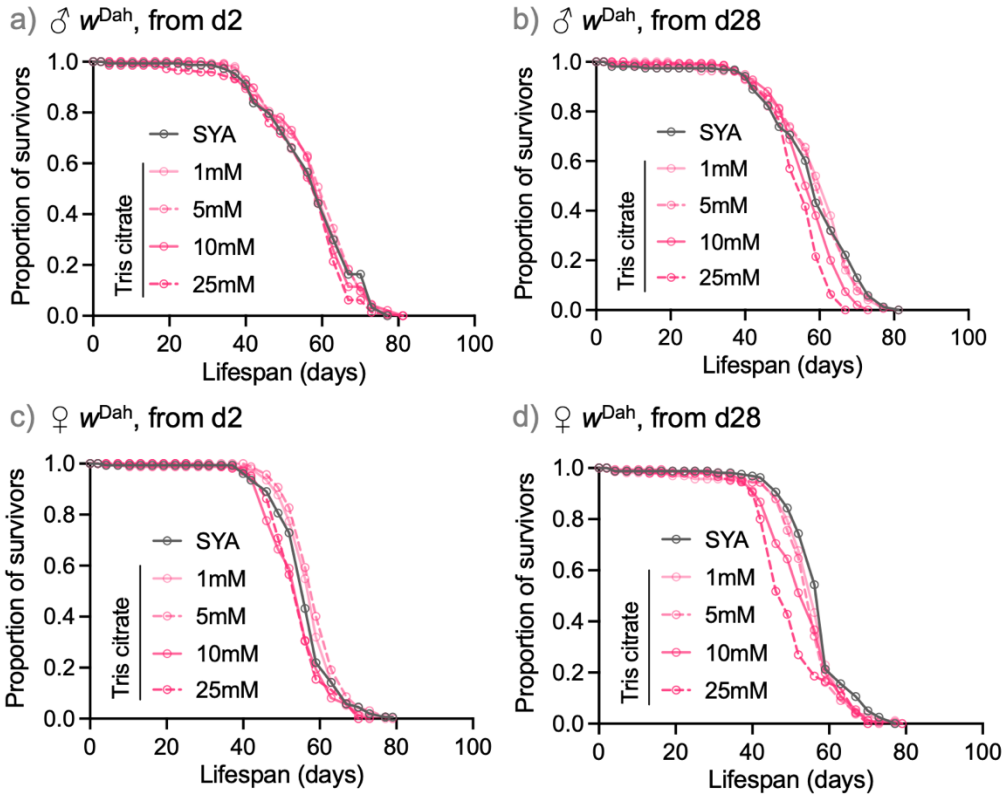


Figure 4.8. Effect of low-dose tris citrate on the survival of w^{Dah} flies. Survival curves of w^{Dah} male (a,b) and female (c,d) flies fed a range of Tris citrate concentrations starting at either d2 (a,c) or d28 (b,d), n=140 flies per condition.

Despite not extending fly survival as previously reported, these drugs at this range of concentrations did not shorten it either. This discrepancy may again be due to different medium composition. In fact, at those concentrations neither of the drugs significantly altered the pH of the food, which is likely related to the relatively high concentration of protein in SYA compared to other fly media. Therefore, higher concentrations of these drugs were tested.

4.3.2. High-dose alkalotic compounds alter resistance to acidotic stress

At a 100 mM concentration, both $NaHCO_3$ and Tris base altered the pH of the food from ~4.5 to ~7 and ~8, respectively. This has the disadvantage of potentially altering food properties and the physiological response to different food pH, such as differences in feeding behaviour, or selection of different microbiota populations (Deshpande et al., 2015). To control whether the effect of the drugs was dependent on food pH, pH-matched controls for both drugs were added by adjusting the pH of the medium with NaOH.

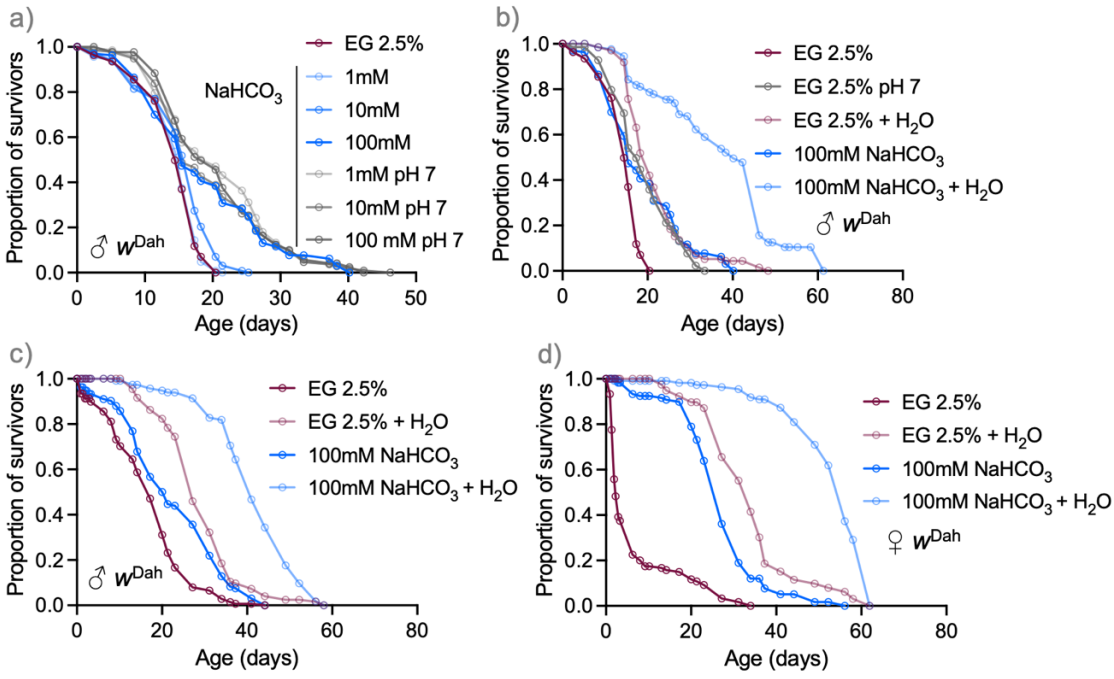


Figure 4.9. Effect of high-dose NaHCO3 on acidotic stress resistance. Survival curves of w^{Dah} male (a-c) and female (d) flies treated with 2.5% EG ± 1-100 mM $NaHCO_3$ ± an extra water source from d2 of adulthood, n=140 flies per condition.

Before repeating lifespans under these conditions, the effect of the drugs on rescuing fly haemolymph acidification was tested. If lower doses could rescue acidification but not lifespan, this would challenge the hypothesis that haemolymph acidification modulates lifespan. To test that, an experiment was set up where both low and high doses of either $NaHCO_3$ or Tris base were given to male flies under EG-induced acidotic stress. Control conditions where the pH was adjusted to the pH of the highest dose, either 7 for $NaHCO_3$ or 8.3 for Tris base, were added (Figures 4.9a, 4.10a).

Consistent with their lack of effect on lifespan, lower doses of either drug (up to 10 mM) with non-adjusted pH failed to rescue the survival of flies under acidotic stress (Figures 4.9a, 4.10a). Conversely, higher doses of $NaHCO_3$ extended survival, as did all conditions where food pH was increased with NaOH, except at 100 mM of Tris base (Figure 4.10a). This is likely due to side-effects of a higher Tris base concentration and not its effect on acid-base, since the other pH-matched conditions had an effect on survival.

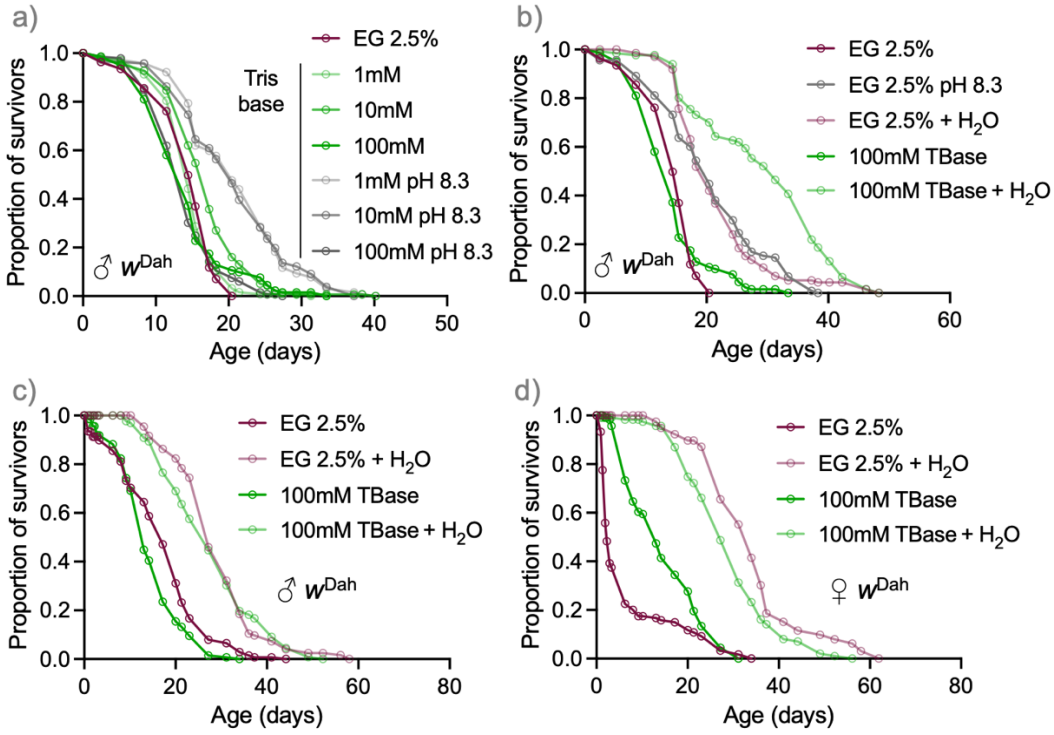


Figure 4.10. Effect of high-dose Tris base on acidotic stress resistance. Survival curves of w^{Dah} male (a-c) and female (d) flies treated with 2.5% EG ± 1-100 mM Tris base ± an extra water source from d2 of adulthood, n=140 flies per condition.

Given that high drug concentrations may also further increase the osmolarity of the medium (as does adjusting pH with NaOH), the addition of the drugs may cause dehydration despite their effect on acidotic stress, limiting the benefit of these interventions. To test if that was the case, flies were provided with an additional source of water as an agar solution. Adding water resulted in an additive, potentially synergistic, effect with both alkalotic compounds to significantly extend fly survival under acidotic stress, in both sexes (Figures 4.9b-d, 4.10b-d).

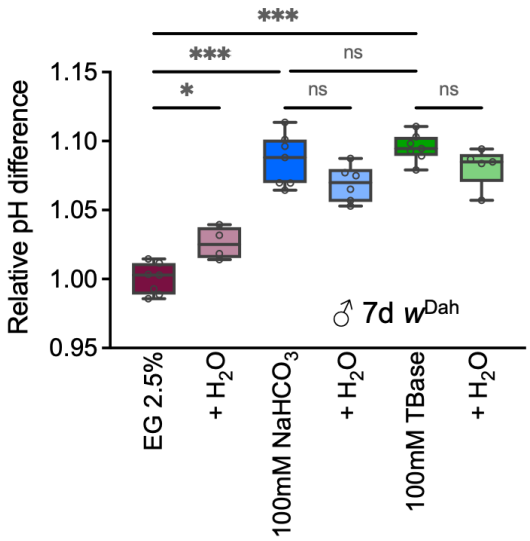


Figure 4.11. Alkalotic compounds rescue EG-induced haemolymph acidification. Haemolymph pH was measured using the pyranine method in *w*^{Dah} male flies after 7 days of treatment with 2.5% EG ± 100 mM $NaHCO_3$ or Tris base ± an extra water source. Data are box-plots of n=4-7 replicates per condition. Statistical analysis was based on ANOVA with Tukey correction for multiple comparisons. ns, p>0.05; *, p<0.05; ***, p<0.001.

Although this likely occurs due to counteracting the compound-related osmolarity effects on haemolymph, added water by itself increased the survival of flies under EG-induced stress. This may occur because: 1) EG acts itself as a strong osmole (Liamis et al., 2010), and 2.5% may be sufficient to cause osmotic stress and dehydration; and 2) water consumption may increase tubule secretion rates and therefore accelerate excess acid excretion.

Likely, it is a combination of both factors. Added water alone can indeed increase haemolymph pH under acidotic stress, although to a lower degree compared to the alkalotic compounds (Figure 4.11). However, it does not further increase haemolymph pH when combined to alkalotic compounds, suggesting its additive effect

occurs due to factors beyond acid-base balance, such as prevention of osmotic stress. Despite partially rescuing the side-effects of high dose Tris base (Figure 4.10b-d), the synergistic effect of water is more pronounced when given with $NaHCO_3$, resulting in significant lifespan extension to a median comparable to flies raised in control conditions, despite the constant acidotic stress (Figure 4.9b-d).

This further illustrates that acid-base balance can *per se* significantly affect fly survival, and poses the question whether these compounds can also prevent age-related haemolymph acidification at higher concentrations to extend fly survival.

4.3.3. High-dose $NaHCO_3$ extends fly lifespan, even from middle-age

Flies were first given alkalotic compounds throughout their lifespans at a range of doses that include the higher 100 mM concentration and a pH-matched control. Then, in independent repeats flies were fed media supplemented with 100 mM of alkalotic compounds from both 2 or 28 days of age. They were also given these compounds intermittently (2 days per week) since continuous higher pH might inhibit essential reactions or paradoxically lead to the downregulation of genes that are essential for acid excretion or buffering. A pH-matched condition was set up for each repeat. An added water control was also set with the alkalotic drugs to account for their potential osmotic effect.

As observed under acidotic stress, chronic intake of 100 mM Tris base shortened fly survival (Figure 4.12a, c-d). Given the pH-matched control neither altered nor extended survival (Figure 4.12a, c-d), this effect may result from the known side-effects of excess Tris base, such as hypoglycaemia, respiratory depression, vomiting and hypotension (Nahas et al., 1998). Tris base at 10 mM showed a small but significant lifespan extension in males flies when given from either day 2 or 28 (Figure 4.12a-b), but this effect was not consistently replicated (Figure 4.7a-b). There might be specific conditions where Tris base may extend fly survival as it was seen before (Massie et al., 1981), such as when given in media with a higher sugar content to prevent hypoglycaemia, for example. Contrary to its effect under acidotic stress, added water did not rescue high-dose Tris base-dependent shortened lifespan, independently of sex or treatment regimen (Figure 4.12c-f).

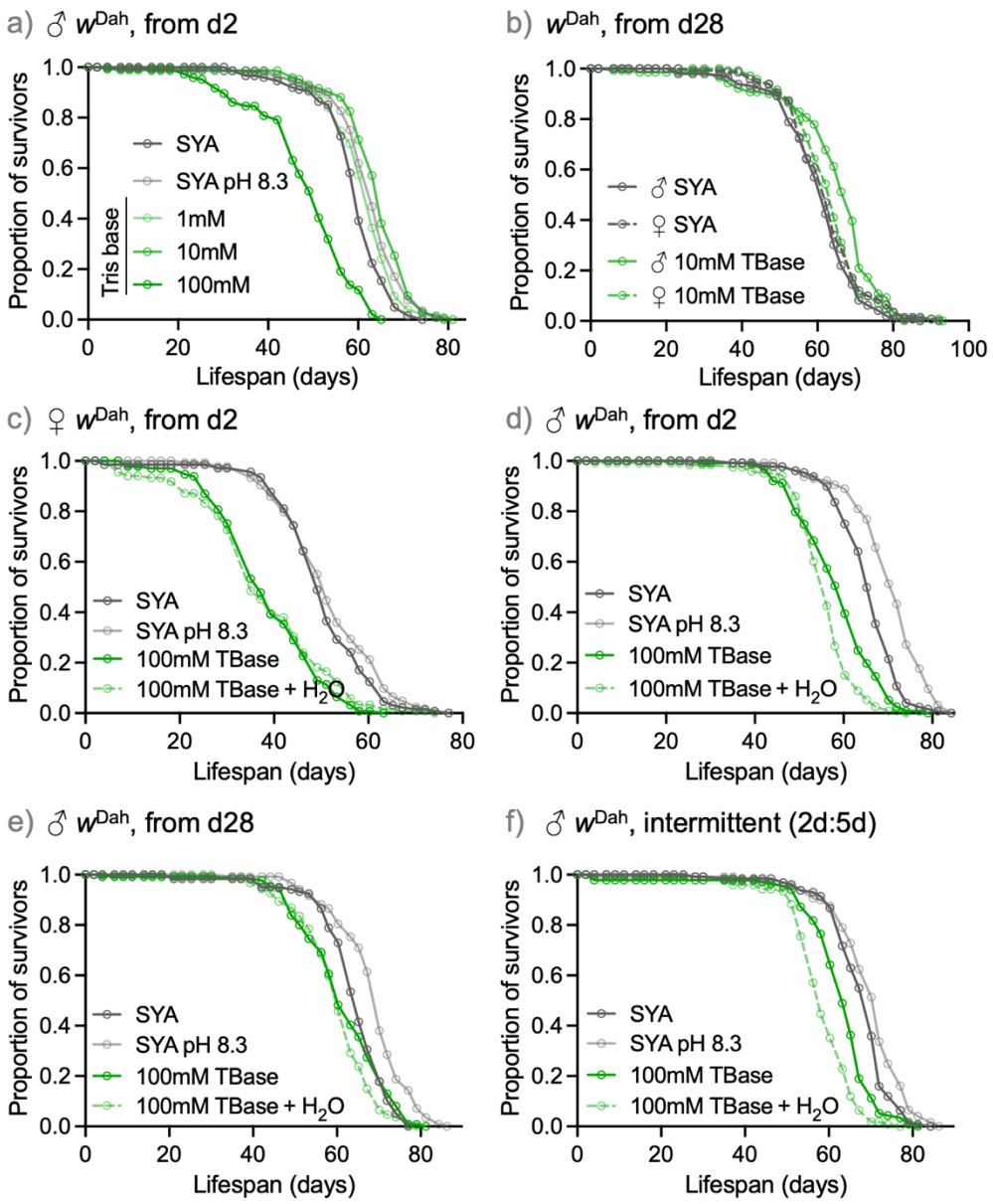


Figure 4.12. Effect of high-dose tris base on the survival of *w*^{Dah} flies. Survival curves of *w*^{Dah} male (a,b,d,e,f) and female (b,c) flies treated with 1-100 mM Tris base ± an extra water source (c-f) from d2 (a,c,d) or d28 (b,e) of adulthood, or intermittently – treated for 2 days a week with Tris base and fed on standard SYA the other 5 days (f); n=140 flies per condition.

Chronic intake of $NaHCO_3$ significantly extended the lifespan of both male and female flies (Figure 4.13a-c). This effect might partially depend on food pH as matching it with NaOH can result in a comparable effect size in both sexes (Figure 4.13a-b). In males, $NaHCO_3$ can also extend lifespan independently of food pH (Figure 4.13c-e). $NaHCO_3$ prolonged survival when administered both from day 2 or day 28, and also intermittently. From these three independent interventions, it seems the longer the flies are on $NaHCO_3$-supplemented food, the longer they live. Contrary to

its effect under acidotic stress, added water did not further extend lifespan in any condition, suggesting the excess sodium was not sufficient to cause osmotic stress.

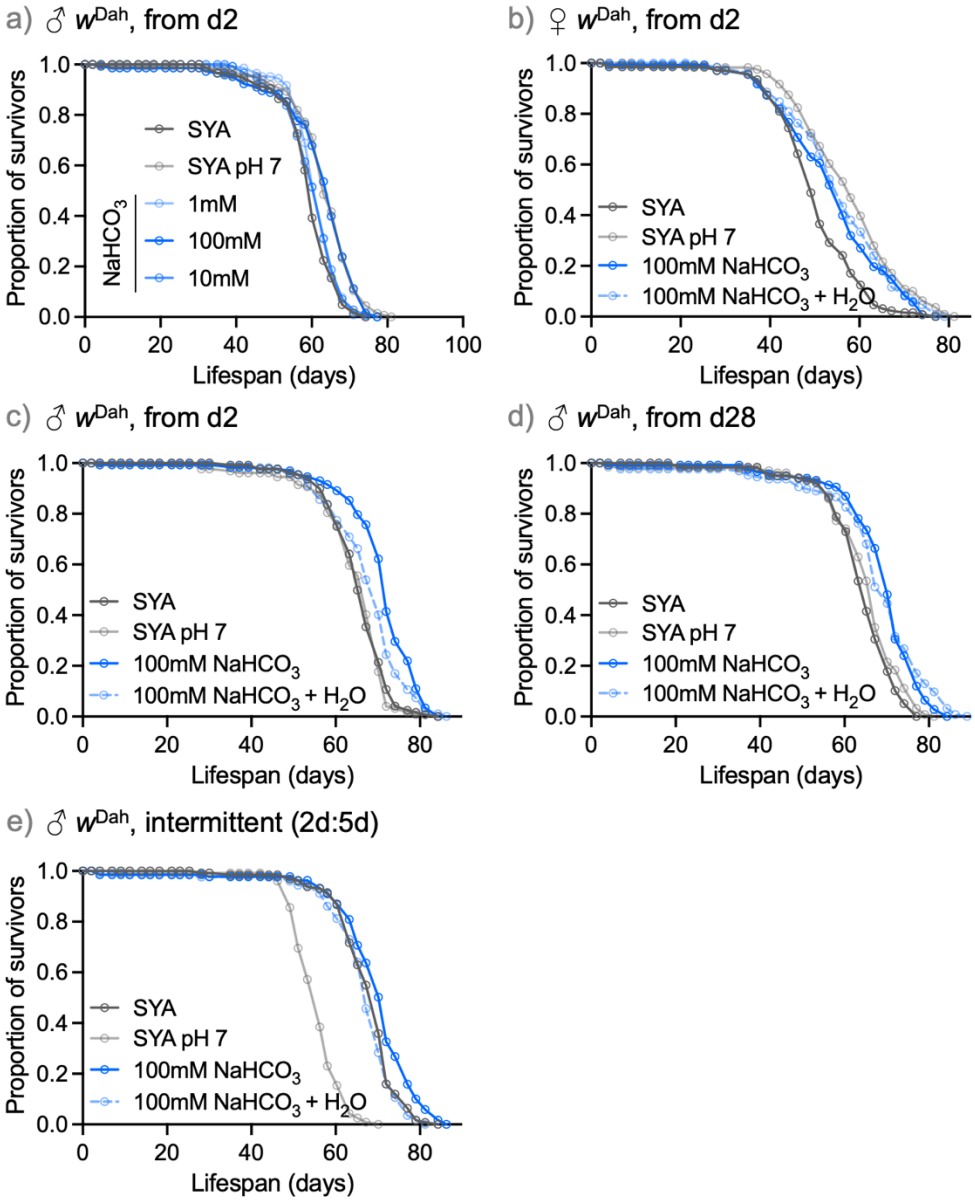


Figure 4.13. Effect of high-dose $NaHCO_3$ on the survival of *w*^{Dah} flies. Survival curves of *w*^{Dah} male (a,c,d,e) and female (b) flies treated with 1-100 mM $NaHCO_3$ ± an extra water source (b-e) from d2 (a-c) or d28 (d) of adulthood, or intermittently – treated for 2 days a week with $NaHCO_3$ and fed on standard SYA the other 5 days (e); n=140 flies per condition.

Altering food pH with NaOH in Stewart's view increases [SID] the same way $NaHCO_3$ does, and so it will also alter the acid-base status of haemolymph. Food pH *per se* may affect survival in part independently of haemolymph acid-base balance, by altering feeding rates or selecting microbiota (Deshpande et al., 2015). To test the

potential impact of food pH on survival, defined medium was buffered to a wide pH range (2 to 8) with different buffers (due to different pK_a): 0.1 M sodium phosphate (pH 2, 3, 6, 7 and 8), 0.1 M sodium acetate (pH 4 and 5) and 0.1 M Tris buffer (pH 8). To alter the pH of the defined medium, high buffer concentration was needed due to the buffering capacity of the other food components. To control for sodium concentration and ionic strength (300 mM, 30 mM in final medium), buffers were adjusted with different amounts of NaCl. The resulting high concentration of sodium likely caused osmotic stress, but to the same extent in all conditions. Under these conditions, lifespan was not dependent on food pH but on the type of buffer (Figure 4.14).

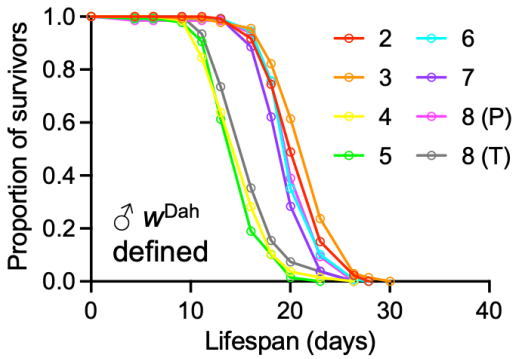


Figure 4.14. Effect of Na^+-matched medium pH on survival. Survival curves of w^{Dah} male flies fed defined media with adjusted pH ranging from 2 to 8; 0.1 M sodium phosphate buffer was used to adjust pH to 2, 3, 6, 7 and 8; 0.1 M sodium acetate to pH 4 and 5; and 0.1 M Tris base buffer to pH 8; n=140 flies per condition. P, phosphate buffer; T, Tris base buffer.

Indeed, the previously reported changes in fly survival under different pH primarily occurred in food buffered differently, which collectively suggests survival may depend on the type of buffer salt rather than on food pH itself (Deshpande et al., 2015). In the same study, food pH was also altered in a narrower range (5 to 9) by the same phosphate buffer and flies raised under the most acidic food condition survived for longer (Deshpande et al., 2015). However, the ionic strength of the buffer at each pH was not matched in this study. In this range, phosphate buffer at pH 9 has a significantly higher concentration of sodium compared to the same buffer at pH 5, so we can interpret the same result as lifespan shortening in a sodium-dependent, rather than pH-dependent, manner.

It would be important to follow up these experiments by measuring feeding in flies raised on food with different pH and with added compounds where a lifespan

effect was seen, as well as testing the impact of these interventions on the survival of axenic flies.

4.4. Key messages and interpretation

In this chapter, fly haemolymph acid-base balance was pharmacologically altered and correlated with survival. The main conclusions from the results presented here are:

- Metabolic acidosis can be modelled in flies by adding EG to their diet
- Survival shortens and haemolymph acidifies in an EG dose-dependent manner
- Flies become more sensitive to acidotic stress with age
- Alkalotic compounds rescue acidotic stress-associated shortened survival and water has an additive effect
- Sodium bicarbonate extends fly lifespan independently of sex and even when started from middle-age

Altering haemolymph to lower or higher pH pharmacologically results in shortened or extended lifespan, respectively. This observation suggests age-related acid-base imbalance can itself affect fly survival, which would make it a hallmark of ageing by definition (López-Otín et al., 2013).

Buffers are rough tools that can alter fly physiology beyond systemic acid-base balance. Sodium from $NaHCO_3$, for example, can alter haemolymph osmolarity and Tris base can have gastrointestinal side-effects (Nahas et al., 1998). It is therefore difficult to step beyond correlation between systemic acid-base balance and survival with this approach. Alkalotic compounds may, however, be used in combination with other strategies that alter haemolymph pH and survival to a similar extend to test whether: 1) the survival effect is cumulative and hence partly pH-independent; or 2) survival is not further extended by redundant strategies, suggesting pH dependence. In the next chapter, I will explore potential genetic approaches that may serve as independent strategies to alter haemolymph pH and test this hypothesis further.

Here, age-related haemolymph acidification was proposed to be metabolic rather than respiratory in origin. To test this hypothesis, other parameters would need to be measured in the haemolymph besides pH. These would include at least strong ions and partial pressure of CO_2. Given the limited amount of haemolymph obtained from each extraction (~1 µL), this would be technically impractical and time-

consuming. However, modelling CO_2 retention by raising the flies in incubators with higher partial pressure of CO_2 and assessing how it alters their physiology and survival could be an interesting follow-up experiment.

This chapter presents a novel model of metabolic acidosis in flies. EG-induced haemolymph acidification results from the production of excess acid in young flies with a functional but overwhelmed excretory system. EG also causes osmotic stress, which combined with acidosis, significantly shortens fly survival in a dose-dependent manner. Consistent with the idea that these factors are responsible for the increased mortality, both alkalotic compounds and added water increase the survival of flies under acidotic and osmotic stress. Their added effects and potential synergy result in the rescue of fly lifespan to a median survival comparable with flies raised under control conditions.

The loss of resilience upon acidotic stress with age suggests that the mechanisms required to either buffer or excrete excess acid become overwhelmed or insufficient with age. How these mechanisms change with age will be explored in the next two chapters.

Chapter 5. Extracellular buffers and proteome in ageing

5.1. Introduction

Loss of resistance to acidotic stresses with age can occur when the buffering capacity is overwhelmed. In this chapter, I explore how fly haemolymph may change with age, both in terms of its buffering capacity and its proteome.

From a descriptive view of acid-base physiology, a buffer is a system that maintains a solution's acid-base balance upon the addition of acids or bases. Accordingly, the buffer strength of a solution is generally defined as the amount of acid or base that must be added to a solution to produce a unit pH change (Harrison, 2001). Effectively, buffers are seen as weak electrolytes whose dissociation is altered to keep pH in a certain range. From a quantitative standpoint, weak acids simply alter the point about which $[H^+]$ changes, for a given range of [SID] values. Their presence actually increases pH changes rather than decreasing them in response to the addition of strong ions to the solution. However, weak electrolytes are important to set the pH range of solutions. Accordingly, the buffer strength represents only the number of strong ions per litre that must be added or removed from the solution in order to alter [SID] and change the pH by one unit (Kellum & Elbers, 2009). Despite the theorical difference in interpretation, the observation is the same: the presence of weak electrolytes is crucial to maintain solution pH in a physiological range.

5.2. Extracellular buffering

Any weak acid or base can work as a buffer in an aqueous solution. Under normal conditions, carbonic acid is the main buffer in both the interstitial fluid and blood. In blood, circulating proteins are also important buffers, largely due to the imidazole group of histidine, the only amino acid with a side-chain group whose pKa is similar to blood pH at body temperature.

5.2.1. The carbonic acid - bicarbonate buffer

The main extracellular weak acid determining the range of physiological pH in both humans and insects is carbonic acid. As previously mentioned, it balances the concentration of H^+ and HCO_3^- with the partial pressure of CO_2, represented in the following equation:

$$CO_2 + 2H_2O \rightleftharpoons H_2CO_3 \rightleftharpoons HCO_3^- + H^+$$

This equation shifts to the left when excess acid is present in solution, consuming bicarbonate and forming CO_2 to be released by the respiratory system. Conversely, it shifts to the right when excess CO_2 accumulates to form bicarbonate and H^+, whose concentration is mainly regulated by the kidneys.

In humans, the plasma concentration of H_2CO_3 is approximately 1.2 mM and the concentration of HCO_3^- is ~24 mM. Using the Henderson-Hasselbalch equation with the pK_a of carbonic acid at body temperature (6.1),

$$pH = 6.1 + \log\frac{24}{1.2} = 7.4$$

which again demonstrates that carbonic acid is the main electrolyte determining blood pH in humans. There are other plasma components that act as buffers, primarily proteins and organic acids, but given its relative greater importance in normal acid-base conditions, I focused on the carbonic acid - bicarbonate system.

5.2.2. Carbonic anhydrases

The hydration of CO_2 has slow kinetics, taking approximately 30 s to occur in the absence of catalysis (Kellum & Elbers, 2009). Carbonic anhydrases (CAs) are enzymes that catalyse this reaction. In their presence, CO_2 hydration occurs in milliseconds (Casey et al., 2010; Kellum & Elbers, 2009). This makes these enzymes essential for effective maintenance of acid-base balance, particularly in extracellular fluids. Because of the importance of acid-base reactions in nature, these ancient enzymes are present in most living organisms (Frost, 2014). There are 5 different classes of CAs (α, β, γ, δ, and ζ). The α class has the widest distribution among species and is the only CA found in mammals (Syrjänen et al., 2013). *Drosophila* also has a mitochondrial β-CA (Syrjänen et al., 2010).

How ageing may alter the activity of these enzymes in human blood is unknown, but changes in protein expression can be found in publicly available datasets on how the plasma proteome is altered by ageing in humans (Lehallier et al., 2019; Tanaka et al., 2018). From the analysis of age-related changes in CA isoforms, the two datasets give conflicting results. There are 16 isoforms of CAs in humans. Data from Tanaka et al. show a significant age-related decrease of CA 2, 3, 4 and 6, but not significant of 1, 7, 9, 10 and 13; other CA isoforms were not detected in the plasma (Tanaka et al., 2018). Lehallier et al. show a decrease of CA 6 and 10, no change in 1, 2, 5 and 9,

and surprisingly, an increase in CA 3 (Lehallier et al., 2019), which was the isoform more significantly decreased in the previous dataset. Despite the differences, these datasets suggest the expression of CAs may change in human plasma with ageing, overall tending to decrease, which might alter buffering efficacy.

5.3. Carbonic anhydrases in *Drosophila*

I used the fly model to further study potential changes in the activity and expression of CAs in extracellular fluids. Similarly to humans, the main fly extracellular buffer is the carbonic acid - bicarbonate system (Harrison, 2001; Massie et al., 1981). Accordingly, *Drosophila* needs CAs to catalyse this buffering reaction. There are 14 CAs and 2 CA-related proteins described in the fly (Table 4). Although different among themselves and to human CAs at the sequence level (sequence similarity under 50%), they have a similar structure, conserved catalytic and binding sites, and are predicted to perform the same function (Bateman et al., 2023).

To test whether extracellular buffering efficiency declines with age, I aimed to measure CA activity in fly haemolymph over time. The adapted method is based on measuring the enzyme's esterase activity in the absence or presence of a specific inhibitor. The difference in reaction rates determines CA activity. Esterase activity of CAs occurs through the same catalytic pocket responsible for their hydratase activity, implicating it can be a readout of hydratase activity (Piazzetta et al., 2017; Uda et al., 2015). Given the low sample volume of extracted haemolymph, this is a more practical and time-efficient method compared to the gold standard method of directly measuring the hydration of CO_2 (Uda et al., 2015). Hence, it is also used in commercial kits to measure the carbonic anhydrase activity in human plasma (e.g., ab284550, Abcam; MAK404, Sigma Aldrich).

5.3.1. Carbonic anhydrase activity in whole fly homogenates

CA activity has previously been quantified in whole fly lysates by an electrometric method based on measuring how much time it takes for the pH of a solution to change upon mixture with a saturated CO_2 solution, i.e., the rate of CO_2 hydration, in the presence or absence of the enzyme (Massie et al., 1981; Wilbur & Anderson, 1948). Using this method, whole fly CA activity is shown to decline with age in male flies, although it is variable and seems to stabilise in old age (Massie et al., 1981). With this

method, homogenates of 100 male flies were needed for a final reaction volume of 5 mL and activity was not normalised for protein concentration. As stated previously, these volumes would make it unfeasible to use this method to quantify CA activity in haemolymph, so an indirect, esterase activity-based method was used.

Gene symbol	Protein symbol	Isoforms	Expression profile	Similarity to human CAs
CAH1	CA1	-	SG, hindgut, midgut	CA7 47% CA2 46%
CAH2	CA2	A	MTs, Midgut, Eye	CA7 37% CA2 36%
		B	Low expression	-
CAH3	CA3	A	MTs	CA7 38%
		B	Low expression	-
		C	Low expression	-
		D	Low expression	-
		E	Low expression	-
CAH4	CA4	A	Testis	CA6 37%
		C	Testis	-
CAH5	CA5	-	Testis	-
CAH6	CA6	-	Low expression	-
CAH7	CA7	A	TA ganglion, brain	CA6 34%
		B	Low expression	-
		C	Fat body	-
CAH8	CA8	A	Spermatheca	-
		B	Spermatheca	-
CAH9	CA9	-	SG, hindgut	-
CAH13	CA13	-	Testis	CA1 29%
CAH14	CA14	-	Testis	-
CAH15	CA15	-	Testis	-
CAH16	CA16	B	Accessory glands	-
		C	Accessory glands	-
		D	Accessory glands	-
CARPA	CARPA	B	Low expression	CARP10 40%
		C	TA ganglion, brain	-
CARPB	CARPB	A	Fat body	CARP10 41%
		B	Fat body	-
		C	Fat body	-
CAHβ	CAHβ	A	Fat body, crop	-
		B	Low expression	-

Table 4. List of fly carbonic anhydrases. Includes CA expression profile based on FlyAtlas2 (Leader et al., 2018) and sequence similarity to human CAs based on UniProt (Bateman et al., 2023). MTs, Malpighian tubules; TA, Thoracoabdominal; SG, salivary glands.

After establishing the method with human CA (see Section 2.6.1), fly lysates were used to independently verify previously reported CA activity changes (Massie et al., 1981). Male flies (25) were homogenised in 1 mL of assay buffer with 1% (v/v) of protease inhibitor (EO0491, Thermo Scientific). Lysates were serially diluted and esterase activity was measured as described (Section 2.6.1). The rate of nitrophenol formation linearly increased over time in a lysate concentration-dependent manner (Figure 5.1a-b).

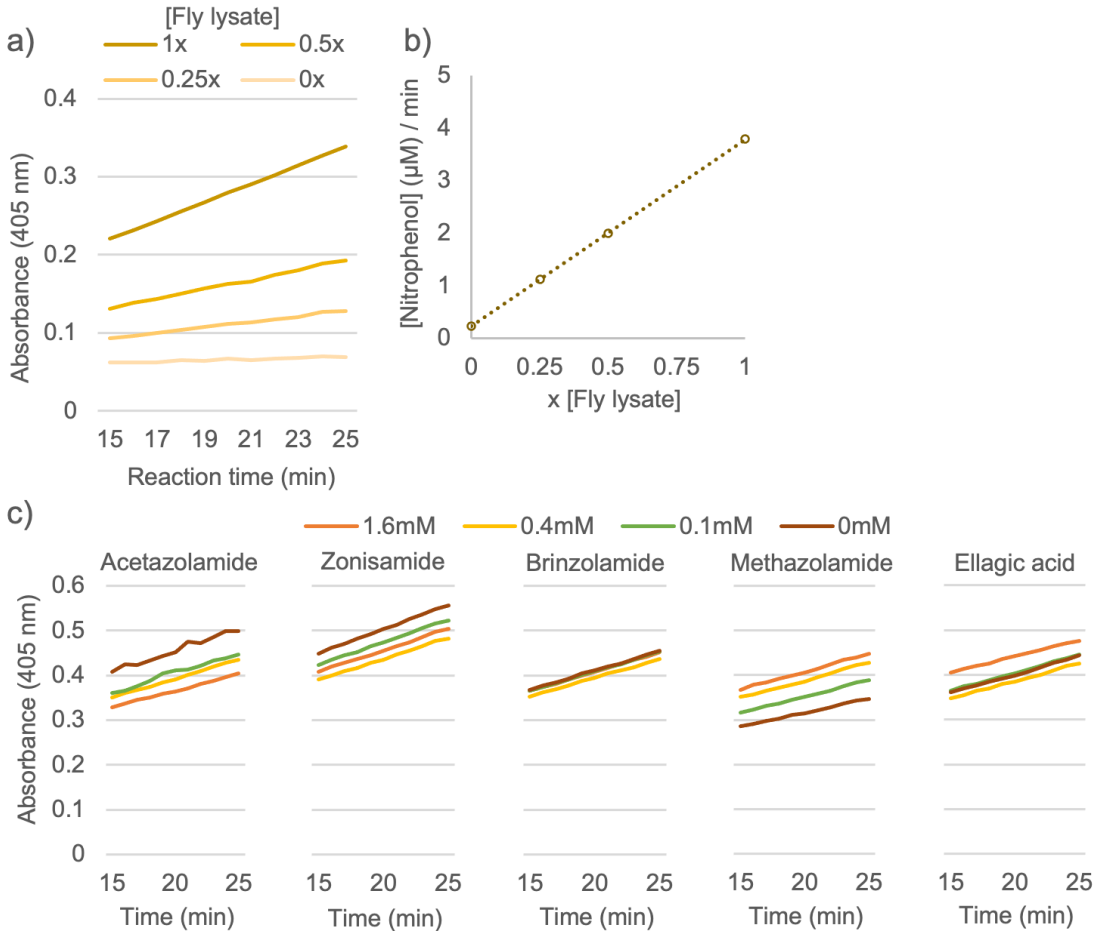


Figure 5.1. CA activity in whole fly lysate: a) Nitrophenol production (absorbance at 405 nm) over time in the linear range dependent on the concentration of serially diluted fly lysate; b) Rate of nitrophenol production is linearly dependent on concentration of fly lysate; c) The effect of different inhibitors on nitrophenol production over time in the linear range.

To get CA-dependent esterase activity, different concentrations of CA inhibitors were added to the reaction. Despite completely inhibiting human CA activity at even the lowest concentration (Section 2.6.1), sulfonamides, including Acz, and ellagic acid did not significantly alter whole fly esterase activity (Figure 5.1c). This observation suggests that this method is not suitable to measure CA activity with age in whole fly

lysates. The lack of measurable effect may be due to the vast number of proteins with potential esterase activity in the whole fly which can disguise the effect of CA-specific activity, so extracted haemolymph samples were tested next.

5.3.2. Carbonic anhydrase activity in fly haemolymph

Like in whole fly lysate, the rate of nitrophenol formation linearly increased over time in serially diluted haemolymph in a concentration-dependent manner (Figure 5.2a-b). However, CA inhibitors, even at their highest concentration, did not significantly alter esterase activity in the haemolymph (Figure 5.2c).

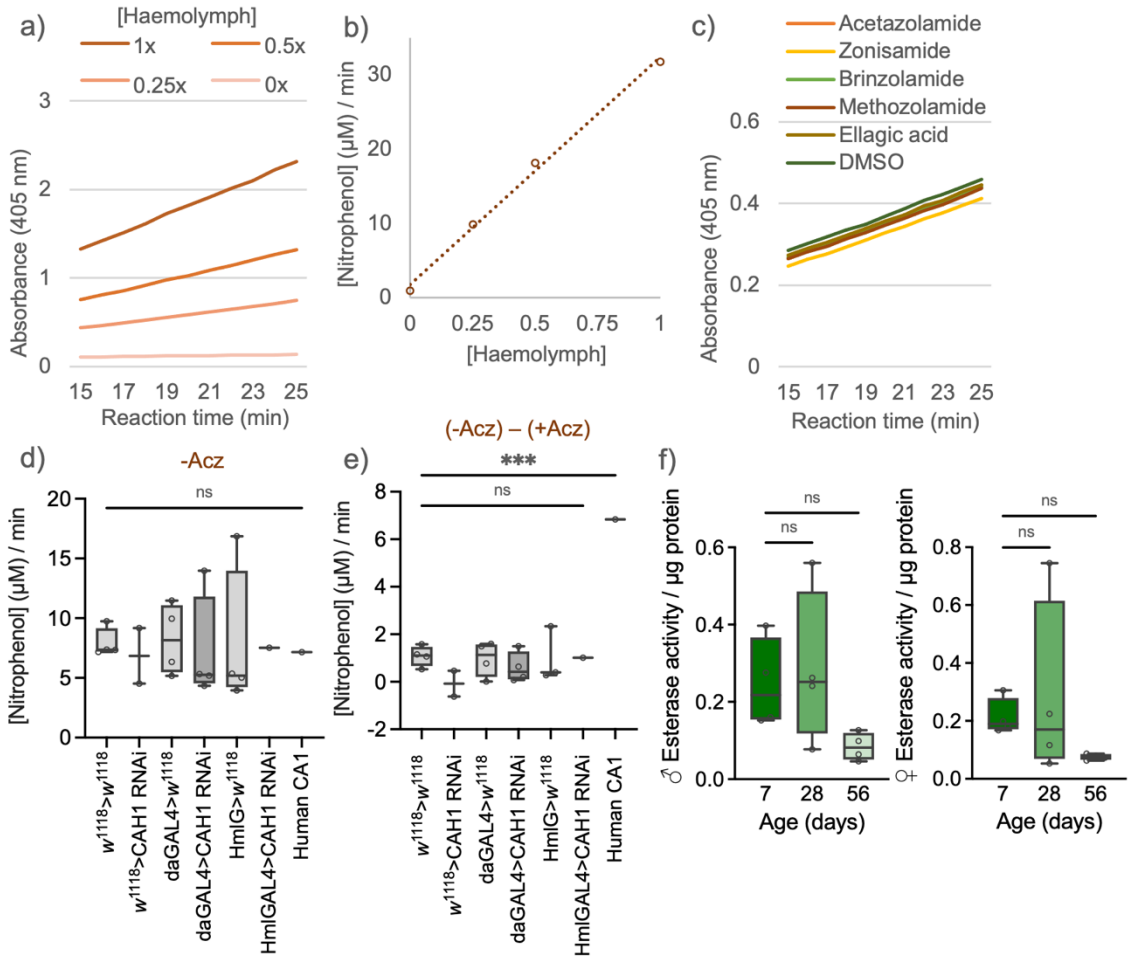


Figure 5.2. CA activity in fly haemolymph: a) Nitrophenol production (absorbance at 405 nm) over time in the linear range dependent on the concentration of serially diluted fly haemolymph; b) Rate of nitrophenol production is linearly dependent on concentration of fly haemolymph; c) The effect of different inhibitors at the highest concentration (1.6 mM) compared to control (DMSO) on nitrophenol production over time in the linear range; d) The rate of nitrophenol production in the absence of inhibitor (1.6 mM Acz) is comparable between

fly haemolymph and positive control (Human CA1), and ubiquitous (daGAL4>CAH1 RNAi) or haemocyte (HmlGAL4>CAH1 RNAi) knockdown of *CAH1* does not alter rate of production compared to the controls; e) The rate of nitrophenol production is fully attributable to CAs in the positive control (i.e., Acz inhibits the reaction) but practically no inhibition occurs in fly haemolymph; f) Rate of nitrophenol production (esterase activity) tends to decrease with age in both male and female fly haemolymph. Data are box-plots of n=1-4 replicates per condition. Statistical analysis was based on ANOVA with Tukey correction for multiple comparisons. ns, $p>0.05$; ***, $p<0.001$.

To test the relative impact of haemolymph CA independently of the inhibitors, *CAH1*, the only CA isoform found in fly haemolymph at the protein level (see Section 5.3.3), was knocked down both ubiquitously and in haemocytes. *CAH1* knock down did not alter the rate of nitrophenol formation (Figure 5.2d). While addition of acetazolamide did not significantly alter esterase activity in any of the fly haemolymph samples, it completely inhibited the activity of human CA1, the positive control (Figure 5.2e). Esterase activity in the positive control can thus be completely attributed to the presence of CA, while in flies the difference between activities by the addition of acetazolamide is negligible (Figure 5.2e), despite comparable esterase activities in the absence of the inhibitor (Figure 5.2d). Although the catalytic pocket responsible for CA esterase activity is the same as for its hydratase activity, the esterase activity has substantially lower reaction rates, even in human isoforms (Piazzetta et al., 2017; Uda et al., 2015). These experiments suggest either: 1) CA activity is disguised by the presence of other proteins with esterase activity in the haemolymph, compared to isolated human CA; or 2) CA inhibitors do not alter fly CA esterase activity. In either case, this assay cannot be used to measure CA activity in flies with age. Esterase activity tends to decline in fly haemolymph with age independently of sex (Figure 5.2f), but whether CA activity contributes to that effect could not be determined.

Given esterase activity can be used to measure CA activity in human plasma, and not just isolated enzymes, human and fly protein sequences were compared to explore whether sulfonamides can effectively bind to and alter CA activity in flies. The sequence of fly CAs was primarily compared to human CA1, used in the assay as positive control. Acz is known to bind human CAs in the catalytic pocket that is conserved in fly isoforms, around Thr199 (Figure 5.3a, yellow arrow) which is needed for the binding (Figure 5.3b). Leu198 interaction, despite weak, also contributes to the

binding of acetazolamide, as does Thr200 (Fisher et al., 2012; Vidgren et al., 1990). Human CA2 binding to acetazolamide is stronger compared to CA1 and CA3 (Vidgren et al., 1990). Given the conservation of these 3 amino acids in the fly CA isoforms and the functional effects of acetazolamide in fly physiology in multiple contexts (Francis et al., 2016; Lu et al., 2019), fly CAs are likely to bind and be inhibited by sulfonamides. The strength of the bond and how it affects esterase activity in the fly is yet to be determined.

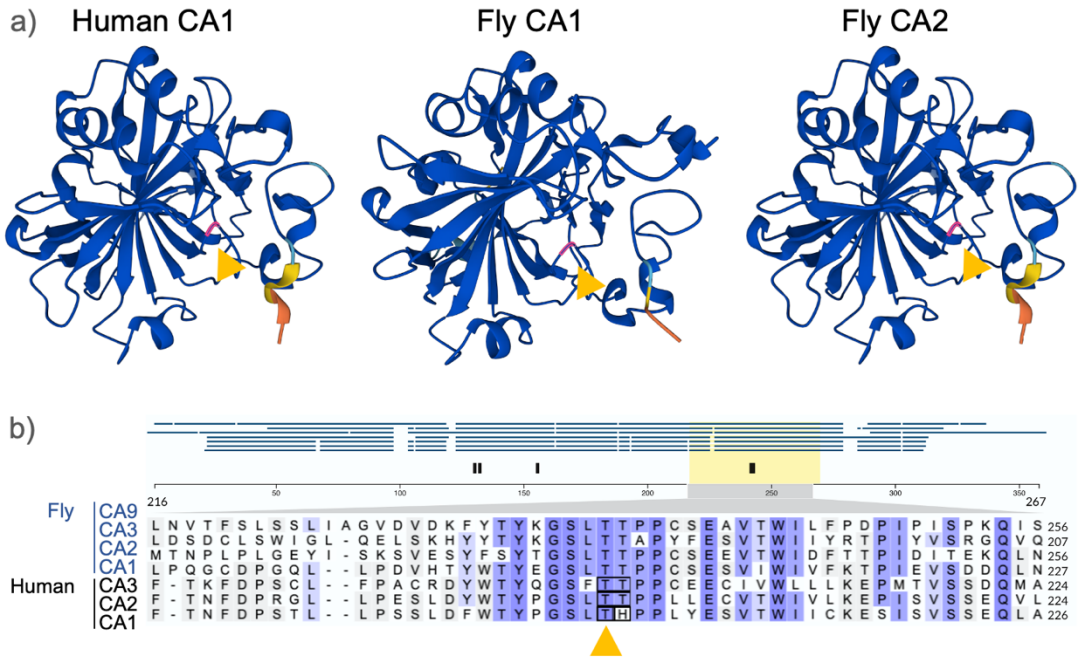


Figure 5.3. Acetazolamide binding site in human and fly CA: a) Modelling of human CA1 compared to fly CA1 and CA2; b) Sequence similarity between selected fly and human CAs shows conserved catalytic pocket, based on UniProt (Bateman et al., 2023); yellow arrow points to Thr199 in the CA catalytic pocket.

Because enzyme activity could not be measured, the next strategy was to identify which isoforms are present in fly haemolymph and alter their expression genetically to assess how it may alter survival in the presence and absence of acidotic stress.

5.3.3. Carbonic anhydrase 1 is present in fly haemolymph

The first step to alter the expression of CAs in the haemolymph was to identify which isoforms were present there. CA 1 and CARPB were previously detected by mass

spectrometry in the haemolymph of *Drosophila* larvae (Handke et al., 2013). In an independent haemolymph proteomics dataset of adult female flies, only CA 1 was present (unpublished data, Cochemé lab).

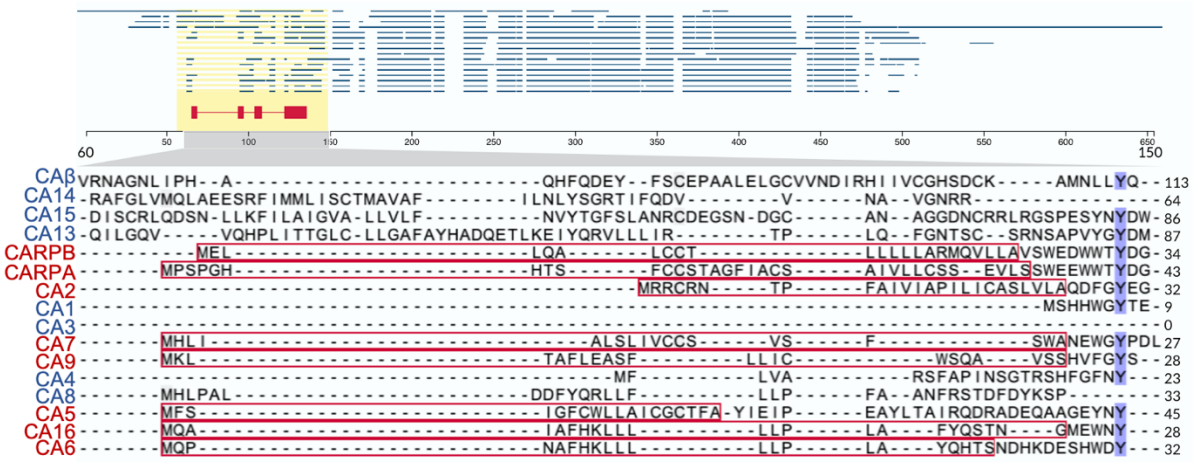


Figure 5.4. Signal peptides in fly carbonic anhydrases. Predicted signal peptides among all fly CAs in red, based on UniProt (Bateman et al., 2023).

To focus the search on CAs and explore how their expression might change with age in the haemolymph, haemolymph proteomics was performed in samples from young, middle-aged and old w^{Dah} males. An *in-silico* digestion (using a tool from expasy.org) prior to the experiment revealed at least one specific tryptic peptide for each of them and multiple for most (Appendix 1). For proteins to be present in the haemolymph they can either be secreted or from within circulating cells. Proteins can be predicted to be secreted by the presence of signal peptides in their sequence. Signal peptides are short sequences that control protein secretion and translocation. Using SignalP 6.0 (Teufel et al., 2022), a machine learning model that detects signal peptides, 8 CA isoforms are predicted to be secreted or translocated (Figure 5.4), and thus could potentially be present in the haemolymph.

Proteomic analysis detected 6 razor and unique peptides of CA 1, correspondent to 26.3% sequence coverage. No other isoforms were detected, including any of the ones predicted to be secreted. Some isoforms may be present in the extracellular portion of specific tissues. Despite their absence in collected haemolymph, they may still impact extracellular acid-base balance in their local microenvironment.

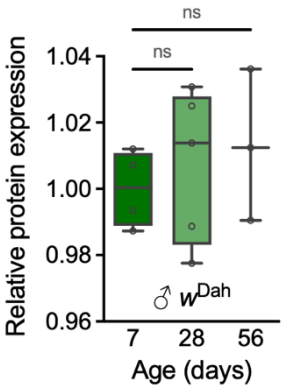


Figure 5.5. CA1 expression in fly haemolymph with age. Relative CA1 intensities detected by proteomics in male w^{Dah} fly haemolymph with age. Data are box-plots of n=3-5 detected CA1 peptides out of n=5 replicates per condition. Statistical analysis was based on ANOVA with Tukey correction for multiple comparisons. ns, p>0.05.

The expression of CA 1 in the haemolymph was found not to change with age in males (Figure 5.5). Other age-related changes on haemolymph proteome are briefly described at the end of this chapter. Because it is not predicted to be secreted or translocated, CA 1 is likely to be present in the cytoplasm of haemocytes. These are cells circulating in the haemolymph which have subpopulations with different functions, primarily innate immune response (Tattikota et al., 2020). Haemocyte CA 1 may be orthologous to the human CA 1 present in erythrocytes, despite the absence of this cell type in flies. Although its expression is unaltered with age, its activity may change. As discussed, measuring CA activity is technically challenging. As an alternative approach to test the effect of CA1 on buffering capacity and how it may alter fly survival given the increased sensibility to acidotic stress with age, the expression of its gene (*CAH1*) in haemocytes was altered.

5.3.4. Changes in *CAH1* gene expression and survival

To drive gene expression changes selectively to fly haemocytes, a haemocyte-specific GAL4 driver was used, hemolectin-GAL4 (Hml-GAL4) (see Section 2.1.4). *Hml* is expressed ubiquitously in haemocytes, particularly in plasmatocyte populations, which constitute over 90% of haemolymph cells (Tattikota et al., 2020). However, it also has low expression in other organs, including the brain, the eye and the fat body (Leader et al., 2018). To control for potential haemocyte-independent effects, a ubiquitous driver, daughterless-GAL4 (daGAL4), was also used. In this driver, GAL4 sits under

the promoter of *da*, a gene with low but ubiquitous expression in the whole fly body. This gene is also present ubiquitously in haemocyte subsets, but in a lower percentage of cells compared to *Hml*, under 40% (Tattikota et al., 2020).

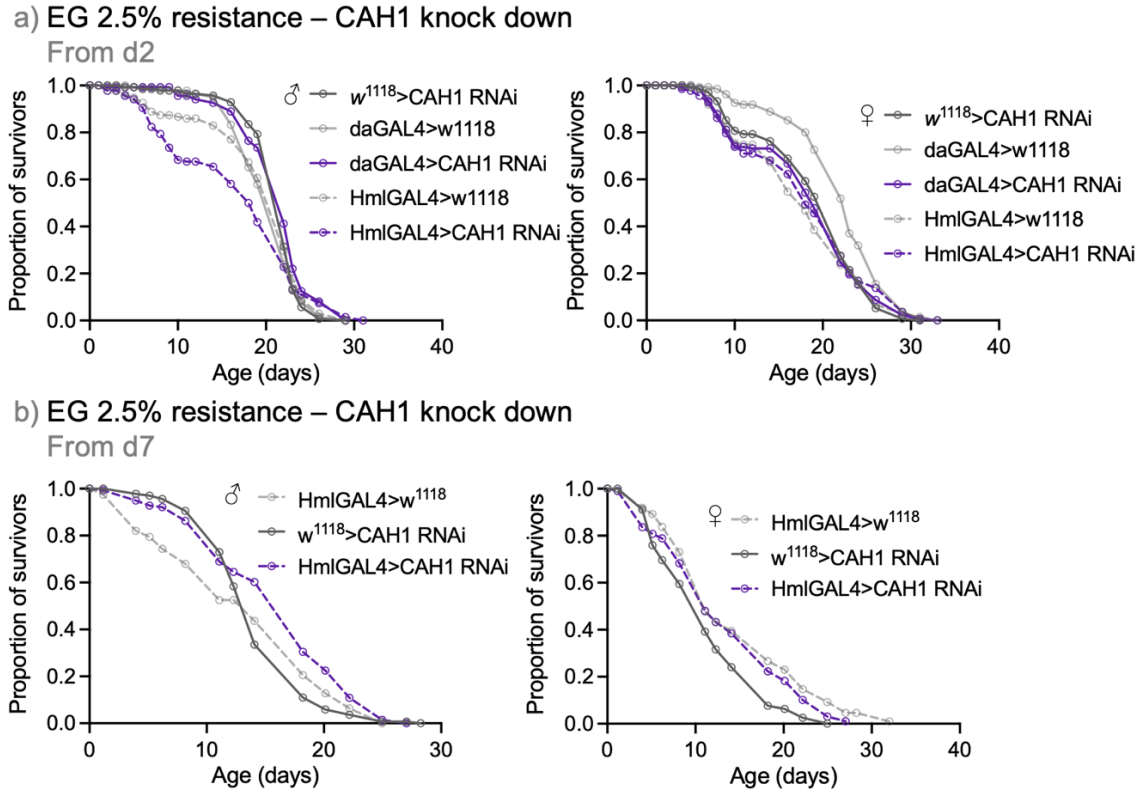


Figure 5.6. Effect of *CAH1* knockdown on acidotic stress resistance. Survival curves of male (left) and female (right) flies in which *CAH1* was knocked down ubiquitously (daGAL4>CAH1 RNAi) or specifically in haemocytes (HmlGAL4>CAH1 RNAi), and their respective controls (in grey), when treated with 2.5% EG from d2 (a) or d7 (b); n=140 flies per condition.

First, given its function as a catalytic factor for the main extracellular buffering reaction, the role of *CAH1* in survival under acidotic stress was assessed. Haemocyte knock down of *CAH1* in male flies seemed to decrease their survival when 2.5% EG was fed from day 2 of life (Figure 5.6a), but this effect was not seen in females, nor was it replicated when acidotic stress when started from day 7 (Figure 5.6b).

The effect of altering *CAH1* gene expression in fly haemocytes and ubiquitously on lifespan was tested next. *CAH1* knock down did not alter the lifespan of male flies compared to the controls (Figure 5.7a). Surprisingly, it extended female lifespan in a haemocyte-dependent manner, since knock down driven by daGAL4 had no effect on survival (Figure 5.7a).

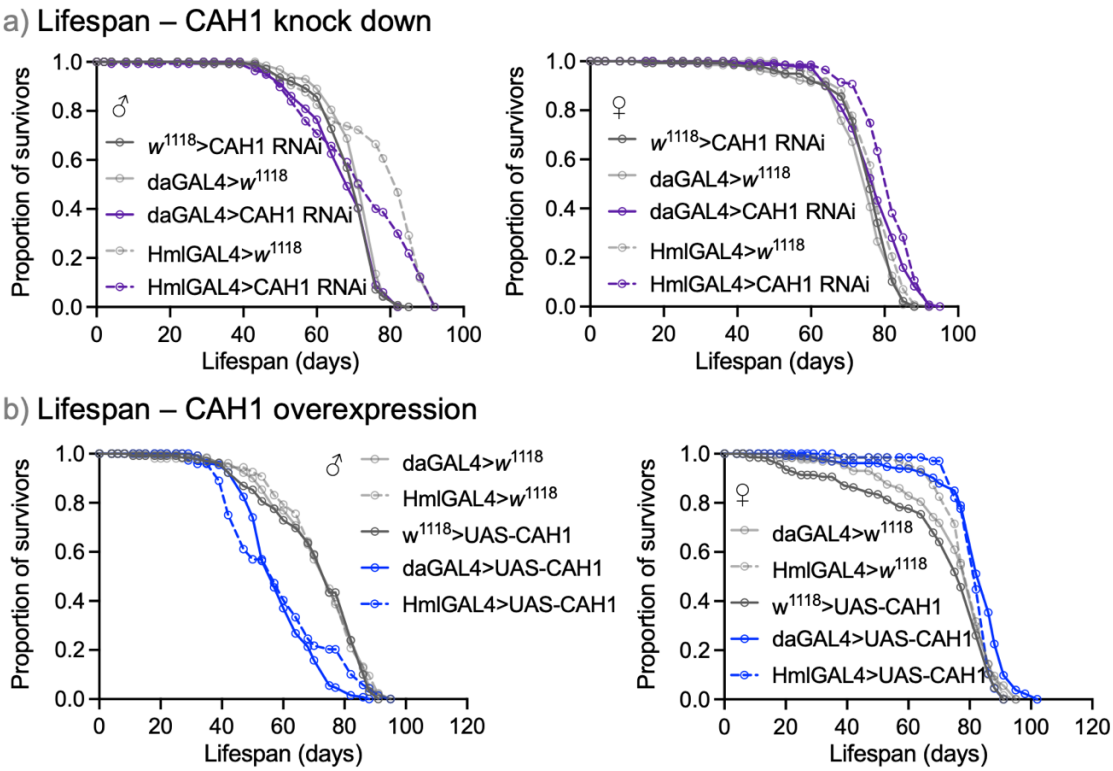


Figure 5.7. Changes in *CAH1* gene expression and lifespan: a) Survival curves of male (left) and female (right) flies in which CAH1 was knocked down ubiquitously (daGAL4>CAH1 RNAi) or specifically in haemocytes (HmlGAL4>CAH1 RNAi), and their respective controls (in grey); b) Survival curves of male (left) and female (right) flies in which CAH1 was ubiquitously overexpressed (daGAL4>UAS-CAH1) or specifically in haemocytes (HmlGAL4>UAS-CAH1), and their respective controls (in grey); n=140 flies per condition.

Conversely, overexpressing *CAH1* in males with either driver significantly shortened their survival to a similar extent (Figure 5.7b). Male-specific shortened survival upon *CAH1* overexpression may be due to the effect of this gene in the fly nervous system, where both drivers can induce its overexpression. *CAH1* expression and CA 1 activity in fly motor neurons was shown to induce locomotor defects as well as to decrease the survival of male flies before (Lu et al., 2019).

Overexpression extended female median lifespan with a comparable effect between both drivers (Figure 5.7b). Given both knocking down and overexpressing *CAH1* resulted in similar lifespan benefits, its effects are likely to be tissue-specific. Because daGAL4-driven overexpression also extended female fly lifespan while knock down had no effect, the lifespan-extending mechanism of *CAH1* overexpression may be haemocyte-independent. Similarly to males, in female flies overexpressing *CAH1* lower locomotor activity was also observed (not quantified), despite their longer

lifespan, which may be attributed to the same neurological effect described in males. However, other factors must benefit the health of females specifically to ultimately extend their survival.

5.3.5. Ubiquitous CAH1 overexpression lowers metabolic rate and fecundity

Consistent with their apparent lower activity, female flies overexpressing *CAH1* ubiquitously seem to have lower metabolic rate (Figure 5.8a). Lower metabolic rate has been correlated with extended longevity across species and is one of the arguments for the rate of living theory of ageing (Hulbert et al., 2007; Pearl, 1928). However, this theory has been challenged over time by many counterexamples, including within the *Drosophila* genus (Hulbert et al., 2004, 2007; Promislow & Haselkorn, 2002). Besides, the observation that males have shorter survival upon *CAH1* overexpression, independently of their lower locomotor activity, suggests a different mechanism for lifespan extension.

One difference that may also justify lower metabolic rate in female flies and has been associated to lifespan extension is their decreased fecundity (Figure 5.8b). This was even more pronounced when the overexpression was driven by Act5CGAL4, a driver with GAL4 under the promotor of the ubiquitous and highly expressed gene *actin 5C* (Figure 5.8b) Reduced energy requirements for producing and laying eggs in female flies may extend their lifespan by allowing energy to be used for somatic cell maintenance instead, in the light of the disposable soma theory of ageing (Kirkwood, 2017; Partridge et al., 1999). Indeed, female fly reproductive trade-off is seen across multiple lifespan-extending interventions, although this can be uncoupled (Bjedov et al., 2010; Mason et al., 2018). Lower metabolic rate associated with decreased fecundity may also decrease feeding and extend lifespan by preventing the side effects of overnutrition (see Chapter 7).

CAHß, another CA isoform, was shown to be required for female fertility, possibly caused by a defective migration of border cells, considered essential for normal egg fertilisation (Syrjänen et al., 2015). *CAH1* is normally not expressed in the ovary. Upon its overexpression driven by daGAL4, it may interfere in this process. However, given *Hml* is also not expressed in the ovary, the effect of *CAH1* overexpression driven by HmlGAL4 cannot be explained by this mechanism.

The benefits of *CAH1* overexpression may thus be related to its overexpression in tissues where both driver-associated genes are normally expressed besides the central nervous system, such as the fat body or the rectal ampulla. Given the potential role of the rectal ampulla in acid-base regulation (Cohen et al., 2020), overexpressing *CAH1* there may promote acid excretion. Beyond acid excretion, which is further explored in the next chapter, *CAH1* may be important for intracellular acid-base homeostasis and promote health that way. Those mechanisms were not explored here but may be interesting to follow up on.

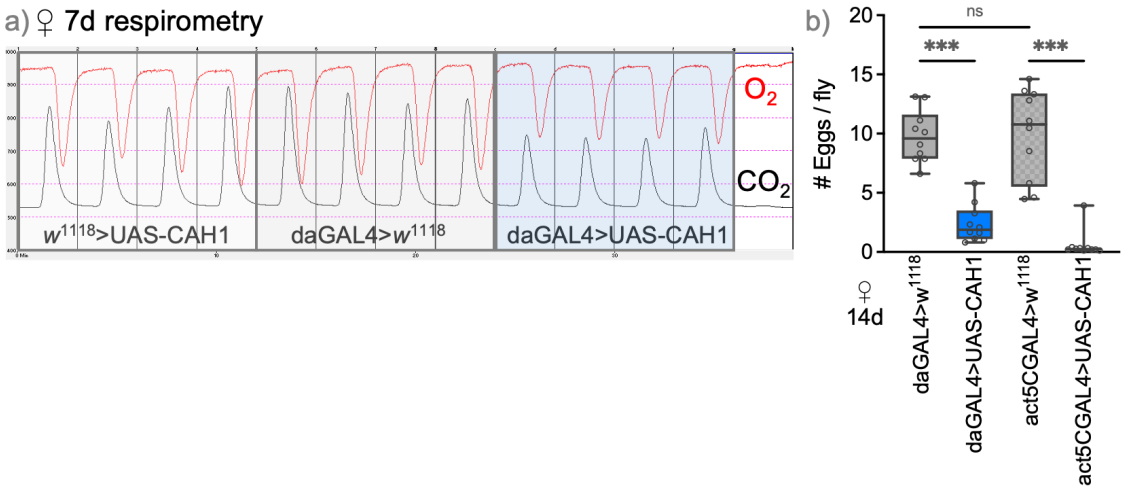


Figure 5.8. Effect of CAH1 overexpression in female fly metabolic rate and fecundity: a) Representative graph of O_2/CO_2 respirometry of 7-day-old female flies in which CAH1 was overexpressed ubiquitously (daGAL4>UAS-CAH1, blue box) and controls (white boxes); each box contains five columns that correspond to 5 replicates (n=3 flies each) of measured O_2/CO_2 peaks after a 48 min cycle; b) Egg laying over 24 h of 14-day-old female flies in which CAH1 was overexpressed ubiquitously with either the daGAL4 (daGAL4> UAS-CAH1) or the act5CGAL4 (act5CGAL4>UAS-CAH1), and respective controls; n=10 groups of 15 flies; Statistical significance was determined by ANOVA with Tukey correction for multiple comparisons; ns, $p>0.05$; ***, $p<0.001$.

5.4. Fly haemolymph proteome changes with age

From the fly haemolymph untargeted proteome analysis used to detect extracellular CAs and their expression with age, age-related changes in the haemolymph proteome were observed and are briefly presented here. Proteomics was performed by Alex Montoya from the LMS Mass Spectrometry Facility. Downstream analysis was started

by Alex Montoya using Perseus software and further analysis was performed with his advice.

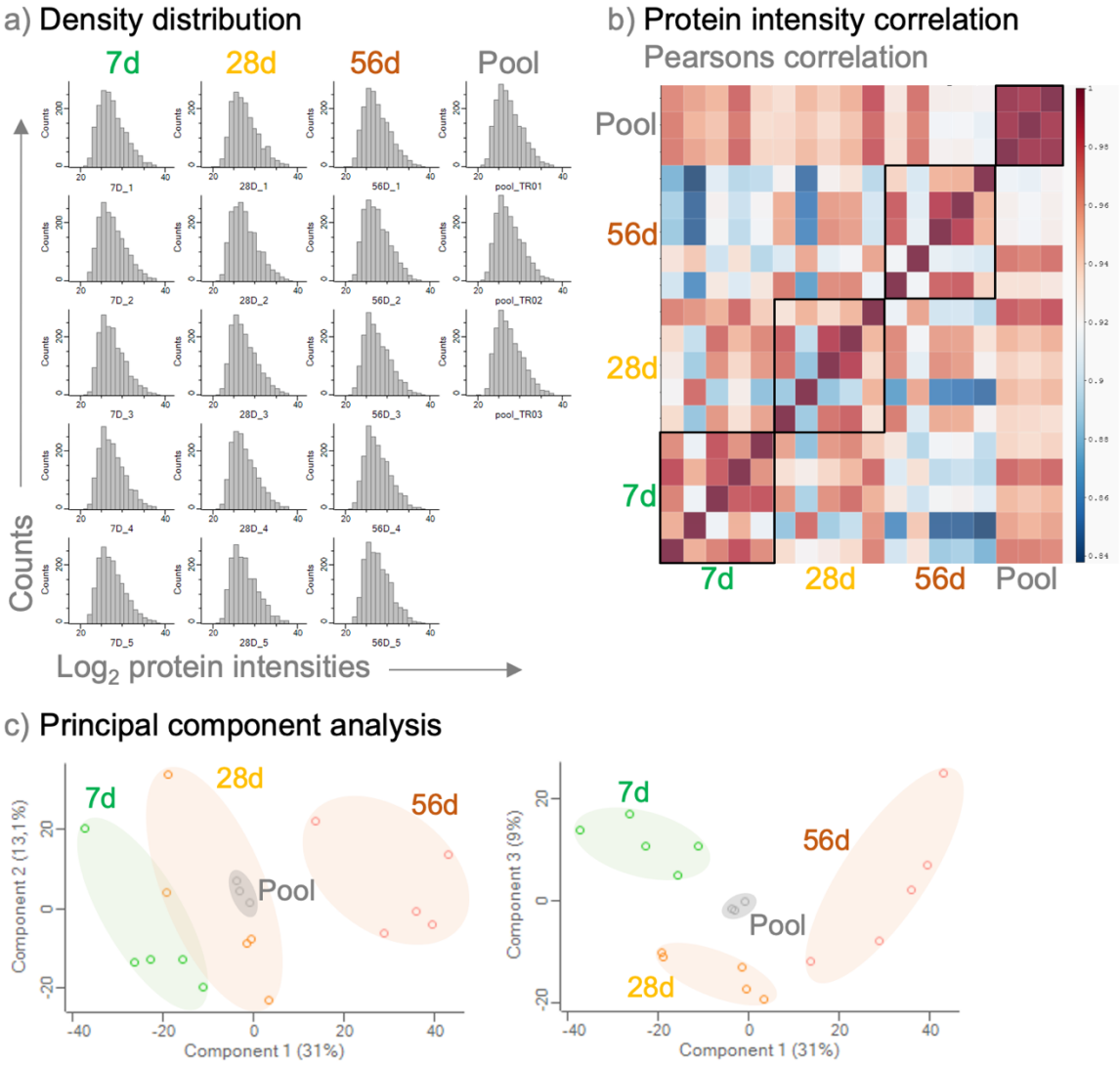


Figure 5.9. Fly haemolymph proteome changes with age: a) Density distributions of protein intensities (log2) for each male w^{Dah} haemolymph sample; b) Heatmap of correlations among (label-free quantitation, LFQ) protein intensities of all samples (Pearsons correlation analysis); c) Principal component analysis of LFQ protein intensities between component 1 and 2 (left), and 1 and 3 (right); drawn areas are merely indicative of age clusters.

There were 2137 proteins detected, 1898 of which with at least 2 razor and unique peptides (i.e., peptides found in different proteins used for the quantification of the protein with the larger number of associated peptides). Globally, there were no missed cleavages in 82.8% of proteins. Both the number of proteins detected and the missed cleavage frequencies per sample were similar across all conditions. The

density distributions of protein intensities were normal and comparable among all samples (Figure 5.9a). Protein intensities generally correlated among samples with of same age group and with samples of pooled haemolymph from the 3 different ages, which later served to normalise protein expression (Figure 5.9b). On principal component analysis, samples of the same age and pooled samples clustered among themselves and these clusters separated by age, indicating differences across all conditions (Figure 5.9c).

5.4.1. Functional analysis of proteome changes with age

After normalising the data to respective mean protein intensity in pooled samples, relative differences across ages were analysed for all proteins (minimum 4 protein intensities out of five replicates per group, FDR=0.05). Clustering the ANOVA significant hits by age group with hierarchical clustering analysis, three different patterns emerge (Figure 5.10a). One where proteins increase with age (cluster A), another where protein expression decreases at 28 days but increases in old age (cluster B), and a third one where protein expression declines with age (cluster C).

To understand the biological role of proteins changing in these patterns, I performed a gene ontology enrichment analysis. By analysing the enrichment of genes related to proteins from each cluster in the KEGG pathway database, proteasome was the only process enriched in both clusters A and B. No pathway was significantly enriched in cluster C. Components of the proteasome are not expected to be present in extracellular fluid, which suggests the expression of proteasome components increase in old age in haemocytes. Given the proteasome is responsible for the targeted degradation of intracellular proteins, its overexpression with age may be a mechanism to deal with the increased number of defective proteins with age. Defective proteins may accumulate with age due to increased rates of translation errors, as shown in the fly before (Martinez-Miguel et al., 2021). It may also occur as a compensatory mechanism as the rate of protein degradation may decline with time due to loss of ability to recognise and degrade proteins. In any case, proteasome function with age may be important to explore further since it shapes innate immune response and effective immune response is important for health and survival (Kammerl & Meiners, 2016).

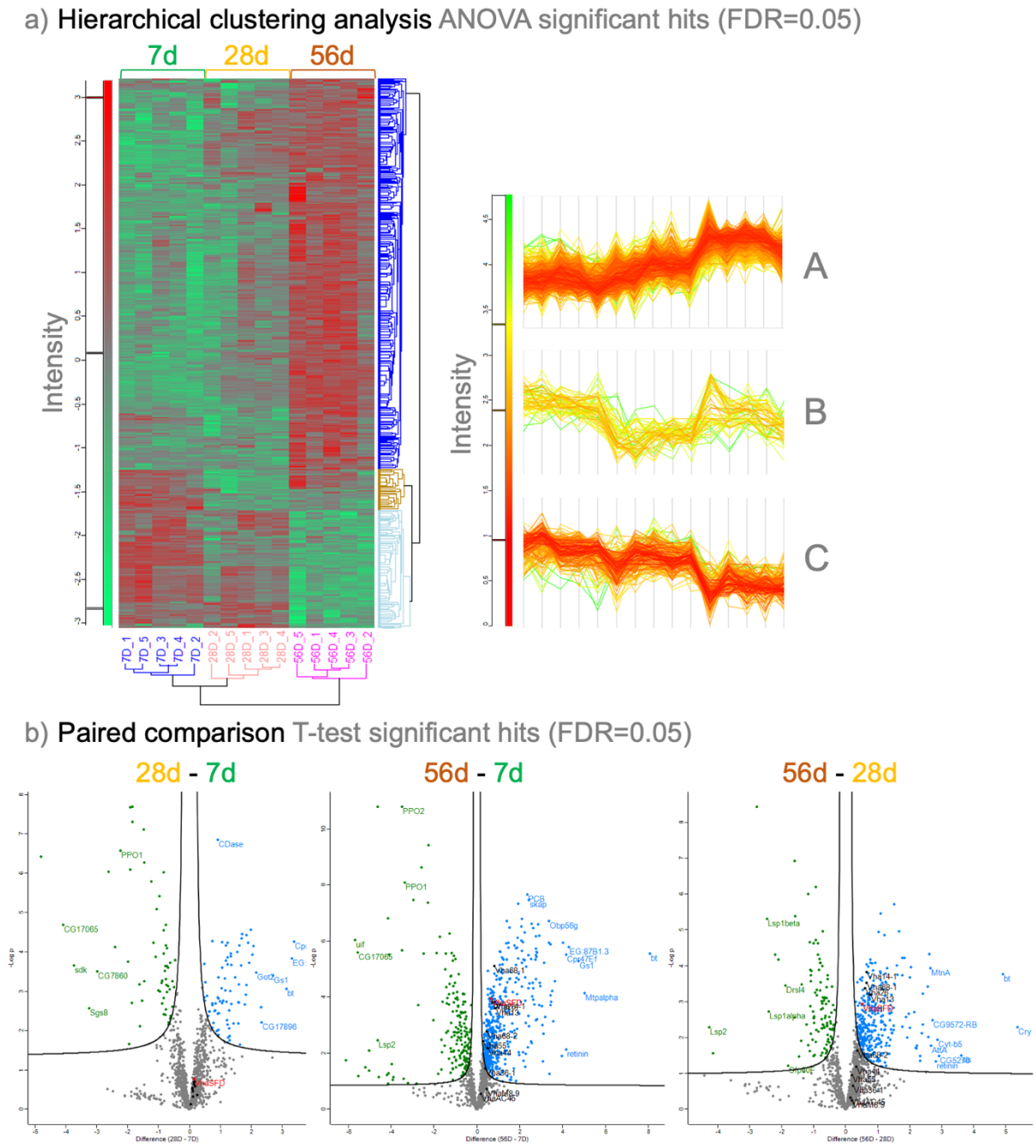


Figure 5.10. Functional analysis of haemolymph proteome with age: a) Hierarchical clustering analysis of proteins whose expression in male *w*^{Dah} fly haemolymph changes with age; ANOVA significant hits, false discovery rate (FDR) =0.05, minimum 4 protein intensities out of five replicates per group; A, B and C are clusters of proteins with the same expression pattern with age; b) Volcano plots of paired comparison of protein expression in the haemolymph of male *w*^{Dah} flies of different ages; t-test significant hits, FDR=0.05, S0=0.1, minimum 4 protein intensities out of five replicates per group.

To further explore age-related changes in proteome, paired comparisons were also performed between two timepoints by t-test (FDR=0.05). In old age compared to

either young or middle-age, fly haemolymph has significantly higher expression of several v-ATPase subunits (Figure 5.10b). These proteins are further explored in the next chapter in the context of acid excretion, but in haemocytes they may be more relevant from a proteostasis perspective, and their expression changes in the same direction as components of the proteasome. V-ATPase pumps protons into the lysosomal lumen within cells whose internal low pH activates hydrolytic enzymes and is crucial for macroautophagy of intracellular components and digestion of extracellular materials (Eaton et al., 2021). Both loss of proteostasis and disabled macroautophagy are primary hallmarks of ageing (López-Otín et al., 2023). Exploring the role of both proteasome components and v-ATPase subunits in haemocytes and how it changes with age may thus be an important avenue of research to find new strategies to maintain immune function with ageing.

5.4.2. Exploring the role of v-ATPase changes in haemocytes

As a preliminary exploration of the role of v-ATPase in haemocytes, the regulatory subunit of v-ATPase encoded by the fly *VhaSFD* gene was overexpressed in haemocytes. No effect on survival was observed (Figure 5.11), which suggests the naturally occurring overexpression of v-ATPase subunits with age may not alter survival outcomes. However, a deeper study of the role of v-ATPase in haemocytes may lead to the discovery of new targets to maintain immune function and health over the lifespan.

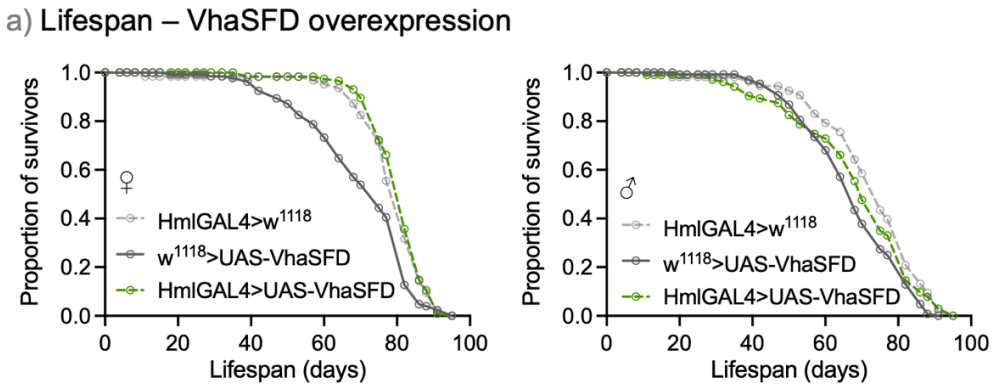


Figure 5.11. Changes in haemocytes *VhaSFD* gene expression and survival. Survival curves of female (left) and male (right) flies in which *VhaSFD* was overexpressed specifically in haemocytes (HmlGAL4>UAS-VhaSFD), and respective controls (in grey); n=140 flies per condition.

5.5. Key messages and interpretation

In this chapter, fly haemolymph was analysed both in terms of its buffering capacity and its proteome changes with age. The key messages are:

- Measuring carbonic anhydrase activity in fly haemolymph may not be feasible
- CA 1 is the only isoform detected in fly haemolymph at the protein level
- Expression of CA 1 does not change with age
- *CAH1* knockdown in haemocytes does not consistently alter fly sensitivity to acidotic stress
- *CAH1* overexpression shortens male fly survival, but extends the lifespan of female flies, likely in a haemocyte-independent manner
- Haemolymph proteome changes with age and reveals increased expression of proteostasis- and macroautophagy-related proteins in old age

From these results, it is unclear whether haemolymph buffering capacity changes with age. Further experiments are also needed to dissect how it may impact acidotic stress resistance and survival.

The activity of CAs, the enzymes that catalyse the principal buffering reaction in the haemolymph, could not be assessed and may prove unfeasible from a practical perspective. Although not technically impossible, high volumes of haemolymph would be needed to directly measure CO_2 hydration with an electrometric method and a new setting would be needed to optimise it for lower volumes. Given the electrometric method is based on pH changes over time, a microelectrode would be needed to measure haemolymph pH in the microliter range in a stable manner. The lowest volume of sample a commercially available microelectrode can measure the pH of currently is 0.5 µL (9810BN, Thermo Scientific). We tested this microelectrode in fly haemolymph and found it technically challenging to submerge the electrode in samples and get consistent readings. In this lower volume range, pH measurements are less accurate and precise. The whole setting would need to be adapted to those volumes and the haemolymph isolated from room air, which would be particularly difficult.

Other experiments can be tried to explore haemolymph buffering capacity more generally, such as an adapted form of titration. Again, given the haemolymph sample volumes in the microliter range, classical titration experiments would be challenging. However, using a narrow range pH-sensitive dye, it may be possible to mix

haemolymph with a low molarity strong anion (e.g., HCl) solution of known pH and infer the relative buffering capacity by measuring how much the pH of haemolymph changes after the addition of a strong acid.

In this chapter, CA 1 was shown to be the only CA isoform detected in the haemolymph at the protein level by proteomics. Surprisingly, in an in-depth study of larval haemolymph cell populations and their gene expression, *CAH1* is reported to be expressed in less than 1% of specific haemocyte clusters (Tattikota et al., 2020). Conversely, *CAH2* is expressed in 37% of cells of a specific crystal cell cluster (CC2), *CAH3* is expressed in 10-20% of all haemocyte clusters, *CARPB* and *CAHß* in less than 2% of most clusters, and *CAH7* and *CAH13* in less than 1% of specific clusters. No other isoform is expressed in any of the clusters of this dataset (Tattikota et al., 2020). Even though this dataset is from larval haemolymph, it suggests that other undetected CA isoforms may be present in adult haemocytes.

The expression of *CAH2* in a crystal cell cluster is particularly interesting. This cluster, CC2, is defined mainly by the presence of the enzymes prophenoloxidase 1 and 2 (PPO1 and PPO2). These two enzymes are important for melanisation, a form of innate immune response in flies, and critical for survival upon wounding in both larvae and adults (Tattikota et al., 2020). Interestingly, PPO1 and PPO2 are two of the proteins whose expression most significantly decreases with age in the haemolymph proteome (Figure 5.10b). This suggests either their translation or degradation is altered with age, or crystal cells are lost with age. If the latter is true, then the expression of CA 2 in haemolymph may also decrease and impair its potential buffering capacity. The role of PPO1 and PPO2 loss in immune dysfunction with ageing and their potential interaction with CA 2 should be explored.

In light of this study and given the inconsistent role of modulating *CAH1* on fly lifespan, potential benefits of overexpressing *CAH1* beyond haemocytes should be tested. In the next chapter, I discuss its role in tubule-specific acid excretion, but studying its function in the rectal ampulla and in the fat body may be interesting. CA 1 may have a tubule-independent role in acid excretion or catalyse intracellular reactions that maintain metabolic homeostasis. *CAH1* overexpression may also have a supraphysiological effect in haemocytes by increasing buffering capacity in cells where a cytoplasmatic CA may be lacking or lowly expressed.

Whether extracellular buffering capacity is lost with ageing needs to be explored further. However, independently of acute buffering and resilience upon acidotic stress,

chronic acid-base changes in extracellular fluids likely occur due to insufficient acid excretion with or without associated increased acid production. These factors are explored in the next chapters.

Chapter 6. Excretory regulation of acid-base balance

6.1. Introduction

Independently of buffering, for haemolymph acidification to chronically occur, insufficient rates of acid excretion for a given rate of endogenous acid production are necessary. Here, I discuss the role of fly excretory tract physiology on acid excretion and explore how different theoretically required proteins affect survival.

6.1.1. *Drosophila* excretory system

Similar to other insects, the fly excretory tract is composed of two pairs of Malpighian tubules, the hindgut and the rectal ampulla (Figure 6.1).

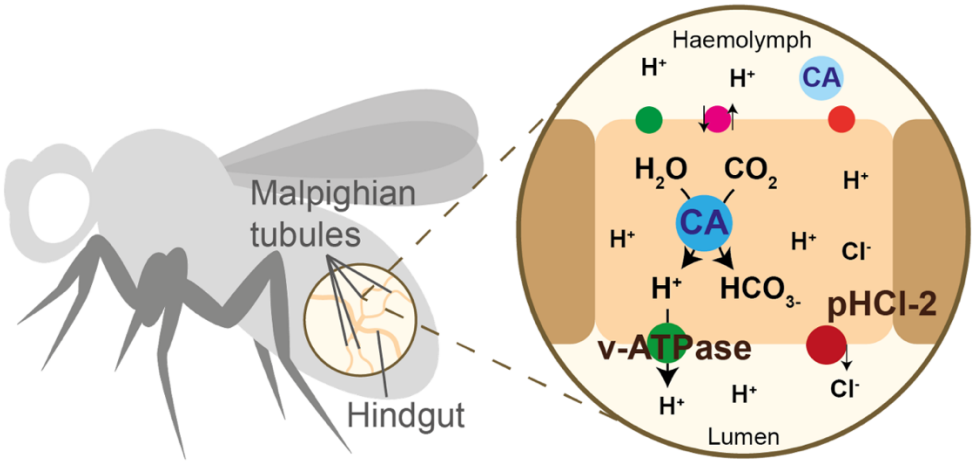


Figure 6.1. Fly excretory system and proteins of interest. Malpighian tubules join with the fly intestinal tract at the midgut-hindgut junction. The tubule epithelium contains proteins that are either conserved in mammals (e.g., CA, v-ATPase) or have equivalent functions (e.g., pHCl-2, chloride transport) proposed to be essential for active acid excretion.

The fly excretory tract performs comparable functions to mammalian kidneys: osmoregulation, ionic homeostasis, clearance of xenobiotics and excretion of metabolic waste products. There are two main anatomical differences that make its physiology substantially different from mammals: 1) Malpighian tubules, seen as orthologous to kidney tubules, are attached to the intestinal tract, at the midgut-hindgut junction (Figure 6.2a); and 2) Malpighian tubules are not preceded by filtering units and their cells are joined by septate junctions that close the paracellular space (Cohen

et al., 2020). Respectively, these implicate that: 1) fly excreta are a combination of urine produced by the tubules with digestion waste from the intestinal tract; and 2) haemolymph is not filtered and active secretion of molecules must occur.

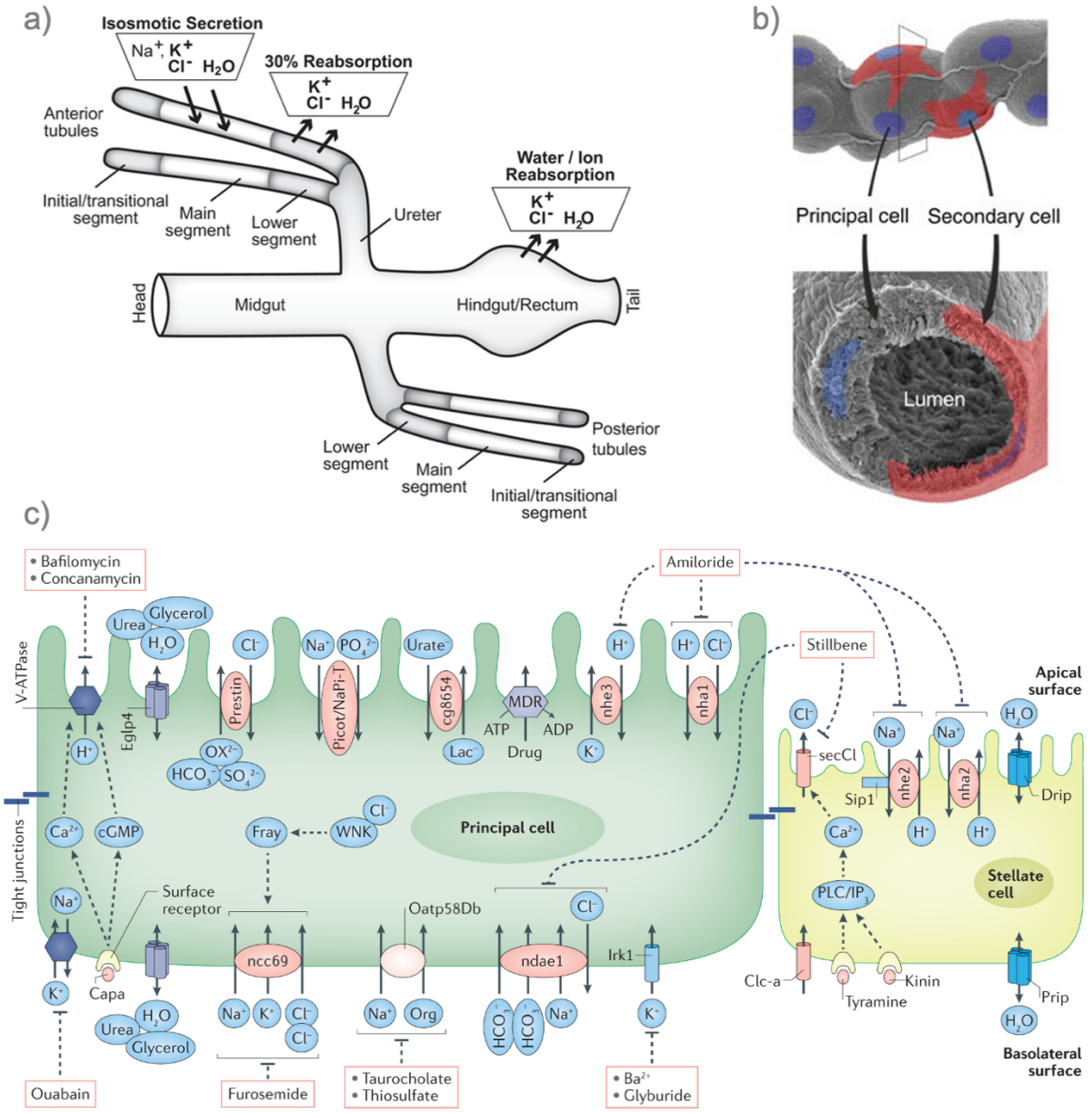


Figure 6.2. General physiology, cell composition and function of the fly excretory tract: a) Scheme of spatial secretion and reabsorption of water and strong ions (Rodan, 2019); b) Cellular composition of the Malpighian tubules, secondary cells are either stem or stellate cells (Halberg et al., 2015); c) Diagram of transport proteins and ion channels expressed in the two main Malpighian tubule cell types whose function is similar to those expressed in the mammalian kidney tubule, pharmacological inhibitors in red boxes; Capa, cardio acceleratory peptide 2b; Clc-a, Cl^- channel protein 2; Eglp4, entomoglyceroporin 4; IP_3, inositol trisphosphate; Irk1, inwardly rectifying potassium channel 1; Lac^-, lactate; MDR, multidrug

resistance protein homologue; NaPi-T, Na^+-dependent inorganic phosphate cotransporter; ncc69, Na^+/Cl^- cotransporter; ndae1, anion exchange protein; nha, Na^+/H^+ hydrogen antiporter; nhe, Na+/H+ exchanger; Oatp58Db, solute carrier organic anion transporter family member; Org, organic anions; OX^{2-}, oxalate; Picot, putative inorganic phosphate cotransporter; PLC, phospholipase C; secCl, secretory Cl^- channel (Dow et al., 2022).

Tubular secretion happens through different mechanisms depending on the type of molecule. Metabolites, xenobiotics and some ions use membrane transporters which either facilitate their diffusion into the tubules or work by exchanging ions with the same charge (Cohen et al., 2020). Other ions, such as H^+, Na^+ and K^+ can also be transported through active pumps (Figure 6.2c). Water passively follows the osmotic gradient transcellularly to produce an isosmotic filtrate (Nocelli et al., 2016). Water and electrolytes can be reabsorbed downstream, mainly at the rectal ampulla, although the lower segment of the tubule can also reabsorb water and K^+ (O'Donnell & Maddrell, 1995).

Malpighian tubules are composed of a single epithelial layer with three main types of cells: principal, stellate and stem cells (Figure 6.2b). Principal cells have different subpopulations that can be divided according to their location along the tubules (J. Xu et al., 2021). Fluid secretion results from cooperation between principal and stellate cells (Cohen et al., 2020; Nocelli et al., 2016). In principal cells, apical vacuolar-type ATPase (v-ATPase) is thought to be the force behind strong ion secretion by pumping H^+ into the lumen, generating apical membrane voltages above 100 mV and creating a proton gradient that drives Na^+ and K^+ secretion through antiporters. Chloride is then secreted primarily by stellate cells to maintain electrical neutrality, while water secretion is driven by increased lumen osmolarity. In principal cells, mitochondria are located in the apical border and are an essential source of ATP for v-ATPase function (Beyenbach, 2001). In support of this view, both v-ATPase inhibition (by bafilomycin) and inhibition of mitochondrial ATP production (by different strategies) stop electrogenesis and transmembrane transport, thus inhibiting fluid secretion (Beyenbach, 2001; Maddrell & O'Donnell, 1992).

The regulation of epithelial transport can occur either through intrinsic mechanisms or in response to circulating messengers, such as hormones, but not through neuronal cues, as Malpighian tubules are not innervated (Nocelli et al., 2016). Capa proteins, for example, bind to their receptor in principal cells and induce cyclic

GMP and ATP production which activate the apical v-ATPase (Cohen et al., 2020; Terhzaz et al., 2006). Kinin is a diuretic ligand for stellate cells, and raises transcellular chloride flux by targeting Clc-a and SecCl channels (Cabrero et al., 2014; Feingold et al., 2019; O'Donnell et al., 1996).

6.1.2. Fly excretory system in acid-base regulation

The different excretory physiology will necessarily result in different acid-base regulation by these organs compared to humans. However, the essential components, the membrane proteins responsible for ion exchanges, are either conserved or have orthologous counterparts in flies.

Acid-base physiology in flies is not fully understood. Mechanisms are often inferred from studies in other insects, such as locusts (Harrison, 2001). Studies on the expression of transporters in the excretory tract have given circumstantial evidence into where they are located and what that might imply for physiology (Wang et al., 2004). Reviews of fly tubule physiology usually adopt a descriptive view on acid-base and argue that protons pumped by v-ATPase at the apical membrane of principal cells can alter lumen pH *per se* (Cohen et al., 2020; Dow et al., 2022).

From a quantitative perspective, the fly excretory tract can regulate acid base balance only by changing either SID or $[A_{tot}]$ (Kellum & Elbers, 2009), excluding partial pressure of CO_2 given the open respiratory system, as previously discussed (Section 4.1). SID can be affected by Na^+, K^+ and Cl^- channels, as well as transporters of molecules that act as strong anions, such as lactate or sulphate. A_{tot} can be regulated by transport of weak anions, such as phosphate. *Drosophila* has tubular channels capable of transporting all of these variables (Dow et al., 2022; Wang et al., 2004) and acid base balance is likely to result from their combined effects.

Supporting this perspective, interventions that selectively slow strong cation secretion in the Malpighian tubules of another insect cause the secreted fluid to become alkaline, while those that selectively diminish the rate of strong anion transport result in secretion of acidic fluid (Maddrell & O'Donnell, 1992). Strong ion secretion in both cases is driven by v-ATPase stimulation (Maddrell & O'Donnell, 1992).

Because of the primary role of Na^+ on extracellular fluid volume regulation, manipulation of Cl^- excretion is theoretically the only mechanism the excretory tract has to effectively alter haemolymph SID and therefore haemolymph pH, in conditions

where the concentration of other strong anions is negligible. Cl^- secretion in fly tubules is promoted by CAs and by v-ATPase (O'Donnell et al., 1996; Wessing et al., 1997). Interestingly, in the *Drosophila* midgut, all three components were shown to be needed for acid excretion, as individually knocking them down or pharmacologically inhibiting them was sufficient to alkalinise the lumen pH of the acidic copper cell region (Overend et al., 2016; Shanbhag & Tripathi, 2009).

Here, I hypothesise that CAs, the proton pump v-ATPase, and the chloride exchange channel pHCl-2 are the components of a main axis needed to regulate acid-base status in the fly. Indeed, these three components are either conserved or have human orthologues that act co-dependently and whose deficiency in intercalated cells in the collecting tubules of kidneys is known to cause distal renal tubular acidosis (Batlle & Haque, 2012). Each of their roles is explored in the respective sections below.

6.2. Acid excretion capacity with age in *Drosophila*

First, to have an overview of how total acid excretion might change with age, flies were fed a pH-sensitive dye at different ages throughout their lifespan and their excreta were analysed. The more acidic the excreta, the lower their hue becomes, as the colour of the dye changes towards yellow (Cognigni et al., 2011; Wayland et al., 2014). Since haemolymph acidifies with age, it would be expected that the excretory tract would increase the amount of excreted H^+ as a compensatory mechanism if increased net acid production was driving acidification. Instead, excreta pH increased with age in both sexes (Figure 6.3a-b), while the number of deposits declined over time (Figure 6.3c-d). This loss-of-function may be related to increased tubular lithiasis with age (Figure 6.3e), which will be further explored in the next chapter.

These observations suggest that acidification is necessarily a consequence of insufficient acid excretion, independently of potential simultaneous increased rate of production. Not only is the excretory system not compensating for increased haemolymph $[H^+]$, it is also contributing to it by lowering acid excretion, especially in old age (Figure 6.3f).

Loss of tubular function also occurs with age in humans (Denic et al., 2016), and may be responsible for chronic acid-base imbalance in old age (Banerjee et al., 2023; Frassetto et al., 1996, 2020). Remarkably, in patients with pathological renal loss of function, metabolic acidosis is a predictor of bad prognosis, being associated

with higher mortality (Kovesdy et al., 2009). As discussed later and proposed before, besides its acute life threatening effects when severe, acidosis may increase mortality chronically by accelerating other ageing processes (Frassetto et al., 2020).

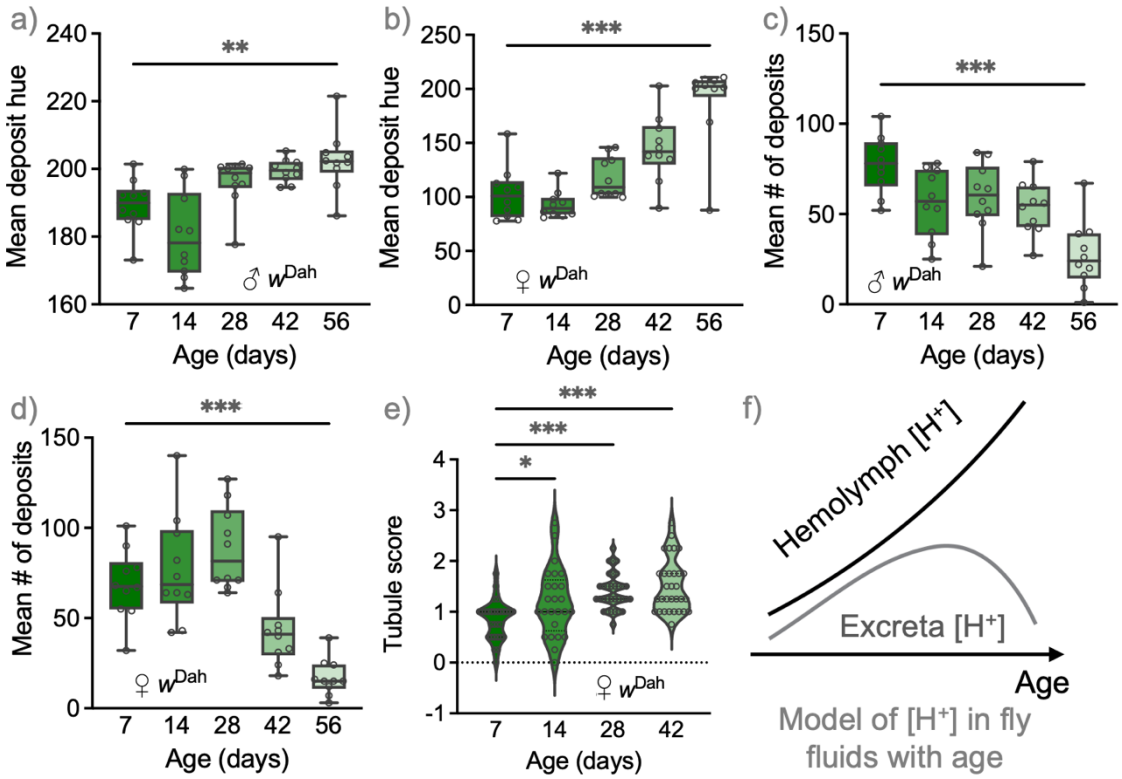


Figure 6.3. Functional assessment of the fly excretory tract with age. Poo plates analysis of mean hue (a,b) and deposit number (c,d) of excreta from male (a,c) and female (b,d) *w*^{Dah} flies, n=10 plates with 5 flies each; e) Tubule scoring of female *w*^{Dah} flies, n=25-32 dissected flies per condition; f) Representation of changes in [H$^+$] in fly fluids with age. Statistical significance determined by ANOVA with Tukey correction for multiple testing; ns, p>0.05; *, p<0.05; **, p<0.01; ***, p<0.001.

Understanding how the excretory system becomes insufficient at excreting H+ with age may reveal new preventive strategies to maintain acid-base balance with age. Hereafter, I explore how proteins important for excretory acid base regulation may drive these changes and affect survival.

6.3. Genetic modulation of acid excretion and survival

As proposed, three different types of proteins may be particularly significant for tubular acid excretion: CAs, v-ATPase and pHCl-2. To explore their potential role in age-

related tubular insufficiency, their gene expression was measured in young, middle-aged and old flies. To test their relative importance in maintaining acid-base balance, their expression was modulated in flies exposed to acidotic stress. Finally, given the potential impact of acid-base balance on survival, the effect of their overexpression on lifespan was measured.

6.3.1. Expression of CAs in fly tubules with age

As discussed in the previous chapter (Section 5.2.2), CAs are essential catalytic enzymes for the carbonic acid-bicarbonate buffering system. In the kidney, they are also important to maintain acid-base balance either by allowing the reabsorption of HCO_3^-, in the descriptive view (DiBartola, 2012), or by promoting Cl^- secretion, in Stewart's model (Kellum & Elbers, 2009). Mammalian CA 2 is highly expressed in kidney intercalated cells and at lower levels in the proximal tubules, loop of Henle, and collecting duct principal cells (Frost, 2014). Its deficiency in humans causes renal tubular acidosis (Sly et al., 1983).

In *Drosophila*, four CA isoforms are expressed in the excretory tract according to the FlyAtlas2 database: *CAH1*, *CAH2*, *CAH3* and *CAH9* (Figure 6.4a, Table 4). CA 1 is cytoplasmatic, while the others are predicted to be located in the plasma membrane (Bateman et al., 2023). Based on qPCR analysis, I found that their expression tends to change in whole flies with age (Figure 6.4b). Whole body expression of *CAH1* and *CAH3* tends to increase with old age, while *CAH2*, the isoform more specifically expressed in both the tubule and the midgut, the two organs where acid excretion occurs, tends to decrease with age. Lower *CAH2* expression specifically in the tubules also seems to occur. Conversely, *CAH3* expression increases with age in the excretory tract, which might be a compensatory mechanism for the loss of *CAH2*, given that both are membrane-bound. Interestingly, contrary to its expression in whole flies, *CAH1* tends to decline with age in the excretory tract.

In light of these results, I focused on CA 1 and CA 2 as the cytoplasmatic and membrane-bound duo theoretically needed for acid excretion in the tubules. *CAH1* shares a common ancestor with mammalian cytoplasmic CAs, whereas *CAH2* descends from the same ancestor as mammalian membrane-bound extracellular CAs (Syrjänen et al., 2013). Since CAs in both cellular locations are needed for effective acid-base regulation, they may have co-evolved.

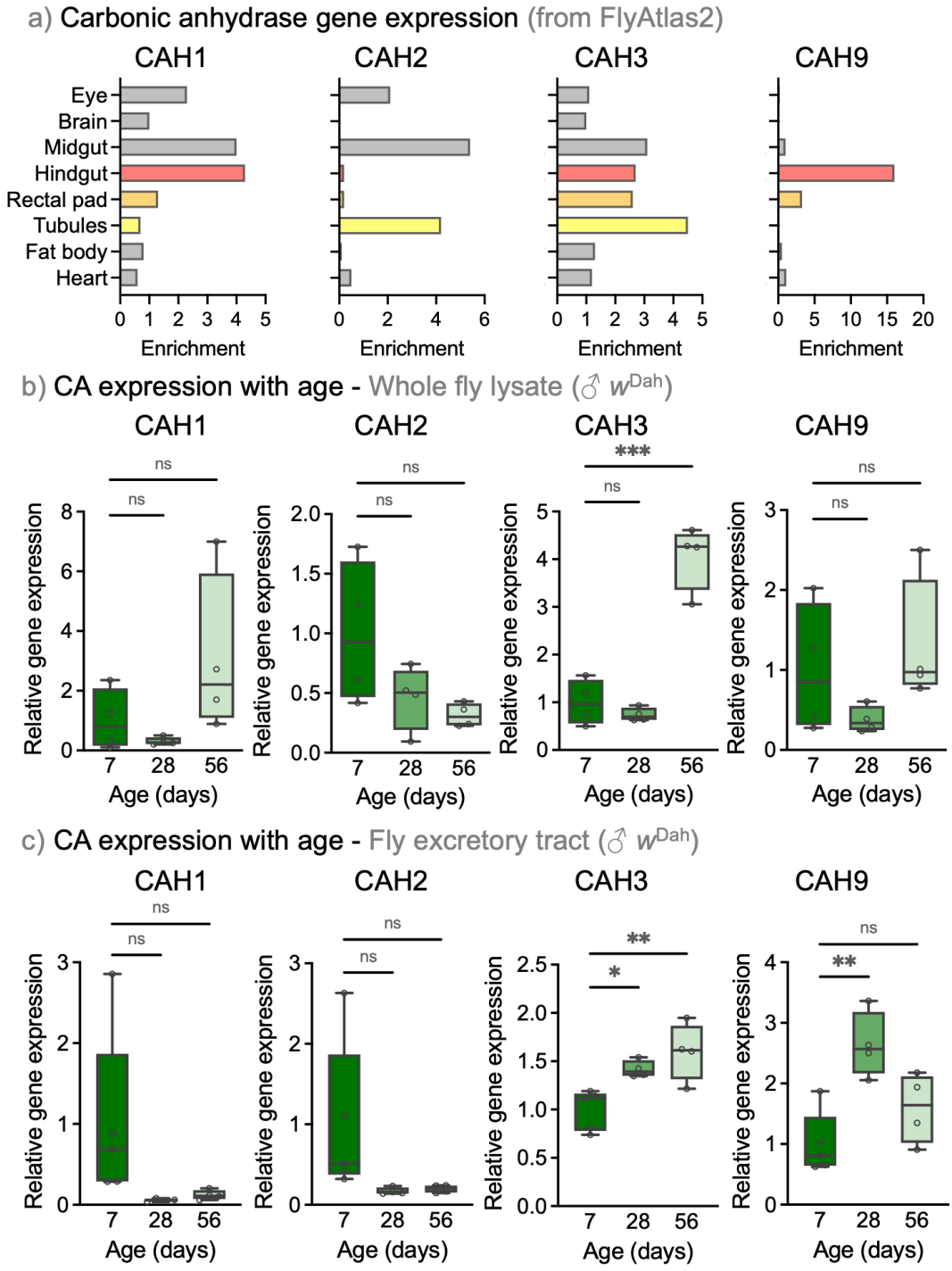


Figure 6.4. CA distribution and changes in gene expression with age: a) Expression profile of selected CAs enriched in the fly excretory tract in male flies (Leader et al., 2018); b) qPCR analysis of CAs gene expression in whole fly lysates of w^{Dah} males with age, n=4 replicates per condition; c) qPCR analysis of CAs gene expression in homogenates of dissected excretory tracts of w^{Dah} male flies with age, n=4-5 replicates per condition. Statistical significance was determined by ANOVA with Tukey correction for multiple comparisons; n/s, p>0.05; *, p<0.05; **, p<0.01; ***, p<0.001.

6.3.2. Tubule-specific expression of CA genes and survival

To test whether a potential loss of *CAH1* and *CAH2* expression with age in the Malpighian tubules can impact haemolymph pH *per se*, these genes were individually knocked down and overexpressed using a tubule-specific driver, urate oxidase-GAL4 (uroGAL4), and their role on survival upon acidotic stress was tested.

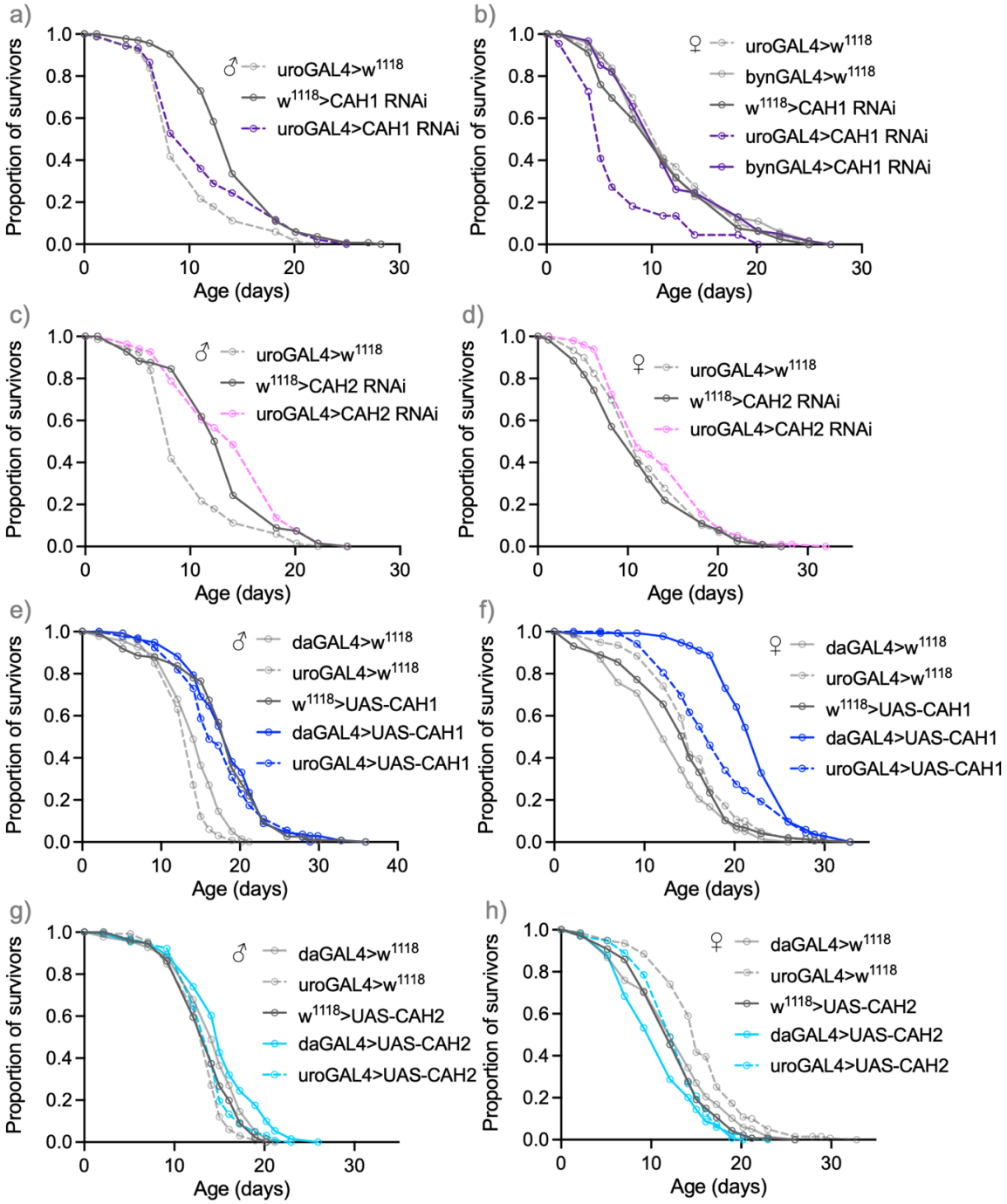


Figure 6.5. Acidotic stress resistance upon changes in expression of CAH1 and CAH2. Survival curves under acidotic stress (2.5% EG) from d7 of male (a,c,e,g) and female (b,d,f,h) flies in which either CAH1 (a,b) or CAH2 (c,d) were knocked down in the Malpighian tubules

(uroGAL4>CAH1 RNAi; uroGAL4>CAH2 RNAi; a-d) or in the hindgut (bynGAL4>CAH1 RNAi; b), and their respective controls (in grey; a-d); or overexpressed either ubiquitously (daGAL4>UAS-CAH1; daGAL4>UAS-CAH2; e-h) or in the Malpighian tubules (uroGAL4>UAS-CAH1; uroGAL4>UAS-CAH2; e-h) and their respective controls (in grey; e-h); n=140 flies per condition.

Knocking down *CAH2* in the tubules did not alter fly resistance to acidosis (Figure 6.5c-d), and neither did *CAH1* knock down in males (Figure 6.5a). In females, lowering *CAH1* in the tubules decreased survival under EG-induced stress (Figure 6.5b). Given its higher expression in the hindgut, a hindgut-specific driver, bynGAL4, was also used to drive *CAH1* to that portion of the excretory tract. There, *CAH1* knockdown had no effect on survival.

In a similar pattern, either overexpressing *CAH2* in both sexes or *CAH1* in males did not alter the outcome of flies under acidotic stress (Figure 6.5e, g-h). Conversely, *CAH1* overexpression in fly tubules extended female survival under those conditions (Figure 6.5f). Interestingly, ubiquitous *CAH1* overexpression in female flies resulted in even longer survival under acidotic stress which correlates with extended lifespan in control conditions (Figure 5.7b). *CAH1* ubiquitous knockdown did not alter EG resistance, which suggests that *CAH1* overexpression in tissues in which it is not usually expressed may result in a supraphysiological effect. Part of that effect is tubule-dependent, given that: 1) *CAH1* has low expression in the tubules under normal conditions (Figure 6.4a); and 2) specific overexpression in the tubules is sufficient to increase acidotic resistance (Figure 6.5f). However, overexpression in haemocytes, where *CAH1* is lowly expressed, as discussed in the previous chapter (Section 5.5), may contribute to the substantially extended survival by increasing haemolymph buffering capacity. This would also correlate to extended lifespan in the absence of acidotic stimulus when *CAH1* in overexpressed in haemocytes (Figure 5.7b).

Tubule-specific overexpression of *CAH1* in female flies was not sufficient to extend their lifespan under control conditions (Figure 6.6b). Consistent with the lack of effect on survival under EG stress, tubule-specific overexpression of *CAH2* in both sexes or *CAH1* in males had no effect on fly lifespan (Figure 6.6a, c-d). Sex-specific effects of *CAH1* expression on fly survival under acidotic stress suggest that tubules may differ between sexes in how their excrete acid.

These results suggest that altering the expression of *CAH2* in fly tubules alone may not be sufficient to increase acid excretion in the tubules under acidotic stress, and hence may also not counteract age-related acidification to extend survival. These observations may also result from compensatory effects on the expression of the other CA genes normally expressed in the tubules, *CAH3* and *CAH9*, as indicated from their age-related increased expression.

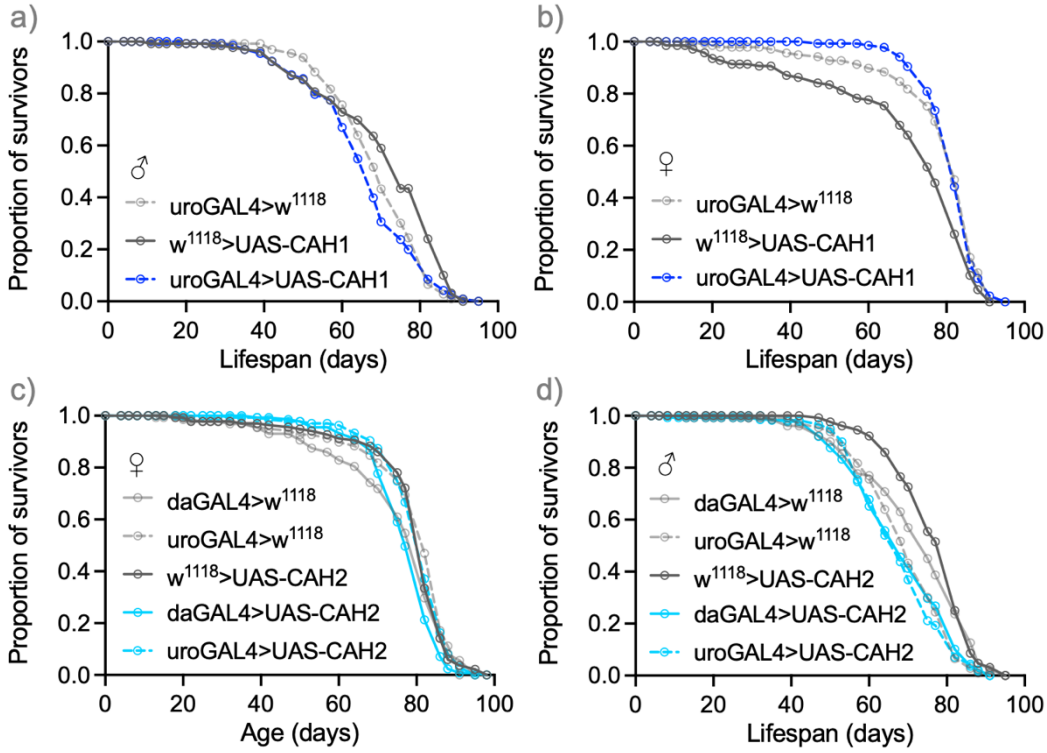


Figure 6.6. Lifespan of flies overexpressing CAH1 or CAH2. Survival curves of male (a,d) and female (b,c) flies in which either CAH1 (a,b) or CAH2 (c,d) were overexpressed either ubiquitously (daGAL4>UAS-CAH1; daGAL4>UAS-CAH2) or in the Malpighian tubules (uroGAL4>UAS-CAH1; uroGAL4>UAS-CAH2) and their respective controls (in grey); n=140 flies per condition.

6.3.3. Expression of v-ATPase subunits in fly tubules with age

V-ATPase is composed of two domains, the membrane-spanning V_0 and the catalytic V_1, each consisting of multiple subunits. V_0 is responsible for proton translocation and V_1 for ATP hydrolysis (Eaton et al., 2021). In humans, this enzyme is expressed in intercalated cells in the kidney. Mutations in subunits of both domains cause distal renal tubular acidosis (Smith et al., 2000; Stover et al., 2002), demonstrating its important role in human acid-base regulation.

In flies, v-ATPase is required for active transport of strong ions into the tubular lumen upon electrogenesis through H^+ pumping. As discussed, v-ATPase is essential for fluid secretion by the tubules (Allan et al., 2005; Maddrell & O'Donnell, 1992). Mutating a single gene of the v-ATPase subunit impairs the function of this channel, decreasing tubular acid excretion (Allan et al., 2005; Davies et al., 1996; Ugur et al., 2016).

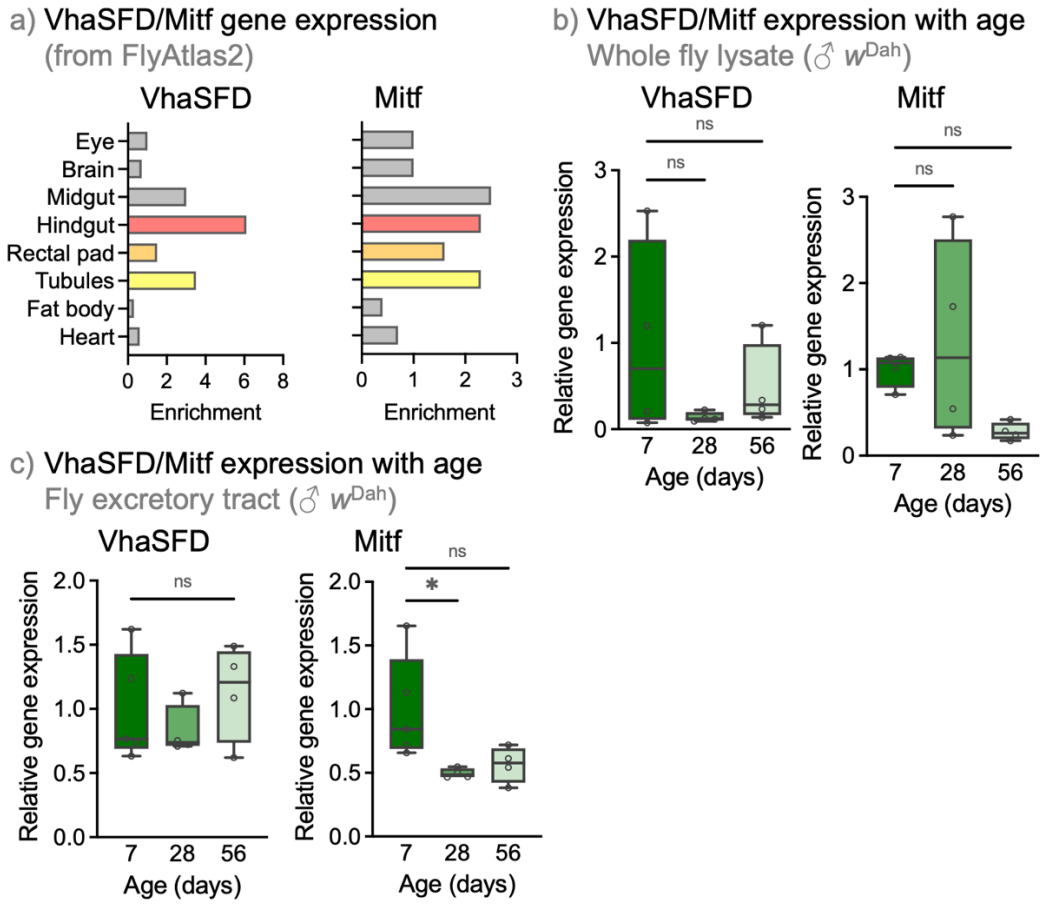


Figure 6.7. *VhaSFD* and *Mitf* distribution and changes in gene expression with age: a) Expression profile of *VhaSFD* and *Mitf* in male flies (Leader et al., 2018); b) qPCR analysis of *VhaSFD* and *Mitf* expression in whole fly lysates of w^{Dah} males with age, n=4 replicates per condition; c) qPCR analysis of *VhaSFD* and *Mitf* expression in homogenates of dissected excretory tracts of w^{Dah} male flies with age, n=4-5 replicates per condition. Statistical significance was determined by ANOVA with Tukey correction for multiple comparisons; n/s, p>0.05; *, p<0.05.

Overexpression of the gene coding for the regulatory v-ATPase subunit, *VhaSFD*, was shown to extend lifespan in a blind screen for conditional mutations that

increase *Drosophila* survival (Landis et al., 2003). While being a promising indication that v-ATPase is important for lifespan, this report is purely descriptive, and does not show if the overexpression of the regulatory *VhaSFD* subunit results in overexpression of other v-ATPase subunits, or overactivity of the H^+ pump, nor does it implicate an effect on pH homeostasis.

One factor that was shown to be a master regulator of v-ATPase, by promoting transcription of all subunits, is the Mitf transcription factor (Zhang et al., 2015). Interestingly, knockdown of the VhaSFD subunit shifts Mitf protein localisation from the cytoplasm to the nucleus, suggesting VhaSFD may regulate itself and other subunits via Mitf interaction (Zhang et al., 2015).

Most v-ATPase subunits have substantially higher expression in the excretory tract compared to other tissues (Figures 6.7a, 6.8a). Consistent with its role as a master regulator of v-ATPase subunit expression, *Mitf* has a similar expression pattern in the fly body (Figure 6.7a). The gene expression of v-ATPase subunits tends to decrease in the whole fly, but surprisingly not in the excretory tract (Figures 6.7b-c, 6.8b-c). This suggests that their expression decreases in other tissues where they are expressed, notably the midgut. In the midgut, v-ATPase is needed for acid excretion in the copper cell region (Overend et al., 2016; Shanbhag & Tripathi, 2009). It would be interesting to measure v-ATPase expression specifically in this tissue and assess midgut lumen pH in flies throughout their lifespan by feeding them a pH-sensitive dye.

The maintenance of most v-ATPase subunit gene expression with age occurs despite lower expression of the Mitf transcription factor (Figure 6.7b-c). One exception is the catalytic subunit Vha68-2. This subunit is one of 3 fly ATP6V1A orthologues, and the one most highly expressed throughout the excretory system. *Vha68-1* is mostly expressed in the central nervous system and *Vha68-3* is specifically expressed in testis (Leader et al., 2018). Since loss of one subunit is sufficient to affect function of the whole complex, v-ATPase activity may decrease with ageing in the excretory system despite maintenance of mRNA levels of most subunits. V-ATPase activity can be measured in flies and has been done before, in the context of cold acclimation (Yerushalmi et al., 2018). Using this method, measuring enzyme activity in the excretory system with age will be more informative into how potential loss of v-ATPase function may contribute to haemolymph acidification.

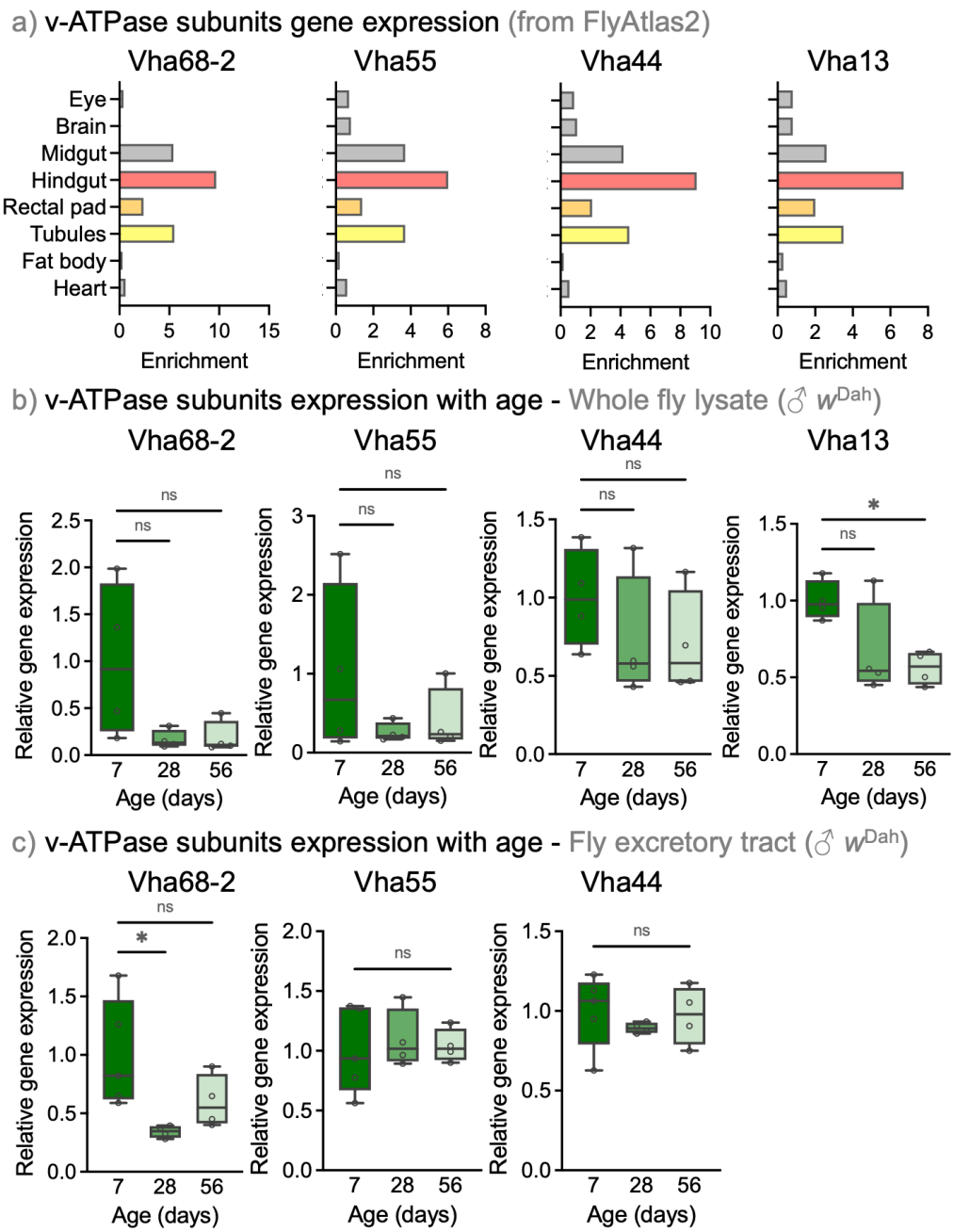


Figure 6.8. Distribution and changes in gene expression of other v-ATPase subunits. a) Expression profile of *Vha68-2*, *Vha55, Vha44* and *Vha13* in male flies (Leader et al., 2018); b) qPCR analysis of *Vha68-2*, *Vha55, Vha44* and *Vha13* expression in whole fly lysates of w^{Dah} males with age, n=4 replicates per condition; c) qPCR analysis of *Vha68-2*, *Vha55, Vha44* and *Vha13* expression in homogenates of dissected excretory tracts of w^{Dah} male flies with age, n=4-5 replicates per condition. Statistical significance was determined by ANOVA with Tukey correction for multiple comparisons; n/s, $p>0.05$; *, $p<0.05$.

6.3.4. Tubule-specific expression of v-ATPase subunit genes and survival

Although only *Vha68-2* showed decreased expression in the excretory tract with age, modulation of gene expression was mainly done on the VhaSFD subunit. As mentioned previously, this regulatory subunit is proposed to control the expression of all other subunits of the v-ATPase through the transcription factor Mitf. As such, altering VhaSFD expression was theorised as a better strategy to manipulate expression of the whole enzyme.

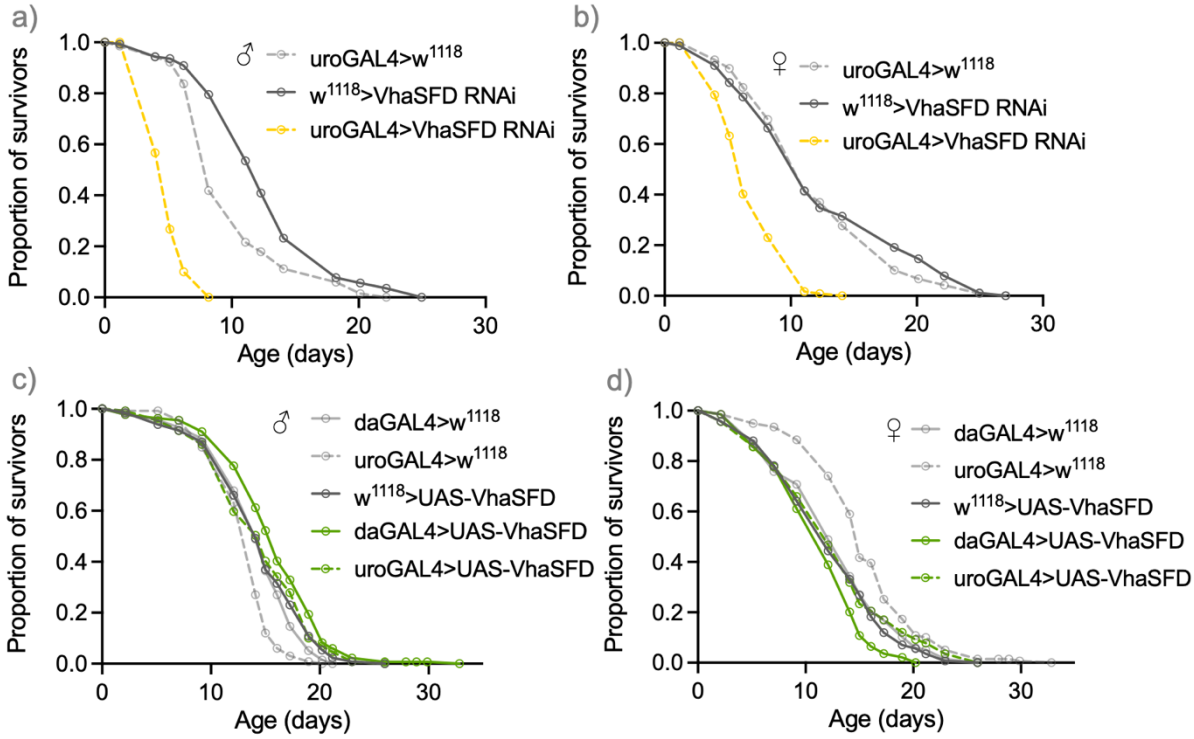


Figure 6.9. Acidotic stress resistance upon changes in *VhaSFD* expression. Survival curves under acidotic stress (2.5% EG) from d7 of male (a,c) and female (b,d) flies in which *VhaSFD* was knocked down in the Malpighian tubules (uroGAL4>VhaSFD RNAi; a-b) or overexpressed either ubiquitously (daGAL4>UAS-VhaSFD; c-d) or in the Malpighian tubules (uroGAL4>UAS-VhaSFD; c-d), and their respective controls (in grey); n=140 flies per condition.

Flies where v-ATPase subunits were knocked down ubiquitously (using the daGAL4 driver) were not viable, consistent with the published lethality of mutant flies for most subunits (Allan et al., 2005). *VhaSFD* knockdown specifically driven to the tubules were viable and resulted in increased sensitivity to acidotic stress, independently of sex (Figure 6.9a-b). Knockdown of other v-ATPase subunits resulted

in the same susceptibility to acidotic stress in both males and females (Figure 6.10), demonstrating again that loss of one subunit is enough to affect the function of this enzyme.

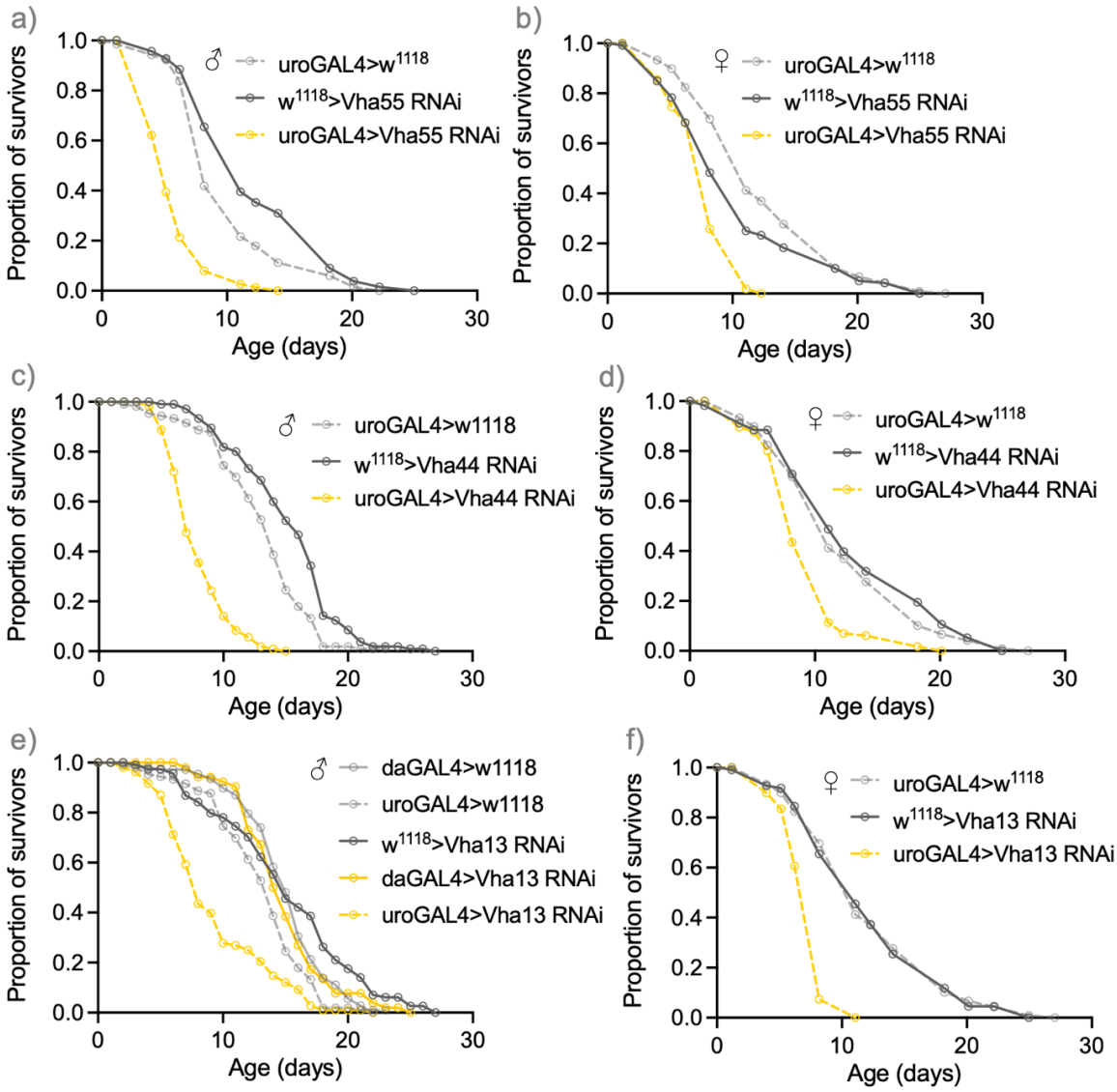


Figure 6.10. Acidotic stress resistance upon knockdown of other v-ATPase subunits. Survival curves under acidotic stress (2.5% EG) from d7 of male (a,c,e) and female (b,d,f) flies in which *Vha55* (a,b), *Vha44* (c,d) or *Vha13* (e,f) were knocked down in the Malpighian tubules (uroGAL4>Vha55 RNAi; uroGAL4>Vha44 RNAi; uroGAL4>Vha13 RNAi; respectively), and their respective controls (in grey); n=140 flies per condition.

Conversely, overexpression of VhaSFD was not sufficient to rescue the survival of flies under EG-induced stress in either males or females (Figure 6.9c-d). Besides, it also did not alter fly lifespan (Figure 6.11a-b), contrary to what was previously

reported in male flies (Landis et al., 2003). This may be due to different levels of overexpression or different control conditions in which VhaSFD overexpression may be more or less advantageous.

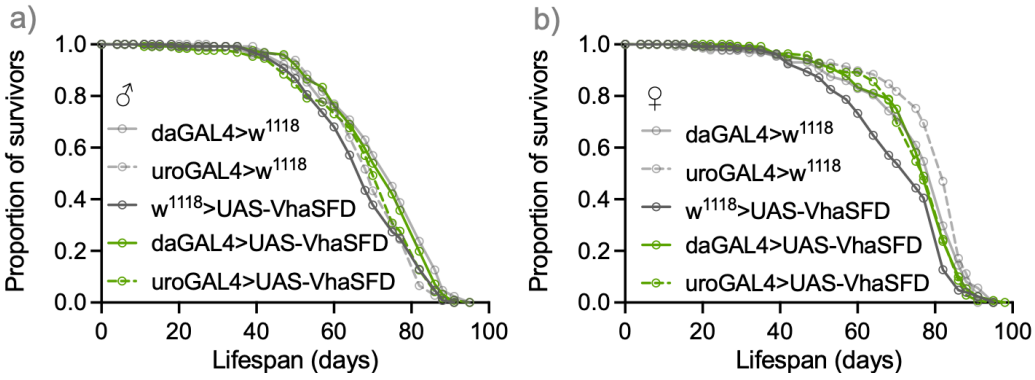


Figure 6.11. Lifespan of flies overexpressing *VhaSFD*. Survival curves of male (a) and female (b) flies in which *VhaSFD* was overexpressed either ubiquitously (daGAL4>UAS-VhaSFD) or in the Malpighian tubules (uroGAL4>UAS-VhaSFD), and their respective controls (in grey); n=140 flies per condition.

6.3.5. Expression of chloride channels in fly tubules with age

From a quantitative perspective, chloride is the most specific ion determining acid base balance (Kellum & Elbers, 2009). From a descriptive view, chloride-bicarbonate exchangers are needed for tubular bicarbonate reabsorption, and hence also crucial for acid-base regulation. Human kidneys express multiple types of chloride channels (Devuyst & Guggino, 2002). The chloride channel ClC-5 is present in intercalated cells where it colocalises with v-ATPase. Mutations of the *CLCN5* gene encoding that channel are found in multiple diseases that can manifest as low-molecular-weight proteinuria, hypercalciuria and nephrocalcinosis, but are not typically associated with metabolic acidosis (Devuyst & Guggino, 2002). An anion exchanger, AE1, is also expressed in intercalated cells and reabsorbs HCO_3^- from the tubular lumen in exchange for Cl^- secretion. Mutations in its encoding gene result in distal renal tubular acidosis (Karet et al., 1998; Ring et al., 2005). Independently of whether this effect is driven by bicarbonate or chloride, these phenotypes show the importance of anion exchangers in acid base regulation.

Flies express chloride channels of the ClC family (mainly *ClC-a* and *ClC-c*) and anion exchangers in both principal and stellate cells (Cohen et al., 2020; Xu et al., 2021). Chloride channels in the stellate cells were shown to allow passive transport of

chloride following electrochemical gradients (Cabrero et al., 2014). By following cation secretion, Cl^- transport through those channels will match the concentration of cations and hence not alter [SID]. This suggests ClC channels do not regulate acid excretion, in line with normal urine acidification in patients with Dent's disease where CLCN5 is mutated (Devuyst & Guggino, 2002). Two anion exchangers have been identified in flies, encoded by *Ndae1* and *AE2*, but *AE2* is lowly expressed in the excretory tract (Leader et al., 2018). *Ndae1* is enriched in fly tubules, but is also present in other tissues, such as the midgut (Figure 6.12a). In this channel, anion exchange is driven by Na^+, and is thought to work by reabsorption of Na^+ and HCO_3^- coupled to secretion of Cl^- and H^+, altering SID and absorbing bicarbonate. This means Ndae1 will necessarily impact pH, and indeed it does so when electrophysiologically tested in *Xenopus* oocytes (Romero et al., 2000; Sciortino et al., 2001). Interestingly, *Ndae1* expression tends to decrease in both whole fly lysate (Figure 6.12b) and excretory tract (Figure 6.12c).

In addition, flies also have pH-sensitive chloride channels encoded by *pHCl-1*, *pHCl-2*, *CG6927* and *secCl*. From these, only *pHCl-2* and *secCl* are expressed in the excretory tract (ref FlyAtlas2?). *pHCl-1* is expressed in the central nervous system and *CG6927* has female-specific expression in the ovaries, heart cells and fat body (Leader et al., 2018). Both pHCl-2 and secCl are expressed in Malpighian tubules and were shown to be required for cAMP- and tyramine-mediated diuretic response, respectively (Feingold et al., 2016, 2019).

pHCl-2 is also expressed in the acidic region of the midgut (Figure 6.12a), where its physiological role was thoroughly explored (Redhai et al., 2020). There, it was reported to act as a zinc sensor. To search for ligands, a range of compounds (including metals, neurotransmitters and amino acids) were tested by electrophysiology in *Xenopus* oocytes. Besides pH, only zinc was shown to have a dose-dependent effect on the activation of this channel. Zinc was delivered as zinc chloride, which dissociates in solution into Zn^+ and Cl^-. Chloride might thus be the main factor activating the channel. Indeed, other metals delivered with chloride, FeCl and CuCl also elicited a response, although comparatively smaller at the same concentration. Given the response to zinc occurred with comparably lower doses and was altered (yet not abolished) in mutants for the potential zinc-binding site, it is likely zinc promotes chloride transport through gating as suggested (Redhai et al., 2020). However, it was not shown to be necessary for the activity of the channel. The direction

of chloride transport in the apical membrane of midgut cells is also not determined (Redhai et al., 2020). Theoretically, it would make sense that upon zinc sensing, signalling food intake (Redhai et al., 2020), chloride would be transported into the lumen to drive acidification of the midgut for digestion. Indeed, similarly to v-ATPase knockdown, when pHCl-2 is knocked down in the midgut, luminal acidification does not occur (Overend et al., 2016; Redhai et al., 2020).

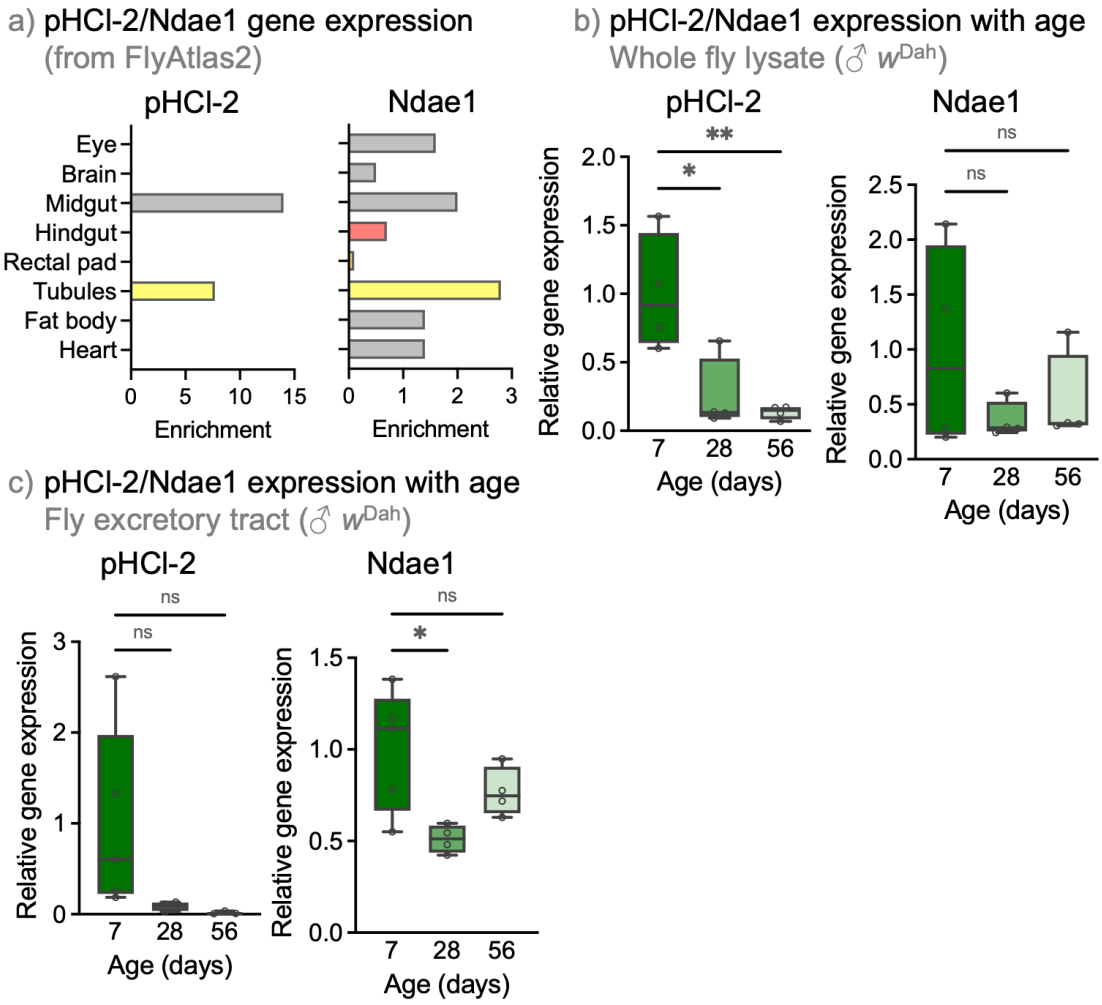


Figure 6.12. *pHCl-2* and *Ndae1* distribution and changes in gene expression with age: a) Expression profile of *pHCl-2* and *Ndae1* in male flies (Leader et al., 2018); b) qPCR analysis of *pHCl-2* and *Ndae1* expression in whole fly lysates of w^{Dah} males with age, n=4 replicates per condition; c) qPCR analysis of *pHCl-2* and *Ndae1* expression in homogenates of dissected excretory tracts of w^{Dah} male flies with age, n=4-5 replicates per condition. Statistical significance was determined by ANOVA with Tukey correction for multiple comparisons; n/s, p>0.05; *, p<0.05; **, p<0.01.

In the tubules, the pHCl-2 channel is expressed at the apical membrane of principal cells and shown to promote cAMP-stimulated diuresis (Feingold et al., 2016). Its function is pH-sensitive, as it is practically non-responsive under pH 7 and has maximum response to pH over 8.5 (Feingold et al., 2016). In this publication, the channel was proposed to respond to extracellular pH. However, pHCl-2 mutants have lower diuresis upon cAMP stimulation and not under basal conditions (Feingold et al., 2016). Given that cAMP acts by stimulating H^+ pumping via v-ATPase, it is more likely that pHCl-2 detects pH changes intracellularly at the apical level where it co-localises with v-ATPase instead, thus allowing differential Cl^- secretion, altering SID and acidifying the urine. This would be in line with its role in acidifying the midgut, where it may have a similar interaction with v-ATPase. It would also explain the diuretic response to cAMP stimulation, which would be paradoxical if pHCl-2 responded to extracellular, luminal pH instead.

Given that pHCl-2 is sensitive to pH changes, highly specific for regions where acid excretion is needed, and shown to be necessary for midgut acid excretion, the potential role pHCl-2 in tubule acid excretion is particularly interesting, since tubule secretion needs to be an active process in *Drosophila*. Indeed, in mammals, where acid-base regulation is based on ion reabsorption, this channel is not conserved probably because it is not needed (Remnant et al., 2016). Besides, the expression of *pHCl-2* tends to decrease with age in both whole fly (Figure 6.12b) and the excretory tract (Figure 6.12c). For these reasons, I decided to focus on this channel and modulate its expression in the tubule, while recognising other channels, particularly secCl and Ndae1, are likely to also play a role in fly acid-base regulation.

6.3.6. Tubule-specific pHCl-2 gene expression and survival

In line with what was done for CAs and v-ATPase, the expression of *pHCl-2* was altered in flies both ubiquitously and specifically in the tubules and survival was measured under control and acidotic stress conditions.

Both knockdown and overexpression of this gene ubiquitously were lethal before eclosion (daGAL4 driver, data not shown). Altering *pHCl-2* gene expression specifically in the tubules did not affect survival under EG-induced stress in male flies (Figure 6.13a, c). In females, *pHCl-2* knockdown decreased survival under acidotic stress (Figure 6.13b), but its overexpression did not substantially alter it (Figure 6.13d), similarly to what was seen with CAs and v-ATPase.

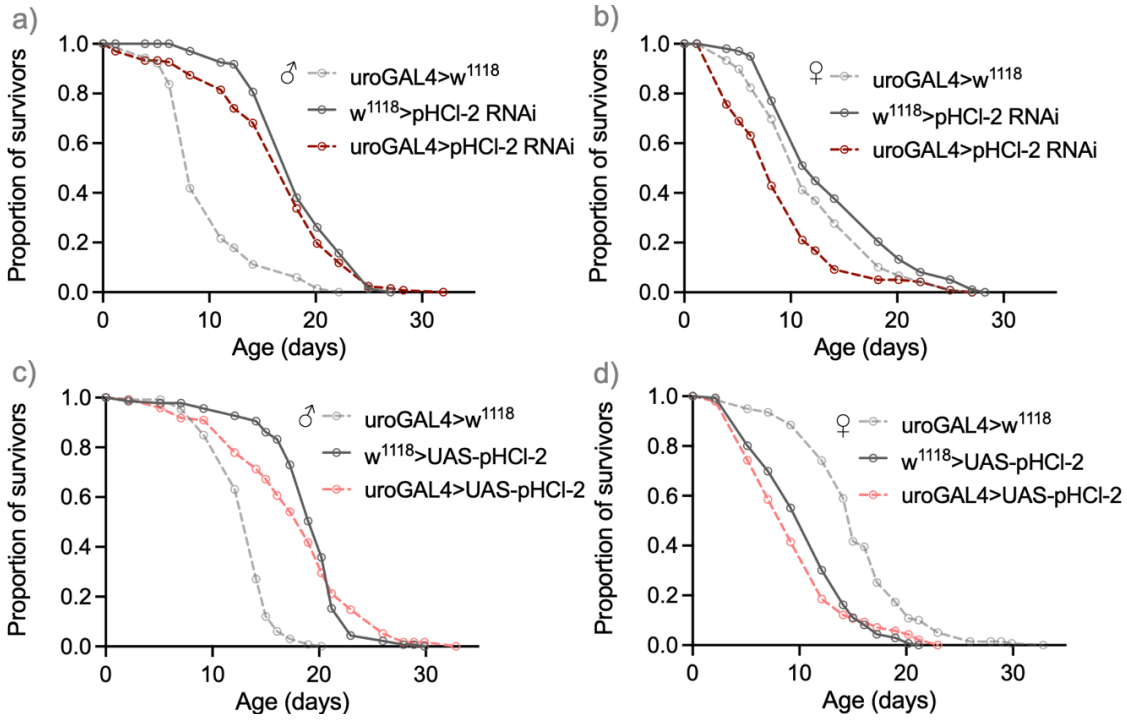


Figure 6.13. Acidotic stress resistance upon changes in *pHCl-2* expression. Survival curves under acidotic stress (2.5% EG) from d7 of male (a,c) and female (b,d) flies in which *pHCl-2* was knocked down (uroGAL4>pHCl-2 RNAi; a-b) or overexpressed (uroGAL4>UAS-pHCl-2; c-d) in the Malpighian tubules, and their respective controls (in grey); n=140 flies per condition.

Under control conditions, overexpression of *pHCl-2* in the tubules did not alter male lifespan (Figure 6.14a) and shortened female survival (Figure 6.14b). Differences in survival of the two control lines, particularly in males and under acidotic stress, suggests genetic background effects. These experiments would ideally have been replicated after backcrossing both lines for a few generations to exclude those effects, but this was not possible due to time constraints.

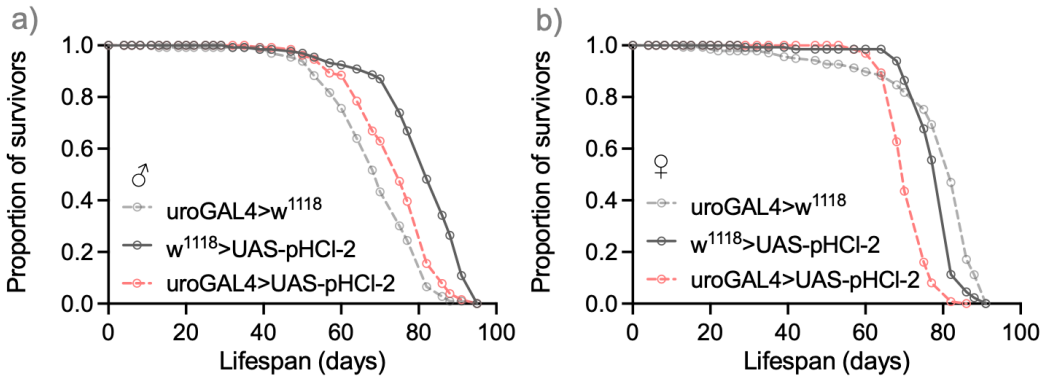


Figure 6.14. Lifespan of flies overexpressing pHCl-2. Survival curves of male (a) and female (b) flies in which *pHCl-2* was overexpressed in the Malpighian tubules (uroGAL4>UAS-pHCl-2), and their respective controls (in grey); n=140 flies per condition.

6.4. Key messages and interpretation

In this chapter, acid excretory capacity was measured in flies over their lifespan and the gene expression of relevant proteins for acid-base regulation was altered to screen them based on how they impact fly capacity to resist acidotic stress. The key results are:

- Flies lose their capacity to excrete acid effectively with age
- The gene expression of pH-regulating proteins in the excretory tract changes with age
- CAs, v-ATPase and pHCl-2 are proposed to form an axis for acid excretion in fly tubules
- Knocking down each of these elements individually shortens female fly survival under acidotic stress
- In male flies, only knockdown of v-ATPase subunits affects survival in response to EG stress
- Overexpression of CAs, v-ATPase and pHCl-2 individually is not sufficient to extend survival both under acidotic or control conditions

Using acidotic stress resistance instead of measuring haemolymph pH directly upon altering the gene expression of acid base-relevant proteins was done for practical reasons, to allow more high-throughput analysis. However, inability to excrete acid should correlate with increased sensitivity to acidotic stress and lower haemolymph pH. Besides measuring haemolymph pH, it will be important to explore the role of each of the discussed proteins further in terms of how their protein expression, enzyme activity and contribution to fluid secretion change with age.

The observation that the acid excretory capacity declines with age as a whole suggests this causes the haemolymph acidification seen with age. The loss-of-function of the excretory system may itself result from being overwhelmed by net acid production influenced by diet, as further explored in the next chapter. However, independently of acid production, insufficient acid excretion necessarily contributes to age-related haemolymph acidification.

As discussed in Chapter 4, besides lowering haemolymph pH, EG shortens survival by osmotic stress. The proteins explored in this chapter, particularly v-ATPase, are needed for normal fluid secretion in fly tubules. Yet, the effects of altering their gene expression in survival under EG is likely to be related to EG-induced acidotic stress only. The way EG creates osmotic stress is by acting as an osmole that attracts water after being filtered (in mammals) or secreted (in flies). Therefore, if normal fluid secretion following ion transport is disrupted by the genetic interventions described in this chapter, EG will either: 1) not be secreted and hence not cause osmotic stress under those conditions; or 2) be secreted by other channels and actually promote fluid secretion.

The hypothesis that acid-base regulation occurs as a result of the interdependence between ion transporters and CAs has been proposed before given their interactions, as the so-called 'transport metabolon' (Deitmer & Becker, 2013). Here, I suggest that acid excretion in fly tubules is mainly dependent on interactions between CAs, v-ATPase and pHCl-2. Other channels will contribute to acid-base balance, but these three elements by themselves should be sufficient to alter acid excretion rates. Each of them individually was indeed shown to increase mortality under acidotic stress when knocked down in female flies.

The observation that only v-ATPase knockdown alters susceptibility to EG in males may be related to: 1) differences in demand, associated with increased production of acid following higher food consumption in females (Wong et al., 2009); 2) differences in fluid secretion rates, which are higher in females (Chintapalli et al., 2012); or 3) intrinsic differences in tubular gene expression between sexes (Chintapalli et al., 2012). In any case, other factors may potentially compensate for decreased *CAH1* and *pHCl-2* expression in males. Similarly, other membrane-bound CAs (CAH3 and 9) may compensate for *CAH2* knockdown, as knocking *CAH2* down did not affect survival under acidotic stress. With ageing, a similar pattern was observed: as *CAH2* expression tends to decline, *CAH3* and *CAH9* expression increases with age.

The common, sex-independent factor needed for survival under acidotic stress is the v-ATPase. This is not surprising given its essential role as the initiator of fluid secretion in the tubules. Even more so, as proposed here, v-ATPase may also initiate acid excretion by activating pHCl-2 through altering intracellular pH apically in a CA-dependent manner to promote Cl^- secretion. Ndae1 is also likely to contribute to either Cl^- secretion or HCO_3^- reabsorption (depending on the view of acid-base) following v-

ATPase-dependent ion transport into the lumen. Ndae1 expression in the excretory tract declines with age, therefore its impact on haemolymph acidification and survival should also be assessed as follow up.

None of the three elements studied here were able to extend the survival of flies in both the presence or absence of acidotic stress when overexpressed. Taking the view that they act together, overexpressing them individually might not significantly improve acid excretion. In the same rationale, if haemolymph acidification affects survival, overexpression of at least these three elements would be needed to promote acid excretion and extend fly lifespan. Indeed, *CAH1*, *CAH2*, *Vha68-2* and *pHCl-2* expressions all tend to decline with age in the excretory tract. Therefore, it would indeed be interesting to recombine all the overexpressor fly lines that I generated into one fly, and to drive their simultaneous overexpression specifically to the whole excretory tract. However, it was not possible to complete the complex recombination schemes as planned, due to unforeseen restrictions during the pandemic, and I was only able to test these lines individually. Generation of the quadruple recombined overexpressor is ongoing, and it will be exciting to assess its effects on survival in the future.

Beyond expression of these elements, their regulation with ageing would also be worth pursuing, following up on the results presented here. From the three elements considered here, regulation of fly v-ATPase is the most thoroughly studied thus far, in the context of fluid secretion. This enzyme is intracellularly regulated by the downstream signals cAMP and cGMP (Cohen et al., 2020). Curiously, the *white* gene, mutated in the fly strains w^{1118} and w^{Dah} used here, is normally highly expressed in tubules relative to other tissues and encodes a protein that transports cGMP (Evans et al., 2008). Although other cGMP transporters are expressed in fly tubules, *white* mutants may be particularly susceptible to conditions with increased demand for cGMP, such as acidotic stress. It would be interesting to compare survival of these strains compared to their wild-type counterparts under acidotic stress.

From studies in other organisms, among other factors (Nishi & Forgac, 2002), v-ATPase is also shown to be regulated by the reversible formation of a disulphide bond between two cysteine residues (Cys254 and Cys532) in subunit V1A (Feng & Forgac, 1994). Interestingly, the small molecule EN6 targets another cysteine (Cys277) of the V1A subunit, increasing the enzyme's catalytic activity and resulting in increased lysosome acidification (Chung et al., 2019). Cys277 is conserved in the

fly V1A subunit. It would be interesting to pharmacologically increase v-ATPase activity in control and knockdown flies for the V1A subunit and measure the effect on acid-base balance and survival. Besides, the V1A disulphide bond is redox-dependent, as first shown in yeast (Oluwatosin & Kane, 1997). Given Cys277 can also be oxidised and its oxidation was shown to change with ageing in different mouse tissues (Xiao et al., 2020), it would be important to study the redox regulation of this enzyme as a whole (Lennicke & Cochemé, 2021), and to study how it impacts and is impacted by acid-base balance.

Finally, loss of tubular function with age may occur due to crystal deposition shown to aggravate with age. This hypothesis and the influence of diet on tubule lithiasis are explored in the next chapter.

Chapter 7. Acid-base imbalance, metabolism and diet-related disease

7.1. Introduction

Haemolymph acidification with age may be promoted by changes in the rate of net endogenous acid production. This endogenous production of acid is strongly diet-dependent. Here, I explore how fly metabolism changes with age, and how diet can promote age-related disease in an acid-base-dependent manner.

In humans, it is estimated that metabolic processes produce ~10,000-15,000 mmol of CO_2 and ~50-100 mEq of non-volatile acid daily (DiBartola, 2012). Under normal conditions, net endogenous acid production (NEAP) is mostly derived from the metabolism of sulphur-containing amino acids. Under pathological conditions, other metabolic sources can significantly impact acid-base balance, such as anaerobic glycolysis, lipolysis, ketogenesis and urea synthesis (DiBartola, 2012). With age-related changes in metabolism, these sources may become important for energy production, leading to increased endogenous acid load. In a recent study correlating metabolic biomarkers with all-cause mortality, lactate (from anaerobic glycolysis) and acetoacetate (from ketogenesis) were shown to significantly associate with increased all-cause mortality (Deelen et al., 2019).

Diet composition determines NEAP (Frassetto et al., 1998). Dietary needs change with age and affect mortality rate in humans. For example, a recent study matching dietary macronutrient composition to mortality with age found that a high ratio of carbohydrate to fat and a lower protein content were associated with the lowest mortality in old age (Senior et al., 2020). Given protein is the main source of non-volatile acids, these results may reflect a different capacity to counter acid load with age. High dietary acid load is itself associated with increased all-cause mortality rate (Hejazi et al., 2022; Park et al., 2015; Xu et al., 2016). However, too low acid load is comparably associated with a higher mortality rate (Hejazi et al., 2022; Xu et al., 2016), likely due to unmet minimal protein needs. Other clinical outcomes, such as muscle mass and strength, have shown benefits of higher protein diets in the elderly (Nowson & O'Connell, 2015). These studies suggest meeting protein needs for function should be balanced with its added acid load to promote both function and overall health, as measured by survival. This balance may be achieved by choosing dietary sources of

protein with lower acidogenic amino acid content. Lower acid load may further explain the longevity benefits of reducing consumption of methionine-rich animal protein compared to plant-based sources, besides the currently proposed mechanisms (Kitada et al., 2019).

Dietary acid load may also contribute to a chronic acid-base imbalance towards acidification by affecting kidney function and thus acid excretion. Indeed, higher NEAP is associated with lower kidney function and the incidence of chronic kidney disease across different cohorts (Banerjee et al., 2014, 2023; Ko et al., 2017; Rebholz et al., 2015; Scialla et al., 2012; Valle-Hita et al., 2022).

This chapter explores the effect of diet and metabolism on age-related haemolymph acidification, and how they can cause age-related disease in flies in an acid-base-dependent manner.

7.2. Metabolic production of acids with age and mortality

7.2.1. *Drosophila* metabolic rate with age

To have an overview on how fly metabolism may change with age in terms of substrate breakdown, respirometry was used to measure O_2 consumption and CO_2 production in young, middle-aged and old flies. Previous reports are conflicting on whether fly baseline metabolic rate lowers with age (Khazaeli et al., 2005; Promislow & Haselkorn, 2002). Importantly, in both studies, metabolic rate was solely based on measurement of CO_2 production. If organic acids build up with age, their buffering into CO_2 by the carbonic acid-bicarbonate system will increase the ratio of CO_2 production to O_2 consumption (i.e., the respiratory quotient, RQ) in respirometry. This can thus alter CO_2 independently of O_2 consumption and disguise potential changes in actual metabolic rate with age.

If an organism would purely breakdown one type of macronutrient, the RQ would be 1 for carbohydrates, ~0.7 for fats and ~0.8-0.9 for proteins, depending on fatty acid and amino acid composition, respectively (Arch et al., 2006). Only metabolism of volatile organic acids or anaerobic glycolysis results in a RQ above 1. In line with previous reports, production of CO_2 in males does not seem to substantially change with age (Figure 7.1a). However, O_2 consumption appears to decline (Figure 7.1a) and is more specific to metabolic rate. Similarly, female O_2 consumption seems to decline with age (Figure 7.1b). In both, the RQ appears to be higher than 1, which

would suggest the metabolism of organic acids or anaerobic glycolysis. However, a quantitative analysis needs to be performed to confirm these findings.

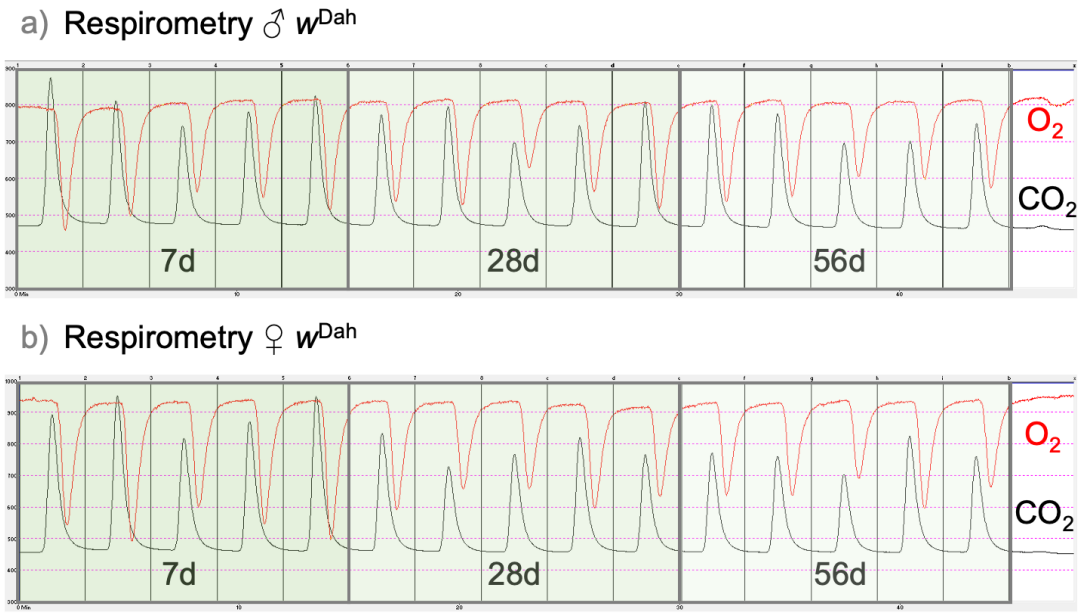


Figure 7.1. Fly metabolic rate with age. Representative graph of O_2/CO_2 respirometry of w^{Dah} male (a) and female (b) flies with age. Each box contains five columns that correspond to 5 replicates (n=5 males or 3 females each) of measured O_2/CO_2 peaks after a 48 min cycle.

7.2.2. Fly haemolymph metabolome changes with age

To test if organic acids or products of anaerobic glycolysis accumulated with age, untargeted metabolomics of the fly haemolymph was performed by gas chromatography-mass spectrometry (GC-MS). I extracted haemolymph from young, middle-aged and old flies (see Section 2.7.2), and these samples were then processed by Joao Mokochinski from the LMS Mass Spectrometry facility, who returned a list of metabolites with peak intensities for each sample. Only metabolites with a retention index within 100 units of their respective library matches (used for compound identification) were considered for downstream analysis, to exclude potential false positives.

Downstream analysis was performed using the online tool MetaboAnalyst 5.0 (Pang et al., 2021). After excluding outliers, based on interquantile range analysis, metabolite peak intensity data were normalised to the respective mean of the peak intensities of pooled samples, transformed (Log10) and autoscaled, i.e., mean-centered and divided by the standard deviation of each variable (Figure 7.2a).

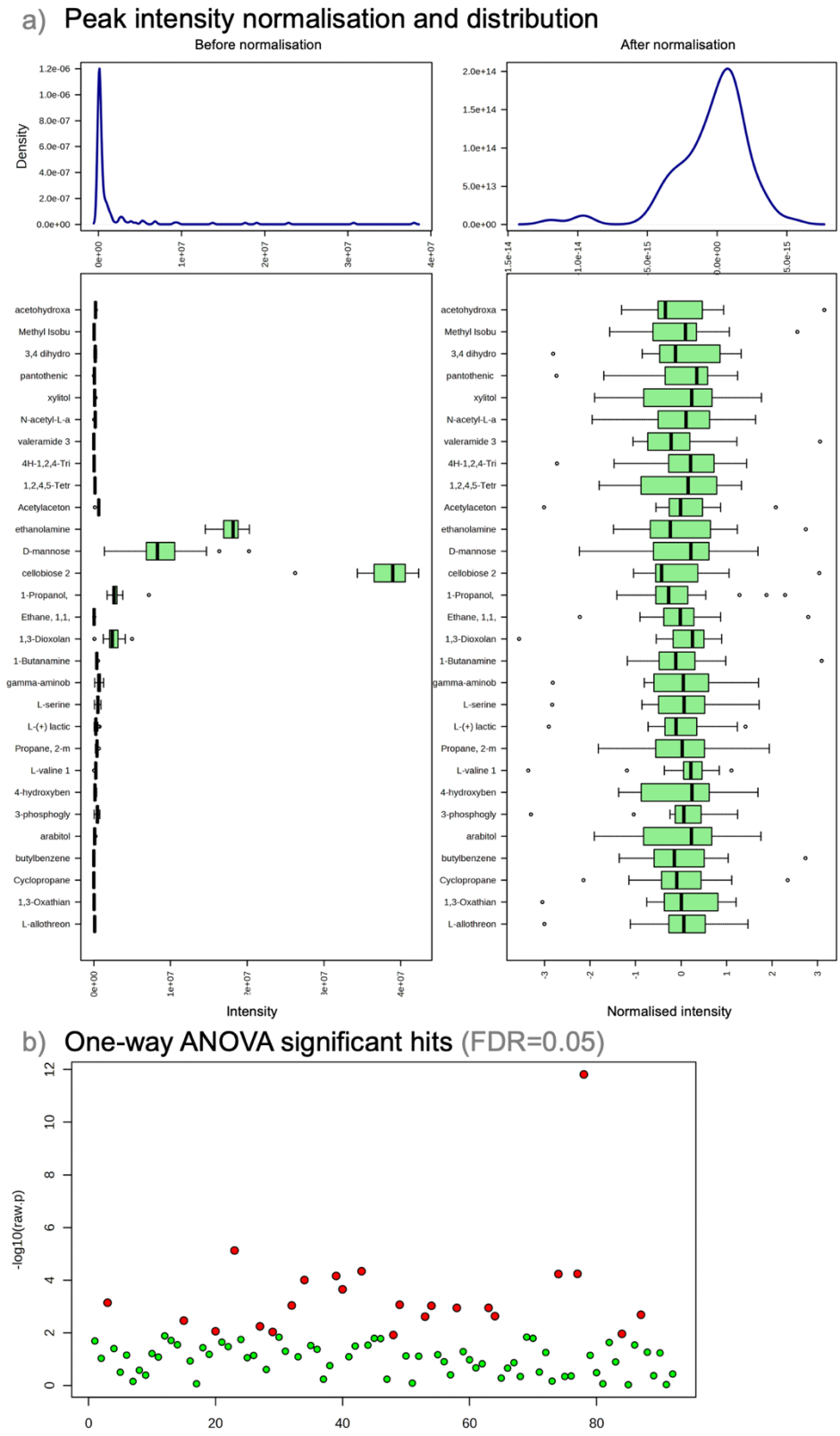


Figure 7.2. Metabolomics data normalisation and ANOVA significant hits: a) Box plots and kernel density plots before and after metabolite peak intensity normalisation to pooled samples; data transformed by Log10, mean-centered and divided by the standard deviation of each variable; b) One-way ANOVA analysis; red dots are significant hits.

ANOVA analysis (FDR=0.05) resulted in 23 significant hits (Figure 7.2b), whose individual peak intensities generally correlated (Pearson R distance measure) with samples of the same age group (Figure 7.3a). By principal component analysis (PCA), samples of the same age and pooled samples also clustered among themselves, and these clusters separated by age, especially at the 56 days timepoint (Figure 7.3b). These significant hits also separate by age following hierarchical clustering (Euclidean distance, Ward's linkage) (Figure 7.4a).

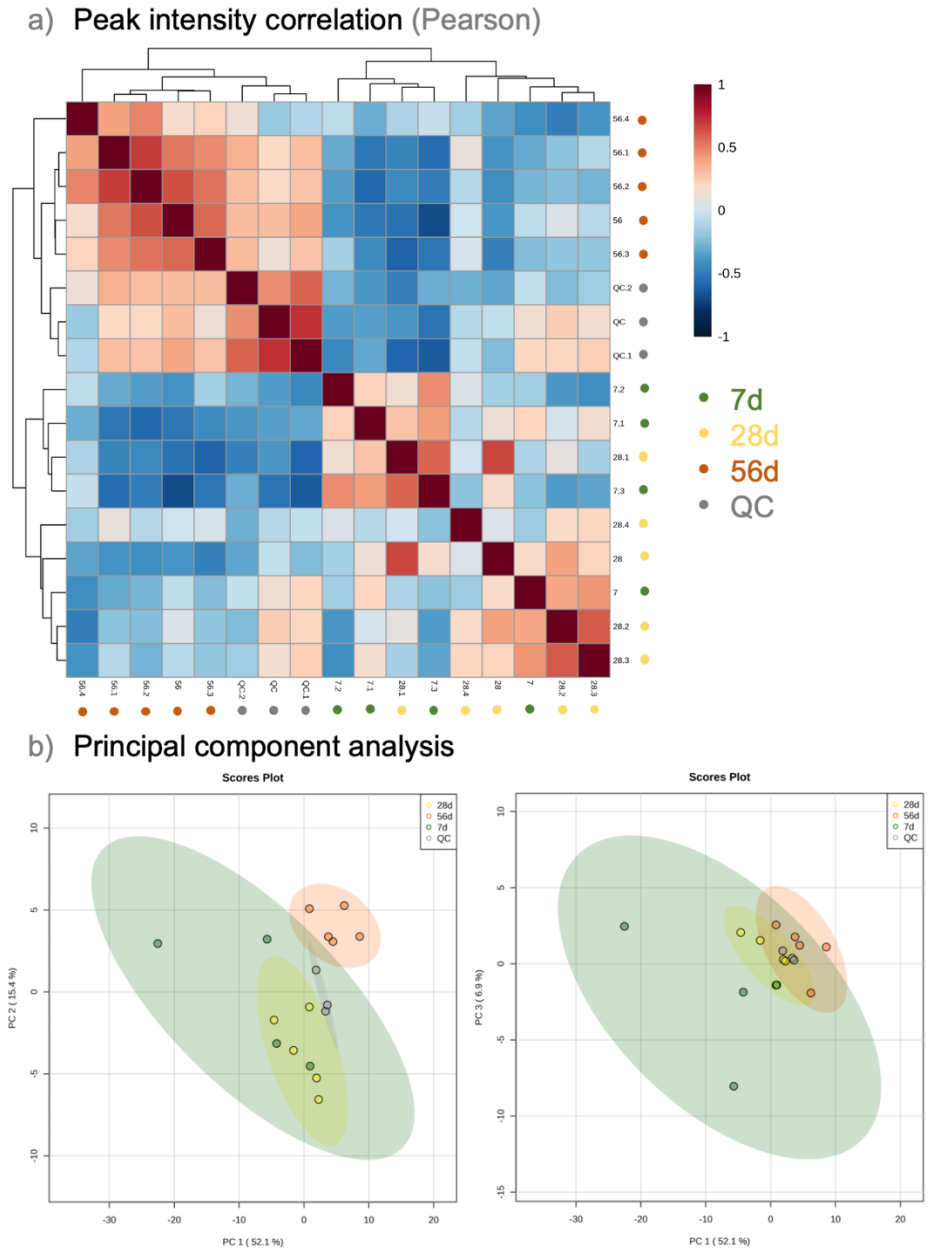


Figure 7.3. Sample correlation heatmap and principal components analysis: a) Heatmap of peak intensity correlations among samples; distance measure: Pearson R; b) Scores plots between principal component 1 and 2 (left), and 1 and 3 (right); explained variances in brackets; n=4-5 haemolymph samples. Green dots, 7d; yellow dots, 28d; red dots, 56d.

To identify biologically meaningful patterns related to the metabolites that significantly change with age, metabolite set enrichment analysis was performed. Over-representation analysis (ORA) was applied using the hypergeometric test to evaluate whether a particular metabolite set is represented more than expected by chance. One-tailed p values are provided after adjusting for multiple testing (Figure 7.4b). Given the resulting low number of significant hits per pathway (maximum 2), this analysis is affected mainly by the total number of metabolites assigned to that pathway and is less likely to represent biologically meaningful features.

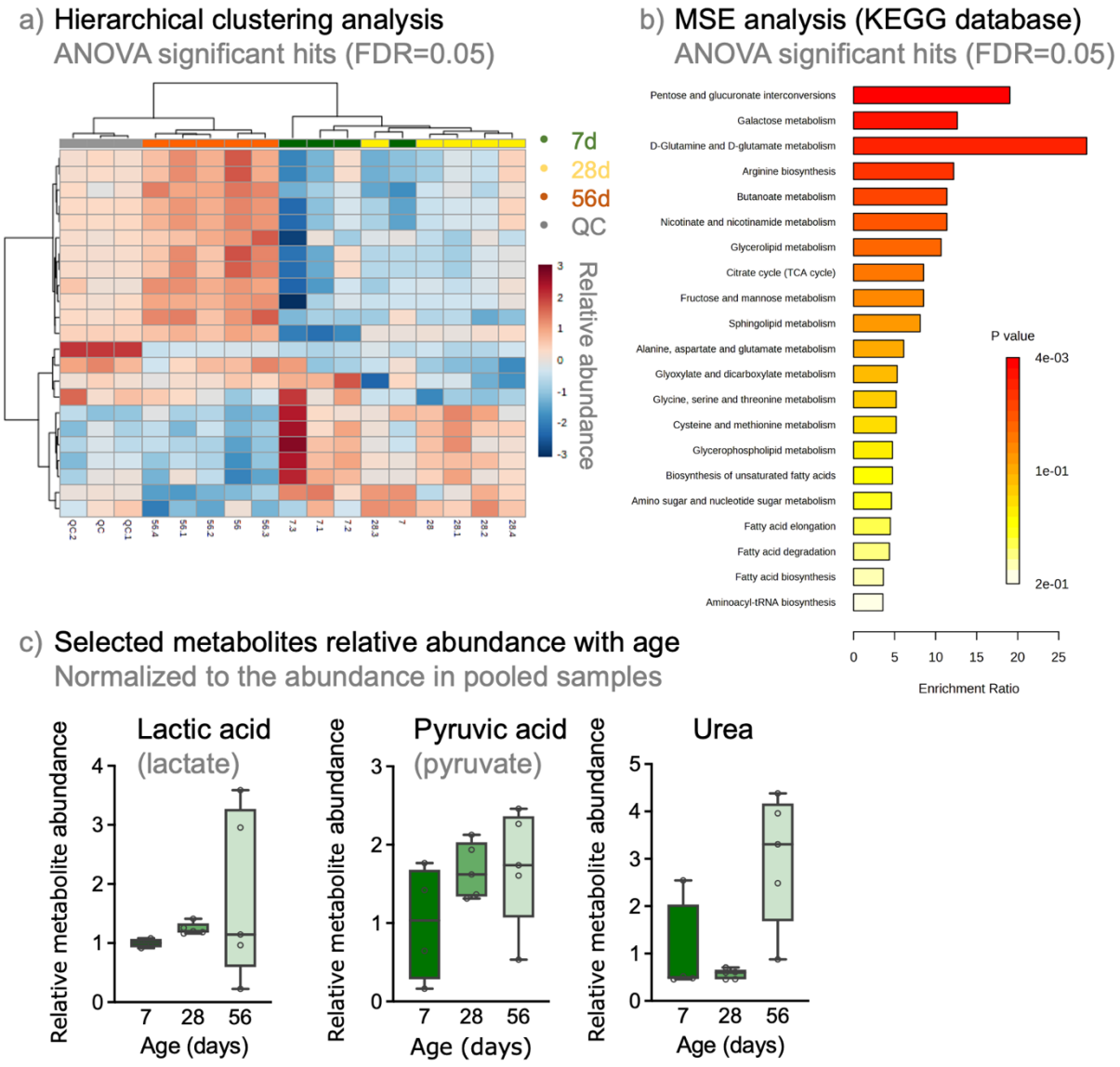


Figure 7.4. Hierarchical clustering and functional analysis of significant hits: a) Heatmap of sample clustering based on hierarchical clustering analysis of relative abundance of ANOVA significant hits; distance measure: Euclidean; Ward's linkage; b) Metabolite set enrichment analysis for ANOVA significant hits; Over-representation analysis in the KEGG database; one-

tailed p values provided after adjusting for multiple testing; c) Relative abundance of lactic acid, pyruvic acid and urea (non-significant); n=4-5 haemolymph samples.

Exploring the hypothesis that anaerobic glycolysis may contribute to increased acid production with age, the trend of lactic acid (measure of lactate) and pyruvic acid (measure of pyruvate) changes with age were individually analysed. Despite being non-significant, both tended to increase with age (Figure 7.4c). It might be worth directly measuring their concentrations in fly haemolymph using biochemical assays.

Given the loss of tubular function with age (see Section 6.2), the concentration of urea in fly haemolymph with age was also explored individually. Unlike in humans, urea is not a measure of filtration rate because flies do not filter their haemolymph, but it can be a measure of excretory capacity to eliminate excess nitrogen. Flies excrete nitrogen primarily through uric acid (see Section 7.3.1), but they may switch to production of either urea or ammonia in conditions where uric acid excretion is overwhelmed or compromised. Interestingly, urea also tends to accumulate in old age (Figure 7.4c).

7.2.3. The potential role of microbiota changes with age

Fly gut microbiota changes with age (Clark & Walker, 2018; Pryor et al., 2020) and may promote differential intestinal absorption of acidogenic nutrients with age that may chronically overwhelm the excretory system capacity to remove acids, even if they do not accumulate in the haemolymph and are thus not detected by metabolomics.

To test the association between age-related haemolymph acidification and the role of microbiota, flies would either need to: 1), be deprived of gut microbiota throughout their lives, to test chronic effects; or 2) be depleted of gut microbiota acutely at different ages, to test preferential absorption of acidogenic components with age. The gold standard procedure to effectively remove adult *Drosophila* microbiota is the addition of a broad-spectrum antibiotic to their food (Heys et al., 2018), which can be given chronically without impacting fly lifespan (Mair et al., 2005). To test if streptomycin could itself affect haemolymph pH, which would limit its use for this purpose, different concentrations of streptomycin (up to 8 times higher than the commonly use dose for microbiota removal) were added to the medium of young flies and haemolymph pH was measured. The same range of concentrations was used to confirm that streptomycin eliminated the microbiota by culturing fly lysates in a

Lactobacillus-selective medium as previously described (Heys et al., 2018). Streptomycin did not alter haemolymph pH (Figure 7.5a) and eliminated bacterial growth, although colony growth was inconsistent in control conditions (Figure 7.5b). Due to time restrictions, I was not able to follow this up and measure haemolymph pH in flies treated with streptomycin at different ages. This would be important to pursue not only in the context of age-related changes, but also following dietary manipulations described hereafter.

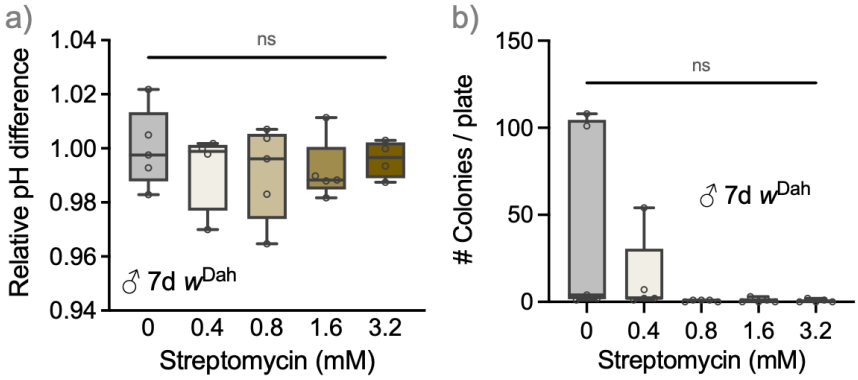


Figure 7.5. Impact of microbiota-related intervention on haemolymph pH: a) Haemolymph pH was measured using the pyranine method in w^{Dah} male flies after 7 days of treatment with 0 – 3.2 mM Streptomycin, n=4-5 replicates per condition; b) Number of colonies grown overnight per bacterial plate cultivated with homogenised w^{Dah} male flies after 7 days of treatment with 0 – 3.2 mM Streptomycin; n=5 replicates per condition. Statistical analysis was based on ANOVA with Tukey correction for multiple comparisons. ns, p>0.05.

7.3. Diet-induced acid-base imbalance and age-related disease

As discussed above, net endogenous acid production is diet-dependent. Diet is an independent risk factor for disease, but interacts with ageing to determine health and survival (Everitt et al., 2006; Fontana et al., 2010; López-Otín et al., 2016; Piper & Bartke, 2008). The oldest known lifespan-extending intervention is calorie restriction (McCay et al., 1935), and most interventions that extend model organism survival involve nutrient-sensing pathways.

The effect of calorie or specific nutrient restriction on animal survival is often compared to control cohorts with *ad libitum* access to food. Compared to the wild environment, *ad libitum* access to food may cause overnutrition instead, while dietary restriction only matches their basic needs, optimising food energy or specific components for health and survival, rather than having an anti-ageing effect as

commonly assumed. On that basis, here I focus on overnutrition through excess of different macronutrients and how it may interact with ageing through acid-base mechanisms to cause disease and shorten lifespan.

7.3.1. Fly tubule lithiasis as an age- and diet-related disease

Overnutrition through excess fats and carbohydrates lowers human life expectancy (Senior et al., 2020). This is often attributed to obesity and its consequences. In flies, excess fats and carbohydrates also shorten their lifespan (Birse et al., 2010; Owusu-Ansah & Perrimon, 2014; van Dam et al., 2020). Similarly, this has been attributed to obesity-like phenotypes and metabolic defects that result from the chronic intake of these diets (Owusu-Ansah & Perrimon, 2014). Here, it is hypothesised that these diets interact with ageing by affecting fly excretory capacity and acid-base balance to ultimately shorten survival.

Indeed, all three types of macronutrients are shown to cause tubule lithiasis in flies when provided in excess (Lang et al., 2019; van Dam et al., 2020). As lithiasis is also promoted by ageing (see Section 6.2), it was used here as an example of how diet may interact with ageing to cause age-related disease.

7.3.2. Excess sugar causes tubule lithiasis in flies

When I started my doctoral studies, there was an ongoing project in the lab determining how excess sugar in the fly diets shortened their survival. Raised under a high sugar diet (HS), adult female flies accumulate triglycerides and develop hyperglycaemia, insulin resistance and glycation damage, which recapitulate metabolic changes seen in mammals fed excess sugar (van Dam et al., 2020). Besides, excess sugar also caused dehydration with extracellular volume depletion with age, which was rescued by providing the flies with an additional source of water (Figure 7.6a).

Flies obtain enough water to meet their needs from their control (SYA) food. A strong indication is the observation that flies given an added water source have the same lifespan as flies raised under standard SYA medium without extra water (Figure 7.6b). However, under HS conditions (20% sucrose, compared to 5% in control food), fly lifespan was significantly decressed, which was fully rescued by exogenous water (Figure 7.6b). Lifespan rescue with water occurs even when the dietary concentration

of sucrose is increased to 40% (Figure 7.6c), demonstrating that dehydration is a major factor driving mortality under HS diets in flies. Importantly, added water did not alter feeding or prevent the metabolic defects mentioned above, establishing that shortened lifespan under excess sugar is independent of its obesogenic effects (van Dam et al., 2020).

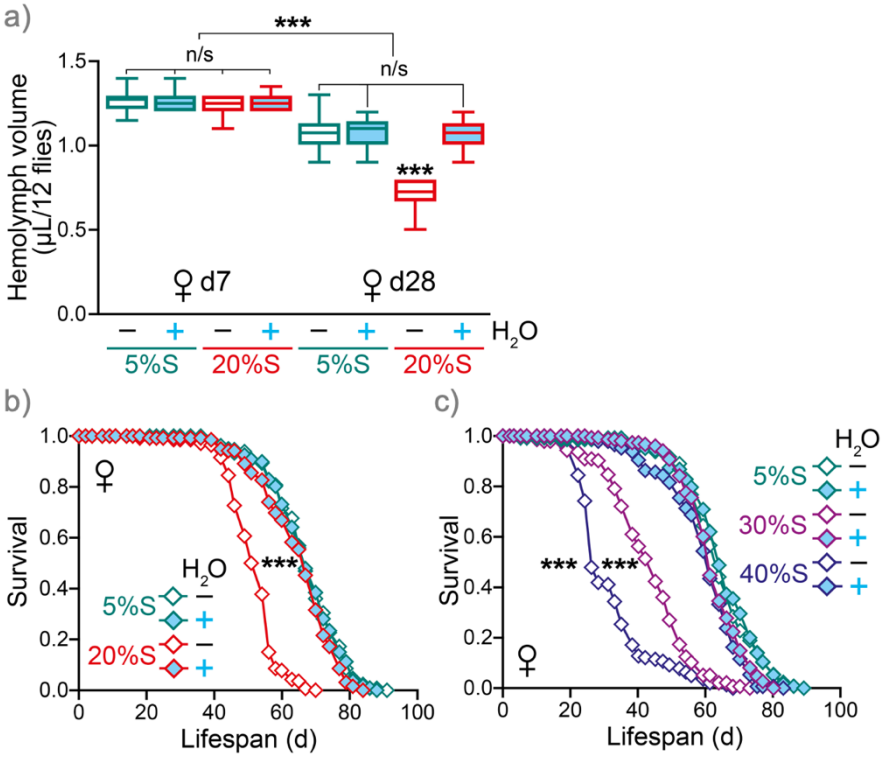


Figure 7.6. HS depletes extracellular volume and shortens fly survival in a water-dependent manner: a) Haemolymph volume of w^{Dah} females pre-treated for 7 and 28 days on standard SYA (5%S) or HS (20%S) ± H_2O; n=12-20 replicates per condition. Data are presented as box-and-whisker plots (min-max error bars), analysed by one-way ANOVA with Tukey correction; n/s, p>0.05; ***, p<0.001; b) Lifespan of w^{Dah} females on 5%S and 20%S ± H2O, n~150 per condition; c) Lifespan of w^{Dah} females on 30%S and 40%S ± H_2O, n~120–135 per condition. (Reprinted from van Dam et al., 2020)

Sugar is one of the main factors determining extracellular fluid osmolarity. Flies have thirst interneurons that respond to increased haemolymph osmolarity by promoting water-seeking behaviour (Landayan et al., 2021). Indeed, flies raised on a HS diet drink more water when acutely exposed to it, suggesting they are thirstier, compared to either flies raised under control conditions or pre-treated with an added source of water (Figure 7.7a-b).

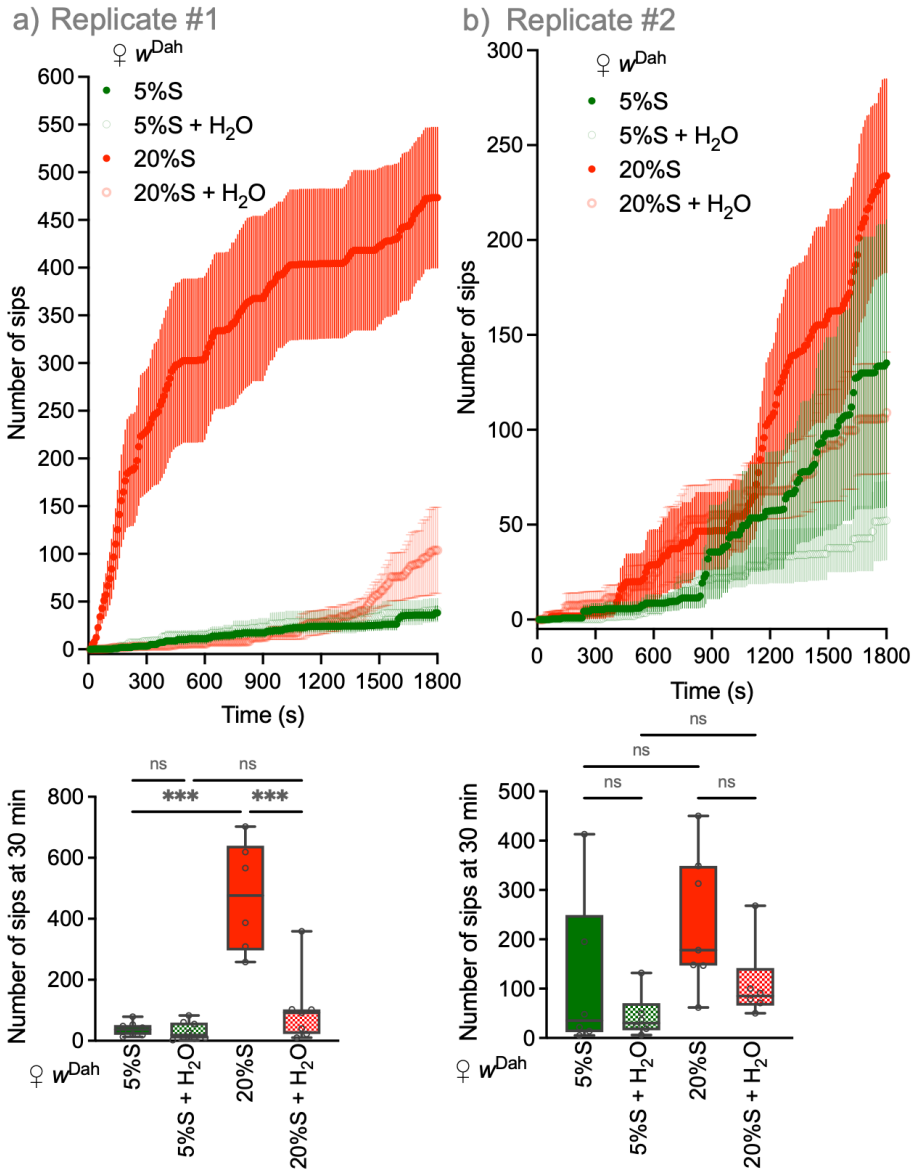


Figure 7.7. Flies raised on a HS diet are thirstier: a-b) Automated FlyPAD analysis showing the cumulative number of fly sips from an agar water source over 30 min. Independent biological repeats of female *w*^{Dah} flies pre-treated for 7 days on standard SYA (5%S) or 20%S diet ± H_2O. Top graphs show cumulative number of sips; data are means ± SEM of n=6–8 individual flies per condition. Bottom graphs are box-and-whisker plots of total number of sips at 30 min; analysed by one-way ANOVA with Tukey correction; n/s, p>0.05; ***, p<0.001.

Excess sugar is likely to cause dehydration due to excretory loss of water upon increased tubular secretion of sugar, as water follows the osmotic gradient. Therefore, higher secretion rates would be expected in flies under a HS diet. Surprisingly, flies raised on HS had significantly lower tubule secretion rates, which were prevented by adding an extra source of water (Figure 7.8a). This suggests: 1) that water loss occurs

through the intestinal tract due to proximal lower absorption or distal increased secretion; and 2) that tubule dysfunction occurs following chronic HS exposure.

Focusing on the excretory tract, the lab found that flies on a HS diet develop lithiasis with age at a higher rate than flies under a control diet or treated with water (Figure 7.8b-c). These stones are composed of uric acid (van Dam et al., 2020), and are thus prevented in flies pre-treated with allopurinol, a xanthine oxidase inhibitor which directly inhibits uric acid production (Figure 7.8d-e). Interestingly, despite shortening the survival of flies under control conditions, allopurinol extended the survival of flies raised on a HS diet (Figure 7.8e), suggesting sugar-related uric acid lithiasis contributes to shortening the survival of flies under HS conditions.

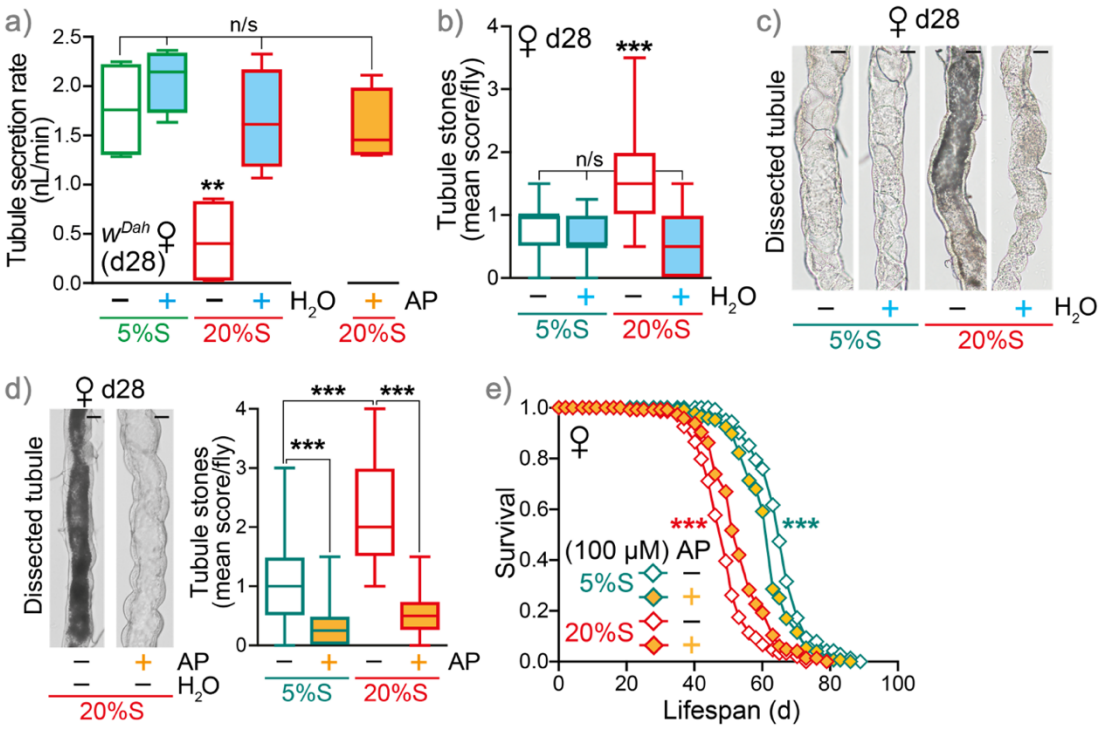


Figure 7.8. HS causes uric acid lithiasis in fly tubules: a) Secretion rates of tubules from w^{Dah} females pre-treated for 28 days on 5%S or 20%S ± H_2O or ± AP (1 mM), n=4 replicates per condition; Data analysed by one-way ANOVA with Tukey correction; n/s, $p > 0.05$; **, $p<0.01$; b) Tubule scoring and c) Representative light microscopy images (Scale bar: 25 µm) of w^{Dah} females after 28 days on 5%S or 20%S ± H_2O, n=50 flies per conditions; Data analysed by Kruskal-Wallis test with Dunn correction; n/s, $p > 0.05$; ***, $p<0.001$; d) Light microscopy images (Scale bar: 25 µm) and tubule scoring of w^{Dah} females after 28 days on 5%S or 20%S ± AP (1 mM), n=25-50 flies per condition; Data analysed by Kruskal-Wallis test with Dunn correction; ***, $p<0.001$); e) Survival curves of w^{Dah} females raised on 5%S or 20%S ± AP (100 µM), n~150 flies per condition. (Reprinted from van Dam et al., 2020)

7.3.3. Excess sugar leads to increased acid excretion

Three main factors determine the risk of uric acid crystal formation: increased uric acid production, dehydration and acidification. HS diet does not appear to cause significant haemolymph acidification (Figure 7.9a-e). Still, consistent with their shorter lifespan, flies raised on HS have accelerated haemolymph acidification with ageing, resulting in lower pH compared to flies raised on a low sugar diet in old age (Figure 7.9f). This suggests that increased acid excretion occurs as a response to sugar-related higher acid production but is insufficient to prevent chronic haemolymph acidification.

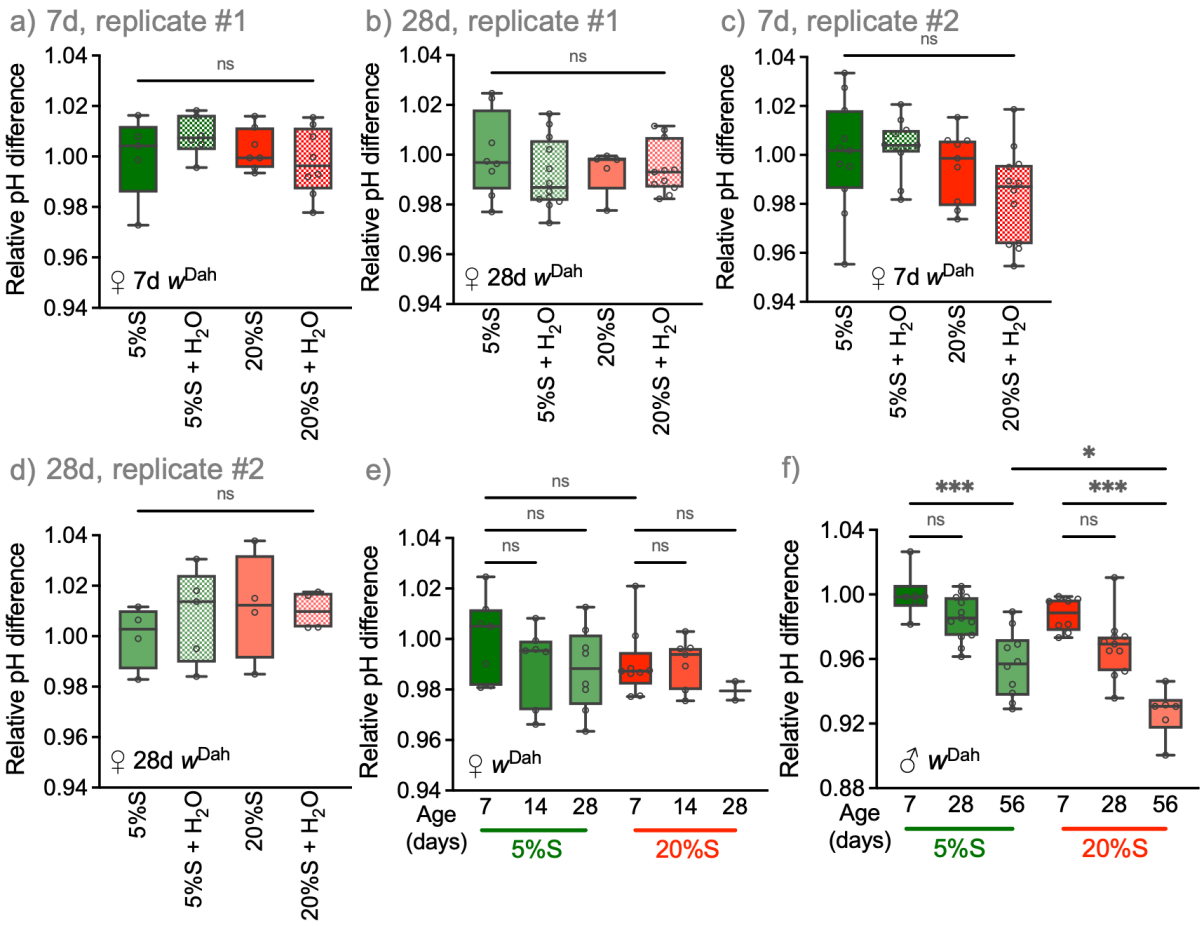


Figure 7.9. Haemolymph pH of flies raised on a HS diet. Independent biological replicates of haemolymph pH in w^{Dah} females treated for 7 (a,c) or 28 days (b,d) on 5%S or 20%S ± H_2O, n=4–12 replicates per condition; e) Haemolymph pH in w^{Dah} females treated for 7, 14 and 28 days on 5%S or 20%S, n=2-9 replicates per condition; f) Haemolymph pH in w^{Dah} males treated for 7, 28 and 56 days on 5%S or 20%S, n=6-13 replicates per condition. Box-and-whisker plots, statistical significance determined by ANOVA with Tukey correction for multiple testing; n/s, p>0.05; *, p<0.05; ***, p<0.001.

To test if a HS diet resulted in increased acid excretion to promote uric acid crystallisation in the tubules, flies were fed pH-dependent dyes (see Section 2.4.2.1). Distally to the insertion of the Malpighian tubules in the hindgut, intestinal lumen becomes more acidic (Figure 7.10a), suggesting that the urine secreted from the tubules under HS is acidic. The final excreta thus have lower pH, which is sex-independent (Figure 7.10b-c). This effect seems to be diet-specific and not related to ageing, as excreta pH does not further decrease in old flies (Figure 7.10d-e). Excreta acidification by a HS diet was inconsistently observed (Figure 7.10f), and seemed to change depending on the yeast batch used to make the media. Indeed, yeast composition may alter the susceptibility to acidification depending on the ratio of acidogenic amino acids in its composition or on its buffering capacity.

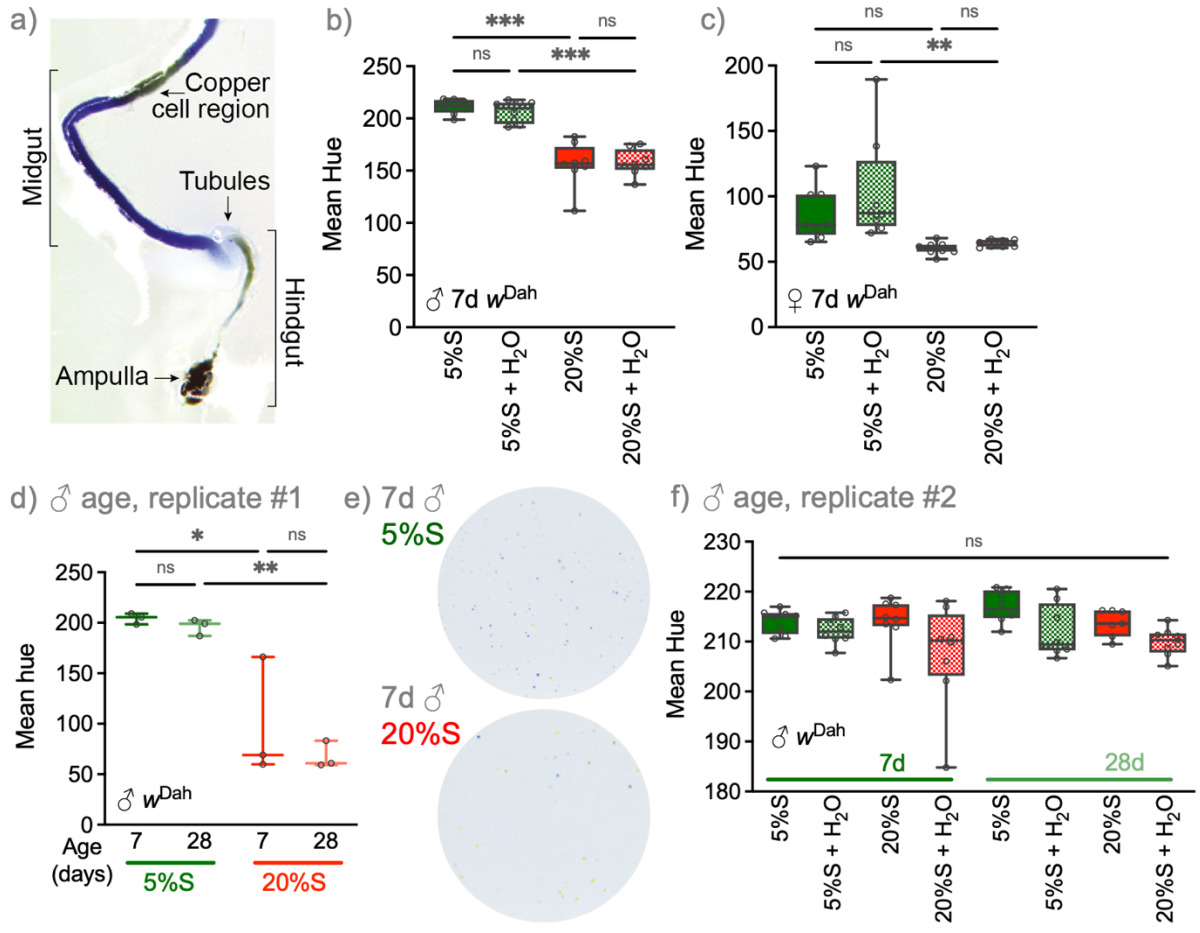


Figure 7.10. HS causes excretory tract acidification: a) Dissected intestine of HS-fed 7-day-old w^{Dah} female after feeding with pH indicator dye (bromophenol blue, 0.5% w/v) showing acidification of the hindgut (after tubule insertion) and the rectal ampulla; the copper cell region in the midgut, known to be acidified, is also apparent. Poo plates analysis of mean deposit hue of: b) male and c) female w^{Dah} flies after 7 days of feeding on 5%S or 20%S ± H_2O, n=10

plates with 5 flies each; d) male w^{Dah} flies after 7 and 28 days of feeding on 5%S or 20%S, n=3 plates with 5 flies each, with e) representative plate lid scans; f) male w^{Dah} flies after 7 and 28 days of feeding on 5%S or 20%S ± H_2O, n=8 plates with 5 flies each. Statistical significance determined by ANOVA with Tukey correction for multiple testing; ns, p>0.05; *, p<0.05; **, p<0.01; ***, p<0.001.

7.3.4. Dietary yeast as a driver of uric acid crystallisation

Flies excrete excess nitrogen from protein metabolism mainly through uric acid, instead of urea (the main human nitrogen waste product) or ammonia. This is an adaptation that insects, terrestrial reptiles and birds have to survive in dry environments (Salway, 2018). The uric acid molecule has a ratio of one hydrogen to one nitrogen atom. This allows it to be excreted within relatively low volumes of water. It is estimated that only 8 mL of water is needed to excrete 1 g of uric acid, while 40 mL of water is needed per g of urea and 400 mL per g of ammonia (Salway, 2018). As a comparison, in aquatic insects, fish and larval amphibians ammonia is the main nitrogen excretory product (Salway, 2018).

Yeast is the only dietary source of protein in our control fly diet. Under high concentrations of sugar in the diet (20% w/v), lowering the percentage of yeast in the media eliminated the lifespan rescue effect associated with water (Figure 7.11). This suggests that lithiasis under HS is also yeast-dependent.

Given uric acid is shown to systemically accumulate when any of the three types of macronutrients are provided in excess (Heinrichsen et al., 2014; Lang et al., 2019; van Dam et al., 2020), diet composition was compared between studies. Importantly, Heinrichsein *et al* do not report the relative percentages of diet components. Whereas in the study where different percentages of dietary yeast were tested, a 5% yeast diet was considered high in protein (Lang et al., 2019). SYA, used as the control diet here, is composed of equal sugar concentration (5%) to that study but 10% yeast (van Dam et al., 2020). Other dietary components may thus lower the threshold for uric acid deposition in the tubules on the high-yeast study, such as osmotic stress.

Flies raised under our control conditions do not suffer osmotic stress (van Dam et al., 2020), but need to excrete a high amount of nitrogen given the high protein concentration in their diet. High uric acid excretion may thus create a susceptibility to

tubule lithiasis. Conditions where uric acid concentration is further increased, excess water is lost, or urine is acidified can promote uric acid crystallisation.

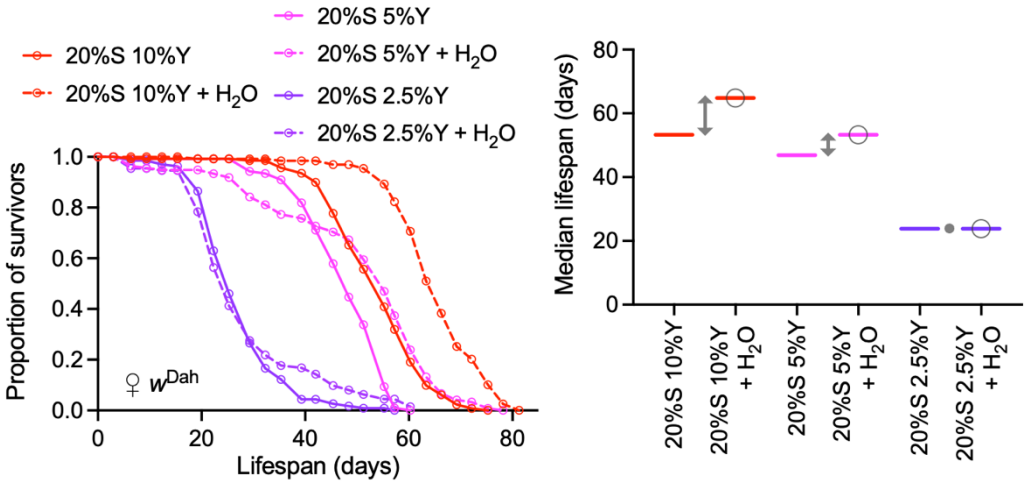


Figure 7.11. Water rescue in HS diets is yeast-dependent. Survival curves of w^{Dah} female flies fed food HS (20%S) with different percentages of yeast (2.5-10%) ± H_2O, and comparison of the effect of water on median lifespan depending on yeast %, n=140 flies per condition.

7.3.5. Dietary yeast concentration does not alter systemic acid-base balance

As previously stated, systemic non-volatile acid is mostly derived from the metabolism of sulphur-containing amino acids, such as methionine and cysteine. As the dietary source of protein in flies, yeast will determine net endogenous acid production and may promote systemic acidification to different degrees depending on its composition.

Protein- and amino acid-specific restriction have been shown to extend fly lifespan to the same extent as dietary restriction (Grandison et al., 2009; Sun et al., 2012). To assess if this correlates with changes in systemic acid-base balance, flies were raised on media containing a range of yeast concentrations, from 5 to 25%. Different studies consider different percentages of yeast as restricted or full-fed. A low-yeast (as opposed to 'fully-fed') condition can refer to concentrations ranging from 0.5% (Lang et al., 2019) to 10% (Grandison et al., 2009). Here, 10% was the control condition (SYA), 5% low-yeast and 25% high-yeast conditions. In this range, yeast % did not significantly alter haemolymph pH, in either sex (Figure 7.12a-b). Haemolymph pH tended to decline with age in all conditions, but acidification does not seem to slow down or accelerate with yeast content (Figure 7.12b).

Methionine is a particularly important amino acid for longevity modulation in animal models, from yeast to rodents (López-Otín et al., 2016). Methionine restriction also extends *Drosophila* lifespan (Lee et al., 2014; Parkhitko et al., 2021; Troen et al., 2007). Due to its acidogenic effect, methionine can be used as a clinical intervention to prevent specific human kidney stones that form under alkaline conditions, as supplementing about two times the daily recommended intake significantly decreases urine pH (Siener et al., 2016; Tiselius et al., 2001).

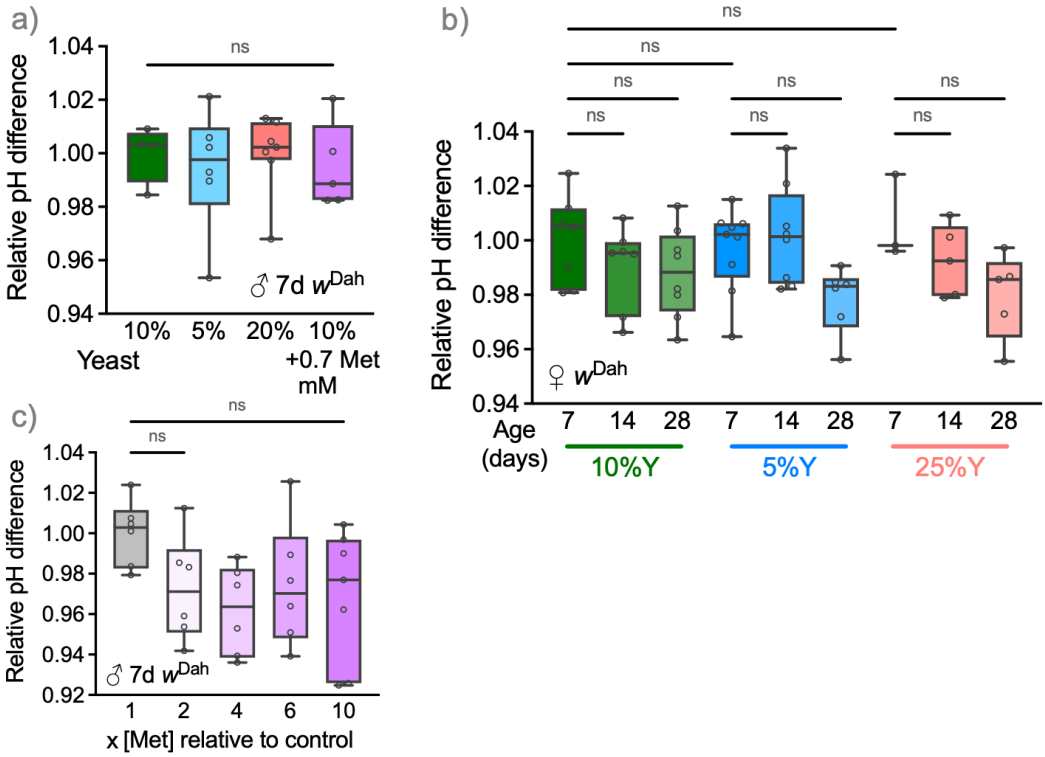


Figure 7.12. Haemolymph pH under HY and methionine diets: a) Haemolymph pH in w^{Dah} males fed for 7 days on SYA with varying yeast (5-20%) and with added 0.7 mM methionine, n=4–7 replicates per condition; b) Haemolymph pH in w^{Dah} females fed for 7, 14 and 28 days on SYA with varying yeast (5-25%), n=3-9 replicates per condition; c) Haemolymph pH in w^{Dah} males fed for 7 days on defined medium with varying concentration of methionine (1-10 times the standard concentration), n=6-7 replicates per condition. Box-and-whisker plots, statistical significance determined by ANOVA with Tukey correction for multiple testing; ns, p>0.05.

Methionine may contribute to urinary acidification and shorten fly survival through uric acid lithiasis. To test if methionine alters fly extracellular pH, I supplemented SYA with 0.7 mM methionine, as done before (Grandison et al., 2009), and defined medium with increasing concentrations of up to 10 times compared to the

control. Both interventions tended to lower haemolymph pH, although the effect was biologically variable (Figure 7.12a, c). If methionine lowers systemic pH, the rate of its oxidation may be exhausted upon doubling its concentration. It would be interesting to repeat these experiments with a higher number of replicates, and in parallel to assess excreta pH and tubule lithiasis under high methionine conditions. From an overall health perspective, it would also be important to test whether alkalotic treatment could counteract the negative effect of high methionine of fly lifespan.

7.3.6. Tubule lithiasis can be uncoupled from survival

Lithiasis can occur as a result of the crystallisation of different compounds. As discussed, flies are particularly susceptible to uric acid lithiasis. However, *Drosophila* has been used to model different kinds of lithiasis (Ali et al., 2018; Wang et al., 2022). The most common form of nephrolithiasis in humans is caused by calcium oxalate stones (Chen et al., 2011; Wang et al., 2022). Flies have been used to model calcium oxalate lithiasis, either by adding low doses of EG to their diet (not observed in our conditions, see Section 4.2.2) or by directly supplementing the diet with oxalate (Ali et al., 2018; Chen et al., 2011; Han et al., 2019). Survival was reported to decrease upon oxalate supplementation in a dose-dependent manner, which was correlated to tubule lithiasis (Chen et al., 2011; Han et al., 2019).

Here, flies were exposed to food with different percentages of sodium oxalate (NaOx) added to it. Consistent with previous reports, oxalate supplementation induced tubule lithiasis also in our SYA medium, that increased in severity in a dose-dependent manner, and may also be age-independent (Figure 7.13a). As reported, higher doses of NaOx resulted in shortened lifespan compared to lower doses. However, I found that low-dose NaOx actually extended fly lifespan (Figure 7.13b), despite increased lithiasis. This suggests that lithiasis *per se* can be uncoupled from lifespan. NaOx can work as an alkalotic compound, given oxalate is metabolisable, resulting in increased SID due to higher Na^+, as previously proposed for other compounds such as potassium citrate (Kellum & Elbers, 2009).

Given the fly susceptibility to form uric acid crystals, the added sodium could potentially promote uric acid lithiasis at higher doses by causing dehydration, independently of oxalate. To test whether lithiasis was indeed caused by calcium oxalate stones upon NaOx treatment, flies were fed allopurinol in addition to NaOx. Allopurinol did not prevent the formation of stones in flies fed NaOx (Figure 7.13c), in

contrast to its effect on lithiasis caused by either HS or high purine diets (van Dam et al., 2020), indicating that NaOx-related stones were not composed of uric acid.

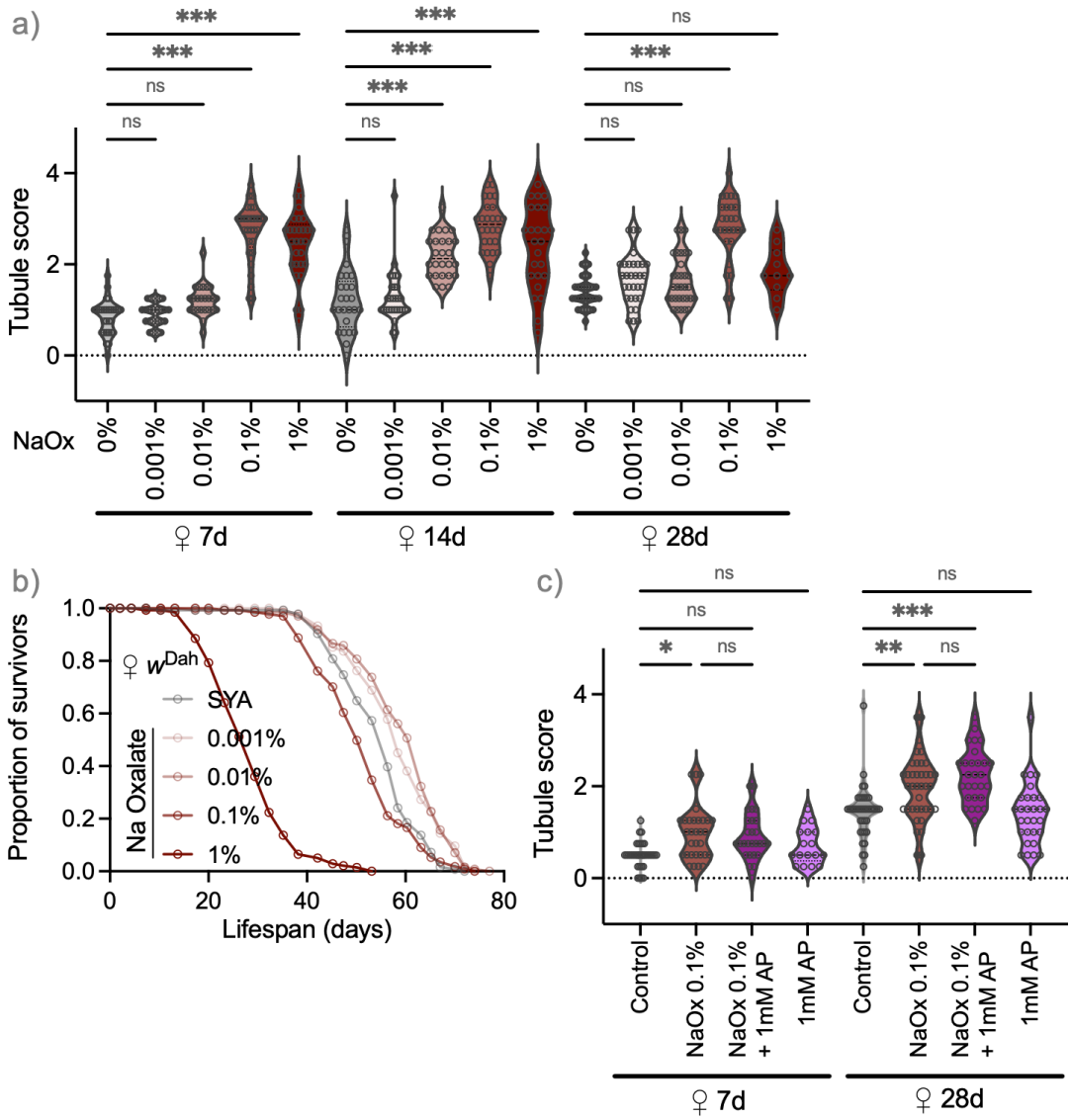


Figure 7.13. Calcium oxalate stones uncouple survival from lithiasis: a) Violin plots, tubule scoring of female *w*^{Dah} flies after 7, 14 and 28 days of feeding on SYA supplemented with varying percentages (w/v) of NaOx (0-1%), n=10-32 dissected flies per condition (note: at 28d, most flies fed 1% are dead, the few survivors may be less susceptible to lithiasis); b) Survival curves of female *w*^{Dah} flies fed on SYA with NaOx (0-1%), n=150 flies per condition; c) Violin plots, tubule scoring of female *w*^{Dah} flies after 7 and 28 days of feeding on SYA ± 0.1% NaOx ± 1 mM AP, n=17-39 dissected flies per condition. Statistical significance determined by ANOVA with Tukey correction for multiple testing; ns, p>0.05; *, p<0.05; **, p<0.01; ***, p<0.001.

To further dissect the correlation between age-related lithiasis and survival, two compounds were given in a range of doses to flies raised on standard SYA diet: allantoin and potassium citrate (K Citrate).

Allantoin is the end-product of uric acid degradation by urate oxidase. Contrary to humans, flies express urate oxidase and can convert uric acid into allantoin. This enzyme is expressed specifically in fly tubules (Leader et al., 2018). The presence of this enzyme in flies means that uric acid accumulation occurs only when the rate of uric acid production is higher than the rate of urate oxidation. This is likely to be the case in flies under relatively high protein diets. Allantoin concentration was shown to increase in flies with ageing and, as expected, in HS and high yeast diets (Yamauchi et al., 2020). To test whether allantoin itself can independently shorten fly survival, it was supplemented to the standard SYA medium. Allantoin did not shorten fly lifespan (Figure 7.14a). In fact, it slightly extended it as previously reported in male flies (Yamauchi et al., 2020), although this effect was not dose-dependent nor replicated in subsequent experiments from our group (Cochemé lab, unpublished data). Given the absence of negative effects from allantoin supplementation on survival, one strategy to prevent uric acid lithiasis in flies may be to increase the rate of uric acid breakdown by either: 1) overexpression of endogenous urate oxidase; or 2) rasburicase (recombinant version of urate oxidase) treatment.

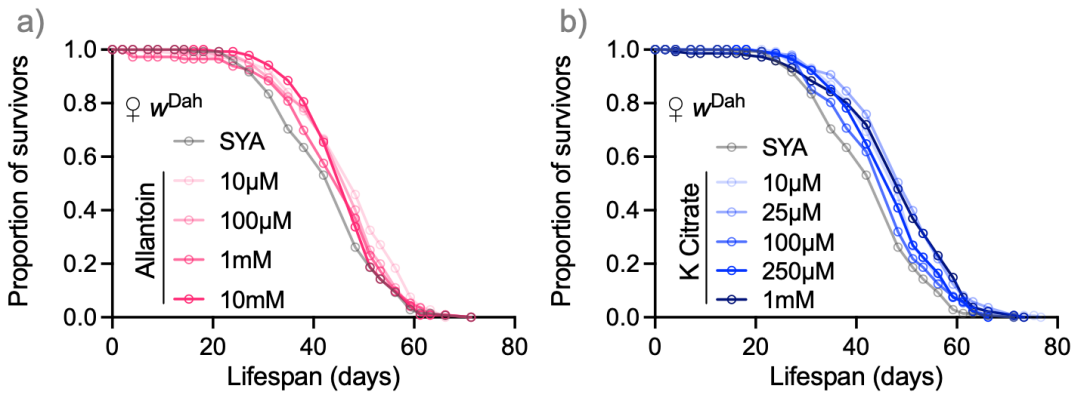


Figure 7.14. Effect of allantoin and potassium citrate on fly survival. Survival curves of female w^{Dah} flies fed on SYA with a) Allantoin (0-10 mM) and b) K Citrate (0-1 mM), n=150 flies per condition.

Potassium citrate is commonly used to prevent nephrolithiasis (Tiselius et al., 2001). Citrate can be metabolised, and potassium increases SID resulting in an

alkalotic effect. From a descriptive view, the alkalotic effect can occur from citrate metabolism into bicarbonate. In humans, potassium citrate can decrease calcium excretion through its alkalotic effect by reducing bone resorption and increasing renal calcium reabsorption (Lambert et al., 2015). Besides, dissociated citrate can bind to calcium which can help prevent formation of calcium-containing stones. Indeed, potassium citrate was shown to partially rescue the lifespan of flies raised on lithogenic diets, although this effect was inconsistent across studies (Chen et al., 2011; Han et al., 2019; Ho et al., 2013). Under control conditions, I found that potassium citrate extended *Drosophila* lifespan (Figure 7.14b). Citrate was reported to extend fly lifespan before, but whether it was supplemented as a salt or added as citric acid to the medium was not described (Fan et al., 2021). In that study, it was argued that citrate extends fly survival by promoting ketogenesis in a TOR- and AMPK-dependent manner. Adding a ketone body (β-hydroxybutyrate) in its sodium salt form to the food also resulted in lifespan extension (Fan et al., 2021). Given β-hydroxybutyrate can be metabolised and increase SID and thus pH, both citrate and β-hydroxybutyrate may alter metabolism and promote survival in an acid-base- and lithiasis-dependent manner. Due to time restrictions, it was not possible to use this drug as a tool to dissect these mechanisms, but this would be an important experiment to perform in the future.

7.3.7. The role of excess fat in tubule lithiasis

Besides sugar and yeast, excess fat (as 20% coconut oil) has previously been shown to result in systemic accumulation of uric acid (Heinrichsen et al., 2014). While studying the role of excess sugar on tubule lithiasis, our group has previously shown that adding fat (as 15% lard) to SYA medium also correlates with the formation of uric acid crystals in fly tubules of w^{Dah} female flies (Cochemé lab, unpublished data). I observed the same phenotype in the w^{1118} strain (Figure 7.15a). Although morphologically high-fat-associated crystals tend to be smaller (Figure 7.15b), in both HS and high fat (HF) the crystals are polychromatic under polarised light microscopy, which is commonly associated with uric acid crystals (Daudon et al., 2016)

Adding 15% lard to control defined medium also results in tubule lithiasis which tended to worsen with age (Figure 7.15c). This is expected since the defined medium was developed to match the amino acid profile of yeast-based SYA. Therefore, using the chemically defined diet, it will be possible in the future to modulate specific amino

acids, such as those that are acidogenic, and test their individual effects on lithiasis development as follow up experiments.

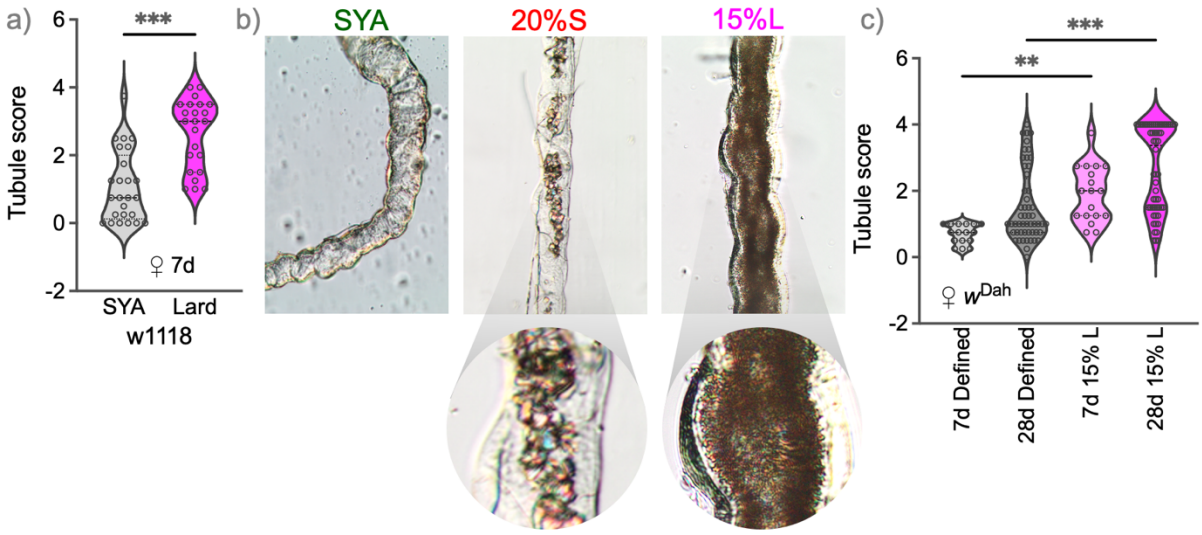


Figure 7.15. High fat diet causes tubule lithiasis in flies. a) Violin plots, tubule scoring of female w^{1118} flies after 7 days of feeding on SYA ± 15% lard, n=23-25 dissected flies per condition; b) Representative polarised light microscopy images of w^{Dah} female tubules after 28 days on standard SYA, HS (20%S) or HF (15%L); c) Violin plots, tubule scoring of female w^{1118} flies after 7 and 28 days of feeding on defined medium ± 15% lard, n=14-56 dissected flies per condition. Statistical significance determined by ANOVA with Tukey correction for multiple testing; **, p<0.01; ***, p<0.001.

7.3.8. Excess fat-related lithogenic factors

Experiments where both lard and yeast were added to media at a range of different concentrations demonstrated that lithiasis developed in a yeast-dependent manner, as proposed for the HS diet (Cochemé lab, unpublished data). This suggests that uric acid lithiasis caused by adding fat to the control diet is related to HF-related factors that further promote uric acid crystal formation, such as dehydration or acidification.

Although flies fed a HF diet are thirsty to the same degree as flies fed a HS diet (Figure 7.16a-b), adding an extra source of water does not rescue their shortened lifespan or prevent tubule stone formation (Cochemé lab, unpublished data), contrary to the effects of water on HS-fed flies. Given water has no effect on HF diets, acidosis was explored as the most likely factor promoting uric acid crystallisation.

Fat metabolism can alter acid-base balance through increased lipolysis or ketogenesis (DiBartola, 2012). HF diets are reported to cause obesity-like phenotypes

in flies (Birse et al., 2010; Heinrichsen & Haddad, 2012). Accumulation of triglycerides correlates with resistance to starvation in flies (Bjedov et al., 2010; van Dam et al., 2020). However, contrary to a HS diet, excess lard shortens fly survival under subsequent starvation (Figure 7.17a-b), despite higher energetic intake compared to the control diet. This suggests that flies raised on a HF diet are either not absorbing or metabolising the excess fat rather than accumulating it.

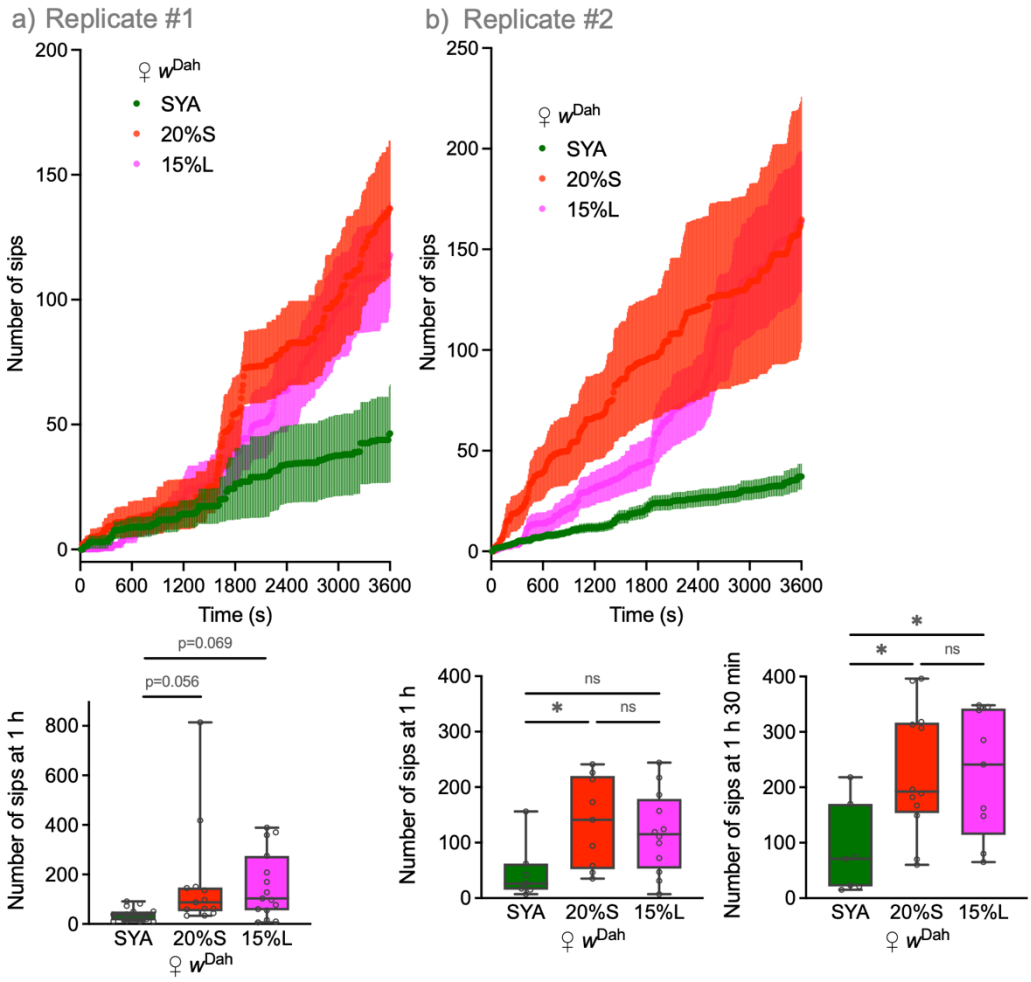


Figure 7.16. High fat diet causes thirst to the same degree as a high sugar diet. a-b) Automated FlyPAD analysis showing the cumulative number of fly sips from an agar water source over 1 h. Independent biological repeats of female *w*^{Dah} flies pre-treated for 7 days on standard SYA, HS (20%S) or HF (15%L). Top graphs show cumulative number of sips; data are means ± SEM of n=7–15 individual flies per condition. Bottom graphs are box-and-whisker plots of total number of sips at 1 h (and 1 h 30 min, for the same replicate); analysed by one-way ANOVA with Tukey correction; n/s, p>0.05; *, p<0.05.

To study substrate utilisation, flies were assessed by respirometry. As previously stated, animals using fat as their sole energy substrate would be expected to have a RQ of about 0.7 (Arch et al., 2006). Flies were either raised on control or HF diet for 7 days and then transferred to respiratory chambers with a matching source of food. In a third condition, flies were raised on a control diet and acutely exposed to a HF diet in the respiratory chamber. Flies fed a HF diet seemed to have a lower metabolic rate (Figure 7.18a-b). However, the RQ appeared to be close to 1 (Figure 7.18a). In fact, in measurements during the dark cycle, RQ seemed to be higher than 1 (Figure 7.18b), although the same is observed in flies raised on a control diet. RQ may be overestimated by increased production of CO_2 due to metabolism of organic acids or anaerobic glycolysis, as discussed (see Section 7.2.1). Detailed quantitative analysis and further replication need to be performed to confirm these results.

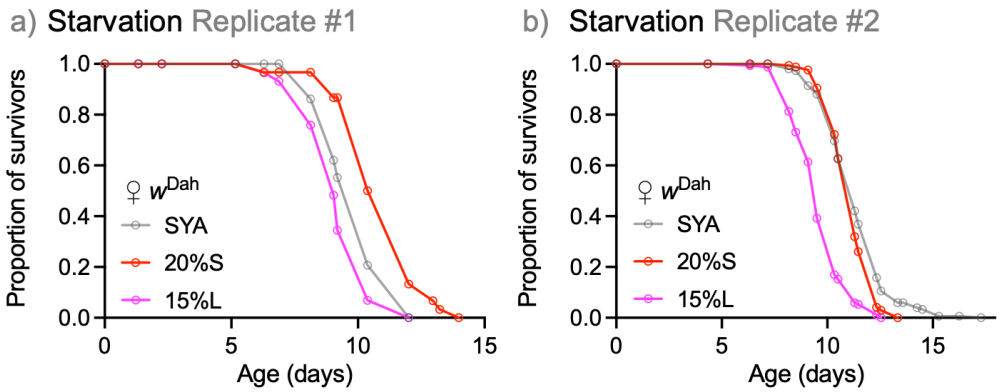


Figure 7.17. High fat diet increases fly mortality under starvation. Independent biological replicates of survival under starvation of female w^{Dah} flies pre-treated for 7 days on standard SYA, HS (20%S) or HF (15%L); a) n=30 flies per condition; b) n=150 flies per condition.

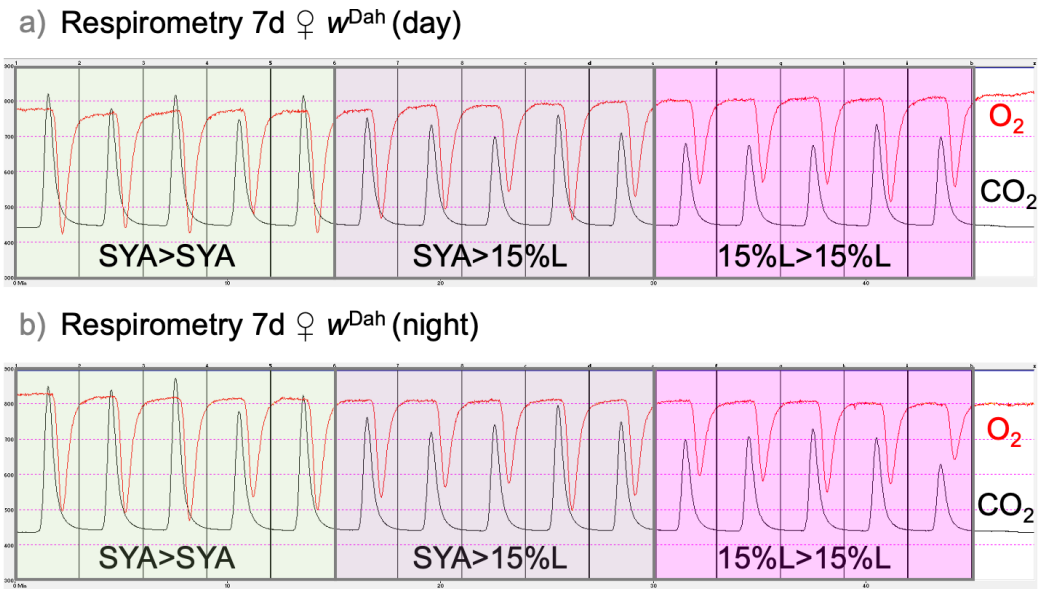


Figure 7.18. Respirometry of flies raised under a high fat diet. Representative graph of O_2/CO_2 respirometry at a) day or b) night of w^{Dah} female flies after 7 days of HF (15%L) feeding (pink box), acute exposure (purple box) or 7 days in control medium (green box). Each box contains five columns that correspond to 5 replicates (n=3 3 females each) of measured O_2/CO_2 peaks after a 48 min cycle.

7.3.8.1. Urine acidification may cause HF diet-related lithiasis

In a report on metabolic and transcriptional changes associated with a HF diet in flies, the most significantly altered metabolite was lactate (Heinrichsen et al., 2014). Ketone bodies were not measured in this study. Since lactate is a strong anion that can alter acid-base balance towards acidification, thereby promoting uric acid lithiasis, I measured the haemolymph pH of flies fed a HF diet. Flies tended to have lower haemolymph pH when raised on a 15% lard diet, although this effect was biologically variable across experiments (Figure 7.19a-c, e). A different fat source, hydrogenated coconut oil, at the same percentage also tended to decrease haemolymph pH (Figure 7.19d). This effect was not caused by tubule lithiasis since adding allopurinol does not rescue haemolymph pH (Figure 7.19e), while it prevented HF-related tubule stone formation (Cochemé lab, unpublished data). Given the experimental variability, it would be important to replicate these results with a higher number of samples.

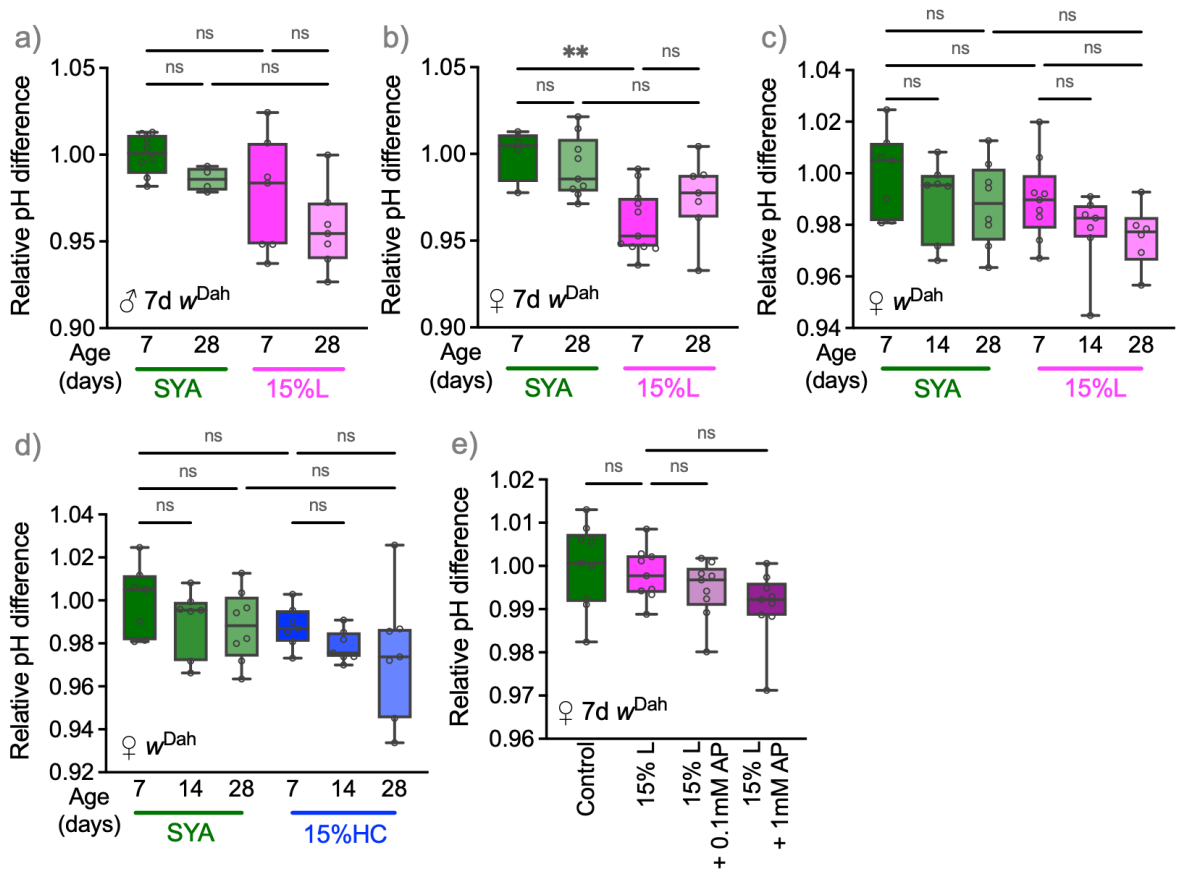


Figure 7.19. Haemolymph pH of flies raised on high fat diets. Haemolymph pH in male (a) and female (b,c) *w*^{Dah} flies fed for 7 (a-c), 14 (c) or 28 days (a-c) on SYA or 15%L, n=4-11 replicates per condition; d) Haemolymph pH in *w*^{Dah} females fed for 7, 14 and 28 days on SYA or 15% hydrogenated coconut oil (HC), n=7-8 replicates per condition; e) Haemolymph pH in *w*^{Dah} females fed for 7 days on SYA ± 15%L ± AP (0.1-1 mM), n=9 replicates per condition. Box-and-whisker plots, statistical significance determined by ANOVA with Tukey correction for multiple testing; n/s, p>0.05; **, p<0.01.

To specifically test the hypothesis that a HF diet may promote uric acid lithiasis by acidifying tubular lumen, proteins related to acid excretion (see Section 6.1.2) were knocked down specifically in the tubules. Knockdown of v-ATPase subunits significantly decreased HF-related tubule stone formation (Figure 7.20a-b), which correlated with their increased susceptibility to acidotic stress (see Section 6.3.4). Conversely, stone formation was not rescued by other proteins whose knockdown altered susceptibility to acidotic stress in females, such as CAH1 and pHCl-2 (Figure 7.20c). This suggests that HF causes lithiasis in v-ATPase-dependent manner. Despite rescuing lithiasis, v-ATPase knockdown will cause systemic acidification due

to decreased acid excretion. Using these conditions, follow-up experiments can fully dissect which factor has the predominant effect on shortening survival.

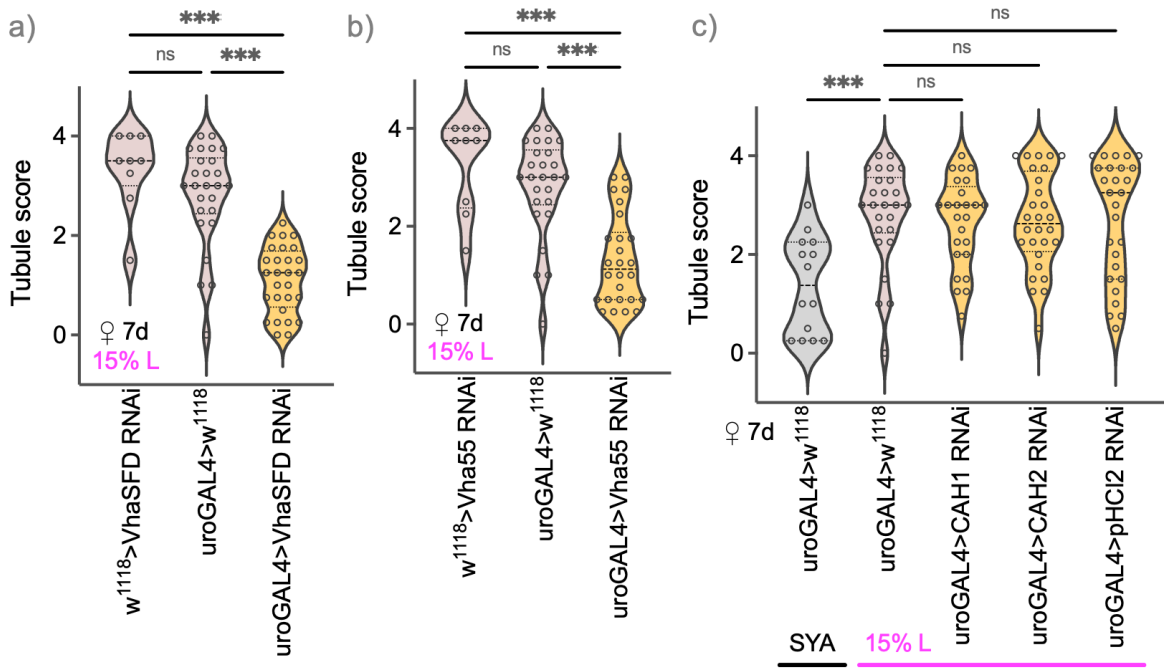


Figure 7.20. The effect of knockdown of acid-excreting proteins on HF-related lithiasis. Violin plots, tubule scoring of 7-day-old female flies fed a HF diet where a) VhaSFD, b) Vha55 or c) CAH1, CAH2 and pHCl-2 were knocked down specifically in the tubules (in yellow), with respective controls (in salmon; or grey for SYA control); n=9-28 dissected flies per condition. Statistical significance determined by ANOVA with Tukey correction for multiple testing; n/s, $p>0.05$; ***, $p<0.001$.

7.4. Key messages and interpretation

In this chapter, the effect of age-related changes in metabolism and of overnutrition of different macronutrients on systemic acid-base balance were tested. The contribution of acid-base as an age- and diet-dependent factor for lithiasis pathophysiology was also explored. The key messages are:

- Haemolymph metabolome changes with age do not include significant organic acid or lactate accumulation
- *Drosophila* is susceptible to uric acid lithiasis
- HS promotes tubule uric acid crystallisation primarily through dehydration
- HF may cause systemic acidification and promote uric acid lithiasis by causing tubule lumen acidification

From previous results of mammalian metabolome studies, and given the apparent change in RQ with age, it was expected that flies would either accumulate organic acids or lactate with age. Indeed, mice show increased lactate and reduced glycolytic intermediates in the liver and muscle with age (Houtkooper et al., 2011), which correlate with age-related mitochondrial dysfunction (López-Otín et al., 2013).

One mouse model overexpressing the enzyme phosphoenolpyruvate carboxykinase (PEPCK) is particularly interesting in this context. Mice overexpressing this enzyme produce negligible levels of lactate and have an extended lifespan, even though they feed more than control mice, and have a higher metabolic rate and resistance to aerobic exercise (Hanson & Hakimi, 2008). PEPCK produces bicarbonate as a by-product and is upregulated in prolonged acidosis in the renal proximal tubule as a compensatory mechanism (Wagner et al., 2006). This makes PEPCK a particularly intriguing factor converging age-related metabolic changes, pH homeostasis and survival. Despite not significantly changing with age in fly haemolymph, lactate may accumulate intracellularly. Besides, lactate was shown to be the metabolite most significantly upregulated by feeding flies a HF diet (Heinrichsen et al., 2014). This suggests overexpressing *Pepck1,* the fly gene encoding PEPCK, may be an interesting strategy to promote acid-base balance with age and prevent acid-related lithiasis.

As previously stated, the control diet used in this study has a relatively high protein content, which is likely to increase baseline susceptibility to uric acid lithiasis since flies excrete uric acid as their form of nitrogen waste. Indeed, flies have the necessary enzymes to form the uric acid cycle originally described by Krebs (Salway, 2018). These enzymes are expressed in the fat body (Leader et al., 2018), suggesting the fat body secretes hypoxanthine as a form of metabolic waste which is then taken up by the tubules where urate oxidase (specifically expressed there) converts it into uric acid. Studying the fat body uric acid cycle or hypoxanthine membrane transport may thus provide other strategies to prevent lithiasis in flies.

A previous report showed that knocking down a Na^+-H^+ exchanger in fly tubules causes uric acid lithiasis, by decreasing tubule lumen pH (Ghimire et al., 2019). This occurred in a control diet composed of only 3.5% yeast, indicating that diets with lower protein content can still induce uric acid lithiasis given other conditions that promote crystallisation are present.

In young flies, control diet *per se* does not cause lithiasis because it lacks the conditions for crystallisation. Added sugar or fat are needed to either cause dehydration or tubule acidification, leading to uric acid crystallisation. Indeed, adding a water source to a HS diet and inhibiting acid excretion in a HF diet, respectively, prevented tubule lithiasis. Importantly, water fully rescued the lifespan of flies raised on a HS diet, despite not ameliorating the associated metabolic defects (Lennicke et al., 2020; van Dam et al., 2020). This demonstrates that short survival under HS is primarily caused by dehydration, not the obesity-like phenotypes caused by sugar as previously assumed.

Water supplementation was also previously shown to abolish the lifespan extension attributed to dietary restriction (Ja et al., 2009), suggesting the control food used in that study shortened fly survival by osmotic stress. Although an independent study showed water-independent life extension under DR (Piper et al., 2010), the first report demonstrates that DR can extend lifespan in conditions where control diets have negative effects, likely related to overfeeding. In flies, the protein to carbohydrate ratio is suggested to be the main dietary determinant of lifespan (Ja et al., 2009). Given protein is the main source of dietary acid load, as discussed (Section 7.2), dietary macronutrient ratio may determine survival by affecting systemic acid-base balance. Here, adding excess yeast (+15%) to the control diet did not significantly alter haemolymph pH. Haemolymph pH is redundantly regulated, so significant changes depend on multiple systems failing, as occurs with ageing. With diet, tubule acid excretion and intracellular buffering systems may disguise haemolymph changes and only be overwhelmed by chronic exposure. Follow up experiments are needed to test these associations.

Diet has complex effects on survival. Here, I focused on the acid-base perspective, but diet can affect all hallmarks of ageing (López-Otín et al., 2013, 2016, 2023). It is important to distinguish the dietary effects from ageing-related factors on mortality rate, but also to understand how they may interact through common mechanisms, such as acid-base balance. Understanding the pathophysiology of overnutrition will create new strategies to prevent age-related disease and help progress ageing research beyond the confounding effects of diet.

Chapter 8. Global discussion and future directions

During my PhD, I set out to test the hypothesis that loss of systemic acid-base homeostasis is a novel hallmark of ageing, i.e., that: 1) systemic acidification occurs during ageing; 2) factors that promote acidification shorten survival (as a simple readout for ageing); and 3) factors that prevent acidification extend lifespan. In this chapter, findings are reviewed collectively and future directions are proposed.

8.1. Loss of acid-base balance as a hallmark of *Drosophila* ageing

8.1.1. Extracellular acidification occurs during ageing

In this study, haemolymph pH was measured spectrophotometrically by mixing it with a dye whose absorption ratio at specific wavelengths is pH-sensitive, by comparison to a standard curve of known pH solutions. Given that solution properties can alter dye absorption and the exposure to air during collection can lead to pH changes through CO_2 loss, despite efforts to limit those factors, interpretation of absolute pH values is limited. In this project, I measured relative differences within the same experiment.

Throughout this study, haemolymph pH was observed to lower with age, independently of fly strain, sex or dietary conditions. Importantly, the rate of acidification correlated with mortality rate, both when manipulated genetically or through temperature.

Consistent with these observations, the pH of whole fly lysates decreases as the flies get older (Massie et al., 1981). Larvae also have higher pH compared to adult flies when both measured in whole lysates or haemolymph directly (Ghosh & O'Connor, 2014; Massie et al., 1981). This suggests: 1) higher pH may be important for *Drosophila* development; or 2) that ageing may occur already at this stage. The idea that ageing occurs through development as a programmed process has been proposed (Magalhães, 2012). From a stochastic standpoint, it is also conceivable that ageing primary drivers act throughout the whole life cycle, and that what differs is the capacity to respond to them. That is what occurs in adult flies: the younger they are, the better they respond to EG-induced acidotic stress. Follow up studies can expand this analysis to fly developmental stages, and test how larvae respond to acidogenic conditions and how that affects their health as adults.

The cause of age-related acid-base imbalance was explored. H^+ can accumulate when the rate of elimination is lower than the rate of production or consumption. Metabolites related to acid-producing metabolic processes were found to not significantly accumulate in fly haemolymph with age, although undetected organic acids may play a role. Besides, neither sulphate nor other inorganic ions were measured, and are needed for a global view on acid production (Poupin et al., 2012). Net acid production can also be indirectly measured by the concentration of sulphate and potassium in urine, as developed for humans (Frassetto et al., 1998). Applying this method to flies may not be technically feasible because the urine produced by Malpighian tubules drains into the hindgut to result in combined excreta with undigested food, which also contains sulphate and potassium and is modified by microbiota.

The advantage of combined excreta is that measuring their pH directly provides a global view of total acid excretion. Tubule secretion rates were found to decline in fly tubules with age (Dornan et al., 2020). As presented here, flies lose the capacity to excrete acid effectively with age. This correlates with a general downtrend in gene expression of proteins that are needed for tubule secretion and are proposed to be required for acid excretion: v-ATPase subunit Vha68-2, CAs and pHCl-2. Upon age-related acidification, these genes would instead be expected to be overexpressed as a compensatory mechanism. This first suggests haemolymph acidification may result from age-related loss of acid excretion, implying loss of systemic acid-base balance is a consequence of ageing.

Alternatively, potential downregulation of these genes may be a manifestation of ageing due to upstream acidification promoted by environmental exposures, such as diet. Diet-related factors that increase acid load are related to decreased kidney function in humans (Banerjee et al., 2023; Hietavala et al., 2018; Rebholz et al., 2015; Toba et al., 2019; Valle-Hita et al., 2022). One of these dietary factors is phosphate. In mammals, high dietary phosphate paradoxically leads to downregulation of *klotho* (Frassetto & Sebastian, 2019; Muñoz-Castañeda et al., 2017), a factor that promotes renal phosphate excretion. Interestingly, klotho promotes nuclear translocation of TFEB. TFEB upregulates the transcription of v-ATPase subunits, and may thus also promote acid excretion in the kidneys, independently of its role on autophagy (Fung et al., 2022). In line with this idea, *klotho* knockout mice accumulate phosphate and develop metabolic acidosis. With ageing, *klotho* gene expression declines, which is

attributed to the consumption of high phosphate diets, and may contribute to systemic acidification in mammals (Frassetto & Sebastian, 2019). In flies, a *klotho*-like gene was identified, but is not well characterised (Rose et al., 2019). Interestingly, a phosphate-lowering drug was shown to extend *Drosophila* lifespan (Bergwitz, 2012). Besides, the expression of *Mitf* (the fly *TFEB* orthologue) is shown here to decline with age in fly Malpighian tubules.

Age-related systemic acidification also occurs in humans (Frassetto et al., 1996), but the relative pH decline is more pronounced in fly haemolymph compared to human blood. This may be related to a tighter control of pH in human blood due to, for example: 1) the presence of erythrocytes; 2) more effective acid excretion through kidney filtration; or 3) the presence of chemoreceptors that quickly respond to blood acid-base changes through respiratory mechanisms. Despite loss of effective response through these elements with age (Conde et al., 2006; Denic et al., 2016; Dos Santos et al., 2018; Frassetto et al., 1996; Woodman et al., 2005), they provide extra levels of regulation compared to the fly.

Fly haemolymph is more comparable to lymph, the fluid resulting from the collection of tissue-specific interstitial fluid by the lymphatic system and redirected to the circulatory system. There is currently no available data on how mammalian lymph pH changes with age. Recently, the role of lymph in diet-induced metabolic disease has been explored (Cao et al., 2021). However, the lymphatic system has mostly been studied in the context of cancer and inflammation (Wiig & Swartz, 2012). Lowering the pH of their microenvironment is a strategy used by several types of cancer to evade immune cells, by inhibiting their function (Erra Díaz et al., 2018). Lower lymph pH favours metastasis (Robey et al., 2009) and decreases lymph flow (Moeller et al., 2019) contributing to oedema, a common sign in oncologic patients with invasive tumours (Rockson et al., 2019). This demonstrates that decreased pH in lymphatic fluid can have pathophysiological consequences, including decreased immune function and oedema, also commonly seen in aged cancer-free patients. To measure whether lymph pH changes with ageing in mammals to the same extent as haemolymph pH, we are collaborating with the Trevaskis group at Monash University, Australia. As hypothesised, mouse lymph pH collected from the thoracic duct decreases with age (3 weeks v. 32 weeks), and the relative age-difference is comparable to that observed in flies (personal communication, Trevaskis group).

Overall, loss of acid-base balance occurs with ageing and is seen across multiple species, including humans. To explore the direction of causality between ageing and loss of acid-base balance, the effect of factors that promote or prevent it on fly lifespan was measured.

8.1.2. Factors that promote acidification shorten survival

Arguably, any essential physiological process can shorten survival if sufficiently dysregulated. Since acid-base homeostasis is fundamental for biological functions, it is then predictable that organisms have a lower survival under acidotic stress conditions. Accordingly, metabolic acidosis is directly correlated with increased mortality in humans, from studies based on either chronic acidosis in the context of advanced chronic kidney disease (Raikou, 2016; Tangri et al., 2021), or on acute acidosis in a critical care setting (Cheng et al., 2021; Gunnerson et al., 2006; Hu et al., 2017; Jamme et al., 2018; Wernly et al., 2020; Yang et al., 2017). While these conditions may not translate the effect of sub-clinical age-related acidosis on mortality, higher estimated dietary acid load is also associated with increased human all-cause mortality (Park et al., 2015; Xu et al., 2016).

Here, interventions were aimed to model chronic systemic acidification throughout fly lifespan rather than acute acidosis. Even with 2.5% EG in their diet, flies responded by increasing acid excretion and survived for ~2-3 weeks. This suggests 2.5% EG promotes acidification, but its toxic effect is not immediate. After 1 week of 2.5% EG treatment, haemolymph pH dropped to values comparable to haemolymph pH of old flies under standard conditions. Besides, shortening of survival after EG exposure occurred in a dose-dependent manner, and even at lower doses. Adding $NaHCO_3$ and an extra water source to EG-containing medium prevented EG-related haemolymph acidification and osmotic stress, respectively. When combined, these interventions rescued fly lifespan to levels comparable to flies raised on standard conditions, despite the constant dietary acidotic stress. This demonstrates that the effect of EG on survival is dependent on haemolymph acidification and osmotic stress, rather than other potential toxic effects.

As independent methods to increase dietary acid load and confirm effects on fly survival, high phosphate and sulphate diets can be explored. In addition, measuring the composition of standard diets, and specifically of acidogenic components such as

sulphates and sulphur-containing amino acids, may clarify the variation in fly lifespan exposed to different diets.

Promoting haemolymph acidification by knocking down the gene expression of proteins proposed to be necessary for acid excretion in fly tubules – v-ATPase, CA1, pHCl-2 – resulted in shorter female survival under acidotic stress. In male flies, only knockdown of v-ATPase subunits increased mortality on acidotic stress. The effect of these tubule-specific interventions on survival under standard conditions should be measured as follow-up. In humans, mutations in orthologues of these genes cause distal renal tubular acidosis (Batlle & Haque, 2012). Given their rarity, data on the long-term outcomes of these inherited diseases is very limited, but early and sustained alkalotic treatment improves the prognosis (Lopez-Garcia et al., 2019; F. Santos & Gil-Peña, 2023).

Another factor known to lower pH directly by altering the dissociation constants of water and weak electrolytes is higher temperature. Flies are ectotherms and when raised on a higher temperature have an increased rate of haemolymph acidification which correlated with shorter lifespan. The effect is proposed to be pathophysiological because young flies raised on a higher temperature do not have significantly lower haemolymph pH. This suggests the excretory system can compensate for the effect of temperature on pH, but this response is more rapidly overwhelmed than in flies raised at lower temperatures.

Collectively, different interventions that lower haemolymph pH – dietary, genetic and environmental – shorten fly survival. Correlations between either acidogenic diets or metabolic acidosis and mortality suggest age-related systemic acidification may also impact human lifespan.

8.1.3. Factors that prevent acidification extend survival

Extending the survival of any organism raised under standard conditions is a more complex challenge. To measure the impact on survival, I aimed to maintain or increase haemolymph pH throughout life with three different strategies: 1) pharmacologically, with alkalotic drugs; 2) genetically, by overexpressing genes that either catalyse buffer reactions or promote acid excretion; and 3) environmentally, by raising flies at a lower temperature.

$NaHCO_3$, an alkalotic treatment used in clinical practice, extended fly lifespan under standard conditions, independently of sex and even when started later in life or given intermittently. Incubating flies at a lower temperature slowed the rate of haemolymph acidification and also extended their survival.

Genetic interventions were less successful. *CAH1* ubiquitous overexpression extended the lifespan of female flies, which correlated with resistance to acidotic stress. However, these effects are female-specific and seem to be haemocyte-independent, suggesting the survival effect is independent of improved haemolymph buffering capacity. It was not technically possible to measure CA activity with age in fly haemolymph. In humans, erythrocyte CA activity is decreased in low dietary zinc conditions, which impairs the physiological response to exercise (Lukaski, 2005). With ageing, changes in erythrocyte CA activity are unexplored, but zinc deficiency is common in the elderly (Cabrera, 2015). From a chronic perspective, loss of buffering capacity may contribute to systemic acidification, but the imbalance is likely to start from increased acid load or decreased excretion.

In an attempt to improve acid excretion in flies, CAs, the v-ATPase regulatory subunit and pHCl-2 were individually overexpressed specifically in fly tubules. Their overexpression did not extend fly lifespan under standard conditions. It also failed to consistently rescue survival under acidotic stress, suggesting their individual overexpression is not sufficient to promote acid excretion. As discussed, these proteins are likely to be interdependent, which implies combined overexpression of at least these 3 elements would be needed to improve acid excretion capacity.

From these observations, it is not possible to conclude that preventing haemolymph acidification promotes survival. The effects of $NaHCO_3$ and temperature on lifespan are correlative and may be independent of their acid-base effects. Given the broad effects of these interventions, it is challenging to decisively attribute causality to pH changes. One way to tackle this problem in fly lifespan interventions has been to use combinatorial strategies. If different interventions alter lifespan through the same mechanism, it is likely that their independent effects would not be additive. This approach is also limited, particularly in the context of acid-base balance. Interventions that significantly extend fly lifespan (e.g., temperature) do not rescue age-related acidification, despite slowing down its rate. Additional strategies (e.g., $NaHCO_3$) could therefore further extend lifespan despite acting through the same mechanism.

Future efforts should focus on finding the primary cause of age-related acidification. As discussed, loss of acid excretion can cause age-related acidification *per se*. However, finding exactly what acids accumulate may allow for more effective genetic strategies to rescue age-related acidification. Measuring inorganic ions in the haemolymph would be important, since organic acids were not found to significantly accumulate with age. Phosphate and sulphate, in particular, may indicate a primary dietary cause to both tubular dysfunction and age-related acidification.

8.1.4. Limitations of survival as a readout for ageing

In the absence of comprehensive and robust biomarkers or functional scores for fly ageing, survival was used as a simple readout for all the interventions presented here. Survival is commonly used as a measure of ageing, from the assumption that even when raised under ideal environmental conditions, living organisms eventually die due to the critical failure of one or more essential organs as a result of ageing. This approach has some limitations: 1) ideal conditions are an elusive concept – diet, for example, does not perfectly match individual nutritional needs; 2) the threshold for critical loss-of-function to affect survival is organ- and organism-dependent; and 3) different cohorts and individuals within a cohort succumb to different causes of death.

Having lifespan as the primary outcome in ageing research finds interventions that simply prolong life, and do not necessarily act through ageing mechanisms. Human life expectancy has increased as a result of antibiotics and, although infections may accelerate ageing, survival is extended primarily through preventing death from acute infection. To find interventions that prolong disability-free life, targeting ageing needs to be the broader outcome. From the definition of ageing proposed in this thesis (see Section 1.2), three criteria would need to be met to define an intervention as anti-ageing: 1) maintenance of functional biomarkers with age; 2) improved resilience to stressors; and 3) lower mortality rate with age. Complementary studies are needed to measure the effects of acid-base interventions on functional phenotypes.

This limitation may apply to processes currently categorised as hallmarks of ageing. A particularly important modulator of longevity is diet (López-Otín et al., 2016). The first evidence showing that longevity is susceptible to intervention dates back to 1935, with the finding that mice kept under DR live longer (McCay et al., 1935). As discussed, DR may extend survival by preventing common consequences of

overnutrition in different animal models. Different mechanisms have been proposed for the effect of DR and mimetic strategies on lifespan (López-Otín et al., 2016). Here, overnutrition was explored in the acid-base context.

8.2. Acid-base imbalance as a promoter of age-related disease

8.2.1. Overnutrition can induce age-related disease through pH imbalance

Overnutrition is an independent risk factor for disease. Excess fats and carbohydrates lower human life expectancy (Senior et al., 2020). This is often attributed to obesity and its consequences. *Drosophila* has been used as a model for diet-induced obesity and metabolic syndrome (Birse et al., 2010; Na et al., 2013; Owusu-Ansah & Perrimon, 2014; van Dam et al., 2020). When fed excess sugar, flies have metabolic defects often seen in metabolic syndrome: triglyceride accumulation, hyperglycaemia and insulin resistance (van Dam et al., 2020). However, we have found that these metabolic defects do not shorten fly lifespan, as they are still observed when HS-fed flies are provided with an extra source of water which fully rescues their survival.

This demonstrates that overnutrition can have health consequences beyond the typical metabolic side-effects. Flies fed excess sugar die earlier due to osmotic stress which correlates with tubular uric acid lithiasis. As previously discussed, flies may be predisposed to forming uric acid crystals because uric acid is their main way of excreting excess nitrogen. With age, fly tubules accumulate crystals, even when raised on a standard diet. This may be promoted by the high protein content in their diet (10% yeast), as yeast concentrations can promote uric acid lithiasis independently of excess sugar (Lang et al., 2019). Interestingly, adding fat to the fly diet also promotes uric acid lithiasis, showing overnutrition caused by each type of macronutrient in excess can result in the same phenotype.

The factors that promote uric acid lithiasis are macronutrient dependent. Uric acid crystallisation is promoted by: 1) increased uric acid production, either by protein nitrogen excretion or glucose via the pentose-phosphate pathway; 2) dehydration, due to the osmotic effect of glucose; and 3) acidic environment, promoted by metabolism of sulphur-containing amino acids, anaerobic glycolysis, lipolysis or ketogenesis. Contrary to excess sugar, added fat did not shorten fly survival through osmotic stress, and is proposed to promote uric acid lithiasis through tubule acidification. Knocking down v-ATPase subunits to block acid excretion in the tubules prevents fat-induced

lithiasis. Despite preventing lithiasis, v-ATPase knockdown will likely aggravate systemic acidification. Using this setting, it is possible to test whether survival is shortened primarily by lithiasis or acid-base imbalance. This would be a key follow-up experiment.

In humans, overnutrition can also promote disease through acid-base, independently of its obesogenic effects. From an evolutionary perspective, it was proposed that with the advent of agriculture, dietary changes occurred too fast for humans to adapt, resulting in a mismatch between the nutrient composition of the diet and genetically determined nutritional requirements for optimal systemic acid-base status (Sebastian et al., 2002). Western diets in particular have a high ratio of animal protein compared to vegetables and fruits, leading to increased NEAP (Frassetto et al., 2020). Without having an effect on weight, short-term consumption of a lower NEAP-associated diet showed systemic metabolic improvements (Frassetto et al., 2009). High dietary NaCl was also found to be acidogenic (Frassetto et al., 2007), in accordance with the observed acidosis following intravenous administration of saline (0.9% NaCl) solutions, although these may occur through different mechanisms (Kellum & Elbers, 2009).

Increased NEAP can have direct effects on age-related disease (DiNicolantonio & O'Keefe, 2021; Frassetto et al., 2020; Vormann & Goedecke, 2002). Lower extracellular pH decreases bone mineral density, for example, as a compensatory mechanism to increase SID, by increasing osteoclast and decreasing osteoblast activity to release alkali from bone (DiNicolantonio & O'Keefe, 2021). With age, bone density declines, increasing the risk of fractures. Consumption of higher animal protein compared to vegetable sources is strongly associated with the frequency of hip fractures in the elderly (Frassetto & Sebastian, 2019b; Li et al., 2022). This is related to higher NEAP, since animal sources of protein have higher content of sulphur-containing amino acids than vegetable sources (Frassetto & Sebastian, 2019b). With ageing, sarcopenia and increased nitrogen waste may also be promoted by lower extracellular pH. In postmenopausal women, alkalotic treatment was shown to lower urinary nitrogen excretion, a marker of protein breakdown (Frassetto et al., 1997). Besides these, as discussed, higher NEAP and dietary phosphate contribute to the progression of chronic kidney disease (Toba et al., 2019)

8.2.2. Acid-base and hallmarks of ageing may interact to cause disease

Beyond the direct effects, systemic acidification can promote the development of age-related disease through interactions with other ageing processes. These interactions are understudied but current evidence hints to speculative mechanisms through which they may cause age-related diseases.

In mammalian fibroblasts, for example, exposure to extracellular low pH (6.5) results in elevated mutagenesis and impaired DNA repair (Yuan et al., 2000). This may directly promote carcinogenesis or lead cells into an irreversible cell-cycle arrest state, senescence. Senescent cells accumulate with age in different organs where they promote age-related disease, including lung fibrosis, chronic kidney disease, liver steatosis, obesity-associated metabolic syndrome, type-2 diabetes, atherosclerosis, Alzheimer's and Parkinson's diseases (López-Otín et al., 2023). These cells typically have lower intracellular pH (Johmura et al., 2021; Triana-Martínez et al., 2019), which may be primarily promoted by their extracellular environment. They adapt to further intracellular pH drops by upregulating kidney-type glutaminase (KGA) expression and producing ammonia (Johmura et al., 2021). The KGA transcript contains an AU-rich element (ARE) which increases mRNA stability through HuC binding under acidic conditions. Besides their recognised role in renal response to acidosis (Ibrahim et al., 2008), it would be interesting to study how ARE-containing transcripts in different tissues may respond to age-related acidification.

Acidic extracellular pH was also shown to inhibit macroautophagy in rat cardiomyocytes (Zhao et al., 2016). Autophagy promotes cardiomyocyte survival under nutrient or energy stress. Impaired macroautophagy can also occur through organellar pH imbalance, related to loss of lysosome acidity needed for hydrolases to function (Song et al., 2020). Either inherited or age-related loss of effective autophagy causes chronic diseases, including neurodegenerative (Klionsky et al., 2021; Ramirez et al., 2006; Song et al., 2020). Neurological diseases are particularly susceptible to extracellular acid-base imbalance, since synaptic transmission is highly sensitive to changes in pH. Astrocytes were recently found to buffer extracellular H^+ in the brain to support normal function (Theparambil et al., 2020). It would be interesting to study whether their buffering capacity is lost with age in patients with neurodegenerative diseases.

Acidosis induces insulin resistance in humans (Bellasi et al., 2016; Kraut & Madias, 2010; Smeha et al., 2022), in part by lowering binding of insulin to its receptor

(Baldini & Avnet, 2018), causing hyperinsulinemia. Chronically, this may promote age- and diet-related metabolic diseases, such as metabolic syndrome and type 2 diabetes (Templeman et al., 2017). Inhibiting the IIS pathway is associated with longer lifespan across species, including mammals (López-Otín et al., 2023). However, insulin resistance and hyperinsulinemia are major risk factors for age-related diseases, and lowering circulating insulin extends mammalian lifespan (Templeman et al., 2017). This dichotomy is still not fully elucidated, but it may relate to: 1) signalling downstream of the insulin receptor modified by insulin-independent processes; 2) insulin-mediated downstream signalling that is independent of conventionally defined insulin resistance (based on impaired insulin-stimulated glycaemic changes); and 3) tissue specific effects, as evidenced by mammalian studies knocking out the insulin receptor in different organs (Biddinger & Kahn, 2006). For example, insulin regulates the mitogen-activated protein kinase pathway. This effect is maintained in insulin resistance in specific tissues and can promote age-related diseases, such as atherosclerosis (Barzilai & Ferrucci, 2012).

These examples suggest further research efforts should be made into understanding how acid-base balance may impact hallmarks of ageing and other processes that are impaired with age, such as redox signalling, both systemically and in a tissue-specific manner, to ultimately cause disease.

8.3. Outlook and future directions

This study explores the influence of acid-base homeostasis in ageing. Extracellular acidification occurs with age, may be a hallmark of ageing, and is promoted by diet. Besides diet, other environmental exposures, such as air pollution, temperature or infections, the sum of which during life is termed the exposome, are risk factors for age-related disease (Shiels et al., 2021). These factors may also promote systemic acidification (Figure 8.1).

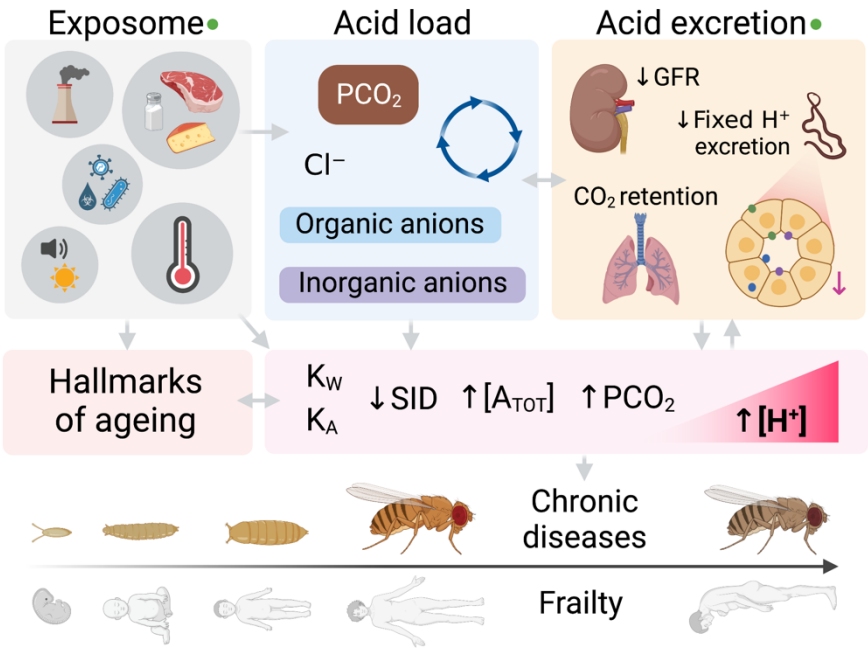


Figure 8.1. Acid-base balance as a convergent target for ageing interventions. Loss of acid-base balance with age is a common consequence of chronic exposure to exposome factors (e.g., air pollution; diet; infections, xenobiotics and drugs; noise and light; temperature) and insufficient excretion of acid that ultimately increase [H^+] systemically. Green dots represent the potential initiating factors. Systemic acidification can interact with (other) hallmarks of ageing to increase the risk of chronic diseases and frailty with age. (Designed with BioRender.com)

Future studies should focus on testing causation. From the findings presented here, the cause of age-related acidification originates either from the exposome (which subsequently overwhelms excretory capacity, supporting the stochastic view on ageing) or primarily from insufficient excretion (which may be a programmed process). Independently of the upstream cause, systemic acidification can promote age-related disease. Maintaining acid-base balance may be thus a target for preventive medicine to promote healthy lifespan.

Supplementary table 1

List of primers used in this study for genomic DNA PCR and Sanger sequencing.

Label	Primer direction	Sequence (5' to 3')
UAS_HSP_UP	Forward	CAACTGCAACTACTGAAATCTGCC
pUAST-up	Forward	AAGTAACCAGCAACCAAGTAA
CAH1_rev	Reverse	TACTTCCACTTGAGCGGAGC
CAH2_rev	Reverse	AATCGTATCGTTCTCGCCCC
VhaSFD_rev	Reverse	AAGCCCAGTTGATCGTCCTG

Supplementary table 2

Tris-HCl (50 mM) buffer solution composition

Final pH	Tris base* (mL)	1 M HCl (μL)	MilliQ water (μL)
6.6	19	971	29
6.8		954	46
7		929	71
7.2		893	107
7.3		869	131
7.4		840	160
7.6		768	232
7.8		676	324

*Tris base stock solution: 1.211g in 190mL MilliQ water

Supplementary table 3

Sorensen's phosphate (100 mM) buffer solution composition

Final pH	0.2 M NaH_2PO_4 (mL)	0.2 M Na_2HPO_4 (mL)	MilliQ water (mL)
6.0	87.7	12.3	100
6.2	81.5	18.5	
6.4	73.5	26.5	
6.6	62.2	37.5	
6.8	51	49	
7	39	61	
7.2	28	72	
7.3	23	77	
7.4	19	81	
7.6	13	87	
7.8	8.5	91.5	

NaH_2PO_4 (Sigma, S8282); Na_2HPO_4 (Sigma, S7907)

Supplementary table 4

List of primers used in this study for qPCR (span exon-exon junctions, specific to gene but not isoform).

Label	Primer direction	Sequence (5' to 3')	Product length
CAH1	Forward	ACCATACAGTCGACGCTCCA	487
	Reverse	CGCCAGCAATAGCCAGGATT	
CAH2	Forward	CGAGGACGAGATCCCAAGTG	257
	Reverse	TTGATTTGTCGCCCACCTGA	
CAH3	Forward	CATCGCTGGATTCCGATTGC	146
	Reverse	GCGAGACACATAGATGGGGG	
CAH9	Forward	CTGCTGGTCTCAAGCTGTCA	358
	Reverse	GGATCCCCGGTTGTTCTTGT	
Vha13	Forward	ACCACGGCGAGGAATTAGAG	129
	Reverse	CCTCCTTGCCTTGCGTTTAC	
Vha44	Forward	GCAGTCTGCTGACCAGGAAT	463
	Reverse	GGCAGTCCGTATCTCAGCAC	
Vha55	Forward	GAACTTCATCTCGCAGGGCAA	131
	Reverse	AGAATTCGGCCAGGATGGAG	
Vha55 (2)	Forward	CAGCCCCGCTTGACTTACA	274
	Reverse	TGAACACACGGCCCAACATA	
VhaSFD	Forward	GCCCGAGGAGAACATTGATATG	446
	Reverse	ACTTGGGCATGGTCTCATGG	
PEPCK1	Forward	TGAACGCAAAGTCCTCGACA	213
	Reverse	CGCAGACATTGCCGGAGATAA	
Mitf	Forward	GCAACGAGTGTCTCTGAGC	193
	Reverse	GTCGCCTTCGCTCAATCATA	
PMCA	Forward	CTGTAACTGGAGACGGCACA	487
	Reverse	TCGAGTATAACATCGCCGACA	
pHCl-2	Forward	TCTTCAACAGAATCTGGCCGC	376
	Reverse	CTGCCTTCGGTTAGGCAGAT	
Ndae1	Forward	TGATGGGTCTGCCTTGGTTC	363
	Reverse	TCATGGTGAACAGGTGGACG	
Uro	Forward	ACTACCAGGGCAACAACTCG	369
	Reverse	TGACCGTTTGTTTGGGATCTGT	
RPL32	Forward	TGCTAAGCTGTCGCACAAAT	
	Reverse	TTCGATCCGTAACCGATG	
Actin 5C	Forward	CACACCAAATCTTACAAAATGTGT	
	Reverse	AATCCGGCCTTGCACATG	

REFERENCES

Afanas'ev, I. (2010). Signaling and Damaging Functions of Free Radicals in Aging-Free Radical Theory, Hormesis, and TOR. *Aging and Disease*, *1*(2), 75–88. http://www.ncbi.nlm.nih.gov/pubmed/22396858

Ali, S. N., Dayarathna, T. K., Ali, A. N., Osumah, T., Ahmed, M., Cooper, T. T., Power, N. E., Zhang, D., Kim, D., Kim, R., St. Amant, A., Hou, J., Tailly, T., Yang, J., Luyt, L., Spagnuolo, P. A., Burton, J. P., Razvi, H., & Leong, H. S. (2018). Drosophila melanogaster as a function-based high-throughput screening model for anti-nephrolithiasis agents in kidney stone patients. *Disease Models & Mechanisms*. https://doi.org/10.1242/dmm.035873

Allan, A. K., Du, J., Davies, S. A., & Dow, J. A. T. (2005). Genome-wide survey of V-ATPase genes in Drosophila reveals a conserved renal phenotype for lethal alleles. *Physiological Genomics*, *22*(2), 128–138. https://doi.org/10.1152/physiolgenomics.00233.2004

Arch, J. R. S., Hislop, D., Wang, S. J. Y., & Speakman, J. R. (2006). Some mathematical and technical issues in the measurement and interpretation of open-circuit indirect calorimetry in small animals. *International Journal of Obesity*, *30*(9), 1322–1331. https://doi.org/10.1038/sj.ijo.0803280

Austad, S. N., & Fischer, K. E. (2016). Sex Differences in Lifespan. *Cell Metabolism*, *23*(6), 1022–1033. https://doi.org/10.1016/j.cmet.2016.05.019

Baldini, N., & Avnet, S. (2018). The Effects of Systemic and Local Acidosis on Insulin Resistance and Signaling. *International Journal of Molecular Sciences*, *20*(1), 126. https://doi.org/10.3390/ijms20010126

Balgi, A. D., Diering, G. H., Donohue, E., Lam, K. K. Y., Fonseca, B. D., Zimmerman, C., Numata, M., & Roberge, M. (2011). Regulation of mTORC1 signaling by pH. *PLoS ONE*, *6*(6). https://doi.org/10.1371/journal.pone.0021549

Banerjee, T., Crews, D. C., Wesson, D. E., Tilea, A., Saran, R., Rios Burrows, N., Williams, D. E., & Powe, N. R. (2014). Dietary acid load and chronic kidney disease among adults in the United States. *BMC Nephrology*, *15*(1), 137. https://doi.org/10.1186/1471-2369-15-137

Banerjee, T., Sebastian, A., & Frassetto, L. (2023). Association of diet-dependent

systemic acid load, renal function, and serum albumin concentration. *Journal of Renal Nutrition*. https://doi.org/10.1053/j.jrn.2023.01.007

Banse, S. A., & Hunter, C. P. (2012). Vampiric isolation of extracellular fluid from Caenorhabditis elegans. *Journal of Visualized Experiments : JoVE*, *61*, 1–7. https://doi.org/10.3791/3647

Barardo, D., Thornton, D., Thoppil, H., Walsh, M., Sharifi, S., Ferreira, S., Anžič, A., Fernandes, M., Monteiro, P., Grum, T., Cordeiro, R., De-Souza, E. A., Budovsky, A., Araujo, N., Gruber, J., Petrascheck, M., Fraifeld, V. E., Zhavoronkov, A., Moskalev, A., & de Magalhães, J. P. (2017). The DrugAge database of aging-related drugs. *Aging Cell*, *16*(3), 594–597. https://doi.org/10.1111/acel.12585

Barzilai, N., & Ferrucci, L. (2012). Insulin Resistance and Aging: A Cause or a Protective Response? *The Journals of Gerontology Series A: Biological Sciences and Medical Sciences*, *67*(12), 1329–1331. https://doi.org/10.1093/gerona/gls145

Bateman, A., Martin, M.-J., Orchard, S., Magrane, M., Ahmad, S., Alpi, E., Bowler-Barnett, E. H., Britto, R., Bye-A-Jee, H., Cukura, A., Denny, P., Dogan, T., Ebenezer, T., Fan, J., Garmiri, P., da Costa Gonzales, L. J., Hatton-Ellis, E., Hussein, A., Ignatchenko, A., … Zhang, J. (2023). UniProt: the Universal Protein Knowledgebase in 2023. *Nucleic Acids Research*, *51*(D1), D523–D531. https://doi.org/10.1093/nar/gkac1052

Bateman, J. R., Lee, A. M., & Wu, C. (2006). Site-Specific Transformation of *Drosophila* via ϕC31 Integrase-Mediated Cassette Exchange. *Genetics*, *173*(2), 769–777. https://doi.org/10.1534/genetics.106.056945

Batlle, D., & Haque, S. K. (2012). Genetic causes and mechanisms of distal renal tubular acidosis. *Nephrology Dialysis Transplantation*, *27*(10), 3691–3704. https://doi.org/10.1093/ndt/gfs442

Bellasi, A., Di Micco, L., Santoro, D., Marzocco, S., De Simone, E., Cozzolino, M., Di Lullo, L., Guastaferro, P., & Di Iorio, B. (2016). Correction of metabolic acidosis improves insulin resistance in chronic kidney disease. *BMC Nephrology*, *17*(1), 158. https://doi.org/10.1186/s12882-016-0372-x

Bergwitz, C. (2012). Dietary phosphate modifies lifespan in *Drosophila*. *Nephrology Dialysis Transplantation*, *27*(9), 3399–3406. https://doi.org/10.1093/ndt/gfs362

Beyenbach, K. W. (2001). Energizing Epithelial Transport with the Vacuolar H + - ATPase. *Physiology*, *16*(4), 145–151. https://doi.org/10.1152/physiologyonline.2001.16.4.145

Biddinger, S. B., & Kahn, C. R. (2006). FROM MICE TO MEN: Insights into the Insulin Resistance Syndromes. *Annual Review of Physiology*, *68*(1), 123–158. https://doi.org/10.1146/annurev.physiol.68.040104.124723

Birse, R. T., Choi, J., Reardon, K., Rodriguez, J., Graham, S., Diop, S., Ocorr, K., Bodmer, R., & Oldham, S. (2010). High-Fat-Diet-Induced Obesity and Heart Dysfunction Are Regulated by the TOR Pathway in *Drosophila*. *Cell Metabolism*, *12*(5), 533–544. https://doi.org/10.1016/j.cmet.2010.09.014

Bitto, A., Ito, T. K., Pineda, V. V., LeTexier, N. J., Huang, H. Z., Sutlief, E., Tung, H., Vizzini, N., Chen, B., Smith, K., Meza, D., Yajima, M., Beyer, R. P., Kerr, K. F., Davis, D. J., Gillespie, C. H., Snyder, J. M., Treuting, P. M., & Kaeberlein, M. (2016). Transient rapamycin treatment can increase lifespan and healthspan in middle-aged mice. *ELife*, *5*(AUGUST), 1–17. https://doi.org/10.7554/eLife.16351

Bjedov, I., Toivonen, J. M., Kerr, F., Slack, C., Jacobson, J., Foley, A., & Partridge, L. (2010). Mechanisms of Life Span Extension by Rapamycin in the Fruit Fly *Drosophila melanogaster*. *Cell Metabolism*, *11*(1), 35–46. https://doi.org/10.1016/j.cmet.2009.11.010

Böhme, I., & Bosserhoff, A. (2020). Extracellular acidosis triggers a senescence-like phenotype in human melanoma cells. *Pigment Cell & Melanoma Research*, *33*(1), 41–51. https://doi.org/10.1111/pcmr.12811

Brand, A. H., & Perrimon, N. (1993). Targeted gene expression as a means of altering cell fates and generating dominant phenotypes. *Development*, *118*(2), 401–415. https://doi.org/10.1242/dev.118.2.401

Broughton, S. J., Piper, M. D. W., Ikeya, T., Bass, T. M., Jacobson, J., Driege, Y., Martinez, P., Hafen, E., Withers, D. J., Leevers, S. J., & Partridge, L. (2005). Longer lifespan, altered metabolism, and stress resistance in *Drosophila* from ablation of cells making insulin-like ligands. *Proceedings of the National*

Academy of Sciences, *102*(8), 3105–3110. https://doi.org/10.1073/pnas.0405775102

Burns, D. M. (2000). Cigarette Smoking among the Elderly: Disease Consequences and the Benefits of Cessation. *American Journal of Health Promotion*, *14*(6), 357–361. https://doi.org/10.4278/0890-1171-14.6.357

Cabrera, Á. J. R. (2015). Zinc, aging, and immunosenescence: an overview. *Pathobiology of Aging & Age-Related Diseases*, *5*(1), 25592. https://doi.org/10.3402/pba.v5.25592

Cabrero, P., Terhzaz, S., Romero, M. F., Davies, S. A., Blumenthal, E. M., & Dow, J. A. T. (2014). Chloride channels in stellate cells are essential for uniquely high secretion rates in neuropeptide-stimulated *Drosophila* diuresis. *Proceedings of the National Academy of Sciences*, *111*(39), 14301–14306. https://doi.org/10.1073/pnas.1412706111

Cao, E., Watt, M. J., Nowell, C. J., Quach, T., Simpson, J. S., De Melo Ferreira, V., Agarwal, S., Chu, H., Srivastava, A., Anderson, D., Gracia, G., Lam, A., Segal, G., Hong, J., Hu, L., Phang, K. L., Escott, A. B. J., Windsor, J. A., Phillips, A. R. J., … Trevaskis, N. L. (2021). Mesenteric lymphatic dysfunction promotes insulin resistance and represents a potential treatment target in obesity. *Nature Metabolism*, *3*(9), 1175–1188. https://doi.org/10.1038/s42255-021-00457-w

Carvalho, G. B., Drago, I., Hoxha, S., Yamada, R., Mahneva, O., Bruce, K. D., Soto Obando, A., Conti, B., & Ja, W. W. (2017). The 4E-BP growth pathway regulates the effect of ambient temperature on *Drosophila* metabolism and lifespan. *Proceedings of the National Academy of Sciences*, *114*(36), 9737–9742. https://doi.org/10.1073/pnas.1618994114

Casey, J. R., Grinstein, S., & Orlowski, J. (2010). Sensors and regulators of intracellular pH. In *Nature Reviews Molecular Cell Biology*. https://doi.org/10.1038/nrm2820

Castillo-Quan, J. I., Kinghorn, K. J., & Bjedov, I. (2015). Genetics and Pharmacology of Longevity. In *Advances in Genetics* (Vol. 90, pp. 1–101). https://doi.org/10.1016/bs.adgen.2015.06.002

Castillo-Quan, J. I., Tain, L. S., Kinghorn, K. J., Li, L., Grönke, S., Hinze, Y.,

Blackwell, T. K., Bjedov, I., & Partridge, L. (2019). A triple drug combination targeting components of the nutrient-sensing network maximizes longevity. *Proceedings of the National Academy of Sciences*, *116*(42), 20817–20819. https://doi.org/10.1073/pnas.1913212116

Chakraborty, T. S., Gendron, C. M., Lyu, Y., Munneke, A. S., DeMarco, M. N., Hoisington, Z. W., & Pletcher, S. D. (2019). Sensory perception of dead conspecifics induces aversive cues and modulates lifespan through serotonin in *Drosophila*. *Nature Communications*, *10*(1), 2365. https://doi.org/10.1038/s41467-019-10285-y

Chen, Y.-H., Liu, H.-P., Chen, H.-Y., Tsai, F.-J., Chang, C.-H., Lee, Y.-J., Lin, W.-Y., & Chen, W.-C. (2011). Ethylene glycol induces calcium oxalate crystal deposition in Malpighian tubules: a *Drosophila* model for nephrolithiasis/urolithiasis. *Kidney International*, *80*(4), 369–377. https://doi.org/10.1038/ki.2011.80

Cheng, Y., Zhang, Y., Tu, B., Qin, Y., Cheng, X., Qi, R., Guo, W., Li, D., Wu, S., Zhu, R., Zhao, Y., Tang, Y., & Wu, C. (2021). Association Between Base Excess and Mortality Among Patients in ICU With Acute Kidney Injury. *Frontiers in Medicine*, *8*(December), 1–10. https://doi.org/10.3389/fmed.2021.779627

Chintapalli, V. R., Terhzaz, S., Wang, J., Al Bratty, M., Watson, D. G., Herzyk, P., Davies, S. A., & Dow, J. A. T. (2012). Functional Correlates of Positional and Gender-Specific Renal Asymmetry in *Drosophila*. *PLoS ONE*, *7*(4), e32577. https://doi.org/10.1371/journal.pone.0032577

Chung, C. Y., Shin, H. R., Berdan, C. A., Ford, B., Ward, C. C., Olzmann, J. A., Zoncu, R., & Nomura, D. K. (2019). Covalent targeting of the vacuolar H+-ATPase activates autophagy via mTORC1 inhibition. *Nature Chemical Biology*, *15*(8), 776–785. https://doi.org/10.1038/s41589-019-0308-4

Clark, R. I., & Walker, D. W. (2018). Role of gut microbiota in aging-related health decline: insights from invertebrate models. *Cellular and Molecular Life Sciences*, *75*(1), 93–101. https://doi.org/10.1007/s00018-017-2671-1

Cognigni, P., Bailey, A. P., & Miguel-Aliaga, I. (2011). Enteric Neurons and Systemic Signals Couple Nutritional and Reproductive Status with Intestinal Homeostasis. *Cell Metabolism*, *13*(1), 92–104. https://doi.org/10.1016/j.cmet.2010.12.010

Cohen, E., Sawyer, J. K., Peterson, N. G., Dow, J. A. T. T., & Fox, D. T. (2020). Physiology, development, and disease modeling in the *Drosophila* excretory system. *Genetics*, *214*(2), 235–264. https://doi.org/10.1534/genetics.119.302289

Conde, S. V., Obeso, A., Rigual, R., Monteiro, E. C., & Gonzalez, C. (2006). Function of the rat carotid body chemoreceptors in ageing. *Journal of Neurochemistry*, *99*(3), 711–723. https://doi.org/10.1111/j.1471-4159.2006.04094.x

da Costa, J. P., Vitorino, R., Silva, G. M., Vogel, C., Duarte, A. C., & Rocha-Santos, T. (2016). A synopsis on aging—Theories, mechanisms and future prospects. *Ageing Research Reviews*, *29*, 90–112. https://doi.org/10.1016/j.arr.2016.06.005

Daudon, M., Frochot, V., Bazin, D., & Jungers, P. (2016). Crystalluria analysis improves significantly etiologic diagnosis and therapeutic monitoring of nephrolithiasis. *Comptes Rendus Chimie*, *19*(11–12), 1514–1526. https://doi.org/10.1016/j.crci.2016.04.010

Davies, S. A., Goodwin, S. F., Kelly, D. C., Wang, Z., Sözen, M. A., Kaiser, K., & Dow, J. A. T. (1996). Analysis and Inactivation of vha55, the Gene Encoding the Vacuolar ATPase B-subunit in Drosophila melanogaster Reveals a Larval Lethal Phenotype. *Journal of Biological Chemistry*, *271*(48), 30677–30684. https://doi.org/10.1074/jbc.271.48.30677

De Grey, A. D. N. J., Ames, B. N., Andersen, J. K., Bartke, A., Campisi, J., Heward, C. B., McCarter, R. J. M., & Stock, G. (2002). Time to Talk SENS: Critiquing the Immutability of Human Aging. *Annals of the New York Academy of Sciences*, *959*(1), 452–462. https://doi.org/10.1111/j.1749-6632.2002.tb02115.x

Deelen, J., Kettunen, J., Fischer, K., van der Spek, A., Trompet, S., Kastenmüller, G., Boyd, A., Zierer, J., van den Akker, E. B., Ala-Korpela, M., Amin, N., Demirkan, A., Ghanbari, M., van Heemst, D., Ikram, M. A., van Klinken, J. B., Mooijaart, S. P., Peters, A., Salomaa, V., … Slagboom, P. E. (2019). A metabolic profile of all-cause mortality risk identified in an observational study of 44,168 individuals. *Nature Communications*, *10*(1), 1–8. https://doi.org/10.1038/s41467-019-11311-9

Deitmer, J. W., & Becker, H. M. (2013). Transport metabolons with carbonic anhydrases. *Frontiers in Physiology*, *4*(October), 2–5. https://doi.org/10.3389/fphys.2013.00291

Denic, A., Glassock, R. J., & Rule, A. D. (2016). Structural and Functional Changes With the Aging Kidney. *Advances in Chronic Kidney Disease*, *23*(1), 19–28. https://doi.org/10.1053/j.ackd.2015.08.004

Deprez, M.-A., Eskes, E., Wilms, T., Ludovico, P., & Winderickx, J. (2018). pH homeostasis links the nutrient sensing PKA/TORC1/Sch9 ménage-à-trois to stress tolerance and longevity. *Microbial Cell*, *5*(3), 119–136. https://doi.org/10.15698/mic2018.03.618

Deshpande, S. A., Yamada, R., Mak, C. M., Hunter, B., Obando, A. S., Hoxha, S., & Ja, W. W. (2015). Acidic Food pH Increases Palatability and Consumption and Extends *Drosophila* Lifespan. *The Journal of Nutrition*, *145*(12), 2789–2796. https://doi.org/10.3945/jn.115.222380

Devuyst, O., & Guggino, W. B. (2002). Chloride channels in the kidney: lessons learned from knockout animals. *American Journal of Physiology-Renal Physiology*, *283*(6), F1176–F1191. https://doi.org/10.1152/ajprenal.00184.2002

DiBartola, S. P. (2012). Introduction to Acid-Base Disorders. In *Fluid, Electrolyte, and Acid-Base Disorders in Small Animal Practice* (4th ed.). Elsevier Inc. https://doi.org/10.1016/B978-1-4377-0654-3.00016-0

Dietzl, G., Chen, D., Schnorrer, F., Su, K.-C., Barinova, Y., Fellner, M., Gasser, B., Kinsey, K., Oppel, S., Scheiblauer, S., Couto, A., Marra, V., Keleman, K., & Dickson, B. J. (2007). A genome-wide transgenic RNAi library for conditional gene inactivation in *Drosophila*. *Nature*, *448*(7150), 151–156. https://doi.org/10.1038/nature05954

DiNicolantonio, J. J., & O'Keefe, J. (2021). Low-grade metabolic acidosis as a driver of chronic disease: a 21st century public health crisis. *Open Heart*, *8*(2), e001730. https://doi.org/10.1136/openhrt-2021-001730

Dornan, A. J., Halberg, K. A., Beuter, L.-K., Davies, S.-A., & Dow, J. A. T. (2020). The septate junction protein Snakeskin is critical for epithelial barrier function and tissue homeostasis in the Malpighian tubules of adult *Drosophila*. *BioRxiv*.

https://doi.org/10.1101/2020.12.14.422678

Dos Santos, E., Sacramento, J. F., Melo, B. F., & Conde, S. V. (2018). Carotid Body Dysfunction in Diet-Induced Insulin Resistance Is Associated with Alterations in Its Morphology. In *Advances in Experimental Medicine and Biology* (Vol. 1071). https://doi.org/10.1007/978-3-319-91137-3_13

Dow, J. A. T., Simons, M., & Romero, M. F. (2022). Drosophila melanogaster: a simple genetic model of kidney structure, function and disease. *Nature Reviews Nephrology*, *18*(7), 417–434. https://doi.org/10.1038/s41581-022-00561-4

Duncan, S. H., Louis, P., Thomson, J. M., & Flint, H. J. (2009). The role of pH in determining the species composition of the human colonic microbiota. *Environmental Microbiology*, *11*(8), 2112–2122. https://doi.org/10.1111/j.1462-2920.2009.01931.x

Eaton, A. F., Merkulova, M., & Brown, D. (2021). The H + -ATPase (V-ATPase): from proton pump to signaling complex in health and disease. *American Journal of Physiology-Cell Physiology*, *320*(3), C392–C414. https://doi.org/10.1152/ajpcell.00442.2020

Ebeling, M., Rau, R., Malmström, H., Ahlbom, A., & Modig, K. (2021). The rate by which mortality increase with age is the same for those who experienced chronic disease as for the general population. *Age and Ageing*, *50*(5), 1633–1640. https://doi.org/10.1093/ageing/afab085

Erra Díaz, F., Dantas, E., & Geffner, J. (2018). Unravelling the interplay between extracellular acidosis and immune cells. *Mediators of Inflammation*, *2018*. https://doi.org/10.1155/2018/1218297

Estrella, V., Swietach, P., Luddy, K., Abrahams, D., Enriquez-Navas, P., Reshetnyak, Y., Damaghi, M., & Gillies, R. J. (2019). Abstract 1140: A new twist on an old strategy: Can the lymph node environment help cancers escape immune surveillance. *Cancer Research*, *79*(13 Supplement), 1140 LP – 1140. https://doi.org/10.1158/1538-7445.AM2019-1140

European Commission Directorate-General for Economic and Financial Affairs. (2018). The 2018 Ageing Report Economic and Budgetary Projections for the EU Member States (2016-2070). In *Economic and Financial Affairs* (Vol. 2018).

https://doi.org/10.2765/615631

Evans, J. M., Day, J. P., Cabrero, P., Dow, J. A. T., & Davies, S. (2008). A new role for a classical gene: White transports cyclic GMP. *Journal of Experimental Biology*, *211*(6), 890–899. https://doi.org/10.1242/jeb.014837

Everitt, A. V., Hilmer, S. N., Brand-Miller, J. C., Jamieson, H. A., Truswell, A. S., Sharma, A. P., Mason, R. S., Morris, B. J., & Couteur, D. G. Le. (2006). Dietary approaches that delay age-related diseases. *Clinical Interventions in Aging*, *1*(1), 11–31. https://doi.org/10.2147/ciia.2006.1.1.11

Fan, S., Lin, C., Wei, Y., Yeh, S., Tsai, Y., Lee, A. C., Lin, W., & Wang, P. (2021). Dietary citrate supplementation enhances longevity, metabolic health, and memory performance through promoting ketogenesis. *Aging Cell*, *20*(12), 1–15. https://doi.org/10.1111/acel.13510

Feingold, D., Knogler, L., Starc, T., Drapeau, P., O'Donnell, M. J., Nilson, L. A., & Dent, J. A. (2019). secCl is a cys-loop ion channel necessary for the chloride conductance that mediates hormone-induced fluid secretion in *Drosophila*. *Scientific Reports*, *9*(1), 7464. https://doi.org/10.1038/s41598-019-42849-9

Feingold, D., Starc, T., O'Donnell, M. J., Nilson, L., & Dent, J. A. (2016). The orphan pentameric ligand-gated ion channel pHCl-2 is gated by pH and regulates fluid secretion in *Drosophila* Malpighian tubules. *Journal of Experimental Biology*, *219*(17), 2629–2638. https://doi.org/10.1242/jeb.141069

Feng, Y., & Forgac, M. (1994). Inhibition of vacuolar H(+)-ATPase by disulfide bond formation between cysteine 254 and cysteine 532 in subunit A. *Journal of Biological Chemistry*, *269*(18), 13224–13230. https://doi.org/10.1016/S0021-9258(17)36822-9

Firrman, J., Liu, L., Mahalak, K., Tanes, C., Bittinger, K., Tu, V., Bobokalonov, J., Mattei, L., Zhang, H., & Van den Abbeele, P. (2022). The impact of environmental pH on the gut microbiota community structure and short chain fatty acid production. *FEMS Microbiology Ecology*, *98*(5), 1–9. https://doi.org/10.1093/femsec/fiac038

Fisher, S. Z., Aggarwal, M., Kovalevsky, A. Y., Silverman, D. N., & McKenna, R. (2012). Neutron Diffraction of Acetazolamide-Bound Human Carbonic

Anhydrase II Reveals Atomic Details of Drug Binding. *Journal of the American Chemical Society*, *134*(36), 14726–14729. https://doi.org/10.1021/ja3068098

Fontana, L., Partridge, L., & Longo, V. D. (2010). Extending Healthy Life Span--From Yeast to Humans. *Science*, *328*(5976), 321–326. https://doi.org/10.1126/science.1172539

Francis, S., Taylor-Wells, J., Gross, A., & Bloomquist, J. (2016). Toxicity and Physiological Actions of Carbonic Anhydrase Inhibitors to Aedes aegypti and *Drosophila melanogaster*. *Insects*, *8*(1), 2. https://doi.org/10.3390/insects8010002

Frassetto, L. A., Morris, R. C., & Sebastian, A. (1996). Effect of age on blood acid-base composition in adult humans: role of age-related renal functional decline. *The American Journal of Physiology*, *271*(6 Pt 2), F1114-22. https://doi.org/10.1152/ajprenal.1996.271.6.F1114

Frassetto, L. A., Morris, R. C., & Sebastian, A. (1997). Potassium Bicarbonate Reduces Urinary Nitrogen Excretion in Postmenopausal Women. *The Journal of Clinical Endocrinology & Metabolism*, *82*(1), 254–259. https://doi.org/10.1210/jcem.82.1.3663

Frassetto, L. A., Morris, R. C., & Sebastian, A. (2007). Dietary sodium chloride intake independently predicts the degree of hyperchloremic metabolic acidosis in healthy humans consuming a net acid-producing diet. *American Journal of Physiology-Renal Physiology*, *293*(2), F521–F525. https://doi.org/10.1152/ajprenal.00048.2007

Frassetto, L. A., Schloetter, M., Mietus-Synder, M., Morris, R. C., & Sebastian, A. (2009). Metabolic and physiologic improvements from consuming a paleolithic, hunter-gatherer type diet. *European Journal of Clinical Nutrition*, *63*(8), 947–955. https://doi.org/10.1038/ejcn.2009.4

Frassetto, L. A., & Sebastian, A. (1996). Age and Systemic Acid-Base Equilibrium: Analysis of Published Data. *The Journals of Gerontology Series A: Biological Sciences and Medical Sciences*, *51A*(1), B91–B99. https://doi.org/10.1093/gerona/51A.1.B91

Frassetto, L. A., & Sebastian, A. (2019a). Aging, metabolic acidosis and renal failure:

Interactive accelerating processes. *Medical Hypotheses*, *124*(September 2018), 95–97. https://doi.org/10.1016/j.mehy.2019.02.015

Frassetto, L. A., & Sebastian, A. (2019b). Aging, metabolic acidosis and renal failure: Interactive accelerating processes. *Medical Hypotheses*, *124*(10), 95–97. https://doi.org/10.1016/j.mehy.2019.02.015

Frassetto, L. A., Sebastian, A., & DuBose Jr, T. D. (2020). How metabolic acidosis and kidney disease may accelerate the aging process. *European Journal of Clinical Nutrition*, *74*(S1), 27–32. https://doi.org/10.1038/s41430-020-0693-5

Frassetto, L. A., Todd, K. M., Morris, R. C., & Sebastian, A. (1998). Estimation of net endogenous noncarbonic acid production in humans from diet potassium and protein contents. *The American Journal of Clinical Nutrition*, *68*(3), 576–583. https://doi.org/10.1093/ajcn/68.3.576

Frost, S. C. (2014). Physiological functions of the alpha class of carbonic anhydrases. *Sub-Cellular Biochemistry*, *75*, 9–30. https://doi.org/10.1007/978-94-007-7359-2_2

Fung, T., Iyaswamy, A., Sreenivasmurthy, S., Krishnamoorthi, S., Guan, X.-J., Zhu, Z., Su, C.-F., Liu, J., Kan, Y., Zhang, Y., Wong, H., & Li, M. (2022). Klotho an Autophagy Stimulator as a Potential Therapeutic Target for Alzheimer's Disease: A Review. *Biomedicines*, *10*(3), 705. https://doi.org/10.3390/biomedicines10030705

Galet, C., Zhou, Y., Eyck, P. Ten, & Romanowski, K. S. (2018). Fall injuries, associated deaths, and 30-day readmission for subsequent falls are increasing in the elderly us population: A query of the who mortality database and national readmission database from 2010 to 2014. *Clinical Epidemiology*, *10*, 1627–1637. https://doi.org/10.2147/CLEP.S181138

Gems, D., Pletcher, S., & Partridge, L. (2002). Interpreting interactions between treatments that slow aging. *Aging Cell*, *1*(1), 1–9. https://doi.org/10.1046/j.1474-9728.2002.00003.x

Genders, A. J., Martin, S. D., McGee, S. L., & Bishop, D. J. (2019). A physiological drop in ph decreases mitochondrial respiration, and HDAC and Akt signaling, in l6 myocytes. *American Journal of Physiology - Cell Physiology*, *316*(3), C404–

C414. https://doi.org/10.1152/ajpcell.00214.2018

Gerschman, R., Gilbert, D. L., Nye, S. W., Dwyer, P., & Fenn, W. O. (1954). Oxygen Poisoning and X-irradiation: A Mechanism in Common. *Science*, *119*(3097), 623–626. https://doi.org/10.1126/science.119.3097.623

Ghimire, S., Terhzaz, S., Cabrero, P., Romero, M. F., Davies, S. A., & Dow, J. A. T. (2019). Targeted renal knockdown of Na + /H + exchanger regulatory factor Sip1 produces uric acid nephrolithiasis in *Drosophila*. *American Journal of Physiology-Renal Physiology*, *317*(4), F930–F940. https://doi.org/10.1152/ajprenal.00551.2018

Ghosh, A. C., & O'Connor, M. B. (2014). Systemic Activin signaling independently regulates sugar homeostasis, cellular metabolism, and pH balance in *Drosophila melanogaster*. *Proceedings of the National Academy of Sciences*. https://doi.org/10.1073/pnas.1319116111

Gloor, G. B., Preston, C. R., Johnson-Schlitz, D. M., Nassif, N. A., Phillis, R. W., Benz, W. K., Robertson, H. M., & Engels, W. R. (1993). Type I repressors of P element mobility. *Genetics*, *135*(1), 81–95. https://doi.org/10.1093/genetics/135.1.81

Graham, K. A., Reaich, D., Channon, S. M., Downie, S., Gilmour, E., Passlick-Deetjen, J., & Goodship, T. H. J. (1996). Correction of acidosis in CAPD decreases whole body protein degradation. *Kidney International*, *49*(5), 1396–1400. https://doi.org/10.1038/ki.1996.196

Grandison, R. C., Piper, M. D. W., & Partridge, L. (2009). Amino-acid imbalance explains extension of lifespan by dietary restriction in *Drosophila*. *Nature*, *462*(7276), 1061–1064. https://doi.org/10.1038/nature08619

Green, M. L., Hatch, M., & Freel, R. W. (2005). Ethylene glycol induces hyperoxaluria without metabolic acidosis in rats. *American Journal of Physiology-Renal Physiology*, *289*(3), F536–F543. https://doi.org/10.1152/ajprenal.00025.2005

Grönke, S., Clarke, D.-F., Broughton, S., Andrews, T. D., & Partridge, L. (2010). Molecular Evolution and Functional Characterization of *Drosophila* Insulin-Like Peptides. *PLoS Genetics*, *6*(2), e1000857.

https://doi.org/10.1371/journal.pgen.1000857

Gunnerson, K. J., Saul, M., He, S., & Kellum, J. A. (2006). Lactate versus non-lactate metabolic acidosis: a retrospective outcome evaluation of critically ill patients. *Critical Care (London, England)*, *10*(1), R22. https://doi.org/10.1186/cc3987

Halberg, K. A., Terhzaz, S., Cabrero, P., Davies, S. A., & Dow, J. A. T. (2015). Tracing the evolutionary origins of insect renal function. *Nature Communications*, *6*(1), 6800. https://doi.org/10.1038/ncomms7800

Hales, K. G., Korey, C. A., Larracuente, A. M., & Roberts, D. M. (2015). Genetics on the Fly: A Primer on the *Drosophila* Model System. *Genetics*, *201*(3), 815–842. https://doi.org/10.1534/genetics.115.183392

Han, S., Zhao, C., Pokhrel, G., Sun, X., Chen, Z., & Xu, H. (2019). Hydroxycitric Acid Tripotassium Inhibits Calcium Oxalate Crystal Formation in the *Drosophila Melanogaster* Model of Hyperoxaluria. *Medical Science Monitor*, *25*, 3662–3667. https://doi.org/10.12659/MSM.913637

Handke, B., Poernbacher, I., Goetze, S., Ahrens, C. H., Omasits, U., Marty, F., Simigdala, N., Meyer, I., Wollscheid, B., Brunner, E., Hafen, E., & Lehner, C. F. (2013). The Hemolymph Proteome of Fed and Starved *Drosophila* Larvae. *PLoS ONE*, *8*(6), e67208. https://doi.org/10.1371/journal.pone.0067208

Hanson, R. W., & Hakimi, P. (2008). Born to run; the story of the PEPCK-Cmus mouse. *Biochimie*, *90*(6), 838–842. https://doi.org/10.1016/j.biochi.2008.03.009

Harman, D. (1956). Aging: A Theory Based on Free Radical and Radiation Chemistry. *Journal of Gerontology*, *11*(3), 298–300. https://doi.org/10.1093/geronj/11.3.298

Harrison, J. F. (2001). Insect acid-base physiology. *Annual Review of Entomology*, *46*(1), 221–250. https://doi.org/10.1146/annurev.ento.46.1.221

Hayflick, L. (2020). The greatest risk factor for the leading cause of death is ignored. *Biogerontology*, *0123456789*(Shock 1951). https://doi.org/10.1007/s10522-020-09901-y

Heinrichsen, E. T., & Haddad, G. G. (2012). Role of High-Fat Diet in Stress Response of *Drosophila*. *PLoS ONE*, *7*(8), e42587.

https://doi.org/10.1371/journal.pone.0042587

Heinrichsen, E. T., Zhang, H., Robinson, J. E., Ngo, J., Diop, S., Bodmer, R., Joiner, W. J., Metallo, C. M., & Haddad, G. G. (2014). Metabolic and transcriptional response to a high-fat diet in *Drosophila melanogaster*. *Molecular Metabolism*, *3*(1), 42–54. https://doi.org/10.1016/j.molmet.2013.10.003

Hejazi, E., Emamat, H., Sharafkhah, M., Saidpour, A., Poustchi, H., Sepanlou, S., Sotoudeh, M., Dawsey, S., Boffetta, P., Abnet, C. C., Kamangar, F., Etemadi, A., Pourshams, A., Malekshah, A. F., Berennan, P., Malekzadeh, R., & Hekmatdoost, A. (2022). Dietary acid load and mortality from all causes, CVD and cancer: results from the Golestan Cohort Study. *British Journal of Nutrition*, *128*(2), 237–243. https://doi.org/10.1017/S0007114521003135

Henry, J. R., & Harrison, J. F. (2004). Plastic and evolved responses of larval tracheae and mass to varying atmospheric oxygen content in *Drosophila melanogaster*. *Journal of Experimental Biology*, *207*(20), 3559–3567. https://doi.org/10.1242/jeb.01189

Heys, C., Lizé, A., Blow, F., White, L., Darby, A., & Lewis, Z. J. (2018). The effect of gut microbiota elimination in *Drosophila melanogaster*: A how-to guide for host–microbiota studies. *Ecology and Evolution*, *8*(8), 4150–4161. https://doi.org/10.1002/ece3.3991

Hietavala, E.-M., Ihalainen, J., Frassetto, L., Schumann, M., Eklund, D., Pitkänen, H., Häkkinen, K., & Mero, A. (2018). Effects of 12-Week Low or Moderate Dietary Acid Intake on Acid–Base Status and Kidney Function at Rest and during Submaximal Cycling. *Nutrients*, *10*(3), 323. https://doi.org/10.3390/nu10030323

Ho, C. Y., Chen, Y. H., Wu, P. Y., Chang, C. H., Chen, H. Y., Man, K. M., Shen, J. L., Tsai, F. J., Lin, W. Y., Lee, Y. J., & Chen, W. C. (2013). Effects of commercial citrate-containing juices on urolithiasis in a *Drosophila* model. *Kaohsiung Journal of Medical Sciences*. https://doi.org/10.1016/j.kjms.2013.01.003

Hoffman, J. M., Dudeck, S. K., Patterson, H. K., & Austad, S. N. (2021). Sex, mating and repeatability of Drosophila melanogaster longevity. *Royal Society Open Science*, *8*(8), 210273. https://doi.org/10.1098/rsos.210273

Houtkooper, R. H., Argmann, C., Houten, S. M., Canńo, C., Jeninga, E. H., Andreux, Ṕeńelope A., Thomas, C., Doenlen, R., Schoonjans, K., & Auwerx, J. (2011). The metabolic footprint of aging in mice. *Scientific Reports*, *1*. https://doi.org/10.1038/srep00134

Hu, J., Wang, Y., Geng, X., Chen, R., Xu, X., Zhang, X., Lin, J., Teng, J., & Ding, X. (2017). Metabolic acidosis as a risk factor for the development of acute kidney injury and hospital mortality. *Experimental and Therapeutic Medicine*, *13*(5), 2362–2374. https://doi.org/10.3892/etm.2017.4292

Hulbert, A. J., Clancy, D. J., Mair, W., Braeckman, B. P., Gems, D., & Partridge, L. (2004). Metabolic rate is not reduced by dietary-restriction or by lowered insulin/IGF-1 signalling and is not correlated with individual lifespan in *Drosophila melanogaster*. *Experimental Gerontology*. https://doi.org/10.1016/j.exger.2004.04.006

Hulbert, A. J., Pamplona, R., Buffenstein, R., & Buttemer, W. A. (2007). Life and Death: Metabolic Rate, Membrane Composition, and Life Span of Animals. *Physiological Reviews*, *87*(4), 1175–1213. https://doi.org/10.1152/physrev.00047.2006

Ibrahim, H., Lee, Y. J., & Curthoys, N. P. (2008). Renal response to metabolic acidosis: Role of mRNA stabilization. *Kidney International*, *73*(1), 11–18. https://doi.org/10.1038/sj.ki.5002581

Inouye, S. K., Studenski, S., Tinetti, M. E., & Kuchel, G. A. (2007). Geriatric Syndromes: Clinical, Research, and Policy Implications of a Core Geriatric Concept. *Journal of the American Geriatrics Society*, *55*(5), 780–791. https://doi.org/10.1111/j.1532-5415.2007.01156.x

Itskov, P. M., Moreira, J.-M., Vinnik, E., Lopes, G., Safarik, S., Dickinson, M. H., & Ribeiro, C. (2014). Automated monitoring and quantitative analysis of feeding behaviour in *Drosophila*. *Nature Communications*, *5*(1), 4560. https://doi.org/10.1038/ncomms5560

Ja, W. W., Carvalho, G. B., Zid, B. M., Mak, E. M., Brummel, T., & Benzer, S. (2009). Water- and nutrient-dependent effects of dietary restriction on *Drosophila* lifespan. *Proceedings of the National Academy of Sciences*, *106*(44), 18633–18637. https://doi.org/10.1073/pnas.0908016106

Jaber, S., Paugam, C., Futier, E., Lefrant, J.-Y., Lasocki, S., Lescot, T., Pottecher, J., Demoule, A., Ferrandière, M., Asehnoune, K., Dellamonica, J., Velly, L., Abback, P.-S., de Jong, A., Brunot, V., Belafia, F., Roquilly, A., Chanques, G., Muller, L., … Kipnis, E. (2018). Sodium bicarbonate therapy for patients with severe metabolic acidaemia in the intensive care unit (BICAR-ICU): a multicentre, open-label, randomised controlled, phase 3 trial. *The Lancet*, *392*(10141), 31–40. https://doi.org/10.1016/S0140-6736(18)31080-8

Jamme, M., Ben Hadj Salem, O., Guillemet, L., Dupland, P., Bougouin, W., Charpentier, J., Mira, J.-P., Pène, F., Dumas, F., Cariou, A., & Geri, G. (2018). Severe metabolic acidosis after out-of-hospital cardiac arrest: risk factors and association with outcome. *Annals of Intensive Care*, *8*(1), 62. https://doi.org/10.1186/s13613-018-0409-3

Jin, K. (2010). Modern Biological Theories of Aging. *Aging and Disease*, *1*(2), 72–74. https://doi.org/10.1093/jn/119.6.952

Johmura, Y., Yamanaka, T., Omori, S., Wang, T.-W., Sugiura, Y., Matsumoto, M., Suzuki, N., Kumamoto, S., Yamaguchi, K., Hatakeyama, S., Takami, T., Yamaguchi, R., Shimizu, E., Ikeda, K., Okahashi, N., Mikawa, R., Suematsu, M., Arita, M., Sugimoto, M., … Nakanishi, M. (2021). Senolysis by glutaminolysis inhibition ameliorates various age-associated disorders. *Science*, *371*(6526), 265–270. https://doi.org/10.1126/science.abb5916

Kammerl, I. E., & Meiners, S. (2016). Proteasome function shapes innate and adaptive immune responses. *American Journal of Physiology-Lung Cellular and Molecular Physiology*, *311*(2), L328–L336. https://doi.org/10.1152/ajplung.00156.2016

Karet, F. E., Gainza, F. J., Györy, A. Z., Unwin, R. J., Wrong, O., Tanner, M. J. A., Nayir, A., Alpay, H., Santos, F., Hulton, S. A., Bakkaloglu, A., Ozen, S., Cunningham, M. J., di Pietro, A., Walker, W. G., & Lifton, R. P. (1998). Mutations in the chloride-bicarbonate exchanger gene AE1 cause autosomal dominant but not autosomal recessive distal renal tubular acidosis. *Proceedings of the National Academy of Sciences*, *95*(11), 6337–6342. https://doi.org/10.1073/pnas.95.11.6337

Keeble, E., Roberts, H. C., Williams, C. D., Van Oppen, J., & Conroy, S. P. (2019).

Outcomes of hospital admissions among frail older people: A 2-year cohort study. *British Journal of General Practice*, *69*(685), E555–E560. https://doi.org/10.3399/bjgp19X704621

Kellum, J. A. (2005). Clinical review: reunification of acid-base physiology. *Critical Care (London, England)*, *9*(5), 500–507. https://doi.org/10.1186/cc3789

Kellum, J. A., & Elbers, P. W. G. (2009). *Stewart's Textbook of Acid-Base*. AcidBase.org. https://books.google.co.uk/books?id=4U%5C_50yjaD2IC

Khazaeli, A. A., Van Voorhies, W., & Curtsinger, J. W. (2005). Longevity and Metabolism in *Drosophila melanogaster*. *Genetics*, *169*(1), 231–242. https://doi.org/10.1534/genetics.104.030403

Kirkwood, T. B. L. (2017). The Disposable Soma Theory. In *The Evolution of Senescence in the Tree of Life* (pp. 23–39). Cambridge University Press. https://doi.org/10.1017/9781139939867.002

Kitada, M., Ogura, Y., Monno, I., & Koya, D. (2019). The impact of dietary protein intake on longevity and metabolic health. *EBioMedicine*, *43*, 632–640. https://doi.org/10.1016/j.ebiom.2019.04.005

Klionsky, D. J., Petroni, G., Amaravadi, R. K., Baehrecke, E. H., Ballabio, A., Boya, P., Bravo-San Pedro, J. M., Cadwell, K., Cecconi, F., Choi, A. M. K., Choi, M. E., Chu, C. T., Codogno, P., Colombo, M. I., Cuervo, A. M., Deretic, V., Dikic, I., Elazar, Z., Eskelinen, E., … Pietrocola, F. (2021). Autophagy in major human diseases. *The EMBO Journal*, *40*(19), 1–64. https://doi.org/10.15252/embj.2021108863

Ko, B., Chang, Y., Ryu, S., Kim, E. M., Lee, M. Y., Hyun, Y. Y., & Lee, K. (2017). Dietary acid load and chronic kidney disease in elderly adults: Protein and potassium intake. *PLOS ONE*, *12*(9), e0185069. https://doi.org/10.1371/journal.pone.0185069

Kontis, V., Bennett, J. E., Mathers, C. D., Li, G., Foreman, K., & Ezzati, M. (2017). Future life expectancy in 35 industrialised countries: projections with a Bayesian model ensemble. *The Lancet*, *389*(10076), 1323–1335. https://doi.org/10.1016/S0140-6736(16)32381-9

Kovesdy, C. P., Anderson, J. E., & Kalantar-Zadeh, K. (2009). Association of serum

bicarbonate levels with mortality in patients with non-dialysis-dependent CKD. *Nephrology Dialysis Transplantation*, *24*(4), 1232–1237. https://doi.org/10.1093/ndt/gfn633

Kraut, J. A., & Madias, N. E. (2010). Metabolic acidosis: Pathophysiology, diagnosis and management. *Nature Reviews Nephrology*, *6*(5), 274–285. https://doi.org/10.1038/nrneph.2010.33

Kuro-o, M., Matsumura, Y., Aizawa, H., Kawaguchi, H., Suga, T., Utsugi, T., Ohyama, Y., Kurabayashi, M., Kaname, T., Kume, E., Iwasaki, H., Iida, A., Shiraki-Iida, T., Nishikawa, S., Nagai, R., & Nabeshima, Y. I. (1997). Mutation of the mouse klotho gene leads to a syndrome resembling ageing. *Nature*, *390*(6655), 45–51. https://doi.org/10.1038/36285

Kurosu, H., Yamamoto, M., Clark, J. D., Pastor, J. V., Nandi, A., Gurnani, P., McGuinness, O. P., Chikuda, H., Yamaguchi, M., Kawaguchi, H., Shimomura, I., Takayama, Y., Herz, J., Kahn, C. R., Rosenblatt, K. P., & Kuro-o, M. (2005). Suppression of Aging in Mice by the Hormone Klotho. *Science*, *309*(5742), 1829–1833. https://doi.org/10.1126/science.1112766

Kurtz, I., Kraut, J., Ornekian, V., & Nguyen, M. K. (2008). Acid-base analysis: a critique of the Stewart and bicarbonate-centered approaches. *American Journal of Physiology-Renal Physiology*, *294*(5), F1009–F1031. https://doi.org/10.1152/ajprenal.00475.2007

Lambert, H., Frassetto, L., Moore, J. B., & Torgerson, D. (2015). *The effect of supplementation with alkaline potassium salts on bone metabolism : a meta-analysis*. 1311–1318. https://doi.org/10.1007/s00198-014-3006-9

Landayan, D., Wang, B. P., Zhou, J., & Wolf, F. W. (2021). Thirst interneurons that promote water seeking and limit feeding behavior in *Drosophila*. *ELife*, *10*, 1–19. https://doi.org/10.7554/eLife.66286

Landis, G. N., Bhole, D., & Tower, J. (2003). A search for doxycycline-dependent mutations that increase Drosophila melanogaster life span identifies the VhaSFD, Sugar baby, filamin, fwd and Cct1 genes. In *Genome Biology*. http://genomebiology.com/2003/4/2/R8

Lang, S., Hilsabeck, T. A., Wilson, K. A., Sharma, A., Bose, N., Brackman, D. J.,

Beck, J. N., Chen, L., Watson, M. A., Killilea, D. W., Ho, S., Kahn, A., Giacomini, K., Stoller, M. L., Chi, T., & Kapahi, P. (2019). A conserved role of the insulin-like signaling pathway in diet-dependent uric acid pathologies in *Drosophila melanogaster*. *PLOS Genetics*, *15*(8), e1008318. https://doi.org/10.1371/journal.pgen.1008318

Lardner, A. (2001). The effects of extracellular pH on immune function. *Journal of Leukocyte Biology*, *69*(4), 522–530. https://doi.org/10.1189/jlb.69.4.522

Leader, D. P., Krause, S. A., Pandit, A., Davies, S. A., & Dow, J. A. T. (2018). FlyAtlas 2: A new version of the *Drosophila melanogaster* expression atlas with RNA-Seq, miRNA-Seq and sex-specific data. *Nucleic Acids Research*, *46*(D1), D809–D815. https://doi.org/10.1093/nar/gkx976

Lee, B. C., Kaya, A., Ma, S., Kim, G., Gerashchenko, M. V, Yim, S. H., Hu, Z., Harshman, L. G., & Gladyshev, V. N. (2014). Methionine restriction extends lifespan of *Drosophila melanogaster* under conditions of low amino-acid status. *Nature Communications*, *5*(1), 3592. https://doi.org/10.1038/ncomms4592

Lehallier, B., Gate, D., Schaum, N., Nanasi, T., Lee, S. E., Yousef, H., Losada, P. M., Berdnik, D., Keller, A., Verghese, J., Sathyan, S., Franceschi, C., Milman, S., Barzilai, N., & Wyss-Coray, T. (2019). Undulating changes in human plasma proteome across lifespan are linked to disease. *Nature Medicine*, *25*(December), 751115. https://doi.org/10.1101/751115

Lehmann, F.-O. (2001). Matching Spiracle Opening to Metabolic Need During Flight in *Drosophila*. *Science*, *294*(5548), 1926–1929. https://doi.org/10.1126/science.1064821

Leibrock, C. B., Voelkl, J., Kohlhofer, U., Quintanilla-Martinez, L., Kuro-o, M., & Lang, F. (2016). Bicarbonate-sensitive calcification and lifespan of klotho-deficient mice. *American Journal of Physiology-Renal Physiology*, *310*(1), F102–F108. https://doi.org/10.1152/ajprenal.00037.2015

Lennicke, C., & Cochemé, H. M. (2020). Redox signalling and ageing: insights from *Drosophila*. *Biochemical Society Transactions*, *48*(2), 367–377. https://doi.org/10.1042/BST20190052

Lennicke, C., & Cochemé, H. M. (2021). Redox metabolism: ROS as specific

molecular regulators of cell signaling and function. *Molecular Cell*, *81*(18), 3691–3707. https://doi.org/10.1016/j.molcel.2021.08.018

Lennicke, C., dos Santos, E., & Cochemé, H. M. (2020). Sugar-induced dysregulation of purine metabolism impacts lifespan. *Aging*, *12*(24), 24479–24480. https://doi.org/10.18632/aging.104223

Li, C.-F., Liu, Y.-P., Liu, C.-Y., Zhu, H.-L., Wu, B.-H., Li, B.-L., & Chen, Y.-M. (2022). Dietary Acid Load Was Positively Associated with the Risk of Hip Fracture in Elderly Adults. *Nutrients*, *14*(18), 3748. https://doi.org/10.3390/nu14183748

Liamis, G., Milionis, H. J., & Elisaf, M. (2010). Pharmacologically-Induced Metabolic Acidosis. *Drug Safety*, *33*(5), 371–391. https://doi.org/10.2165/11533790-000000000-00000

Lighton, J. R. B. (2008). *Measuring Metabolic Rates*. Oxford University Press. https://doi.org/10.1093/acprof:oso/9780195310610.001.0001

Lighton, J. R. B., & Schilman, P. E. (2007). Oxygen Reperfusion Damage in an Insect. *PLoS ONE*, *2*(12), e1267. https://doi.org/10.1371/journal.pone.0001267

Linneweber, G. A., Jacobson, J., Busch, K. E., Hudry, B., Christov, C. P., Dormann, D., Yuan, M., Otani, T., Knust, E., de Bono, M., & Miguel-Aliaga, I. (2014). Neuronal Control of Metabolism through Nutrient-Dependent Modulation of Tracheal Branching. *Cell*, *156*(1–2), 69–83. https://doi.org/10.1016/j.cell.2013.12.008

Livak, K. J., & Schmittgen, T. D. (2001). Analysis of Relative Gene Expression Data Using Real-Time Quantitative PCR and the 2−ΔΔCT Method. *Methods*, *25*(4), 402–408. https://doi.org/10.1006/meth.2001.1262

Lopez-Garcia, S. C., Emma, F., Walsh, S. B., Fila, M., Hooman, N., Zaniew, M., Bertholet-Thomas, A., Colussi, G., Burgmaier, K., Levtchenko, E., Sharma, J., Singhal, J., Soliman, N. A., Ariceta, G., Basu, B., Murer, L., Tasic, V., Tsygin, A., Decramer, S., … Bockenhauer, D. (2019). Treatment and long-term outcome in primary distal renal tubular acidosis. *Nephrology Dialysis Transplantation*, *34*(6), 981–991. https://doi.org/10.1093/ndt/gfy409

López-Otín, C., Blasco, M. A., Partridge, L., Serrano, M., & Kroemer, G. (2013). The Hallmarks of Aging. *Cell*, *153*(6), 1194–1217.

https://doi.org/10.1016/j.cell.2013.05.039

López-Otín, C., Blasco, M. A., Partridge, L., Serrano, M., & Kroemer, G. (2023). Hallmarks of aging: An expanding universe. *Cell*, *186*(2), 243–278. https://doi.org/10.1016/j.cell.2022.11.001

López-Otín, C., Galluzzi, L., Freije, J. M. P., Madeo, F., & Kroemer, G. (2016). Metabolic Control of Longevity. *Cell*, *166*(4), 802–821. https://doi.org/10.1016/j.cell.2016.07.031

Lu, D., Peng, X., Jia, S., Li, G., & Tan, N. (2019). Carbonic Anhydrase I modifies SOD1-induced motor neuron toxicity in *Drosophila* via ER stress pathway. *Journal of Neuroscience and Neurological Disorders*, *3*(2), 135–144. https://doi.org/10.29328/journal.jnnd.1001024

Lukaski, H. C. (2005). Low dietary zinc decreases erythrocyte carbonic anhydrase activities and impairs cardiorespiratory function in men during exercise. *The American Journal of Clinical Nutrition*, *81*(5), 1045–1051. https://doi.org/10.1093/ajcn/81.5.1045

Mackenzie, S. M., Brooker, M. R., Gill, T. R., Cox, G. B., Howells, A. J., & Ewart, G. D. (1999). Mutations in the white gene of *Drosophila melanogaster* affecting ABC transporters that determine eye colouration. *Biochimica et Biophysica Acta (BBA) - Biomembranes*, *1419*(2), 173–185. https://doi.org/10.1016/S0005-2736(99)00064-4

Maddrell, S. H. P., & O'Donnell, M. J. (1992). Insect malpighian tubules: V-ATPase action in ion and fluid transport. *Journal of Experimental Biology*, *172*(1), 417–429. https://doi.org/10.1242/jeb.172.1.417

Magalhães, J. P. (2012). Programmatic features of aging originating in development: aging mechanisms beyond molecular damage? *The FASEB Journal*, *26*(12), 4821–4826. https://doi.org/10.1096/fj.12-210872

Mair, W., Goymer, P., Pletcher, S. D., & Partridge, L. (2003). Demography of Dietary Restriction and Death in Drosophila. *Science*, *301*(5640), 1731–1733. https://doi.org/10.1126/science.1086016

Mair, W., Piper, M. D. W., & Partridge, L. (2005). Calories Do Not Explain Extension of Life Span by Dietary Restriction in *Drosophila*. *PLoS Biology*, *3*(7), e223.

https://doi.org/10.1371/journal.pbio.0030223

Mannick, J. B., Morris, M., Hockey, H.-U. P. U., Roma, G., Beibel, M., Kulmatycki, K., Watkins, M., Shavlakadze, T., Zhou, W., Quinn, D., Glass, D. J., & Klickstein, L. B. (2018). TORC1 inhibition enhances immune function and reduces infections in the elderly. *Science Translational Medicine*, *10*(449), 1–11. https://doi.org/10.1126/scitranslmed.aaq1564

Martinez-Miguel, V. E., Lujan, C., Espie--Caullet, T., Martinez-Martinez, D., Moore, S., Backes, C., Gonzalez, S., Galimov, E. R., Brown, A. E. X., Halic, M., Tomita, K., Rallis, C., von der Haar, T., Cabreiro, F., & Bjedov, I. (2021). Increased fidelity of protein synthesis extends lifespan. *Cell Metabolism*, *33*(11), 2288-2300.e12. https://doi.org/10.1016/j.cmet.2021.08.017

Mason, J. S., Wileman, T., & Chapman, T. (2018). Lifespan extension without fertility reduction following dietary addition of the autophagy activator Torin1 in *Drosophila melanogaster*. *PLOS ONE*, *13*(1), e0190105. https://doi.org/10.1371/journal.pone.0190105

Massie, H. R., Williams, T. R., & Colacicco, J. R. (1981). Changes in pH with age in *Drosophila* and the influence of buffers on longevity. *Mechanisms of Ageing and Development*. https://doi.org/10.1016/0047-6374(81)90098-1

Massonneau, J., Ouellet, C., Lucien, F., Dubois, C. M., Tyler, J., & Boissonneault, G. (2018). Suboptimal extracellular <scp>pH</scp> values alter <scp>DNA</scp> damage response to induced double-strand breaks. *FEBS Open Bio*, *8*(3), 416–425. https://doi.org/10.1002/2211-5463.12384

McCay, C. M., Crowell, M. F., & Maynard, L. A. (1935). The Effect of Retarded Growth Upon the Length of Life Span and Upon the Ultimate Body Size. *The Journal of Nutrition*, *10*(1), 63–79. https://doi.org/10.1093/jn/10.1.63

McKillip, E., & Klueg, K. (2006). Processing Clones for Whatman FTA Discs. *CGB Technical Report*, *2006*(2). https://doi.org/10.2506/cgbtr-200602

Medvedev, Z. A. (1990). An attempt at a rational classification of theories of ageing. *Biological Reviews of the Cambridge Philosophical Society*, *65*(3), 375–398. https://doi.org/10.1111/j.1469-185x.1990.tb01428.x

Miquel, J., Lundgren, P. R., Bensch, K. G., & Atlan, H. (1976). Effects of temperature

on the life span, vitality and fine structure of *Drosophila melanogaster*. *Mechanisms of Ageing and Development*, *5*(C), 347–370. https://doi.org/10.1016/0047-6374(76)90034-8

Mitch, W. E., Medina, R., Grieber, S., May, R. C., England, B. K., Price, S. R., Bailey, J. L., & Goldberg, A. L. (1994). Metabolic acidosis stimulates muscle protein degradation by activating the adenosine triphosphate-dependent pathway involving ubiquitin and proteasomes. *Journal of Clinical Investigation*, *93*(5), 2127–2133. https://doi.org/10.1172/JCI117208

Mo, D., Chen, Y., Jiang, N., Shen, J., & Zhang, J. (2020). Investigation of Isoform Specific Functions of the V-ATPase a Subunit During *Drosophila* Wing Development. *Frontiers in Genetics*, *11*(July), 1–11. https://doi.org/10.3389/fgene.2020.00723

Moeller, A. L., Hjortdal, V. E., Boedtkjer, D. M. B., & Boedtkjer, E. (2019). Acidosis inhibits rhythmic contractions of human thoracic ducts. *Physiological Reports*, *7*(8), 1–17. https://doi.org/10.14814/phy2.14074

Mołoń, M., Dampc, J., Kula-Maximenko, M., Zebrowski, J., Mołoń, A., Dobler, R., Durak, R., & Skoczowski, A. (2020). Effects of Temperature on Lifespan of *Drosophila melanogaster* from Different Genetic Backgrounds: Links between Metabolic Rate and Longevity. *Insects*, *11*(8), 470. https://doi.org/10.3390/insects11080470

Muñoz-Castañeda, J. R., Herencia, C., Pendón-Ruiz de Mier, M. V., Rodriguez-Ortiz, M. E., Diaz-Tocados, J. M., Vergara, N., Martínez-Moreno, J. M., Salmerón, M. D., Richards, W. G., Felsenfeld, A., Kuro-O, M., Almadén, Y., & Rodríguez, M. (2017). Differential regulation of renal Klotho and FGFR1 in normal and uremic rats. *The FASEB Journal*, *31*(9), 3858–3867. https://doi.org/10.1096/fj.201700006R

Na, J., Musselman, L. P., Pendse, J., Baranski, T. J., Bodmer, R., Ocorr, K., & Cagan, R. (2013). A *Drosophila* Model of High Sugar Diet-Induced Cardiomyopathy. *PLoS Genetics*, *9*(1), e1003175. https://doi.org/10.1371/journal.pgen.1003175

Nahas, G. G., Sutin, K. M., Fermon, C., Streat, S., Wiklund, L., Wahlander, S., Yellin,

P., Brasch, H., Kanchuger, M., Capan, L., Manne, J., Helwig, H., Gaab, M., Pfenninger, E., Wetterberg, T., Holmdahl, M., & Turndorf, H. (1998). Guidelines for the Treatment of Acidaemia with THAM. *Drugs*, *55*(2), 191–224. https://doi.org/10.2165/00003495-199855020-00003

Nahas, G. G., Verosky, M., & Schwartz, I. (1964). Urinary Excretion of THAM Citrate Orally Administered. *Experimental Biology and Medicine*, *116*(2), 378–382. https://doi.org/10.3181/00379727-116-29253

Niccoli, T., & Partridge, L. (2012). Ageing as a Risk Factor for Disease. *Current Biology*, *22*(17), R741–R752. https://doi.org/10.1016/j.cub.2012.07.024

Nishi, T., & Forgac, M. (2002). The vacuolar (H+)-ATPases — nature's most versatile proton pumps. *Nature Reviews Molecular Cell Biology*, *3*(2), 94–103. https://doi.org/10.1038/nrm729

Nocelli, R., Cintra-Socolowski, P., Roat, T., Silva-Zacarin, E., & Malaspina, O. (2016). Comparative physiology of Malpighian tubules: form and function. *Open Access Insect Physiology*, 13. https://doi.org/10.2147/OAIP.S72060

Nowson, C., & O'Connell, S. (2015). Protein Requirements and Recommendations for Older People: A Review. *Nutrients*, *7*(8), 6874–6899. https://doi.org/10.3390/nu7085311

O'Donnell, M. J., Dow, J. A., Huesmann, G. R., Tublitz, N. J., & Maddrell, S. H. (1996). Separate control of anion and cation transport in malpighian tubules of *Drosophila Melanogaster*. *Journal of Experimental Biology*, *199*(5), 1163–1175. https://doi.org/10.1242/jeb.199.5.1163

O'Donnell, M. J., & Maddrell, S. H. (1995). Fluid reabsorption and ion transport by the lower Malpighian tubules of adult female *Drosophila*. *Journal of Experimental Biology*, *198*(8), 1647–1653. https://doi.org/10.1242/jeb.198.8.1647

Oluwatosin, Y. E., & Kane, P. M. (1997). Mutations in the CYS4 Gene Provide Evidence for Regulation of the Yeast Vacuolar H+-ATPase by Oxidation and Reduction in Vivo. *Journal of Biological Chemistry*, *272*(44), 28149–28157. https://doi.org/10.1074/jbc.272.44.28149

Osanai, T., Tanaka, M., Izumiyama, K., Mikami, K., Kitajima, M., Tomisawa, T.,

Magota, K., Tomita, H., & Okumura, K. (2018). Intracellular protons accelerate aging and switch on aging hallmarks in mice. *Journal of Cellular Biochemistry*, *119*(12), 9825–9837. https://doi.org/10.1002/jcb.27302

Overend, G., Luo, Y., Henderson, L., Douglas, A. E., Davies, S. A., & Dow, J. A. T. (2016). Molecular mechanism and functional significance of acid generation in the *Drosophila* midgut. *Scientific Reports*, *6*(1), 27242. https://doi.org/10.1038/srep27242

Owusu-Ansah, E., & Perrimon, N. (2014). Modeling metabolic homeostasis and nutrient sensing in *Drosophila*: implications for aging and metabolic diseases. *Disease Models & Mechanisms*, *7*(3), 343–350. https://doi.org/10.1242/dmm.012989

Pamarthy, S., Kulshrestha, A., Katara, G. K., & Beaman, K. D. (2018). The curious case of vacuolar ATPase: regulation of signaling pathways. *Molecular Cancer*, *17*(1), 41. https://doi.org/10.1186/s12943-018-0811-3

Pang, Z., Chong, J., Zhou, G., de Lima Morais, D. A., Chang, L., Barrette, M., Gauthier, C., Jacques, P.-É., Li, S., & Xia, J. (2021). MetaboAnalyst 5.0: narrowing the gap between raw spectra and functional insights. *Nucleic Acids Research*, *49*(W1), W388–W396. https://doi.org/10.1093/nar/gkab382

Park, M., Jung, S. J., Yoon, S., Yun, J. M., & Yoon, H. (2015). Association between the markers of metabolic acid load and higher all-cause and cardiovascular mortality in a general population with preserved renal function. *Hypertension Research*, *38*(6), 433–438. https://doi.org/10.1038/hr.2015.23

Parkhitko, A. A., Wang, L., Filine, E., Jouandin, P., Leshchiner, D., Binari, R., Asara, J. M., Rabinowitz, J. D., & Perrimon, N. (2021). A genetic model of methionine restriction extends *Drosophila* health- and lifespan. *Proceedings of the National Academy of Sciences*, *118*(40), 1–12. https://doi.org/10.1073/pnas.2110387118

Partridge, L., Deelen, J., & Slagboom, P. E. (2018). Facing up to the global challenges of ageing. *Nature*, *561*(7721), 45–56. https://doi.org/10.1038/s41586-018-0457-8

Partridge, L., Fuentealba, M., & Kennedy, B. K. (2020). The quest to slow ageing through drug discovery. *Nature Reviews Drug Discovery*, *19*(8), 513–532.

https://doi.org/10.1038/s41573-020-0067-7

Partridge, L., Prowse, N., & Pignatelli, P. (1999). Another set of responses and correlated responses to selection on age at reproduction in *Drosophila melanogaster*. *Proceedings of the Royal Society of London. Series B: Biological Sciences*, *266*(1416), 255–261. https://doi.org/10.1098/rspb.1999.0630

Pearl, R. (1928). *The rate of living*. University Press London.

Pfeiffer, J., Johnson, D., & Nehrke, K. (2008). Oscillatory Transepithelial H+ Flux Regulates a Rhythmic Behavior in *C. elegans*. *Current Biology*. https://doi.org/10.1016/j.cub.2008.01.054

Piazzetta, P., Marino, T., & Russo, N. (2017). Mechanistic Explanation of the Weak Carbonic Anhydrase's Esterase Activity. *Molecules*, *22*(6), 1009. https://doi.org/10.3390/molecules22061009

Piper, M. D. W., & Bartke, A. (2008). Diet and Aging. *Cell Metabolism*, *8*(2), 99–104. https://doi.org/10.1016/j.cmet.2008.06.012

Piper, M. D. W., Blanc, E., Leitão-Gonçalves, R., Yang, M., He, X., Linford, N. J., Hoddinott, M. P., Hopfen, C., Soultoukis, G. A., Niemeyer, C., Kerr, F., Pletcher, S. D., Ribeiro, C., & Partridge, L. (2014). A holidic medium for *Drosophila melanogaster*. *Nature Methods*, *11*(1), 100–105. https://doi.org/10.1038/nmeth.2731

Piper, M. D. W., & Partridge, L. (2016). Protocols to Study Aging in *Drosophila*. *Methods in Molecular Biology (Clifton, N.J.)*, *1478*, 291–302. https://doi.org/10.1007/978-1-4939-6371-3_18

Piper, M. D. W., & Partridge, L. (2018). *Drosophila* as a model for ageing. *Biochimica et Biophysica Acta (BBA) - Molecular Basis of Disease*, *1864*(9), 2707–2717. https://doi.org/10.1016/j.bbadis.2017.09.016

Piper, M. D. W., Wong, R., Grandison, R. C., Bass, T. M., Martinez, P. M., & Partridge, L. (2010). Water-independent effects of dietary restriction in Drosophila. *Proceedings of the National Academy of Sciences*, *107*(14), 54–56. https://doi.org/10.1073/pnas.0914686107

Poupin, N., Calvez, J., Lassale, C., Chesneau, C., & Tomé, D. (2012). Impact of the diet on net endogenous acid production and acid–base balance. *Clinical*

Nutrition, *31*(3), 313–321. https://doi.org/10.1016/j.clnu.2012.01.006

Promislow, D. E. L., & Haselkorn, T. S. (2002). Age-specific metabolic rates and mortality rates in the genus *Drosophila*. *Aging Cell*, *1*(1), 66–74. https://doi.org/10.1046/j.1474-9728.2002.00009.x

Pryor, R., Martinez-Martinez, D., Quintaneiro, L., & Cabreiro, F. (2020). The Role of the Microbiome in Drug Response. *Annual Review of Pharmacology and Toxicology*, *60*(1), 417–435. https://doi.org/10.1146/annurev-pharmtox-010919-023612

Rae, M. J., Butler, R. N., Campisi, J., De Grey, A. D. N. J. N. J., Finch, C. E., Gough, M., Martin, G. M., Vijg, J., Perrott, K. M., & Logan, B. J. (2010). The Demographic and Biomedical Case for Late-Life Interventions in Aging. *Science Translational Medicine*, *2*(40), 40cm21-40cm21. https://doi.org/10.1126/scitranslmed.3000822

Raikou, V. D. (2016). Metabolic acidosis status and mortality in patients on the end stage of renal disease. *Journal of Translational Internal Medicine*, *4*(4), 170–177. https://doi.org/10.1515/jtim-2016-0036

Ramirez, A., Heimbach, A., Gründemann, J., Stiller, B., Hampshire, D., Cid, L. P., Goebel, I., Mubaidin, A. F., Wriekat, A.-L., Roeper, J., Al-Din, A., Hillmer, A. M., Karsak, M., Liss, B., Woods, C. G., Behrens, M. I., & Kubisch, C. (2006). Hereditary parkinsonism with dementia is caused by mutations in ATP13A2, encoding a lysosomal type 5 P-type ATPase. *Nature Genetics*, *38*(10), 1184–1191. https://doi.org/10.1038/ng1884

Reaich, D., Channon, S. M., Scrimgeour, C. M., Daley, S. E., Wilkinson, R., & Goodship, T. H. J. (1993). Correction of acidosis in humans with CRF decreases protein degradation and amino acid oxidation. *American Journal of Physiology-Endocrinology and Metabolism*, *265*(2), E230–E235. https://doi.org/10.1152/ajpendo.1993.265.2.E230

Rebholz, C. M., Coresh, J., Grams, M. E., Steffen, L. M., Anderson, C. A. M., Appel, L. J., & Crews, D. C. (2015). Dietary Acid Load and Incident Chronic Kidney Disease: Results from the ARIC Study. *American Journal of Nephrology*, *42*(6), 427–435. https://doi.org/10.1159/000443746

Redhai, S., Pilgrim, C., Gaspar, P., Giesen, L. van, Lopes, T., Riabinina, O., Grenier, T., Milona, A., Chanana, B., Swadling, J. B., Wang, Y.-F., Dahalan, F., Yuan, M., Wilsch-Brauninger, M., Lin, W., Dennison, N., Capriotti, P., Lawniczak, M. K. N., Baines, R. A., … Miguel-Aliaga, I. (2020). An intestinal zinc sensor regulates food intake and developmental growth. *Nature*, *580*(7802), 263–268. https://doi.org/10.1038/s41586-020-2111-5

Regenmortel, M. H. V. Van. (2004). Reductionism and complexity in molecular biology. *EMBO Reports*, *5*(11), 1016–1020. https://doi.org/10.1038/sj.embor.7400284

Reijenga, J., van Hoof, A., van Loon, A., & Teunissen, B. (2013). Development of methods for the determination of pKa values. *Analytical Chemistry Insights*, *8*(1), 53–71. https://doi.org/10.4137/ACI.S12304

Reiter, L. T., Potocki, L., Chien, S., Gribskov, M., & Bier, E. (2001). A Systematic Analysis of Human Disease-Associated Gene Sequences In Drosophila melanogaster. *Genome Research*, *11*(6), 1114–1125. https://doi.org/10.1101/gr.169101

Remnant, E. J., Williams, A., Lumb, C., Yang, Y. T., Chan, J., Duchêne, S., Daborn, P. J., Batterham, P., & Perry, T. (2016). Evolution, expression, and function of nonneuronal ligand-gated chloride channels in *Drosophila melanogaster*. *G3: Genes, Genomes, Genetics*, *6*(7), 2003–2012. https://doi.org/10.1534/g3.116.029546

Ring, T., Frische, S., & Nielsen, S. (2005). *Clinical review : Renal tubular acidosis – a physicochemical approach*. 573–580. https://doi.org/10.1186/cc3802

Robey, I. F., Baggett, B. K., Kirkpatrick, N. D., Roe, D. J., Dosescu, J., Sloane, B. F., Hashini, A. I., Morse, D. L., Raghunand, N., Gatenby, R. A., & Gillies, R. J. (2009). Bicarbonate increases tumor pH and inhibits spontaneous metastases. *Cancer Research*, *69*(6), 2260–2268. https://doi.org/10.1158/0008-5472.CAN-07-5575

Rockson, S. G., Keeley, V., Kilbreath, S., Szuba, A., & Towers, A. (2019). Cancer-associated secondary lymphoedema. *Nature Reviews Disease Primers*, *5*(1). https://doi.org/10.1038/s41572-019-0072-5

Rodan, A. R. (2019). The Drosophila Malpighian tubule as a model for mammalian tubule function. *Current Opinion in Nephrology and Hypertension*, *28*(5), 455–464. https://doi.org/10.1097/MNH.0000000000000521

Romero, M. F., Henry, D., Nelson, S., Harte, P. J., Dillon, A. K., & Sciortino, C. M. (2000). Cloning and characterization of a Na+-driven anion exchanger (NDAE1). A new bicarbonate transporter. *Journal of Biological Chemistry*. https://doi.org/10.1074/jbc.M003476200

Rose, E., Lee, D., Xiao, E., Zhao, W., Wee, M., Cohen, J., & Bergwitz, C. (2019). Endocrine regulation of MFS2 by branchless controls phosphate excretion and stone formation in *Drosophila* renal tubules. *Scientific Reports*, *9*(1), 8798. https://doi.org/10.1038/s41598-019-45269-x

Rotstein, B., & Paululat, A. (2016). On the Morphology of the *Drosophila* Heart. *Journal of Cardiovascular Development and Disease*, *3*(2), 15. https://doi.org/10.3390/jcdd3020015

Salway, J. G. (2018). The Krebs Uric Acid Cycle: A Forgotten Krebs Cycle. *Trends in Biochemical Sciences*, *43*(11), 847–849. https://doi.org/10.1016/j.tibs.2018.04.012

Santos, F., & Gil-Peña, H. (2023). Long-term complications of primary distal renal tubular acidosis. *Pediatric Nephrology (Berlin, Germany)*, *38*(3), 635–642. https://doi.org/10.1007/s00467-022-05546-w

Sasaki, A., Nishimura, T., Takano, T., Naito, S., & Yoo, S. K. (2021). *white* regulates proliferative homeostasis of intestinal stem cells during ageing in *Drosophila*. *Nature Metabolism*, *3*(4), 546–557. https://doi.org/10.1038/s42255-021-00375-x

Scialla, J. J., Appel, L. J., Astor, B. C., Miller, E. R., Beddhu, S., Woodward, M., Parekh, R. S., & Anderson, C. A. M. (2012). Net endogenous acid production is associated with a faster decline in GFR in African Americans. *Kidney International*, *82*(1), 106–112. https://doi.org/10.1038/ki.2012.82

Sciortino, C. M., Shrode, L. D., Fletcher, B. R., Harte, P. J., & Romero, M. F. (2001). Localization of endogenous and recombinant Na + -driven anion exchanger protein NDAE1 from *Drosophila melanogaster*. *American Journal of Physiology-Cell Physiology*, *281*(2), C449–C463.

https://doi.org/10.1152/ajpcell.2001.281.2.C449

Scott, A. J., Ellison, M., & Sinclair, D. A. (2021). The economic value of targeting aging. *Nature Aging*. https://doi.org/10.1038/s43587-021-00080-0

Sebastian, A., Frassetto, L. A., Sellmeyer, D. E., Merriam, R. L., & Morris, R. C. (2002). Estimation of the net acid load of the diet of ancestral preagricultural *Homo sapiens* and their hominid ancestors. *The American Journal of Clinical Nutrition*, *76*(6), 1308–1316. https://doi.org/10.1093/ajcn/76.6.1308

Senior, A. M., Nakagawa, S., Raubenheimer, D., & Simpson, S. J. (2020). Global associations between macronutrient supply and age-specific mortality. *Proceedings of the National Academy of Sciences*, *117*(48), 30824–30835. https://doi.org/10.1073/pnas.2015058117

Shanbhag, S., & Tripathi, S. (2009). Epithelial ultrastructure and cellular mechanisms of acid and base transport in the *Drosophila* midgut. *Journal of Experimental Biology*, *212*(11), 1731–1744. https://doi.org/10.1242/jeb.029306

Shi, Q., Maas, L., Veith, C., Van Schooten, F. J., & Godschalk, R. W. (2017). Acidic cellular microenvironment modifies carcinogen-induced DNA damage and repair. *Archives of Toxicology*, *91*(6), 2425–2441. https://doi.org/10.1007/s00204-016-1907-4

Shiels, P. G., Painer, J., Natterson-Horowitz, B., Johnson, R. J., Miranda, J. J., & Stenvinkel, P. (2021). Manipulating the exposome to enable better ageing. *Biochemical Journal*, *478*(14), 2889–2898. https://doi.org/10.1042/BCJ20200958

Shirakabe, A., Ikeda, Y., Sciarretta, S., Zablocki, D. K., & Sadoshima, J. (2016). Aging and Autophagy in the Heart. *Circulation Research*, *118*(10), 1563–1576. https://doi.org/10.1161/CIRCRESAHA.116.307474

Siener, R., Struwe, F., & Hesse, A. (2016). Effect of L-Methionine on the Risk of Phosphate Stone Formation. *Urology*, *98*, 39–43. https://doi.org/10.1016/j.urology.2016.08.007

Siesjö, B. K. (1972). Symposium on acid-base homeostasis. The regulation of cerebrospinal fluid pH. *Kidney International*, *1*(5), 360–374. https://doi.org/10.1038/ki.1972.47

Singleton, K., & Woodruff, R. I. (1994). The Osmolarity of Adult *Drosophila* Hemolymph and Its Effect on Oocyte-Nurse Cell Electrical Polarity. *Developmental Biology*, *161*(1), 154–167. https://doi.org/10.1006/dbio.1994.1017

Sly, W. S., Hewett-Emmett, D., Whyte, M. P., Yu, Y. S., & Tashian, R. E. (1983). Carbonic anhydrase II deficiency identified as the primary defect in the autosomal recessive syndrome of osteopetrosis with renal tubular acidosis and cerebral calcification. *Proceedings of the National Academy of Sciences*, *80*(9), 2752–2756. https://doi.org/10.1073/pnas.80.9.2752

Smeha, L., Fassula, A. S., Franco Moreno, Y. M., Gonzalez-Chica, D. A., & Nunes, E. A. (2022). Dietary acid load is positively associated with insulin resistance: a population-based study. *Clinical Nutrition ESPEN*, *49*, 341–347. https://doi.org/10.1016/j.clnesp.2022.03.025

Smith, A. N., Skaug, J., Choate, K. A., Nayir, A., Bakkaloglu, A., Ozen, S., Hulton, S. A., Sanjad, S. A., Al-Sabban, E. A., Lifton, R. P., Scherer, S. W., & Karet, F. E. (2000). Mutations in ATP6N1B, encoding a new kidney vacuolar proton pump 116-kD subunit, cause recessive distal renal tubular acidosis with preserved hearing. *Nature Genetics*, *26*(1), 71–75. https://doi.org/10.1038/79208

Song, Q., Meng, B., Xu, H., & Mao, Z. (2020). The emerging roles of vacuolar-type ATPase-dependent Lysosomal acidification in neurodegenerative diseases. *Translational Neurodegeneration*, *9*(1), 17. https://doi.org/10.1186/s40035-020-00196-0

Southall, T. D., Elliott, D. A., & Brand, A. H. (2008). The GAL4 System: A Versatile Toolkit for Gene Expression in *Drosophila*. *Cold Spring Harbor Protocols*, *2008*(7), pdb.top49. https://doi.org/10.1101/pdb.top49

Stewart, J., Manmathan, G., & Wilkinson, P. (2017). Primary prevention of cardiovascular disease: A review of contemporary guidance and literature. *JRSM Cardiovascular Disease*, *6*, 204800401668721. https://doi.org/10.1177/2048004016687211

Stover, E. H., Borthwick, K. J., Bavalia, C., Eady, N., Fritz, D. M., Rungroj, N., Giersch, A. B. S., Morton, C. C., Axon, P. R., Akil, I., Al-Sabban, E. A., Baguley, D. M., Bianca, S., Bakkaloglu, A., Bircan, Z., Chauveau, D., Clermont, M.-J.,

Guala, A., Hulton, S. A., … Karet, F. E. (2002). Novel ATP6V1B1 and ATP6V0A4 mutations in autosomal recessive distal renal tubular acidosis with new evidence for hearing loss. *Journal of Medical Genetics*, *39*(11), 796–803. https://doi.org/10.1136/jmg.39.11.796

Sun, X., Komatsu, T., Lim, J., Laslo, M., Yolitz, J., Wang, C., Poirier, L., Alberico, T., & Zou, S. (2012). Nutrient-dependent requirement for SOD1 in lifespan extension by protein restriction in *Drosophila melanogaster*. *Aging Cell*, *11*(5), 783–793. https://doi.org/10.1111/j.1474-9726.2012.00842.x

Syrjänen, L., Tolvanen, M. E. E., Hilvo, M., Vullo, D., Carta, F., Supuran, C. T., & Parkkila, S. (2013). Characterization, bioinformatic analysis and dithiocarbamate inhibition studies of two new α-carbonic anhydrases, CAH1 and CAH2, from the fruit fly *Drosophila melanogaster*. *Bioorganic and Medicinal Chemistry*, *21*(6), 1516–1521. https://doi.org/10.1016/j.bmc.2012.08.046

Syrjänen, L., Tolvanen, M., Hilvo, M., Olatubosun, A., Innocenti, A., Scozzafava, A., Leppiniemi, J., Niederhauser, B., Hytönen, V. P., Gorr, T. A., Parkkila, S., & Supuran, C. T. (2010). Characterization of the first beta-class carbonic anhydrase from an arthropod (*Drosophila melanogaster*) and phylogenetic analysis of beta-class carbonic anhydrases in invertebrates. *BMC Biochemistry*, *11*(1), 28. https://doi.org/10.1186/1471-2091-11-28

Syrjänen, L., Valanne, S., Kuuslahti, M., Tuomela, T., Sriram, A., Sanz, A., Jacobs, H. T., Rämet, M., & Parkkila, S. (2015). β carbonic anhydrase is required for female fertility in *Drosophila melanogaster*. *Frontiers in Zoology*, *12*(1), 1–10. https://doi.org/10.1186/s12983-015-0111-3

Tanaka, T., Biancotto, A., Moaddel, R., Moore, A. Z., Gonzalez-Freire, M., Aon, M. A., Candia, J., Zhang, P., Cheung, F., Fantoni, G., Semba, R. D., & Ferrucci, L. (2018). Plasma proteomic signature of age in healthy humans. *Aging Cell*, *17*(5), 1–13. https://doi.org/10.1111/acel.12799

Tangri, N., Reaven, N. L., Funk, S. E., Ferguson, T. W., Collister, D., & Mathur, V. (2021). Metabolic acidosis is associated with increased risk of adverse kidney outcomes and mortality in patients with non-dialysis dependent chronic kidney disease: an observational cohort study. *BMC Nephrology*, *22*(1), 185. https://doi.org/10.1186/s12882-021-02385-z

Tattikota, S. G., Cho, B., Liu, Y., Hu, Y., Barrera, V., Steinbaugh, M. J., Yoon, S.-H., Comjean, A., Li, F., Dervis, F., Hung, R.-J., Nam, J.-W., Ho Sui, S., Shim, J., & Perrimon, N. (2020). A single-cell survey of *Drosophila* blood. *ELife*, *9*, 1–35. https://doi.org/10.7554/eLife.54818

Templeman, N. M., Flibotte, S., Chik, J. H. L., Sinha, S., Lim, G. E., Foster, L. J., Nislow, C., & Johnson, J. D. (2017). Reduced Circulating Insulin Enhances Insulin Sensitivity in Old Mice and Extends Lifespan. *Cell Reports*, *20*(2), 451–463. https://doi.org/10.1016/j.celrep.2017.06.048

Terhzaz, S., Southall, T. D., Lilley, K. S., Kean, L., Allan, A. K., Davies, S. A., & Dow, J. A. T. (2006). Differential Gel Electrophoresis and Transgenic Mitochondrial Calcium Reporters Demonstrate Spatiotemporal Filtering in Calcium Control of Mitochondria. *Journal of Biological Chemistry*, *281*(27), 18849–18858. https://doi.org/10.1074/jbc.M603002200

Teufel, F., Almagro Armenteros, J. J., Johansen, A. R., Gíslason, M. H., Pihl, S. I., Tsirigos, K. D., Winther, O., Brunak, S., von Heijne, G., & Nielsen, H. (2022). SignalP 6.0 predicts all five types of signal peptides using protein language models. *Nature Biotechnology*, *40*(7), 1023–1025. https://doi.org/10.1038/s41587-021-01156-3

Theparambil, S. M., Hosford, P. S., Ruminot, I., Kopach, O., Reynolds, J. R., Sandoval, P. Y., Rusakov, D. A., Barros, L. F., & Gourine, A. V. (2020). Astrocytes regulate brain extracellular pH via a neuronal activity-dependent bicarbonate shuttle. *Nature Communications*, *11*(1), 1–15. https://doi.org/10.1038/s41467-020-18756-3

Tiselius, H. G., Ackermann, D., Alken, P., Buck, C., Conort, P., & Gallucci, M. (2001). Guidelines on urolithiasis. *European Urology*, *40*(4), 362–371. https://doi.org/10.1159/000049803

Toba, K., Hosojima, M., Kabasawa, H., Kuwahara, S., Murayama, T., Yamamoto-Kabasawa, K., Kaseda, R., Wada, E., Watanabe, R., Tanabe, N., Suzuki, Y., Narita, I., & Saito, A. (2019). Higher estimated net endogenous acid production with lower intake of fruits and vegetables based on a dietary survey is associated with the progression of chronic kidney disease. *BMC Nephrology*, *20*(1), 421. https://doi.org/10.1186/s12882-019-1591-8

Triana-Martínez, F., Picallos-Rabina, P., Da Silva-Álvarez, S., Pietrocola, F., Llanos, S., Rodilla, V., Soprano, E., Pedrosa, P., Ferreirós, A., Barradas, M., Hernández-González, F., Lalinde, M., Prats, N., Bernadó, C., González, P., Gómez, M., Ikonomopoulou, M. P., Fernández-Marcos, P. J., García-Caballero, T., … Collado, M. (2019). Identification and characterization of Cardiac Glycosides as senolytic compounds. *Nature Communications*, *10*(1), 1–12. https://doi.org/10.1038/s41467-019-12888-x

Troen, A. M., French, E. E., Roberts, J. F., Selhub, J., Ordovas, J. M., Parnell, L. D., & Lai, C.-Q. (2007). Lifespan modification by glucose and methionine in *Drosophila melanogaster* fed a chemically defined diet. *AGE*, *29*(1), 29–39. https://doi.org/10.1007/s11357-006-9018-4

Tu, C. K., Thomas, H. G., Wynns, G. C., & Silverman, D. N. (1986). Hydrolysis of 4-nitrophenyl acetate catalyzed by carbonic anhydrase III from bovine skeletal muscle. *Journal of Biological Chemistry*, *261*(22), 10100–10103. https://doi.org/10.1016/S0021-9258(18)67496-4

Tyanova, S., Temu, T., & Cox, J. (2016). The MaxQuant computational platform for mass spectrometry-based shotgun proteomics. *Nature Protocols*, *11*(12), 2301–2319. https://doi.org/10.1038/nprot.2016.136

Uda, N. R., Seibert, V., Stenner-Liewen, F., Müller, P., Herzig, P., Gondi, G., Zeidler, R., Van Dijk, M., Zippelius, A., & Renner, C. (2015). Esterase activity of carbonic anhydrases serves as surrogate for selecting antibodies blocking hydratase activity. *Journal of Enzyme Inhibition and Medicinal Chemistry*, *30*(6), 955–960. https://doi.org/10.3109/14756366.2014.1001754

Ugur, B., Chen, K., & Bellen, H. J. (2016). *Drosophila* tools and assays for the study of human diseases. *Disease Models & Mechanisms*, *9*(3), 235–244. https://doi.org/10.1242/dmm.023762

United Nations, Department of Economic and Social Affairs, P. D. (2019). *World Population Ageing 2019: Highlights*.

Vaccari, T., Duchi, S., Cortese, K., Tacchetti, C., & Bilder, D. (2010). The vacuolar ATPase is required for physiological as well as pathological activation of the Notch receptor. *Development*, *137*(11), 1825–1832. https://doi.org/10.1242/dev.045484

Valle-Hita, C., Becerra-Tomás, N., Díaz-López, A., Vázquez-Ruiz, Z., Megías, I., Corella, D., Goday, A., Martínez, J. A., Alonso-Gómez, Á. M., Wärnberg, J., Vioque, J., Romaguera, D., López-Miranda, J., Estruch, R., Tinahones, F. J., Lapetra, J., Serra-Majem, L., Bueno-Cavanillas, A., Tur, J. A., … Babio, N. (2022). Longitudinal association of dietary acid load with kidney function decline in an older adult population with metabolic syndrome. *Frontiers in Nutrition*, *9*. https://doi.org/10.3389/fnut.2022.986190

van Dam, E., van Leeuwen, L. A. G., dos Santos, E., James, J., Best, L., Lennicke, C., Vincent, A. J., Marinos, G., Foley, A., Buricova, M., Mokochinski, J. B., Kramer, H. B., Lieb, W., Laudes, M., Franke, A., Kaleta, C., & Cochemé, H. M. (2020). Sugar-Induced Obesity and Insulin Resistance Are Uncoupled from Shortened Survival in *Drosophila*. *Cell Metabolism*, *31*(4), 710-725.e7. https://doi.org/10.1016/j.cmet.2020.02.016

Vidgren, J., Liljas, A., & Walker, N. P. C. (1990). Refined structure of the acetazolamide complex of human carbonic anhydrase II at 1.9 Å. *International Journal of Biological Macromolecules*, *12*(6), 342–344. https://doi.org/10.1016/0141-8130(90)90040-H

Vissers, J. H. A., Manning, S. A., Kulkarni, A., & Harvey, K. F. (2016). A *Drosophila* RNAi library modulates Hippo pathway-dependent tissue growth. *Nature Communications*, *7*(1), 10368. https://doi.org/10.1038/ncomms10368

Vogler, G., & Ocorr, K. (2009). Visualizing the Beating Heart in *Drosophila*. *Journal of Visualized Experiments*, *31*, 6–8. https://doi.org/10.3791/1425

Vormann, J., & Goedecke, T. (2002). Acid-base homeostasis: Latent acidosis as a cause of chronic diseases. *Schweizerische Zeitschrift Fur GanzheitsMedizin*, *14*(5), 90–96. https://doi.org/10.1159/000282055

Wagner, C. A., Kovacikova, J., Stehberger, P. A., Winter, C., Benabbas, C., & Mohebbi, N. (2006). Renal acid-base transport: Old and new players. *Nephron - Physiology*, *103*(1), 1–6. https://doi.org/10.1159/000090217

Walton, Z. E., Patel, C. H., Brooks, R. C., Yu, Y., Ibrahim-Hashim, A., Riddle, M., Porcu, A., Jiang, T., Ecker, B. L., Tameire, F., Koumenis, C., Weeraratna, A. T., Welsh, D. K., Gillies, R., Alwine, J. C., Zhang, L., Powell, J. D., & Dang, C. V. (2018). Acid Suspends the Circadian Clock in Hypoxia through Inhibition of

mTOR. *Cell*, *174*(1), 72-87.e32. https://doi.org/10.1016/j.cell.2018.05.009

Wang, H., Abbas, K. M., Abbasifard, M., Abbasi-Kangevari, M., Abbastabar, H., Abd-Allah, F., Abdelalim, A., Abolhassani, H., Abreu, L. G., Abrigo, M. R. M., Abushouk, A. I., Adabi, M., Adair, T., Adebayo, O. M., Adedeji, I. A., Adekanmbi, V., Adeoye, A. M., Adetokunboh, O. O., Advani, S. M., … Murray, C. J. L. (2020). Global age-sex-specific fertility, mortality, healthy life expectancy (HALE), and population estimates in 204 countries and territories, 1950–2019: a comprehensive demographic analysis for the Global Burden of Disease Study 2019. *The Lancet*, *396*(10258), 1160–1203. https://doi.org/10.1016/S0140-6736(20)30977-6

Wang, J., Kean, L., Yang, J., Allan, A. K., Davies, S. A., Herzyk, P., & Dow, J. A. T. (2004). Function-informed transcriptome analysis of *Drosophila* renal tubule. *Genome Biology*, *5*(9), R69. https://doi.org/10.1186/gb-2004-5-9-r69

Wang, S., Ju, Y., Gao, L., Miao, Y., Qiao, H., & Wang, Y. (2022). The fruit fly kidney stone models and their application in drug development. *Heliyon*, *8*(4), e09232. https://doi.org/10.1016/j.heliyon.2022.e09232

Wayland, M. T., Defaye, A., Rocha, J., Jayaram, S. A., Royet, J., Miguel-Aliaga, I., Leulier, F., & Cognigni, P. (2014). Spotting the differences: Probing host/microbiota interactions with a dedicated software tool for the analysis of faecal outputs in *Drosophila*. *Journal of Insect Physiology*, *69*(C), 126–135. https://doi.org/10.1016/j.jinsphys.2014.05.023

Wernly, B., Heramvand, N., Masyuk, M., Rezar, R., Bruno, R. R., Kelm, M., Niederseer, D., Lichtenauer, M., Hoppe, U. C., Bakker, J., & Jung, C. (2020). Acidosis predicts mortality independently from hyperlactatemia in patients with sepsis. *European Journal of Internal Medicine*, *76*(November 2019), 76–81. https://doi.org/10.1016/j.ejim.2020.02.027

Wessing, A., Zierold, K., & Bertram, G. (1997). Carbonic anhydrase supports electrolyte transport in *Drosophila Malpighian* tubules. Evidence by X-ray microanalysis of cryosections. *Journal of Insect Physiology*. https://doi.org/10.1016/S0022-1910(96)00078-9

Wiig, H., & Swartz, M. A. (2012). Interstitial fluid and lymph formation and transport: Physiological regulation and roles in inflammation and cancer. *Physiological*

Reviews, *92*(3), 1005–1060. https://doi.org/10.1152/physrev.00037.2011

Wilbur, K. M., & Anderson, N. G. (1948). Electrometric and colorimetric determination of carbonic anhydrase. *Journal of Biological Chemistry*, *176*(1), 147–154. https://doi.org/10.1016/S0021-9258(18)51011-5

Wong, R., Piper, M. D. W., Wertheim, B., & Partridge, L. (2009). Quantification of Food Intake in *Drosophila*. *PLoS ONE*, *4*(6), e6063. https://doi.org/10.1371/journal.pone.0006063

Woodman, R., Ferrucci, L., & Guralnik, J. (2005). Anemia in older adults. *Current Opinion in Internal Medicine*, *4*(3), 261–266. https://doi.org/10.1097/01.moh.0000154030.13020.85

Xiao, H., Jedrychowski, M. P., Schweppe, D. K., Huttlin, E. L., Yu, Q., Heppner, D. E., Li, J., Long, J., Mills, E. L., Szpyt, J., He, Z., Du, G., Garrity, R., Reddy, A., Vaites, L. P., Paulo, J. A., Zhang, T., Gray, N. S., Gygi, S. P., & Chouchani, E. T. (2020). A Quantitative Tissue-Specific Landscape of Protein Redox Regulation during Aging. *Cell*, *180*(5), 968-983.e24. https://doi.org/10.1016/j.cell.2020.02.012

Xiao, H., Li, T.-K., Yang, J.-M., & Liu, L. F. (2003). Acidic pH induces topoisomerase II-mediated DNA damage. *Proceedings of the National Academy of Sciences*, *100*(9), 5205–5210. https://doi.org/10.1073/pnas.0935978100

Xu, H., Åkesson, A., Orsini, N., Håkansson, N., Wolk, A., & Carrero, J. J. (2016). Modest U-Shaped Association between Dietary Acid Load and Risk of All-Cause and Cardiovascular Mortality in Adults. *The Journal of Nutrition*, *146*(8), 1580–1585. https://doi.org/10.3945/jn.116.231019

Xu, J., Liu, Y., Li, H., Tarashansky, A. J., Kalicki, C. H., Hung, R.-J., Hu, Y., Comjean, A., Kolluru, S. S., Wang, B., Quake, S. R., Luo, L., McMahon, A. P., Dow, J. A. T., & Perrimon, N. (2021). A cell atlas of the fly kidney. *BioRxiv*, 1–54. https://doi.org/https://doi.org/10.1101/2021.09.03.458871

Yamauchi, T., Oi, A., Kosakamoto, H., Akuzawa-Tokita, Y., Murakami, T., Mori, H., Miura, M., & Obata, F. (2020). Gut Bacterial Species Distinctively Impact Host Purine Metabolites during Aging in *Drosophila*. *IScience*, *23*(9), 101477. https://doi.org/10.1016/j.isci.2020.101477

Yang, S. W., Zhou, Y. J., Zhao, Y. X., Liu, Y. Y., Tian, X. F., Wang, Z. J., Jia, D. A., Han, H. Y., Hu, B., Shen, H., Gao, F., Wang, L. Y., Lin, J., Pan, G. Z., Zhang, J., Guo, Z. F., Du, J., & Hu, D. Y. (2017). The serum anion gap is associated with disease severity and all-cause mortality in coronary artery disease. *Journal of Geriatric Cardiology*, *14*(6), 392–400. https://doi.org/10.11909/j.issn.1671-5411.2017.06.008

Yerushalmi, G. Y., Misyura, L., MacMillan, H. A., & Donini, A. (2018). Functional plasticity of the gut and the Malpighian tubules underlies cold acclimation and mitigates cold-induced hyperkalemia in *Drosophila melanogaster*. *Journal of Experimental Biology*. https://doi.org/10.1242/jeb.174904

Yuan, J., Narayanan, L., Rockwell, S., & Glazer, P. M. (2000). Diminished DNA repair and elevated mutagenesis in mammalian cells exposed to hypoxia and low pH. *Cancer*, *60*(16), 4372–4376. https://doi.org/10.1016/s0360-3016(00)80378-8

Zhang, T., Zhou, Q., Ogmundsdottir, M. H., Möller, K., Siddaway, R., Larue, L., Hsing, M., Kong, S. W., Goding, C. R., Palsson, A., Steingrimsson, E., & Pignoni, F. (2015). Mitf is a master regulator of the v-ATPase, forming a control module for cellular homeostasis with v-ATPase and TORC1. *Journal of Cell Science*, *128*(15), 2938–2950. https://doi.org/10.1242/jcs.173807

Zhao, L., Cui, L., Jiang, X., Zhang, J. J., Zhu, M., Jia, J., Zhang, Q., Zhang, J. J., Zhang, D., & Huang, Y. (2016). Extracellular pH regulates autophagy via the AMPK–ULK1 pathway in rat cardiomyocytes. *FEBS Letters*, *590*(18), 3202–3212. https://doi.org/10.1002/1873-3468.12359

Zocchi, L. (2002). Physiology and pathophysiology of pleural fluid turnover. *European Respiratory Journal*, *20*(6), 1545–1558. https://doi.org/10.1183/09031936.02.00062102

Appendix 1

List of peptides resulting from trypsin digestion of CAs and v-ATPase subunits. Specific peptides shown in green.

Carbonic anhydrase 1		
mass	position	peptide sequence
4577.2407	175-215	VTLPQGCDPGQLLPDVHTYW TYEGSLTTPPCSESVIWIVF K
2653.2641	105-128	GSEHTVDGVSYSGELHLVHW NTTK
2137.9297	01-18	MSHHWGYTEENGPAHWAK
2132.0505	70-90	VDVNGADSELTGGPLGDQIF K
1933.0429	131-150	SFGEAAAAPDGLAVLGVFLK
1690.7100	91-104	LEQFHCHWGCTDSK
1588.7635	216-229	TPIEVSDDQLNAMR
1464.8685	249-261	VINNFRPPLPLGK
1284.7674	161-171	VTSLLQFVLHK
1269.4874	238-248	EECPCNEFNGK
1229.6372	28-39	QSPVDITPSSAK
1194.5724	60-69	SLVNPGYCWR
1091.5228	151-160	AGNHHAELDK
1044.4857	19-27	EYPQASGHR
1027.5782	41-50	GSELNVAPLK
936.4785	230-237	NLNAYDVK
873.4465	53-59	YVPEHTK
512.2463	266-270	EIGGH
Carbonic anhydrase 2 isoform A		
mass	position	peptide sequence
3943.8357	218-252	SVESYFSYTGSLTTPPCSEE VTWIDFTTPIDITEK
3464.5930	113-141	TPLGYQFEQFHFHWGENDTI GSEDLINNR
2991.6011	.01-33	NTPFAIVIAPILICASLVLA QDFGYEGR
2566.2969	284-307	NYIEIPIHNMGSIPLVDAEN AAGK
1979.0378	76-93	VVPDNLQMTNNGHTVLVK
1857.8977	182-198	STGGYEGFTNLLSQIDR
1781.8679	166-181	DHGIAVMAFFFQVGDK
1776.1105	310-327	AQAAAVLLPLVVLAALSR
1762.9044	202-217	SVNMTNPLPLGEYISK
1664.8602	50-64	HQSPINIDQVSAVEK
1483.7764	268-279	NNFRPIQPLNDR
1483.6349	34-45	HGPEHWSEDYAR
1482.7111	153-165	NLEYPDFASALDK
1439.6471	94-105	MSYNEDEIPSVR
1267.7157	142-152	AYPAELHVVLR

1026.5214	259-267	LTANDDHLK
944.4876	69-75	LEFFNFK
748.4100	253-258	QLNAFR
671.3722	106-112	GGPLAEK
623.3511	328-332	TSIFR
524.3079	280-283	TLYK
Carbonic anhydrase 2 isoform B		
mass	position	peptide sequence
3943.8357	136-170	SVESYFSYTGSLTTPPCSEE VTWIDFTTPIDITEK
3464.5930	31-59	TPLGYQFEQFHFHWGENDTI GSEDLINNR
2566.2969	203-226	NYIEIPIHNMGSIPLVDAEN AAGK
1857.8977	100-116	STGGYEGFTNLLSQIDR
1781.8679	84-99	DHGIAVMAFFFQVGDK
1776.1105	229-246	AQAAAVLLPLVVLAALSR
1762.9044	120-135	SVNMTNPLPLGEYISK
1483.7764	187-198	NNFRPIQPLNDR
1482.7111	71-83	NLEYPDFASALDK
1439.6471	01-23	MSYNEDEIPSVR
1267.7157	60-70	AYPAELHVVLR
1213.6357	01-20	MTNNGHTVLVK
1139.6055	177-186	LLTANDDHLK
748.4100	171-176	QLNAFR
671.3722	24-30	GGPLAEK
623.3511	247-251	TSIFR
524.3079	199-202	TLYK
Carbonic anhydrase 3 isoform A		
mass	position	peptide sequence
4671.0359	53-92	QQPYIIGGALEQDMYVFEQL HFHWSDCDESGCEHTLEGMK
2754.3270	13-36	AIEHIDDVDPLEYHGHWEPV GVAR
2403.1860	150-171	IHTSASLDSDCLSWIGLQEL SK
2104.0749	178-195	GSLTTAPYFESVTWIIYR
2007.0367	114-132	NKPDGLAVVAFFIQACGEK
1536.6900	93-105	YSMEAHAVHYNSK
1470.7257	37-50	VQNTGTSAMVTFSK
1370.7096	01-20	MPVQSPIEISNR
994.4992	235-242	DPEIFFAR
907.5108	228-234	EIQRPHK
874.4094	172-177	HYYTYK
835.4672	196-202	TPIYVSR
833.4628	203-209	GQVQVFR
789.3923	210-216	NLQSCPK
778.4206	222-227	IVNNYR

738.3127	133-138	DCPEFK
710.3355	108-113	DFTEAK
688.3988	140-145	ITEGIR
573.2991	243-247	NTNPK
Carbonic anhydrase 4 isoform A		
mass	position	peptide sequence
3730.7918	85-118	TVDGSRPSLCISTEGQQVFE ADQLHFHWGSALSK
3387.7009	212-241	YFTYQGSLTTPPCAEAVIWF VFPTPLDVPK
2641.2007	188-211	LDDSCPLEDSMALQDLFASI DSQK
2272.0087	119-138	GSEHCLDGNYYDGEVHIVHK
1945.0245	64-81	SLCDPLSVINNGLTVLMR
1944.9670	38-55	QSPIALWSCNAITCNVPK
1932.8864	164-180	NLEDPNIETPAMNMICK
1816.0115	147-163	EAGLQPNGFAVLALFIR
1484.7240	264-275	ELQDGHDRPVYR
1114.4952	17-25	SHFGFNYDK
1049.5374	01-16	SFAPINSGTR
886.4682	246-251	HFWQLR
821.4304	58-63	FLNYHK
765.4253	258-263	VLNTYR
762.4356	181-187	QVSSITK
736.4174	01-20	MFLVAR
661.3304	29-33	DWNVK
582.2882	139-143	NASYK
575.3187	242-245	ELWK
Carbonic anhydrase 4 isoform C		
mass	position	peptide sequence
3730.7918	01-39	TVDGSRPSLCISTEGQQVFE ADQLHFHWGSALSK
3387.7009	133-162	YFTYQGSLTTPPCAEAVIWF VFPTPLDVPK
2641.2007	109-132	LDDSCPLEDSMALQDLFASI DSQK
2272.0087	40-59	GSEHCLDGNYYDGEVHIVHK
1932.8864	85-101	NLEDPNIETPAMNMICK
1816.0115	68-84	EAGLQPNGFAVLALFIR
1484.7240	185-196	ELQDGHDRPVYR
886.4682	167-172	HFWQLR
765.4253	179-184	VLNTYR
762.4356	102-108	QVSSITK
582.2882	60-64	NASYK
575.3187	163-166	ELWK
Carbonic anhydrase 5		
4820.3803	221-264	LTVGQLLGNIVTGEFFTYNG SLTTPDCAEAVTWTVFPDVL DYPR
4325.7847	35-73	ADEQAAGEYNYDEQGDDWTG TCQSGENQSPIDLIFEDSK

3515.7274	01-31	MFSIGFCWLLAICGCTFAYI EIPEAYLTAIR
3296.6480	82-110	FNNYDQPLQTPLVITNNGHT ANMVIPQTR
3035.4982	111-138	GGQRPSINGSLLPGNFEAQS VHFHWGSR
2753.3095	162-186	NTIYETMGEATMHPDGLAVL GVMFR
1436.7492	208-220	IVQYNSNATITGR
1270.6248	152-161	YDVEMHIVHK
1175.5803	191-200	QTSQHYGLNK
1173.6487	278-286	QRPLINNYR
1158.5650	142-151	GSEHAINFQR
920.4432	287-294	SIQDTNSR
887.5097	201-207	IFNQLPR
715.3409	295-299	DVYYR
701.4093	270-274	LWNLR
668.4453	74-79	IVAIPR
Carbonic anhydrase 6		
mass	position	peptide sequence
3423.8382	78-110	GPLTLLNNGHTAHVEIPETA NGNKPFITGGLLK
3240.6496	227-256	GSLTTPLCEQSVTWTVFSQV LPVPYSSVSK
2641.0644	26-48	DESHWDYETNGQNWGGICST GER
1976.0963	.01-25	LLLLLPLAYQHTSNDHK
1925.0273	202-220	TTIPGGLSLGQMLGNVNPR
1861.8768	113-128	FVAEAFHFHWGSPSSR
1282.6361	139-148	FDVEMHIVHR
1155.5501	129-138	GSEHSINQQR
1115.6492	163-173	DGIAVIGVMLK
1113.6262	49-58	QSPISLNVQK
1054.5567	67-75	IVFGNYDVK
1008.5373	279-286	NGRPVFYR
972.4720	01-20	MQPNAFHK
923.4832	290-298	DLSGAYLGK
910.4152	152-159	YGDIDEAK
894.5771	59-66	SLIVPLPR
848.3937	221-226	DFFTYR
776.4413	268-273	LINNFR
773.4338	188-194	VMSALPR
761.4556	181-187	IFPGLSK
700.3009	262-267	DSEGHR
628.3413	274-278	DIQPR
500.2576	177-180	NPNR
Carbonic anhydrase 7 isoform A		
mass	position	peptide sequence

6914.3881	182-244	SYDSMNKPVLVADSLAVDDL VPSVENYFTYAGSLTTPTCA EAVTWIVLTETFPVTLDQVN EFK
5411.6112	80-126	MVNNGHSIQLSGFDHELTLS GGALLQDFVVEQIHMHWWSE HTINDIR
4238.9660	01-37	MHLIALSLIVCCSVSFSWAN EWGYPDLDNNQDEPFPK
2608.4344	151-175	DGIVVIGVLYHVSNTPNEAI GSIIK
2175.2053	279-301	SGSAGLTASVSLGLMTLILA GQK
1615.7607	137-150	NTIYPNMTMAANFK
1267.7004	268-278	AVVLVEQPEQR
1262.7004	127-136	YPLEVHIVHR
1209.5171	68-76	FENYDEHQK
1035.5945	48-56	QSPINLHVK
989.4646	260-267	ELQSENNR
982.4363	245-252	EIEYDEGK
944.4697	253-259	QLHNNYR
922.4087	38-46	WGGLCDSGK
779.3934	61-67	GEFDALK
574.3559	176-181	SLGAVK
Carbonic anhydrase 8 isoform A		
mass	position	peptide sequence
3605.7699	176-207	SGPFFYQPGLSEIFSSLLHL GNFNASYTVQER
3268.6823	227-256	GSLTTPPCSPVVQWHVFGEV LPISHQDLPK
2919.5906	58-82	AIPLNLPPLIFALYDEFFDE LVTIR
2124.1600	287-303	QHIVPLQQEHLQELIWL
2077.8708	110-127	DCYDAEAVHFHWGSPESK
1934.1109	92-109	VPTTIYGVKPYVTGGLLR
1678.7853	40-55	YPNCGGSEQSPIAISR
1505.7205	01-20	MHLPALDDFYQR
1421.8303	13-24	LLFLLPFAANFR
1411.7831	160-172	YSDGVTVLAVLFK
1388.7029	271-281	NFRPLQSQENR
1296.6517	138-147	FDLEMHIVHR
1244.7208	208-219	LTLGSLLGSLDR
1078.5779	151-159	YLNLEEAVK
1018.4952	83-91	NSGHTVEFK
982.5064	128-136	GSEHLLNGR
892.4199	220-226	GNFYTYK
875.3781	25-31	STDFDYK
735.3936	257-261	FWNLR
685.4144	282-286	LIFHR
683.4562	265-270	GRPLLK
559.2874	36-39	WPEK
Carbonic anhydrase 9		

mass	position	peptide sequence
3806.8659	155-190	YATIGEALNHPDGAAVLGFF FNLDEDEGAGLVTINR
3500.7307	01-33	LTAFLEASFLLICWSQAVSS HVFGYSEPNQR
3291.7219	191-221	HLHLIADANQEATLNVTFSL SSLIAGVDVDK
2766.4422	227-252	GSLTTPPCSEAVTWILFPDP IPISPK
2595.3461	57-79	TTAIHMPAVDMIGYHNLLPY PLK
1996.9551	112-128	LPGEFEVEGLHFHWGDK
1750.9010	94-108	VNVTEVGEDFLPYIR
1678.8031	259-273	QLSDTQDGALVDNFR
1524.8202	80-93	MINNGHTVSITIPK
1316.6238	142-151	YTMEMHIVHR
1174.6426	46-56	TQSPIAITTSR
1139.5803	132-141	GSEHVINDIR
884.4948	274-281	TLQPVGNR
875.4257	300-306	HEGEYLK
870.5043	292-299	HTSIATLK
846.3787	38-45	HHGHCAGK
793.3191	307-311	YDWFY
721.3555	222-226	FYTYK
569.3154	287-291	TGHVR
506.3085	283-286	IFAR
503.2936	253-256	QISR
Carbonic anhydrase 13		
mass	position	peptide sequence
5826.1449	01-54	MFDTALGTVLSVMVQLIILV FGQILGQVVQHPLITTGLCL LGAFAYHADQETLK
4760.2434	393-437	AQQEQASEAAIAASEDEGQL IETIDTTTIITSSSNTSICM TTLMR
4100.9163	273-308	SGFYSYGGSLTHPPCYQGTE WFIFPESLAISDFQLR
3656.8127	217-248	TCTSSYDLLMIGYVFELSAH NPFLDPLVQNLR
3592.6691	443-475	QLEQPSQMPMMAPNQGNFCN PGIVIFSGVNESK
3112.5949	129-155	ELLSWNHYDDLPASITLENT GQTLILR
2772.2958	100-124	SSSSSVEEATFFQSPVNIDE SQIQR
2692.3729	156-180	AQFHGNAPTISGADLLASYT FLELR
2298.0760	78-97	NSAPVYGYDMQHGPHTWLPK
2196.9416	181-198	FHWGWCNSEGSEHTINHR
2195.9444	353-370	MHVELCQAQAQEEHEEER
1989.0302	257-272	VQISPFPISYLMYQFR
1892.8741	478-493	CGIHQDTPEELMIHNR
1885.8935	336-352	VVSLNCFCPYDAAQLSR
1563.7583	507-522	ADAFCGVGDGVNIGIR
1414.7172	371-381	IEQEQQLELER
1321.7838	312-324	LLLGPDGISPIAR

1310.6157	66-77	TPLQFGNTSCSR
1295.6385	325-335	NSRPVQHMGNR
1259.6275	200-209	FPLEMQVMHK
950.4182	498-506	NMGVQNGCK
769.4930	249-255	LVQKPGK
726.5236	60-65	VLLLIR
708.3675	55-59	EIYQR
687.3784	210-216	TGSGIPR
620.2960	523-527	MELVE
591.2984	388-392	ESDLK
546.2882	382-385	ELER
Carbonic anhydrase 14		
mass	position	peptide sequence
5527.7160	204-252	WISQPGSSIELPPFHLESLL QPFGSGYFSYEGTYDNGDVV LPTTWLINR
3208.5264	90-116	MPLHWTYYEDLPMATVLENN GNTVIMR
2688.3490	169-191	CAQLNNNFEYLTLSYLFALS HVK
2494.2729	29-50	FIMMLISCTMAVAFILNLYS GR
2095.0640	117-135	IYTANNFMPQLSGAELLGR
1554.8196	72-85	QPSPITIPESNMIK
1509.7666	01-20	MFLPMIDLCWLK
1480.7477	157-168	HNFCLELQALHR
1450.7358	16-28	AFGLVMQLAEESR
1432.7543	51-63	TIFQDVVNAVGNR
1312.6532	261-271	QLSEFEALYGR
1144.6037	136-144	YQFVEAIFK
840.4574	197-203	QVTDHLK
775.4308	254-260	ISVVDSR
769.3879	290-295	NVYFNI
757.3839	150-156	SEHSIGK
684.3787	284-289	QPLGNR
640.3413	192-196	NEHLK
590.3296	145-149	WGSLK
520.2799	65-68	LEMK
Carbonic anhydrase 15		
mass	position	peptide sequence
10113.6510	171-261	WSWASSLGSEHTLDHHHSPL EMQCLHTDGDGCDGCSSSQG VLMISYMFDLSEHNPFLDVL IQHLAAVEQAGQVVEVPPFP LSYLMSPFYDK
6500.9022	77-132	GSPESYNYDWDQGPHTWDTA CNNQSPINIDMNCVEINYFD TPLIWSHYNSIPLGIR
2611.5010	32-55	FILAIGVALLVLFNVYTGFS LANR
2362.0698	01-23	GCLTCGLLNYLWCSLEDISC R
1833.9381	277-292	GAEWLIYPESLAISER

1770.7904	262-276	FYSYNGSLTEPPCHR
1757.5908	56-73	CDEGSNDGCANAGGDNCR
1279.7117	133-143	LENNGHTLILR
1222.6651	311-321	NARPVQPIGDR
1200.6218	150-161	TPSIDGGDLLGR
930.5254	24-31	LQDSNLLK
806.4155	293-298	QLNEFR
795.4182	322-327	MVYLNR
690.3569	144-149	AAFPER
651.3460	166-170	EISFR
584.2827	162-165	FDFR
Carbonic anhydrase 16 isoform B		
mass	position	peptide sequence
4036.8969	215-250	DFFTYEGSLTTPLCDETVTW IVFTETTTVTMSSVSK
2726.3743	189-214	VPIEDSNATVFGQSSLDQLI GGVSHR
2627.3941	01-30	LLLLLPLAFYQSTNGMEWNY LK
1780.8936	80-96	NNGHSISLDIPVTSNGR
1743.7914	109-122	YYADGLHFHWGSYK
1737.8900	58-70	WVLPGITFWHYYR
1299.7704	159-171	DGLAVVAIMVAIK
1236.6483	135-144	FDAEIHIVHR
1165.6324	44-53	HQSPILLDSR
1139.4673	34-43	DWEDLCSSGK
971.5268	268-275	IVQDLNNR
945.4975	01-20	MQAIAFHK
897.4788	125-132	GSEHLINK
875.5097	97-104	KPFITGGR
851.4886	74-79	RPFYIR
817.4600	182-188	LMEAVVR
807.3645	256-261	DHWGHR
792.4362	262-267	LINNYR
771.4471	150-156	NIAQAVR
734.4348	251-255	FWLLR
660.3675	176-181	STPLSR
657.3606	276-280	TVFYK
Carbonic anhydrase 16 isoform C		
mass	position	peptide sequence
4036.8969	217-252	DFFTYEGSLTTPLCDETVTW IVFTETTTVTMSSVSK
2726.3743	191-216	VPIEDSNATVFGQSSLDQLI GGVSHR
2627.3941	01-30	LLLLLPLAFYQSTNGMEWNY LK
1780.8936	80-96	NNGHSISLDIPVTSNGR
1743.7914	109-122	YYADGLHFHWGSYK

1737.8900	58-70	WVLPGITFWHYYR
1426.8450	159-172	DGLAVVAIMVAIVR
1236.6483	135-144	FDAEIHIVHR
1165.6324	44-53	HQSPILLDSR
1139.4673	34-43	DWEDLCSSGK
971.5268	270-277	IVQDLNNR
945.4975	01-20	MQAIAFHK
897.4788	125-132	GSEHLINK
875.5097	97-104	KPFITGGR
851.4886	74-79	RPFYIR
817.4600	184-190	LMEAVVR
807.3645	258-263	DHWGHR
792.4362	264-269	LINNYR
771.4471	150-156	NIAQAVR
734.4348	253-257	FWLLR
660.3675	178-183	STPLSR
657.3606	278-282	TVFYK
Carbonic anhydrase 16 isoform D		
mass	position	peptide sequence
4036.8969	212-247	DFFTYEGSLTTPLCDETVTW IVFTETTTVTMSSVSK
2726.3743	186-211	VPIEDSNATVFGQSSLDQLI GGVSHR
2627.3941	01-30	LLLLLPLAFYQSTNGMEWNY LK
1780.8936	80-96	NNGHSISLDIPVTSNGR
1743.7914	109-122	YYADGLHFHWGSYK
1737.8900	58-70	WVLPGITFWHYYR
1236.6483	135-144	FDAEIHIVHR
1165.6324	44-53	HQSPILLDSR
1139.4673	34-43	DWEDLCSSGK
1016.5808	159-168	DGLAVVAIMK
971.5268	265-272	IVQDLNNR
945.4975	01-20	MQAIAFHK
897.4788	125-132	GSEHLINK
875.5097	97-104	KPFITGGR
851.4886	74-79	RPFYIR
817.4600	179-185	LMEAVVR
807.3645	253-258	DHWGHR
792.4362	259-264	LINNYR
771.4471	150-156	NIAQAVR
734.4348	248-252	FWLLR
660.3675	173-178	STPLSR
657.3606	273-277	TVFYK
Carbonic anhydrase-related protein A isoform B		

mass	position	peptide sequence
6868.0670	01-62	MPSPGHHTSFCCSTAGFIAC SAIVLLCSSEVLSSWEEWWT YDGISGPSFWGLINPQWNMC NK
4377.1900	222-259	SLLPNTDHYITYEGSTTHPG CWESTVWIIVNKPIYITK
2518.2037	142-163	GSEHFIQGYSFPGEIQIYGF NK
2338.2435	176-197	SQGIVGLSLMVQIGETPNPE LR
2060.9712	126-141	YQFEEIYIHYGTENVR
1766.9521	278-293	APLGNNARPVQSLHHR
1739.9842	76-89	LLFDPYLRPLHIDK
1615.8550	92-106	VSGTLHNTGQSLVFR
1486.6743	164-175	ELYHNMSEAQHK
1411.7440	113-125	QHVNISGGPLAYR
1204.5125	306-315	NQYACPSMYK
1157.6313	324-333	WSPDTGLLIR
1097.5837	66-75	QSPIDVVPDK
1077.5245	268-277	LMQGSESTPK
949.5101	260-266	QELYQLR
923.5196	198-205	IITSTFNK
777.4253	210-216	GFSTPIR
747.3130	316-320	DMYYR
737.3828	297-302	TNIDFK
611.3623	217-221	HISVR
550.3347	206-209	VLYR
Carbonic anhydrase-related protein B isoform A		
mass	position	peptide sequence
5593.5606	126-173	FHEIHMHYGLNDQFGSEHSV EGYTFPAEIQIFGYNSQLYA NFSDALNR
4251.0776	220-257	GLLPDTDHYMTYDGSTTAPA CHETVTWVVLNKPIYITK
4238.0822	83-123	ISGLITNTGHSVIFTAGNDT VANYDGMQTPVNISGGPLSY R
4212.0033	18-53	MQVLLAVSWEDWWTYDGISG PAFWGLINPEWSLCNK
2266.2765	174-195	AQGIVGVSILLQLGDLSNAE LR
2209.2464	276-294	APLGNNYRPPQPLLHRPIR
1917.0734	01-17	MELLQALCCTLLLLLAR
1708.9203	67-80	LLFDPNLRPMHIDK
1167.6116	57-66	QSPVNLEPQR
1109.5408	266-275	LMQGSPDHPK
1005.5033	196-203	MLTDQLER
985.4625	206-214	YGGDEAFVK
912.4066	308-315	AACPTMYR
865.5002	258-264	QQLHALR
737.3828	295-300	TNIDFK
701.3504	316-320	EVYYK
592.3089	321-325	ATSWK

Carbonic anhydrase β isoform A		
mass	position	peptide sequence
3770.7689	62-95	NAGNLIPHAQHFQDEYFSCE PAALELGCVVNDIR
3111.4999	206-230	LESHDLHIHALWFDIYTGDI YYFSR
2256.1693	184-203	LSQINTLQQMSNIASYGFLK
1539.7260	49-61	YTDTHVGDMFVVR
1517.7165	132-144	SWLCTHANTSLER
1374.7263	155-166	DPLIFSSETPLR
1305.6321	235-245	FLPVDEDTVDR
1241.6048	168-177	FVAYIDEEQK
1211.5659	96-106	HIIVCGHSDCK
1176.5176	34-43	AVFFTCMDSR
1121.6136	107-115	AMNLLYQLR
779.3570	116-122	DPDFASK
765.3678	145-149	FQEWR
732.3886	246-251	LSEEVR
722.3719	178-183	FALEDK
699.3308	28-33	DNPEPK
634.3229	17-21	EQMVK
617.3439	44-48	MIPTR
585.3718	127-131	LSPLR
551.2824	22-25	EFQK
521.2388	150-154	DAGMK

Vacuolar H^+ ATPase 100kD subunit 1		
mass	position	peptide sequence
8356.2829	616-690	FAATNDKPYSEACAPSILIT FIDMVLFNTPKPPPENCETY MFMGQHFIQVLFVLVAVGCI PVMLLAKPLLIMQAR
6574.1053	692-755	QANVQPIAGATSDAEAGGVS NSGSHGGGGGHEEEEELSEI FIHQSIHTIEYVLGSVSHTA SYLR
4288.1658	413-450	EMNPAPYTIITFPFLFAVMF GDLGHGAIMALFGLWMIR
4171.2849	781-819	QEGPVGGIVLTCVFAFWAIL TVGILVLMEGLSAFLHTLR
3534.6953	07-38	SEEMALCQLFLQSEAAYACV SELGELGLVQFR
3466.9940	585-612	ISLLYEFIPQLVFLLLLFFY MVLLMFIK
3004.5476	558-582	ISIIFGVIHMIFGVVMSWHN HTYFR
2763.5629	756-780	LWALSLAHAQLAEVLWTMVL SIGLK
2735.3863	473-495	YIIFLMGVFSMYTGLIYNDI FSK
2634.1736	161-183	YPQMADNQNEDEQAQLLGEE GVR
2503.1411	832-855	GQGYAFQPFSFDAIIENGAA AAEE
2483.1336	525-547	GDYEGAPYPFGMDPIWQVAG ANK
2412.3029	343-363	CLIAECWVPLLDIETIQLAL R
2123.0073	224-242	QAMIETPLEDPTNGDQVHK

1909.8960	75-92	DGIPMLDTGESPEAPQPR
1890.0119	327-342	AIYHTLNLFNLDVTQK
1802.8972	496-510	SLNIFGSHWHLSYNK
1738.8718	290-304	IEDLNTVLGQTQDHR
1659.8264	135-148	TQVFFDESVPTVYK
1644.8380	398-412	AFQALIDAYGVASYR
1568.7492	460-472	TDNEIWNIFFGGR
1541.8362	243-255	SVFIIFFQGDQLK
1497.6791	380-391	MQTFENPPTYNR
1403.6623	267-279	ATLYPCPEAPADR
1325.6293	93-103	EMIDLEATFEK
1288.6280	39-49	DLNPDVNAFQR
1173.6051	820-828	LHWVEFQSK
1126.6215	369-379	SGSSVPPILNR
1115.5691	110-119	EVNQNAEALK
1106.6092	121-129	NFLELTELK
1044.6564	193-202	LGFVAGVILR
1025.4577	281-289	EMAMGVMTR
1005.5516	548-555	IIFHNAYK
942.5003	184-192	ASQPGQNLK
873.3948	149-157	SSGAYSSSK
832.4927	518-524	FLQLSPK
808.3869	511-517	STVMENK
782.2807	58-63	CDEMER
773.4152	104-109	LENELR
763.4097	51-56	FVNEVR
732.4039	205-210	LPAFER
724.3446	261-266	ICEGFR
710.3654	01-07	MGSLFR
705.4042	218-223	GNVFLR
693.3718	317-321	NWFVK
671.4450	307-313	VLVAAAK
605.3228	211-214	MLWR
587.3511	454-459	GLAAQK
552.3028	67-70	YLEK
538.3460	130-133	HILR
Vacuolar H^+ ATPase 100kD subunit 2		
mass	position	peptide sequence
7619.5856	667-737	AHANHNGQLTGNIELAEGET PLPTGFSGNEENAGGAHGHD DEPMSEIYIHQAIHTIEYVL STISHTASYLR
4723.2925	479-520	WFNNYNTTTVLTNPNLQLPP NSSAVGVYPFGMDPVWQLAD NK
4607.2860	388-428	ECNPALYTCITFPFLFAVMF GDLGHGLILVLFGAWMVLCE R

4138.2457	763-801	MSGVGGAIGLFIIFGAWCLF TLAILVLMEGLSAFLHTLR
3567.8936	557-585	YASIFLEFVPQILFLLLLFG YMVFMMFFK
3554.5946	07-38	SEEMALCQMFIQPEAAYTSV SELGETGCVQFR
3218.5963	336-366	ALSDGSAAVGSTIPSFLNVI DTNEQPPTFNR
2825.4703	531-555	LSIIFGVLHMVFGVCMSVVN FTHFK
2806.5687	738-762	LWALSLAHAQLSEVLWQMVL SLGLK
2802.3737	593-617	TSFQPETPGCAPSVLIMFIN MMLFK
2671.3914	448-470	YIILLMGLFAMYTGLVYNDV FSK
2512.1950	132-153	VLENTQGFFSDQEVLNLDSS NR
2505.4198	639-660	AFVLIALCCIPWMLLGKPLY IK
2104.9327	236-254	VCTGFHASLYPCPSSHNER
2014.0136	318-335	CLIGECWVPTNDLPVVQK
1981.9501	200-217	SDLDEPLNDPATGHPIYK
1865.8619	105-120	TESEMIELAQNEVNMK
1818.8196	811-825	FYEGMGYAFQPFSFK
1785.7934	624-638	GCNEFMFESQPQLQK
1779.9098	302-316	AIYHTLNLFNMDVTK
1673.8282	373-387	GFQNLIDAYGVASYR
1565.8169	75-88	DGIVLPDIQDDIPR
1513.8049	218-230	TVFVAFFQGEQLK
1466.7175	435-447	NGGEIWNIFFGGR
1309.6998	94-104	EIIDLEAHLEK
1289.6596	39-49	DLNVNVNAFQR
1237.6423	121-130	SNYLELTELR
1197.6222	270-279	LVLSQTEDHR
1182.5246	154-165	AGGDNDAAAQHR
1176.5870	802-810	LHWVEFMSK
1174.6289	289-298	NLPSWSIMVK
1045.6152	168-177	LGFVAGVINR
1004.4418	826-834	AILDGEEEE
981.5767	521-528	IIFLNSFK
943.4421	586-592	WFSYNAR
911.4403	471-478	SMNLFGSR
895.4771	67-73	YIETEIK
768.4039	180-185	VFAFER
764.3243	58-63	CDELER
756.3167	01-06	MGDMFR
750.4144	51-56	FVTEVR
717.4505	282-288	VLATVSK
685.3515	618-623	NTEPPK
677.3981	193-198	GNVFLK
663.3130	255-259	EEMVR

617.3504	265-269	LEDLK
605.3228	186-189	MLWR
554.3045	89-93	APNPR
Vacuolar H^+ ATPase 100kD subunit 3		
mass	position	peptide sequence
5695.6209	547-597	YNETTVYDPAFHVTLDSSHP HFYSGHPYPLGMDPVWAVCG QDSITTTNSLK
4858.5940	831-874	GFANTLPLYYGVPVLMATFF AWAILTVAILVMMEGLSAFL HTLR
4657.1968	150-192	YMVSDMGSELLYSESTVIGL VQDATTTSGAYPAHLNYMIG CIR
4490.0121	17-55	SEDMDLCQLLLHTENAFDCL IEVGHHGAVQFNNVYDEDR
4425.3833	448-486	ELNPAPYTIITFPFLFAVMF GDLGHGILLILFSSLMIWK
4192.9880	772-808	SVDNEEEHEMSEIWIHSGIH TIETVLGSVSHTASYLR
3442.6641	655-685	WMSYGGHKPAPYNAACAPSV LITFINMMLMK
3322.8459	627-654	ADLILVVIPQMIFMLCLFGY LVFLIFYK
3063.5053	385-412	TMPNTTPYPIEADFQPLEDM SAGAILLK
2993.6792	703-729	MIEFALVGIAFCTIPILLAG KPIYLMR
2885.4832	74-97	IVDSLHTYIVQLHVNEIFYP DVDR
2724.3890	600-625	MAIVLGISQMMFGLGLAAAN CVLMNR
2637.4256	512-534	YIILLMGVFSVYMGLVYNIV MAK
2576.3693	809-830	LWALSLAHDQLSDVLWHMVL TK
2404.3009	340-360	YLLAEVYIPSSDVPEVEVIL R
2379.0750	215-233	FSEMPSPVYEYHYGYKPER
2182.1138	493-511	YQINATSENEILNILYAGR
2163.9698	255-273	ICAHYHVNIYDCPSSASQR
2142.8437	365-384	ISGGADNIDSSDEDEMNDMK
1986.8208	687-702	EDPVENCLDYMYPNER
1726.8729	237-251	FAILMMASSTMIWPK
1705.7890	433-447	GFQNLIDAYGMADYK
1674.8234	116-129	IHVEASAVTEHYYR
1374.6987	416-426	LVNHMPPTYFR
1360.6103	535-546	GFNLFGSSWSCR
1350.7092	196-205	FYSFELLLYR
1302.5080	759-769	YTDDDNSETSR
1287.6790	279-289	ELSQEIVNVEK
1207.5598	137-146	MMEHSFALNK
1181.5698	894-903	AFNFPTSNQR
1173.6051	875-883	LHWVEFQSK
1124.5768	65-73	VTQCYELLR
1078.6077	206-214	LCSFNLIIR
1046.4941	884-893	FFGGAGESFK
964.5462	56-63	LLNNLYSK
925.5465	331-339	LVGGVEVPR

910.4451	322-328	VYDLMNR
885.5152	300-307	QILEVAGR
848.4294	748-754	QTIAEMR
776.4665	308-313	DLFIIR
748.3658	293-298	EAELMR
712.3512	109-114	YSDSLK
691.3192	734-738	MQQER
556.2878	13-16	SFFR
518.2820	489-492	EIEK
501.3143	314-317	VNLR
Vacuolar H^+ ATPase 100kD subunit 4		
mass	position	peptide sequence
7205.7255	748-811	LWALSLAHAQLSEVLWTMVL AMGLQMNGYVGAIGLFFIFA VWEFFTIAIMVMMEGLSAFL HTLR
5787.7758	697-747	EIIITEVAEAHESGGHSEED DEPMSEIWIHQAIHTIEYIL STISHTASYLR
4635.3238	398-438	EVNPGLYTCITFPFLFAVMF GDMGHGTILFLLGLWMVIDE K
3632.8330	566-594	YAYIILQFVPQVLFLLLMFG YMCFMMFYK
3563.8149	117-147	TETEILELAANNVNLQTSYL ELSEMIQVLER
3518.7004	19-50	SEVMSLVQMYLQPEAAYDTI AALGEVGCVQFR
3160.5290	598-626	YSPTTDVEADTPGCAPSVLI MFIDMVLFK
3016.6088	339-368	ELELVEVALAAGSASVGSTV PSFINVLDTK
3012.7796	644-669	NLEMIFLVVALLCIPWILLG KPLYIK
2863.4747	540-564	LSIIFGVLHMVFGVCMSVEN FVFFK
2775.3383	457-479	YIIMLMGLFAMYTGFHYNDI FSK
2145.9051	246-264	VCTGFHAHMYPCPSSHSER
2071.8992	148-164	TDQFFSDQESHNFDLNK
1926.0654	495-512	TTVLTNPTLQLNPSVATR
1863.8979	627-643	TETALPGCDVNMFPIQK
1862.9105	513-529	GVYPMGIDPIWQSASNK
1800.7758		WWSCGSNQESNSIFR
1790.9435	312-327	GIYHTLNLFNVDLGSK
1780.9188	275-289	LEDLQVIINQTSDHR
1780.9075	674-689	NRPAGPVEEVDEIVEK
1770.8526	821-835	FYVGNGYPFTPFSFK
1740.9067	228-242	SVFVVFFQGDQLQAR
1710.8519	91-105	VLDLMDDFPPAPQPR
1657.8332	383-397	GFQNLIDAYGIAGYR
1413.7597	174-187	SNGHLGFVAGVISR
1366.6902	445-456	GGEIWNIFFAGR
1351.7467	106-116	EIIDLELHLEK
1176.5870	812-820	LHWVEFMSK
1175.5612	210-220	CDVDVALTDPK

1160.6132	299-308	QLPTWSAMVK
1101.5761	328-337	CLIGEGWVPK
1030.5302	836-844	DILIVVEDD
1011.5873	530-537	IIFLNTYK
950.4843	488-494	WVNVYNR
946.5390	290-298	TCVLQAALK
937.4989	79-86	YVTAELNK
893.4839	480-487	SINVFGTR
883.4420	370-376	EPPTHFR
814.3730	190-195	EYAFER
768.4362	221-227	TGNVLHK
764.3243	70-75	CDELER
747.4247	690-696	IEVTTGK
729.4002	56-61	INAQQR
720.4039	63-68	FIGEVR
691.3886	203-208	GNVFVR
634.3229	265-269	QEMVK
605.3228	196-199	MLWR
601.2875	165-169	MGTHR
560.3038	51-55	DLNAK
Vacuolar H^+ ATPase 100kD subunit 5		
mass	position	peptide sequence
5330.5446	668-717	TNGAPPPKPQSGGGEGHGED DEMGEIFIHQAIHTIEYVLS TVSHTASYLR
4359.1749	590-629	WVVYNDTVEGPLSPACAPSI LILFINMILQGSQDTPEPCK
4353.3621	392-430	EVNPALYACITFPFLFAVMF GDLGHGLILLLFASWLIIK
4314.3980	743-781	YDSYIGGILIYVFFGAWALL TVGILVLIEGLSAFLHTLR
3567.8936	561-589	YASIFLEFLPQVLFLLLLFG YMVFMMFFK
3215.8524	638-665	SIQQVFVVVAIICIPWMLLG KPLYIMIK
2878.4782	718-742	LWALSLAHAQLSEVLWNMVF SMGFK
2787.4976	535-559	LSIIVGVIHMIFGVSMSVVN FAYYK
2751.4142	450-472	YIIFLMGIFSIYTGFIYNDV FSK
2727.3004	347-370	ISESSIPAFMNVIETNEMPP TYTR
2601.2467	132-153	YVLENTEGFFSDQEVINLDV NR
2496.2512	10-32	MALCQLFIQPEAAYASIAEL GEK
2358.1758	322-343	CLIGEGWVPTNDISTVQDAL AR
2069.9385	374-391	FTNGFQNLVDSYGMASYR
2047.9113	240-258	VCTGYHAAVYPCPSSHAER
1897.9865	204-221	ADIDGLVADEETGRPVLK
1895.8996	509-524	TYPFGMDPIWQLADNK
1848.9642	306-321	AIYHILNFFNPDVTGK
1827.0122	79-94	LPVLRPEEEPIAPNPR

1814.8101	473-487	SMNIFGSAWHMNYTR
1743.8053	791-805	FYEGAGYAFEPFAFK
1563.7761	155-169	LDPEDPANLPGAAQR
1513.8049	222-234	TVFVAFFQGEQLK
1482.7951	497-508	YITLRPNDTVYK
1482.6641	112-125	EMSANGASLDANFR
1328.6633	439-449	EEIFNIFFGGR
1307.6226	39-49	DLNEEVSAFQR
1286.6838	95-105	EIVDLEAQLEK
1176.5870	782-790	LHWVEFMSK
1125.6011	274-283	LVLSQSADHR
1102.6619	170-180	GQLAFVAGVIK
1060.5157	488-496	DVVEDENLK
1006.4575	806-814	TILDVSEDD
1001.4397	630-637	EFMFDGQK
995.5924	525-532	IIFLNTFK
885.4022	67-73	YVESEMK
832.3988	184-189	FFSFER
791.4232	297-302	WSIMVR
785.3974	126-131	HMQELK
779.4046	51-56	YVNEVR
768.2651	58-63	CDDMER
756.3167	01-06	MGDMFR
747.3631	106-111	TDNELR
719.4199	197-202	GNIFLR
718.4094	286-292	VLNSASK
709.3450	33-38	GCVQFR
675.4035	433-438	QLSSIK
617.3504	269-273	LEDLK
605.3228	190-193	MLWR
602.3256	264-268	DVNVR
522.3147	293-296	HLPR
520.2799	260-263	EMIK
Vacuolar H^+ ATPase 13kD subunit		
mass	position	peptide sequence
2417.2751	93-112	DPFILEILQYVYNISPEVHK
1716.8949	01-16	MASQTQGIQQLLAAEK
1063.4789	38-46	DEATEEIEK
720.3345	81-86	LADMDR
702.3780	73-78	IDADIR
675.3209	113-117	NYNHK
623.3035	57-61	EFEAK

588.3464	87-91	AIQTR
587.2718	62-66	HMGSR
574.3195	67-72	EGVAAK
545.3042	22-26	VAEAR
Vacuolar H^+ ATPase 14kD subunit 1		
mass	position	peptide sequence
2448.2690	11-34	LISVIGDEDTCVGFLLGGVG EINK
2010.1018	80-98	HVIDAHTSPVPAVLEIPSK
1971.0215	63-79	DDIDIILINQNCAELIR
1355.6147	46-57	NTAVSELEDCFK
1177.5670	115-124	GMFNPEDLVR
1086.5400	37-45	HPNFMVVDK
932.4108	99-106	DHPYDASK
870.4866	01-08	MALHSAIK
603.3460	107-111	DSILR
Vacuolar H^+ ATPase 14kD subunit 2		
mass	position	peptide sequence
4124.2939	62-98	RPDIVIILINQVYADMIRPT VDAHNLAVPTVLEIPSK
2705.3337	11-36	LLAVIGDEDTCVGFLLGGIG EVDEDR
1132.5051	01-10	MSSHTEDLGR
1124.5404	37-45	ETNFMVVER
989.4435	99-106	QHPYDSSR
896.4182	51-57	QIEECFK
811.4672	116-122	VITPPER
575.3399	107-111	DSILK
561.2878	46-50	DTTPK
Vacuolar H^+ ATPase 16kD subunit 1		
mass	position	peptide sequence
3784.8236	01-38	MSSEVSSDNPIYGPFFGVMG AASAIIFSALGAAYGTAK
3258.9229	131-159	LFVGMILILIFAEVLGLYGL IVAIYLYTK
3106.8199	57-87	SIIPVVMAGIIAIYGLVVAV LIAGALEEPSK
2870.5674	93-123	GFIHLGAGLAVGFSGLAAGF AIGIVGDAGVR
1891.9802	39-56	SGTGIAAMSVMRPELIMK
757.3951	124-130	GTAQQPR
701.3617	88-92	YSLYR
Vacuolar H^+ ATPase 16kD subunit 2		
mass	position	peptide sequence
6308.3963	57-121	AIIPVVMAGIIAIYGLVVSV LIAGSIGDDYTMEDSYVHLG AGLSVGLPGLTAGVAIGIAG DAGVR
4440.2505	01-45	MVTAALNEEPSYAFFLGCTG AAVAIIFTTLGASYGTAVSG VGIAK
3258.9229	129-157	LFVGMVLILIFAEVLALYGL IVAIYLYTK
1305.6476	46-56	MAVNRPDMIMK

758.3791	122-128	GTAEQPR
Vacuolar H^+ ATPase 16kD subunit 3		
mass	position	peptide sequence
3390.9320	65-97	SIIPVVMAGIIAIYGLVVSV LIAGSLSDSYTIR
3258.9229	137-165	LFVGMILILIFAEVLGLYGL IVAIYLYTK
3117.5389	16-46	DKPAYSFFFGSMGAASAIIF SALGAAYGTAK
2900.5780	99-129	GYIHLAAGLSVGFAGLAAGF AIGIVGDAGVR
1875.9853	47-64	SGTGIAAMAVMRPELIMK
822.3662	08-15	MATDAADK
757.3951	130-136	GTAQQPR
Vacuolar H^+ ATPase 16kD subunit 4		
mass	position	peptide sequence
3726.7925	01-36	MELSLDEPQCASFFCILGAV CAIVFSTLGAAYGTAK
3419.9625	55-88	AIVPVVMAGIIAIYGLVIAV LLAGSLSSPYSAYK
3224.9716	127-155	LFVAIILILIFAEVLGLYGL IVAIYLFSK
2799.5185	89-119	GFLNLSAGLAVGVSGMGAGI AIGVVGEAGVR
1079.5765	37-47	ASVGISSMSIK
866.4916	48-54	HPQLIMK
729.3890	120-126	ASAQQPK
Vacuolar H^+ ATPase 16kD subunit 5		
mass	position	peptide sequence
4871.4496	40-87	YPPYSPFYGVMGVVFSSVLT SAGAAYGTAVSGTGIAATAV MRPELVMK
3599.1340	162-193	LFIGMILILIFAEVLGLYGL IIGIYLYTVNIK
3507.8270	119-154	YSLPTGYVHLAAGLSVGFAG LAAGYAVGEVGEVGVR
3090.8250	88-118	SIIPVVMAGIIAIYGLVVSV LLSGELAPAPK
2933.3947	01-26	MEMDYYLPVYNGSNSVDVPG LIESLK
1229.6736	29-39	ETSISPIVLDR
834.4944	155-161	HIALQPR
Vacuolar H^+ ATPase 26kD subunit		
mass	position	peptide sequence
1950.9589	171-189	DFLSADTCGGVELLALNGR
1660.8540	157-170	AQINQNVELFIDEK
1577.7086	14-26	HMMAFIEQEANEK
1523.8791	200-212	LDLISQQLVPEIR
1515.8603	119-131	LIVQGLFQIMEPK
1342.6233	88-99	EDHVSSVLDDAR
1311.6427	108-118	NQSEYETVLTK
1261.6317	70-80	IQSSNMLNQAR
1231.6681	146-156	NVLPAAVEQYK
1108.5157	34-42	AEEEFNIEK
1077.5245	01-10	MALSDADVQK
975.4492	53-59	IMEYYEK

926.5305	138-145	EVDVPLVR
915.4894	192-199	VPNTLESR
775.3832	27-33	AEEIDAK
771.4471	45-50	LVQQQR
744.4250	63-68	QVELQK
677.3729	213-218	NALFGR
646.3770	102-107	LGEVTK
502.2732	219-222	NVNR
500.3555	132-135	VILR
Vacuolar H^+ ATPase 36kD subunit 1		
mass	position	peptide sequence
2987.4268	99-126	DNVAGVTLPVFESYQDGSDT YELAGLAR
2218.2580	144-163	LLVELASLQTSFVTLDEVIK
1762.9334	74-89	FTSGDINQVVLQNVTK
1691.7758	232-246	QQANILDEGDDDVLF
1664.8741	183-196	TLAYIISELDELER
1260.7422	169-179	VNAIEHVIIPR
1241.6848	221-231	AELLQQGIDVR
1036.5309	64-73	EAAFSLAEAK
894.4423	56-63	TLMGDVMK
829.4930	07-13	LPIFPSR
809.4152	137-143	NYQSAVK
804.4032	37-43	ADALQMR
778.3950	14-20	GAQMLMK
743.3359	197-201	EEFYR
701.3940	127-133	GGQQLAK
624.3827	29-34	GHGLLK
603.3712	51-55	IIETK
587.3511	23-28	LAGAQK
543.3864	46-50	LILGK
503.2936	164-167	ITNR
503.2824	205-208	IQDK
Vacuolar H^+ ATPase 36kD subunit 2		
mass	position	peptide sequence
3305.6510	169-196	VNALEHVVIPILQNTYNYIC GELEEFER
2603.2120	237-258	NINQTRPPAADTPFDQEQFE ER
2227.1141	286-307	GEPPPPTSFITTHGASLSFA GR
1806.8989	115-133	GVGAFPLAGLSCGGMQVSR
1646.8682	72-86	ANLLGADFKPQMVSR
1524.8056	144-156	ALVEFASLEYQVR
1485.6777	224-235	NMTDEELETYIK
1451.5678	52-63	FDQDMHGDEAMR

1364.6661	157-168	MLEAASLQTNMR
1229.5168	363-373	DVVNEDPPEES
1060.5884	106-114	LNTLELETK
1057.6040	05-13	DILPIFPSR
1028.4895	313-322	ASSGDLYSTK
989.5084	324-332	MLLSSGPER
969.5476	87-95	SHVATVSLR
952.5172	214-221	MAFTELIK
881.4549	64-71	NAIFSMAK
863.4217	334-341	SASNVTER
862.4013	349-355	NSQETQR
762.4178	14-20	ANSVIMK
729.3202	197-201	EDFYR
692.3283	38-43	DAIDMK
672.3311	343-348	SDTPPR
667.3079	357-362	SSQMSK
613.2828	136-140	DSYTK
588.3351	209-213	QLEAK
586.3922	29-34	GVGLLK
561.2627	276-279	EQER
529.3456	23-27	VLAAR
515.3551	101-105	IVGVK
Vacuolar H^+ ATPase 36kD subunit 3		
mass	position	peptide sequence
2996.4887	99-126	DNVAGVTLPIFEPYTDGVDT YELAGLAR
2805.3134	225-249	LLGQMAEAQEVQNILDEDGD EDLLF
2203.2584	144-163	LLVQLASLQTSFVTLDDVIK
1790.9647	74-89	FTTGDINQIVLQNVTK
1722.8796	183-196	TIEYIISELDELER
1260.7422	169-179	VNAIEHVIIPR
1064.5622	64-73	EAAFSLAEVK
907.4740	56-63	TLMGQVMK
837.4213	137-143	NYQSAVR
829.4930	07-13	LPIFPSR
804.4032	37-43	ADALQMR
748.4022	14-20	GAQTLMK
743.3359	197-201	EEFYR
701.3940	127-133	GGQQLAK
624.3827	29-34	GHGLLK
603.3712	51-55	IIETK
560.3402	23-28	LAGATK
543.3864	46-50	LILGK

503.2824	205-208	IQDK
503.2572	221-224	AEQR
Vacuolar H^+ ATPase 44kD subunit		
mass	position	peptide sequence
9207.1044	153-245	SAATCSPATPPAPASAPPHL PPACACDVLAPGSLTGGSLT NLSTSHEPEPEFDVCPCDEC FACAPPSTSATASTLLADEC YSQTASSMLSATR
6214.7928	246-315	CALSTVAAIATGSGLGNGPS TSAAAAAAASNSSGGGGGGG PASCSTLCSSAYFSTSAPTT SSSVHSSMSR
4644.2071	423-462	SSAQQQHETAQLQHQQTTQQ HATPLTPQNHNQYQNQHLSK
4638.2099	782-825	DVLNQLYGHLDGASAGGAVS SADNVDIPGLGFGQSEYFPY VFYK
4170.0625	337-373	SGSHVSQLHLATQQPQHHHS HPHQQPHTNPLQSPVQK
3473.6621	124-150	HQHTHHQNKPQHYHHHHHHH QLPQDLK
2854.3781	528-553	SSPDTDPAEPPEFPLSPAEL PQYLTR
2491.1676	397-417	SPHSVQSDLSDAFDWWFNKP K
2464.9164	374-396	SMSEDEGDASNAHEDGETDE DPK
2334.1322	661-680	SSQLIQEDADYCLFNVTLFK
2294.9951	88-108	LHENLMANNSPGPPDDSMPC R
2230.2369	622-640	EHFILDSEYLTTLLVIVPK
2111.0628	494-512	STPSQLNINNGFNLTPTHR
1816.0003	759-774	YGLPVNFQAILIEPNK
1747.7626	15-29	TCQQTYDTMNNLTSK
1629.8693	46-61	VGTLDQLVGLSDDLGK
1627.7494	01-14	MMSEYWIISAPGDK
1577.8144	734-747	VNFSEAFCALIHVK
1533.7267	463-475	AMTFWHQASTTPR
1519.7427	480-492	SFFNSLADQIYSK
1505.7594	73-85	VANYLGEVLEDQR
1484.6903	699-711	DFVYNEEELAAGK
1483.6886	641-652	VMANDWLTNYEK
1428.5842	513-527	SSPVSSCCGSSSQGR
1348.6274	321-332	LNNNTCSINNNK
1237.6423	62-71	LDTYVEQITR
1146.5823	826-835	VNIDMVEQAK
1133.5156	30-38	QHNLCNNYK
1086.5789	577-586	QIGQIDGDLK
948.5513	751-758	VFVESVLR
944.5233	653-660	ITDMIVPR
937.4738	589-596	SQAYNNLK
925.4236	554-560	FQWDMAK
915.4894	597-604	GNLQNLEK
873.5040	569-576	NIADIISK
869.4879	39-45	FHIPDLK

816.4726	724-730	QFGPLVR
772.4563	614-620	NLADLVK
747.4359	607-613	TGSLLTR
722.3719	682-687	VAEEFK
625.3780	115-119	HLSLR
622.2865	712-716	NEMTK
607.3120	717-721	LMTDK
577.2953	109-112	HHQR
534.3398	695-698	FIVR
522.3034	333-336	LSFR
520.3129	561-564	YPIK
512.2463	476-479	SSYR
503.2936	565-568	QSLR
Vacuolar H^+ ATPase 55kD subunit		
mass	position	peptide sequence
4111.0692	325-361	NGSITQIPILTMPNDDITHP IPDLTGYITEGQIYVDR
2998.3557	226-251	QDFEENGSMENVCLFLNLAN DPTIER
2724.2756	198-222	SVLDDHTDNFAIVFAAMGVN METAR
2463.2666	121-142	GPPILAEDFLDIQGQPINPW SR
2451.2258	143-164	IYPEEMIQTGISAIDVMNSI AR
2336.2271	417-437	AVVGEEALTPDDLLYLEFLT K
2121.1273	168-187	IPIFSAAGLPHNEIAAQICR
1918.0102	272-288	HVLVILTDMSSYAEALR
1896.8836	302-317	GFPGYMYTDLATIYER
1883.8592	394-410	DHSDVSNQLYACYAIGK
1676.9006	452-465	TVFESLDIGWQLLR
1670.8458	257-271	LALTAAEFLAYQCEK
1639.9265	28-43	TVSGVNGPLVILDEVK
1582.8951	367-380	QIYPPVNVLPSLSR
1520.7954	73-87	AVVQVFEGTSGIDAK
1381.6780	88-99	NTLCEFTGDILR
1376.7572	475-486	IPASILAEFYPR
1341.6182	441-451	NFISQGNYENR
1161.6262	110-120	VFNGSGKPIDK
1104.5354	100-109	TPVSEDMLGR
1090.5738	62-72	SGQVLEVSGSK
975.5622	47-54	FAEIVQLR
946.4523	01-08	MNAQQAQR
921.4458	384-392	SAIGEGMTR
910.5105	09-16	EHVLAVSR
862.4417	17-23	DFISQPR
731.4046	55-61	LADGTVR

691.3443	411-416	DVQAMK
686.3467	295-300	EEVPGR
667.3634	362-366	QLHNR
632.3362	289-294	EVSAAR
615.3824	188-193	QAGLVK
599.3875	252-256	IITPR
524.3079	24-27	LTYK
520.2799	470-473	EMLK
504.3180	466-469	IFPK
Vacuolar H^+ ATPase 68kD subunit 1		
mass	position	peptide sequence
3688.8744	398-434	EGSVSIVGAVSPPGGDFSDP VTSATLGIVQVFWGLDK
2814.3719	175-199	YIAPAGNYNLEDIVLETEFD GEITK
2738.5021	80-105	TGKPLSVELGPGIMGSIFDG IQRPLR
2473.2101	19-42	VYAVSGPVVSAEAMSGSAMY ELVR
2370.1129	55-76	LEGDMATIQVYEETSGVTVG DR
2338.1569	230-253	VLDSLFPCVQGGTTAIPGAF GCGK
2195.1454	140-160	VGSHITGGDLYGVVHENTLV K
2071.0804	478-495	EILQEEEDLSEIVQLVGK
2026.9347	287-304	DFPELTCEIDGVTESIMK
1874.8555	596-610	ADYDQLYEDLQQAFR
1781.8526	362-378	LAEMPADSGYPAYLGAR
1749.8694	321-335	EASIYTGITLSEYFR
1747.7558	514-527	DDFLQQNSYSPYDR
1674.7792	263-277	YSNSDVIIYVGCGER
1648.6764	336-350	DMGYNVAMMADSTSR
1591.8267	441-453	HFPSINWLISYSK
1561.7059	569-582	ESMGGIMYQLSSMK
1521.7154	128-139	SEMWEFNPLNVR
1515.7948	306-320	TALVANTSNMPVAAR
1450.7610	106-118	DIGVMTNSIYIPK
1410.7627	43-54	VGYYELVGEIIR
1350.7277	218-229	LPANHPLFTGQR
1332.5848	550-561	HCLESTAQSDNK
1266.6775	200-209	HTMLQVWPVR
1215.5826	540-549	NIMAFYETAR
1134.5942	465-473	NYPEFVPLR
1034.4935	278-286	GNEMSEVLR
1016.4571	457-464	ALDEYYDK
946.5567	254-262	TVISQALSK
937.5214	210-217	HARPVTEK
918.5003	119-127	GVNTTALSR

899.4621	379-385	LATFYER
875.4985	562-568	ITWNTIK
834.4203	496-503	ASLAETDK
788.3719	391-397	CLGNPER
759.4610	504-510	VTLEVAK
756.3749	528-533	VCPFYK
745.3991	351-356	WAEALR
740.3209	13-18	ESEYGR
686.4018	163-168	MIVAPR
676.3810	534-539	TVGMLR
620.3184	01-05	MSNLR
576.2624	589-593	DGEQK
561.2991	357-361	EISGR
548.2311	09-12	DEER
Vacuolar H^+ ATPase 68kD subunit 2		
mass	position	peptide sequence
3688.8744	398-434	EGSVSIVGAVSPPGGDFSDP VTSATLGIVQVFWGLDK
2710.4960	80-105	TGKPLSVELGPGIMGSIFDG IQRPLK
2679.3181	55-79	LEGDMATIQVYEETSGVTVG DPVLR
2471.2308	19-42	VFAVSGPVVTAEAMSGSAMY ELVR
2338.1569	230-253	VLDSLFPCVQGGTTAIPGAF GCGK
2209.1611	140-160	VGSHITGGDLYGLVHENTLV K
2071.0804	478-495	EILQEEEDLSEIVQLVGK
2008.9783	287-304	DFPELSVEIDGVTESIMK
1846.8718	596-610	ADFEQLHEDLQQAFR
1808.8800	184-199	VDDVVLETEFDGEITK
1781.8526	362-378	LAEMPADSGYPAYLGAR
1749.8694	321-335	EASIYTGITLSEYFR
1737.7351	514-527	DDFLQQNSYSSYDR
1674.7792	263-277	YSNSDVIIYVGCGER
1664.6713	336-350	DMGYNVSMMADSTSR
1602.7324	569-582	EAMGNIMYQLSSMK
1591.8267	441-453	HFPSINWLISYSK
1534.7999	106-118	DINELTESIYIPK
1515.7948	306-320	TALVANTSNMPVAAR
1410.7627	43-54	VGYYELVGEIIR
1403.7317	128-139	VASWEFNPLNVK
1316.7433	218-229	LPANHPLLTGQR
1316.6077	550-561	HSVESTAQSENK
1266.6775	200-209	HTMLQVWPVR
1257.5932	540-549	NIIDFYDMAR
1118.5993	465-473	NFPEFVPLR

1034.4935	278-286	GNEMSEVLR
1012.5098	175-183	YIAPSGNYK
986.4465	457-464	ALDDFYDK
954.5367	210-217	QPRPVTEK
946.5567	254-262	TVISQALSK
928.5210	119-127	GVNVPSLSR
901.5254	562-568	ITWNVIR
885.4465	379-385	LASFYER
834.4203	496-503	ASLAETDK
810.3264	07-12	FDDEER
804.3749	528-533	FCPFYK
788.3719	391-397	CLGNPER
773.4767	504-510	ITLEVAK
745.3991	351-356	WAEALR
729.4076	163-168	MIVNPR
676.3810	534-539	TVGMLR
592.3123	01-05	MSNLK
561.2991	357-361	EISGR
519.2409	589-593	DGEAK
Vacuolar H^+ ATPase 68kD subunit 3		
mass	position	peptide sequence
5392.7078	179-229	LEGDMATIQVYEDTSGVSVG DPVYQTGKPLSVELGPGIMG SIFDGIQRPLR
3718.8849	523-559	EGSVSIVGAVSPPGGDFSDP VTSATLSIVQVFWGLDK
2881.3600	300-324	WLAPPGNYCVDEVIVETEFN DEITK
2678.2337	264-287	IDALITGGDIYGSVFENSMM HDHR
2510.2417	143-166	IFGVSGPVVNAEEMAGAAMY ELVR
2479.0547	639-658	DDFLQQNSYSQYDAYCPFFK
2475.1279	665-686	NMMTFYDAAILSVQNTADNE AR
2356.1464	355-378	VLDAFFPCVQGGTTAIPGAF GCGK
2207.0462	74-93	KPVAEPESPHDTVNDEDSLK
2114.9665	582-598	TLDTYYEESNPEFTHLR
2095.9679	May-23	SWVAPLTSFTNSNASNEDR
2066.9773	412-429	DFPQLEVEVNGTMESIMK
1898.0116	604-620	VLQEEDDLAEIVQLVGK
1816.8711	113-128	NEDSGFVIEQVVDTHK
1765.8577	487-503	LAEMPADAGYPAYLGAR
1749.8694	446-460	EASIYTGITLSEYFR
1687.6873	461-475	DMGYHVSMMADSTSR
1674.7792	388-402	YSNSDVIIYVGCGER
1632.6330	129-142	YSSDEEEEEATMGR
1592.7856	566-578	HFPSVNWLQSYSK

1515.7948	431-445	TALVANTSNMPVAAR
1450.7788	230-242	SISELTNSIYVPK
1353.7082	696-707	AANILYELSTMK
1307.7430	167-178	VGHSQLVGEIIR
1291.6562	713-724	LGEATVLESMNK
1282.7113	343-354	LPSNSPLLTGQR
1273.5767	26-37	NSGSLNQDGEPR
1266.6775	325-334	HTMLQVWPVR
1215.6480	725-734	LHDNILSTFR
1175.6167	63-73	SNPVPPPPQSR
1139.5731	252-261	NIAYEFTPGK
1125.4582	735-743	EIEDNVEDY
1085.3995	49-58	CTCPTCACQR
1034.4935	403-411	GNEMSEVLR
1032.5836	38-47	SVPHPTVPAK
955.5207	243-251	GIDTPSLPR
946.5567	379-387	TVISQALSK
921.4160	621-628	SSLNEEDK
885.4465	504-510	LASFYER
868.4887	105-112	SAHIALEK
846.4138	336-342	CRPVEDK
844.5039	687-693	VTWGLIR
802.3690	98-104	STDQSHK
773.4767	629-635	ITLEVAK
747.3454	516-522	CLGSPDR
745.3991	476-481	WAEALR
708.4766	288-293	LILPPR
662.3905	659-664	TIGMLK
619.3450	708-712	FIDPK
561.2991	482-486	EISGR
513.2416	59-62	NDHK
Vacuolar H^+ ATPase AC39 subunit 1		
mass	position	peptide sequence
6030.8947	128-181	CHPLGSFEQMEAIHVASTPA ELYNAVLVDTPLAPFFVDCI SEQDLDEMNIEIIR
4809.5687	86-127	NHAVEPLSNFLDFITYGYMI DNIILLITGTLHQRPISELI PK
2902.4468	46-72	LHLQGTDYGSFLANEPSPLS VSVIDDK
2469.2641	300-319	LDVYAFLQQFHFGVFYAYLK
2452.0939	265-287	TVAEYYAEYAALFDGSGNNP GDK
2267.9882	01-20	MNSSGFMFNIDNGYLEGLCR
2113.9351	198-217	NMGGATADVMCEILAFEADR
1994.9739	29-45	QADYLNLVQCETLEDLK

1606.9050	219-233	AIIITINSFGTELSK
1373.7245	327-338	NIVWIAECVAQK
1368.6293	187-197	AYLEAFYNFCK
1177.6034	246-256	MYPDGLAALAR
1172.6244	77-85	LVIEFQHMR
994.5244	343-350	IDNYIPIF
967.4367	257-264	ADDYEQVK
935.4621	293-299	FFEHEVK
794.3865	239-245	LYPNCGK
664.2719	322-326	EQECR
638.3508	182-186	NTLYK
605.3141	288-292	TLEDK
533.3116	24-28	CGILK
Vacuolar H^+ ATPase AC39 subunit 2		
mass	position	peptide sequence
4743.2440	26-68	HSDYLNLTQCESLEDVMISI QGTDYGLIFGGEQSAPSVEV IER
3742.8454	124-158	MCHPLGEFDQLGAIEVASNS AELFDAVLIDTPIAR
2885.3233	189-214	FYAYCSQLGGNTANVMTNLL SFEADR
2380.2124	299-317	NVQTFLQQYHFGIFYSFIK
2157.1273	98-116	YPFMIDNVALLVAGLNNHR
2038.9612	Jan-17	MSMIFNTEYGYLEALTR
1795.8683	83-97	SHSTEPLTTFMEFIR
1625.9472	216-231	TITIAVNAIGSDIIPK
1479.7359	246-259	IALASMSTLNDTDK
1431.7413	325-336	NIVWISECIAQR
1259.6783	74-82	LLQQYYYIR
1251.5521	280-290	DSDGMITLEDR
1216.5303	262-272	DVCNVFDGYGK
1156.5529	236-245	MFPTCGYLPK
1112.6350	341-350	INAFIPIPLD
1006.5567	171-178	YLDVEIVR
960.4819	163-170	DLPMESLR
924.4244	273-279	MFDNLER
869.4259	291-297	FLMMEAK
659.3623	179-183	AHLYR
644.3726	320-324	QLEVR
623.3399	184-188	AYLEK
562.3017	21-25	NGMLK
519.2521	337-340	QTDR
518.3085	159-162	FVPR
Vacuolar H^+ ATPase AC45 accessory subunit		
mass	position	peptide sequence

5399.5893	316-363	EDFPFGDSWDCVGFVTPGIL MGLFVVALLLVIMFVGVCWM MDINTMDR
4274.0750	231-268	LSVVMDTSVADKPITFDVVY NGGYFSLSNLVYDNNNFR
3588.6621	269-302	SSGVNAPTTFSYSCGNLTLE SAAVNNMYNTLSFK
3391.6725	37-67	TVSQVEFAEQLAALLEDHMV VAFEENGLSSK
3253.8016	05-36	SLIALCVIGAAVAEQTPVFL WGANSVAKPSLK
2861.4719	198-222	STNQFQIFYTALLYNGNPIT VTDLK
2374.0802	68-89	DFLCSNSQAQSCYAQLQGVS PK
1886.8952	126-143	CAVGTALFVTFEDAAESR
1819.0112	165-181	VAYLYLAAPSTAPVVQR
1629.7755	90-103	TYYTSVENPSEALR
1612.8176	144-159	EASLESHDAAIAAISK
1467.7478	303-315	SLQLQAPFDGTYK
1251.6038	186-197	DTAATTGGIMWK
1057.4908	110-119	EHNSIDASGK
903.4782	371-379	TITINAAAE
837.4312	223-230	LTNSSSTK
654.2916	160-164	QFECK
630.3821	120-125	LTTPAK
621.2878	364-368	FDDPK
577.3166	01-04	MLWK
Vacuolar H^+ ATPase M9.7 subunit a		
mass	position	peptide sequence
3336.5465	37-65	CILMLTAACCWLFWLCCYMA QMNPLIGPK
2970.5482	01-28	MGAAFFPVLFFTALWGGVGI AMPIMTPK
957.4788	77-85	SWNNPIVAG
934.5217	29-36	GPHQNLIR
860.4658	69-76	DVVAMIGR
Vacuolar H^+ ATPase M9.7 subunit b		
mass	position	peptide sequence
3721.7604	32-64	GVTQCCLMLTAATCWLFWLC CYMTQLNPLIGPK
3066.6347	01-27	MVSEWVAPIVITSIWAFIGI ICPFFAR
1308.6472	65-75	LSMNEIMIMAR
875.4257	76-82	EWGNEIK
736.3545	83-89	DTMAVTV
Vacuolar H^+ ATPase M9.7 subunit c		
mass	position	peptide sequence
3340.7521	36-64	CIFLLTAVVCWLFWLCCYLA QLNPLLGPK
2233.2129	01-19	MEVFLTIVFFTIFWAAVAK
1185.6626	72-82	IIASSWGNPIK
979.4955	28-35	QPHDDLVR
938.5345	20-27	YGPILFTK
787.4421	65-71	LNGNTIR

Vacuolar H⁺ ATPase M9.7 subunit d		
mass	position	peptide sequence
3245.5874	36-64	CCVILTAVCCYLAWMVTFVM QLNPLTGPR
2842.5880	04-27	HVAFMVITVFWLLFAIIGFL VSYR
1362.7602	69-79	IILGMITYWPR
841.4414	80-86	SIIHDEK
596.2674	28-31	YEER
Vacuolar H⁺ ATPase PPA1 subunit 1		
mass	position	peptide sequence
9065.7587	92-180	NLISVIFCEAVAIYGLITAI VLSGQLEQFSMETALSQAAI QNTNWFSGYLIFGAGLAVGL VNLFCGIAVGIVGSGAALSD AANAALFVK
4719.4676	37-84	VSVGWFLASSNPYMWACLGI GLSVSLSVVGAALGIHTTGT SIVGGGVK
3062.7038	07-33	TVVSQTFLWLFLAVATILTL YFVMTGK
2654.5241	181-205	ILIVEIFGSAIGLFGLIVGI YMTSK
689.3763	01-06	MAAQIR
Vacuolar H⁺ ATPase PPA1 subunit 2		
mass	position	peptide sequence
5395.6906	127-182	LITDSTVMATNMFTGFATFG AGLCVGMVNVACGIAVGIVG SGAALADAANSALFVK
4901.4147	39-86	MGLGWFLYTSNPFLWSGMGI FLACALSVLGAASGIYMIGC SVAGGGVR
3609.8492	05-38	MSFGLFFMLFVLGAASLGAV GIIFANVMVNMGER
2948.6529	94-121	NLISVIFCEAVAIYGLITAI LLSGNVNK
2668.5397	183-207	ILIVEIFGSAIGLFGLIVAI YMTSK
595.3198	122-126	FSSVR
547.2722	208-212	AETIN
Vacuolar H⁺ ATPase SFD subunit isoform A		
mass	position	peptide sequence
3206.6071	01-29	MTTALYLPEENIDMIAATSV LQQQAADIR
2968.6157	214-238	VNFQVQYQLIFCLWVLTFNP LLAAK
2324.0209	32-50	TINWASYMQSQMISEEDYK
2262.1863	84-102	DSTIQYILVLLDDLLQEDR
2201.0356	321-339	LQNSVQDLSSFDEYATEVR
1888.8334	305-320	FDDEDITADVEYLSEK
1883.9571	382-398	DAIILSVACFDIGEYVR
1821.8726	167-182	DQLASNNNEYIQSVAR
1772.8860	414-428	QIVMQHLGHEDPNVR
1704.9240	242-257	FSVIPILADILSDCAK
1573.8307	117-129	QCIWGPFLNLLNR
1494.8314	195-208	FAFVGVDGISTLIR
1429.7533	270-282	NLIEKPEDSSVAK
1389.6983	438-448	LMVHNWEYLGK
1387.7256	156-166	SDLNFYLQFLK
1378.7325	60-72	ASFLAQNSSQVVK

1306.5707	145-155	FACWGHETMPK
1253.5943	130-140	QDGFIVNMSSR
1224.7310	73-83	TLLNLVSHLSK
1152.6986	372-381	ILVHLLETSK
1147.5057	283-292	DHCIAMVQCK
1102.5527	105-114	VDLFHDTAGK
1034.5880	429-437	YEALLAVQK
995.5309	343-350	LEWSPVHK
986.5629	296-303	QLSILEQR
980.5523	405-413	HVLEQLGGK
894.4358	183-189	CLQMMLR
831.5450	263-269	IILAVFR
812.4624	459-467	QGAAPIAGK
807.4359	366-371	NYELLR
761.3424	453-458	ENENQK
717.4141	51-57	AISALDK
681.3202	190-194	VDEYR
617.3001	357-361	ENAQR
589.3668	209-213	ILSTR
572.2939	399-402	HYPR
517.2980	449-452	QLEK
508.2667	354-356	FWR
503.2824	362-365	LNEK
Vacuolar H^+ ATPase SFD subunit isoform B		
mass	position	peptide sequence
3206.6071	01-29	MTTALYLPEENIDMIAATSV LQQQAADIR
2968.6157	288-312	VNFQVQYQLIFCLWVLTFNP LLAAK
2723.3033	200-222	DHHGHQYSPTLAQLQQQHEL AER
2324.0209	32-50	TINWASYMQSQMISEEDYK
2262.1863	84-102	DSTIQYILVLLDDLLQEDR
2201.0356	395-413	LQNSVQDLSSFDEYATEVR
2064.0430	167-185	DQLASNGLAYLQEMAQLAK
1888.8334	379-394	FDDEDITADVEYLSEK
1883.9571	456-472	DAIILSVACFDIGEYVR
1772.8860	488-502	QIVMQHLGHEDPNVR
1704.9240	316-331	FSVIPILADILSDCAK
1605.8053	243-256	CVIPNNEYIQSVAR
1573.8307	117-129	QCIWGPFLNLLNR
1494.8314	269-282	FAFVGVDGISTLIR
1483.6771	229-242	EVGVGSDHQQQDGK
1429.7533	344-356	NLIEKPEDSSVAK
1389.6983	512-522	LMVHNWEYLGK

1387.7256	156-166	SDLNFYLQFLK
1378.7325	60-72	ASFLAQNSSQVVK
1306.5707	145-155	FACWGHETMPK
1253.5943	130-140	QDGFIVNMSSR
1234.6902	187-197	TQTILVHTHGK
1224.7310	73-83	TLLNLVSHLSK
1152.6986	446-455	ILVHLLETSK
1147.5057	357-366	DHCIAMVQCK
1102.5527	105-114	VDLFHDTAGK
1034.5880	503-511	YEALLAVQK
995.5309	417-424	LEWSPVHK
986.5629	370-377	QLSILEQR
980.5523	479-487	HVLEQLGGK
894.4358	257-263	CLQMMLR
831.5450	337-343	IILAVFR
812.4624	533-541	QGAAPIAGK
807.4359	440-445	NYELLR
761.3424	527-532	ENENQK
739.3369	223-228	ANESYR
717.4141	51-57	AISALDK
681.3202	264-268	VDEYR
617.3001	431-435	ENAQR
589.3668	283-287	ILSTR
572.2939	473-476	HYPR
517.2980	523-526	QLEK
508.2667	428-430	FWR
503.2824	436-439	LNEK
Vacuolar H^+ ATPase SFD subunit isoform D		
mass	position	peptide sequence
3206.6071	01-29	MTTALYLPEENIDMIAATSV LQQQAADIR
2968.6157	214-238	VNFQVQYQLIFCLWVLTFNP LLAAK
2324.0209	32-50	TINWASYMQSQMISEEDYK
2262.1863	84-102	DSTIQYILVLLDDLLQEDR
2201.0356	321-339	LQNSVQDLSSFDEYATEVR
1888.8334	305-320	FDDEDITADVEYLSEK
1883.9571	382-398	DAIILSVACFDIGEYVR
1821.8726	167-182	DQLASNNNEYIQSVAR
1772.8860	414-428	QIVMQHLGHEDPNVR
1704.9240	242-257	FSVIPILADILSDCAK
1573.8307	117-129	QCIWGPFLNLLNR
1494.8314	195-208	FAFVGVDGISTLIR
1429.7533	270-282	NLIEKPEDSSVAK

1387.7256	156-166	SDLNFYLQFLK
1378.7325	60-72	ASFLAQNSSQVVK
1306.5707	145-155	FACWGHETMPK
1253.5943	130-140	QDGFIVNMSSR
1224.7310	73-83	TLLNLVSHLSK
1152.6986	372-381	ILVHLLETSK
1147.5057	283-292	DHCIAMVQCK
1102.5527	105-114	VDLFHDTAGK
1034.5880	429-437	YEALLAVQK
995.5309	343-350	LEWSPVHK
986.5629	296-303	QLSILEQR
980.5523	405-413	HVLEQLGGK
894.4358	183-189	CLQMMLR
831.5450	263-269	IILAVFR
807.4359	366-371	NYELLR
717.4141	51-57	AISALDK
681.3202	190-194	VDEYR
617.3001	357-361	ENAQR
589.3668	209-213	ILSTR
572.2939	399-402	HYPR
508.2667	354-356	FWR
503.2824	362-365	LNEK

Appendix 2

Summary of haemolymph proteomics (performed by Alex Montoya)

Sample processing:

Samples were processed using an in-solution digestion procedure. 8 M urea solution (in 20 mM HEPES buffer at pH 8.0) was added to each sample for a final approximate urea concentration of 7 M. Samples were then sequentially reduced and alkylated to final concentrations of 10 mM dithiothreitol (DTT) and 50 mM 2-chloroacetamide (2-CAM) respectively, for 30 min in the dark and at room temperature. 20 mM HEPES buffer was then added to each sample, reducing urea concentration to approximately 1.5 M. 1 µg of Trypsin/LysC protease mix (Pierce, PN:1863467) was added to each sample followed by incubation at 37ºC for 18 h.

Post digestion, samples were acidified to 0.2% trifluoroacetic acid and desalted using reversed-phase spin tips (Glygen Corp, PN: TT2C18) according to the manufacturer's recommendations. Briefly, spin-tips were solvated and equilibrated with successive washes of 60% acetonitrile (ACN) + 0.1% formic acid (FA) and 1% ACN + 0.1% FA. Samples were then loaded onto the spin-tips and washed with 1% ACN + 0.1% FA and then eluted with 60% ACN + 0.1% FA. Eluents were subsequently dried to completion using vacuum centrifugation.

Samples were reconstituted with 0.1% TFA and allowed to mix for 30 min, followed by water bath pulsed sonication for 5 min. Samples were centrifuged at 12,000 g for 5 min and clarified supernatants used for concentration estimation with a quantitative peptide assay kit (Pierce, PN: 23275). Sample volumes were then taken and diluted to a final peptide concentration of 250 ng/µL for analysis by liquid chromatography mass spectrometry (LC-MS).

LC-MS analysis:

Samples analysed by LC-MS/MS analysis an Ultimate 3000 RSLC nano liquid chromatography system (Thermo Scientific) coupled to a Q-Exactive HFX mass spectrometer (Thermo Scientific) via an EASY spray source (Thermo Scientific). Samples were loaded onto a trap column (Acclaim PepMap 100 C18, 100 µm × 2 cm) for desalting and concentration at a flow rate of 8 µL/min (loading pump buffer: 2% acetonitrile, 0.1% TFA). Peptides were then eluted on-line to an analytical column

(Acclaim Pepmap RSLC C18, 75µm×50 cm) at a flow rate of 250nl/min. Peptides were separated using a 90 min gradient, 1-30% of buffer B for 75 min followed by 30-40% buffer B for another 15 min (buffer A: 5% dimethylsulfoxide (DMSO), 0.1% FA; buffer B: 75% acetonitrile (ACN), 20% water, 5% DMSO, 0.1% FA) and subsequent column conditioning and equilibration. Eluted peptides were analysed by the mass spectrometer operating in positive polarity using a data-dependent acquisition (DDA) mode. Ions for fragmentation were determined from an initial MS1 survey scan at 120,000 resolution, followed by HCD (Higher Energy Collision Induced Dissociation) fragmentation of the top 20 most abundant ions at 15,000 MS2 resolution. MS1 and MS2 scan AGC targets were set to 3e6 and 5e4, allowing maximum ion injection times of 25 ms and 100 ms, respectively. A survey scan m/z range of 350-1750 was used, normalised collision energy set to 27%, charge state exclusion enabled with unassigned and +1 charge states rejected and a minimal AGC target of 8e3. Dynamic exclusion was set to 45 s.

Data analysis (database searching and protein quantification):

Data was processed using the MaxQuant (Tyanova et al., 2016) software platform (v1.6.10.43), with database searches carried out by the in-built Andromeda search engine against the relevant Uniprot reference protein database – *Drosophila melanogaster* (Downloaded – 2nd February 2021, entries: 22,039). A reverse decoy database approach was used at a 1% FDR for peptide spectrum matches and protein identifications. Search parameters included: maximum missed cleavages set to 2, variable modifications of methionine oxidation, protein N-terminal acetylation, asparagine deamidation and cyclisation of glutamine to pyro-glutamate. Label-free quantification was enabled with an LFQ minimum ratio count of 1. 'Match between runs' function was enabled, with alignment and matching time windows of 20 and 0.7 min respectively.

Appendix 3

Publications arising from this thesis:

- van Dam, E.*, van Leeuwen, L. A. G.*, **dos Santos, E.***, James, J.*, Best, L.*, Lennicke, C., Vincent, A. J., Marinos, G., Foley, A., Buricova, M., Mokochinski, J. B., Kramer, H. B., Lieb, W., Laudes, M., Franke, A., Kaleta, C., & Cochemé, H. M. (2020). Sugar-Induced Obesity and Insulin Resistance Are Uncoupled from Shortened Survival in *Drosophila*. *Cell Metabolism*, 31(4), 710-725.e7. https://doi.org/10.1016/j.cmet.2020.02.016

- Lennicke, C.*, **dos Santos, E.***, & Cochemé, H. M. (2020). Sugar-induced dysregulation of purine metabolism impacts lifespan. *Aging*, 12(24), 24479–24480. https://doi.org/10.18632/aging.104223

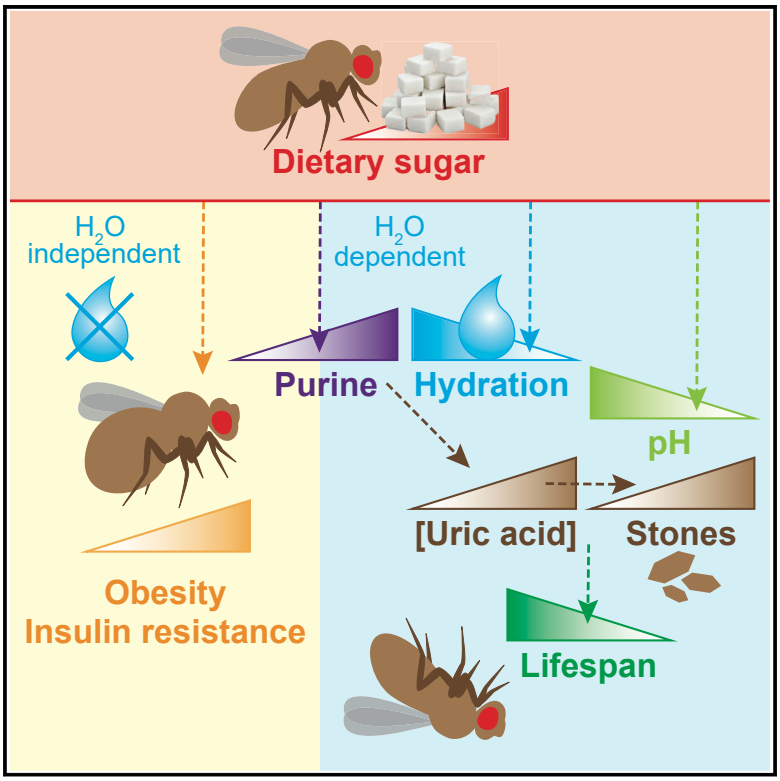
* Equal contribution

Article

Cell Metabolism

Sugar-Induced Obesity and Insulin Resistance Are Uncoupled from Shortened Survival in *Drosophila*

Graphical Abstract



Authors

Esther van Dam,
Lucie A.G. van Leeuwen,
Eliano dos Santos, ..., Andre Franke,
Christoph Kaleta, Helena M. Cochemé

Correspondence

helena.cocheme@lms.mrc.ac.uk

In Brief

van Dam et al. disentangle the physiological effects of high-sugar feeding on survival using adult *Drosophila*. They uncouple diet-induced obesity and insulin resistance from shortened lifespan by rescuing sugar-induced water imbalance. Dietary sugar is linked to kidney dysfunction and dysregulation of purine catabolism in both flies and humans, emphasizing this pathway as a promising target for potential therapeutic interventions.

Highlights

- Sugar-induced lifespan shortening can be uncoupled from obesity and insulin resistance
- A high-sugar diet induces water imbalance in adult *Drosophila*
- High-sugar feeding shortens fly lifespan through dysregulation of purine catabolism
- Dietary sugar intake in humans is associated with circulating purine levels

van Dam et al., 2020, Cell Metabolism *31*, 710–725
April 7, 2020 © 2020 The Authors. Published by Elsevier Inc.
https://doi.org/10.1016/j.cmet.2020.02.016

CellPress

CellPress

Cell Metabolism
Article

Sugar-Induced Obesity and Insulin Resistance Are Uncoupled from Shortened Survival in *Drosophila*

Esther van Dam,[1,2,7] Lucie A.G. van Leeuwen,[1,2,7] Eliano dos Santos,[1,2,7] Joel James,[1,2,7] Lena Best,[3,7] Claudia Lennicke,[1,2] Alec J. Vincent,[1,2] Georgios Marinos,[3] Andrea Foley,[1,2] Marcela Buricova,[1,2] Joao B. Mokochinski,[1,2] Holger B. Kramer,[1,2] Wolfgang Lieb,[4] Matthias Laudes,[5] Andre Franke,[6] Christoph Kaleta,[3] and Helena M. Cochemé[1,2,8,*]

[1]MRC London Institute of Medical Sciences, Du Cane Road, London W12 0NN, UK
[2]Institute of Clinical Sciences, Imperial College London, Hammersmith Hospital Campus, Du Cane Road, London W12 0NN, UK
[3]Institute for Experimental Medicine, Kiel University, 24105 Kiel, Germany
[4]Institute of Epidemiology, Kiel University, 24105 Kiel, Germany
[5]Department of Internal Medicine I, University Hospital Schleswig-Holstein, 24105 Kiel, Germany
[6]Institute of Clinical Molecular Biology, Kiel University, 24105 Kiel, Germany
[7]These authors contributed equally
[8]Lead Contact
*Correspondence: helena.cocheme@lms.mrc.ac.uk
https://doi.org/10.1016/j.cmet.2020.02.016

SUMMARY

High-sugar diets cause thirst, obesity, and metabolic dysregulation, leading to diseases including type 2 diabetes and shortened lifespan. However, the impact of obesity and water imbalance on health and survival is complex and difficult to disentangle. Here, we show that high sugar induces dehydration in adult *Drosophila*, and water supplementation fully rescues their lifespan. Conversely, the metabolic defects are water-independent, showing uncoupling between sugar-induced obesity and insulin resistance with reduced survival *in vivo*. High-sugar diets promote accumulation of uric acid, an end-product of purine catabolism, and the formation of renal stones, a process aggravated by dehydration and physiological acidification. Importantly, regulating uric acid production impacts on lifespan in a water-dependent manner. Furthermore, metabolomics analysis in a human cohort reveals that dietary sugar intake strongly predicts circulating purine levels. Our model explains the pathophysiology of high-sugar diets independently of obesity and insulin resistance and highlights purine metabolism as a pro-longevity target.

INTRODUCTION

Diet-induced obesity and associated metabolic disorders such as type 2 diabetes (T2D) are a major global issue reaching epidemic proportions, widely attributed to the increased consumption of sugary foods and drinks, with serious consequences to human health (WHO, 2016, 2020). Many severe comorbidities are associated with T2D (e.g., nephropathy and cardiomyopathy), and the life expectancy of individuals with T2D is significantly reduced (Chatterjee et al., 2017; DeFronzo et al., 2015). In fact, diet-induced obesity and age are major risk factors for developing T2D, yet despite clear correlations between insulin resistance, obesity, and aging, the exact underlying mechanisms still remain unclear (Chatterjee et al., 2017; DeFronzo et al., 2015). Thirst is an early symptom of hyperglycemia, as excess non-reabsorbed glucose is eliminated via enhanced urine production, resulting in dehydration. Yet the role of water balance in the context of sugar-induced metabolic disease and survival defects is not fully appreciated.

The combination of short lifespan, low costs, and ease of genetic manipulations, together with the evolutionary conservation of central signaling pathways regulating metabolism and energy homeostasis, make the fruit fly *Drosophila melanogaster* a powerful model system to study dietary interventions, metabolic disorders, and aging (Baker and Thummel, 2007; Mattila and Hietakangas, 2017; Owusu-Ansah and Perrimon, 2014;

Context and Significance

Excess consumption of sugar has been implicated in the global epidemic of obesity and metabolic disease. How sugar-rich diets are detrimental to health and longevity is still unclear, and the interplay with water intake is often overlooked. Here, Cochemé and colleagues disentangle the diabetic-like effects of high-sugar diets and shortened survival in *Drosophila* by manipulating water balance. They find that sugar fuels the purine degradation pathway, leading to the accumulation of uric acid as kidney stones. Consistent with the fly data, they show in a human cohort that dietary sugar intake is associated with kidney function and blood purine levels. This work highlights the purine pathway as an unappreciated regulator of survival and a potential therapeutic target for health and lifespan benefits.

 © 2020 The Authors. Published by Elsevier Inc.
This is an open access article under the CC BY license (http://creativecommons.org/licenses/by/4.0/).

Padmanabha and Baker, 2014). Importantly, the endocrine system of the fly is remarkably similar to mammals, and the insulin/insulin-like growth factor signaling (IIS) pathway is strongly evolutionarily conserved (Partridge et al., 2011; Riera et al., 2016; Teleman, 2009).

A high-sugar diet has been used to model diabetic complications in *Drosophila*, applied both to larvae and adults, causing a range of detrimental effects on growth, metabolism, glucose homeostasis, cardiac function, and lifespan (Morris et al., 2012; Musselman et al., 2011; Na et al., 2013; Rovenko et al., 2015). Like humans, adult flies fed a high-sugar diet develop hyperglycemia, insulin resistance, and obesity (Morris et al., 2012; Skorupa et al., 2008). High-sugar feeding also significantly shortens lifespan in flies (Lushchak et al., 2014; Na et al., 2013; Skorupa et al., 2008), which has been attributed to the associated metabolic defects, yet causal evidence is lacking. As flies are a particularly valuable *in vivo* model to study metabolism and aging, it is important to understand the mechanisms underlying the pathophysiology of high-sugar diets in order to strengthen potential translation for diabetes research and therapies.

In this study, we focus on the response of adult flies to a high-sugar diet and the regulation of lifespan. We develop an experimental setup allowing us to distinguish between phenotypes that are directly caused by the sugar and those that are related to other factors such as sugar-induced water imbalance. Strikingly, we show that sugar-induced obesity and insulin resistance are unlinked from organismal aging. Furthermore, we find that the high-sugar diet fuels increased purine catabolism, promoting uric acid accumulation and the formation of stones in the renal tubules, which are exacerbated by dehydration and physiological acidification. In agreement with our results in *Drosophila*, we show that dietary sugar intake is also a strong predictor of renal function and circulating purine levels in a large human cohort. Overall, this study has important implications for high-sugar diets as a paradigm of metabolic disease and offers molecular insights into the complex pathology of diabetes models and their intricate relationship with survival.

RESULTS

High-Sugar Feeding Induces Thirst and Dehydration in Adult *Drosophila*

Drosophila are able to actively regulate water intake in response to diet composition (Fanson et al., 2012). Water imbalance was previously shown to cause the shortened lifespan of adult flies fed a high-salt diet (Piper et al., 2010), stressing the importance of dehydration on survival. Therefore, to assess whether a high-sugar diet induced thirst and dehydration in *Drosophila*, we fed adult wild-type (WT) *white Dahomey* (w^{Dah}) flies a standard laboratory food containing 5% w/v sucrose (5%S), or a high-sugar diet with 4-fold increased levels of sucrose up to 20% w/v (20%S). The protein source, yeast, was maintained constant throughout all experiments (see Table S1 for all media recipes). An exogenous water source was provided to the flies in the form of an agar gel (Figure 1A), a strategy previously used to rescue salt toxicity and explore mechanisms of dietary restriction in adult *Drosophila* (Ja et al., 2009; Piper et al., 2010). To assay thirst, we maintained flies on the 5%S and 20%S diets ± H_2O for 7 days, then measured their drinking from an agar source using the automated FlyPAD system, where proboscis extension completes a circuit between electrodes and registers a signal (Itskov et al., 2014). Flies on the 20%S diet without additional water exhibited a significantly increased number of sips, which was abolished when flies were pre-treated with the 20%S diet supplemented with water (Figures 1B and 1C). As further corroboration, we assayed thirst by two additional independent methods: first, we exposed flies to agar containing blue dye and quantified the amount of water ingested colorimetrically (Figure S1A); and second, we performed an adaptation of the liquid Capillary Feeder (CAFE) system (Ja et al., 2007) to supply drinking water to the vials and measured the volume of water consumed by the flies (Figure S1B). Again, by both of these approaches, flies pre-treated with the 20%S diet were significantly thirstier, which disappeared upon water supplementation. Furthermore, by all three independent drinking assays, WT flies fed the 5%S control food did not drink additional water, indicating that our standard diet does not induce thirst in WT flies (Figures 1B, 1C, S1A, and S1B).

To test for dehydration, we assessed the volume of total hemolymph extracted from flies (i.e., the circulating interstitial fluid, as flies have an open circulatory system). Hemolymph volume on the 20%S diet was unchanged at day 7 (d7), but significantly decreased at day 28 (d28) (Figure 1D). This loss was fully rescued back to control levels by water supplementation (Figure 1D), consistent with the flies being dehydrated upon long-term chronic high-sucrose feeding when unable to replenish their thirst. Together, these data confirm that flies subjected to a high-sucrose diet experience thirst, and that supplementation with drinking water was able to rescue this sugar-induced dehydration. Importantly, this experimental setup allows us to distinguish between the water-dependent and water-independent effects of high-sugar feeding on lifespan and physiology in adult *Drosophila*.

Water Supplementation Fully Rescues the Shortened Lifespan of WT Adult Flies on a High-Sucrose Diet

To explore how this sugar-induced water imbalance affected adult physiology, we focused initially on WT aging. A high-sucrose diet has been reported to shorten adult lifespan (Lushchak et al., 2014; Skorupa et al., 2008), and we confirmed that WT female flies on the 20%S food were dramatically shorter-lived than on the standard 5%S food (~21% decrease in median lifespan; Figures 1E and S1C). Remarkably, supplementation of the 20%S diet with water fully rescued the lifespan back to control levels (Figures 1E and S1C). Furthermore, despite known deleterious effects of age on water balance (Gibbs and Markow, 2001; Zheng et al., 2018), supplementation of the control 5%S food with water had no effect on WT lifespan (Figures 1E and S1C), confirming that WT flies were not under water stress on our standard laboratory diet.

To exclude changes in feeding behavior as a potential confounder in our results, we assessed feeding rates on the high-sucrose diet. Importantly, while WT flies fed less on the 20%S diet compared to standard 5%S, water supplementation did not affect the level of feeding on each respective food type, as measured by observation of proboscis extension (Figure S1D) or excretion of dye-containing food (Figure S1E; Shell et al., 2018). This confirmed that the lifespan rescue of the

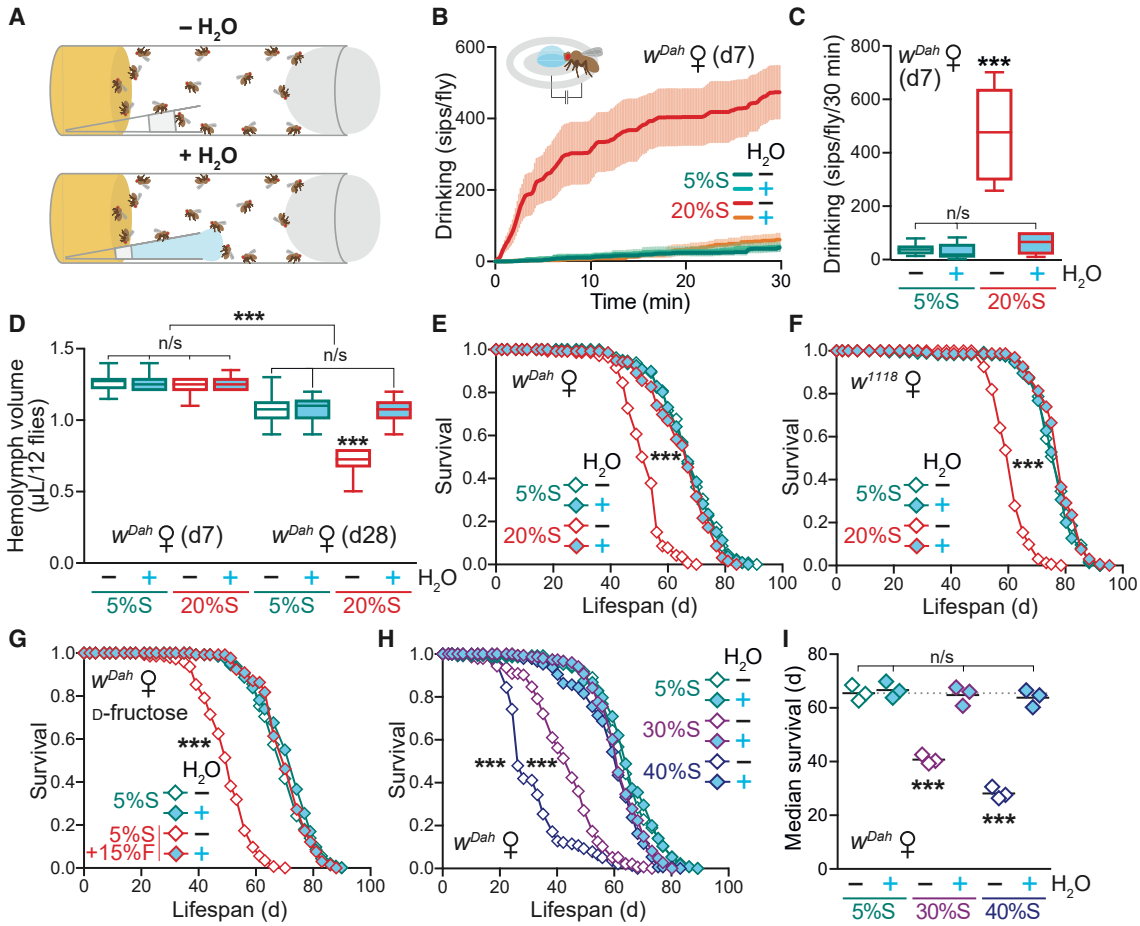


Figure 1. A High-Sucrose Diet that Induces Thirst and Dehydration and Shortens Lifespan in Adult *Drosophila* Is Rescued by Water Supplementation

(A) Scheme of the experimental setup, illustrating the supplementation of media vials with agar-filled tips as an *ad libitum* water source.

(B and C) Drinking assay to quantify the thirst of WT (w^{Dah}) flies in response to a high-sugar diet. Females were pre-treated for 7 days on a standard (5%S) or high-sucrose (20%S) diet ± H_2O. (B) Automated FlyPAD analysis showing the cumulative number of sips from an agar water source over 30 min. Data are means ± SEM of n = 6–8 individual flies per condition. (C) Box-and-whisker plots (min-max error bars) of the data from (B), analyzed by one-way ANOVA with Tukey correction (n/s, $p > 0.05$; ***$p < 0.001$).

(D) Hemolymph volume of WT females pre-treated for 7 and 28 days on 5%S or 20%S ± H_2O. Hemolymph was extracted from groups of 12 flies (n = 12–20 replicates per condition). Data are presented as box-and-whisker plots (min-max error bars), analyzed by one-way ANOVA with Tukey correction (n/s, $p > 0.05$; ***$p < 0.001$).

(E) Lifespan of WT females on 5%S and 20%S ± H_2O (n ~ 150 per condition).

(F) Lifespan of w^{1118} females on 5%S and 20%S ± H_2O (n ~ 165 per condition).

(G) Lifespan of WT females ± H_2O on a control diet (5%S) supplemented with 15% D-fructose (n ~ 150 per condition).

(H) Lifespan of WT females on 30%S and 40%S ± H_2O (n ~ 120–135 per condition).

(I) Summary of median survival ± H_2O for n = 3 independent lifespan experiments on control (5%S) and high sucrose (30%S and 40%S) diets. Data were analyzed by one-way ANOVA with Tukey correction (n/s, $p > 0.05$; ***$p < 0.001$).

Statistical analysis for all survival curves (E, F, G, and H) was performed by log-rank test (n/s, $p > 0.05$; ***$p < 0.001$). See Table S2 for exact n numbers and p values. See also Figure S1.

20%S + H_2O flies was not simply due to decreased ingestion of the "harmful" high-sugar food.

To rule out genetic background effects, we assessed the water response in different fly strains. Presence of the endosymbiont *Wolbachia* is known to affect fly metabolism and lifespan (Ikeya et al., 2009; Toivonen et al., 2007); therefore, we tested a *Wolbachia*-uninfected strain of w^{Dah} and found that it responded similarly to a high-sucrose diet, showing that the process was independent of *Wolbachia* status (Figure S1F). Furthermore, the parental (red-eyed) *Dahomey* strain behaved comparably to w^{Dah} (Figure S1G), indicating that the *white* mutation reported to influence feeding and behavior was not involved. Finally, we also tested the response in females of the isogenic control strain w^{1118} and again found a similar pattern (Figure 1F). Importantly, the water rescue was not gender-specific, as it was also observed in w^{1118} males (Figure S1H) and not linked to egg production, as it occurred in sterile ovo^{D1} mutant females (Figure S1I). We also quantified egg laying directly, which is often

regarded as an indicator of female *Drosophila* health and is frequently associated with a lifespan trade-off (Flatt, 2011). As previously reported for high-sugar diets (Lushchak et al., 2014), we observed lower fecundity on the 20%S food (Figure S1J). Interestingly, water supplementation did not rescue this decreased egg laying (Figure S1J) even though longevity was fully restored to control levels, representing an uncoupling of lifespan and fecundity. To control for the effects of decreased food intake between the 5%S and 20%S diets, which may explain the reduced fecundity, we supplemented the agar tips with a cocktail of essential amino acids (Grandison et al., 2009a); however, this did not improve egg laying on the 20%S food (Figure S1J). Therefore, not all phenotypes in response to a high-sugar diet can be rescued by water supplementation.

To address whether the water rescue of lifespan occurs on other high-sugar diets, we tested the constituent monosaccharides of sucrose, D-fructose and D-glucose. For these experiments, we performed lifespan assays with a standard sucrose base (5%S) supplemented with a 15% w/v excess of each respective sugar. We found that a high D-fructose (Figure 1G) or D-glucose (Figure S1K) diet significantly shortened adult lifespan to a similar extent as high sucrose (Figure S1L) and that this effect was fully rescued by water supplementation, confirming that our initial observations were not specific to sucrose.

To enhance the severity of the dietary challenge, we investigated the response of WT flies at even higher sugar concentrations, within a range used experimentally for *Drosophila*. When sucrose levels were further increased from 20%S to 30%S and 40%S, we found a corresponding dose-dependent decrease in lifespan compared to 5%S by ~38% and ~57%, respectively (Figures 1H and 1I). Remarkably, this greater decline in longevity was still fully rescued by water supplementation (Figure 1I). Overall, we have shown that water supplementation fully and robustly rescued the shortened lifespan from a high sucrose diet across multiple genetic background strains and in a gender-independent manner.

Response of Metabolic Traits to a High-Sucrose Diet and Water Supplementation

The shortened lifespan of adult flies on a high-sugar diet is widely assumed to be a consequence of the associated metabolic defects; namely obesity, glycation, hyperglycemia, and insulin resistance. Therefore, we were interested to investigate how water supplementation affected these high-sugar-induced metabolic phenotypes in the context of rescued lifespan. Consistent with previous reports (Morris et al., 2012; Skorupa et al., 2008), we confirmed that WT adult flies fed a high-sucrose diet had increased adiposity, both by lipid staining of fat body tissue (Figure 2A) and measurement of whole-body triglyceride (TAG) levels (Figure 2B). Remarkably, diet-induced obesity was unaffected by water supplementation, and the 20%S + H_2O flies retained their adiposity levels despite the rescued lifespan (Figure 2B).

Glycation damage has been implicated as an important factor underlying diabetic complications (Goh and Cooper, 2008). Advanced glycation end-products (AGEs), formed when reducing sugars such as D-glucose and D-fructose react non-enzymatically with amino groups on proteins, have been shown to increase in *Drosophila* with age (Jacobson et al., 2010; Oudes et al., 1998) and upon high-sugar feeding (Garrido et al., 2015). Proteins are typically glycated through lysine residues, forming adducts such as carboxy-methyl-lysine (CML). Using an anti-AGE (CML) antibody, we detected elevated glycation adducts in whole flies in response to 20%S feeding (Figures 2C and S2A). Interestingly, glycation levels were not affected by water supplementation, again demonstrating that despite the lifespan rescue, the 20%S + H_2O flies still displayed many of the supposedly harmful traits associated with high-sugar feeding. In contrast, as a control, protein carbonylation, indicative of oxidative damage, was unchanged for all conditions (Figures S2B and S2C).

To evaluate the effect of water supplementation on hyperglycemia induced by high-sugar feeding, we measured the levels of trehalose in the hemolymph, the major circulating sugar in *Drosophila* (Mattila and Hietakangas, 2017). Hemolymph trehalose levels were significantly increased on the 20%S diet, and this hyperglycemic state was retained upon water supplementation (Figure 2D). To monitor insulin resistance, we performed an insulin response test on the abdominal fat body tissue by assessing AKT phosphorylation. The 20%S diet caused insulin resistance, as evidenced from decreased phospho-AKT levels, which was not rescued by water supplementation (Figures 2E, 2F, and S2D). This was further corroborated by measuring glucose uptake into fat body tissue using a fluorescent non-metabolizable glucose analog (Figure 2G). Altogether, while the lifespan of WT flies was completely rescued on the 20%S + H_2O condition to that of "healthy" controls, they remained obese, hyperglycemic, and insulin resistant, which are hallmarks of metabolic disease. Therefore, we show that high-sugar-diet-induced "diabesity" can be fully uncoupled from mortality *in vivo*.

Heightened Sensitivity of *Δfoxo* Mutants in Response to Dietary Sucrose

Dietary sugar is sensed via the IIS pathway, which is a key regulator of growth, metabolism, and lifespan (Partridge et al., 2011; Riera et al., 2016; Teleman, 2009). Null flies for the transcription factor FOXO, the major downstream effector of the IIS pathway, have impaired nutrient sensing and are significantly shorter lived than WT (Slack et al., 2011; Figure S3A). Therefore, we were interested in testing the response of *Δfoxo* flies to a high-sugar diet and the effects of water supplementation. Again, we found that the 20%S diet induced thirst (Figures S3B and S3C) and shortened lifespan (Figures 3A, 3B, and S3A) in *Δfoxo* flies. However, this decreased survival was only partially rescued by water (Figures 3A, 3B, and S3A), suggesting a combination of both water-dependent and directly sugar-related effects. Contrary to WT flies, decreased hemolymph volume was already detectable in the *Δfoxo* mutants at d7 of 20%S treatment (Figure 3C), indicating a hypersensitivity to the dehydration effects of a high-sugar diet. Unexpectedly, and in contrast to WT flies, water supplementation further extended the lifespan of the *Δfoxo* mutant on the standard 5%S diet (Figures 3A and 3B). This result suggests that *Δfoxo* mutants, with their dysregulated IIS, were already experiencing dehydration stress under control sugar conditions.

To explore this observation further, we tested the effect of lowering dietary sucrose levels on survival of the *Δfoxo* mutant. Remarkably, simply decreasing the concentration of sucrose in the food from 5% to 2.5% was sufficient to abolish the

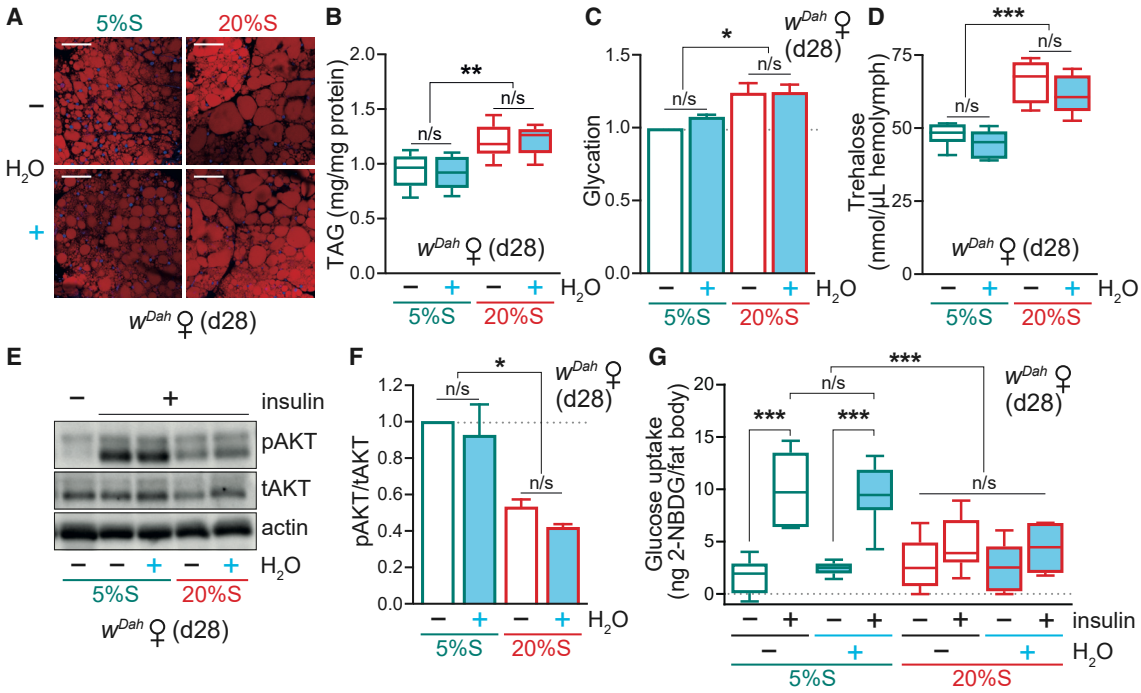


Figure 2. Metabolic Effects of a High-Sucrose Diet and Water Supplementation in WT Adults

(A) Lipid staining by Nile Red of abdominal fat body tissue from d28 WT (w^{Dah}) females fed on 5%S or 20%S ± H_2O, imaged by confocal microscopy. Scale bar: 50 µm.

(B) Whole body TAG levels in d28 WT females fed on 5%S or 20%S ± H_2O. Data (n = 8 replicates, each with n = 4 flies per sample) are presented as box-and-whisker plots (min-max error bars), analyzed by one-way ANOVA with Tukey correction (n/s, $p > 0.05$; **$p < 0.01$).

(C) Glycation damage in whole body d28 WT females fed on 5%S or 20%S ± H_2O, assessed by western blotting (see Figure S2A). Data are means + SEM of n = 4 samples per condition, analyzed by one-way ANOVA with Tukey correction (n/s, $p > 0.05$; *$p < 0.05$).

(D) Circulating trehalose levels in the hemolymph of d28 WT females pre-treated on 5%S or 20%S ± H_2O. Data (n = 6 replicates per condition, each with n = 12 flies per sample) are presented as box-and-whisker plots (min-max error bars), analyzed by one-way ANOVA with Tukey correction (n/s, $p > 0.05$; ***$p < 0.001$).

(E and F) Insulin response of abdominal fat body dissected from d28 WT females fed on 5%S or 20%S ± H_2O (see Figure S2D). (E) Western blot for phospho-AKT with total AKT and actin as controls. (F) Quantification of bands by densitometry. Data are means + SEM of n = 3 experiments (each with n = 5 fat bodies per sample), analyzed by one-way ANOVA with Tukey correction (n/s, $p > 0.05$; *$p < 0.05$).

(G) Glucose uptake into abdominal fat body dissected from d28 WT females fed on 5%S or 20%S ± H_2O (n = 6 replicates for "– insulin" and n = 10 replicates for "+ insulin," each with n = 5 fat bodies per sample). Data are presented as box-and-whisker plots (min-max error bars), analyzed by one-way ANOVA with Tukey correction (n/s, $p > 0.05$; ***$p < 0.001$).

See also Figure S2.

water-dependent lifespan extension (Figure 3D). Lowering the sucrose content further to 1% and 0% resulted in a concomitant decrease in survival, without any water differences (Figures S3D and S3E). Feeding rates of the *Δfoxo* flies were the same on the 1%S, 2.5%S and 5%S diets ± H_2O (Figure S3F), therefore excluding the modulation of lifespan via a dietary restriction mechanism. Consistent with our hypothesis, we performed drinking assays on aged *Δfoxo* flies treated for 21 days (rather than 28 days, since they are short-lived) and found that flies on the 5%S – H_2O diet were thirstier compared to the 5%S + H_2O condition, whereas drinking was unaffected on the 2.5%S diet ± H_2O (Figure 3E), highlighting their hypersensitivity to sucrose levels in the diet. The *Δfoxo* mutants have lower fecundity relative to WT (Slack et al., 2011), which was further decreased upon high-sugar feeding, regardless of H_2O status (Figure S3G), again showing an uncoupling between fecundity and longevity.

Importantly, as with WT flies, the 20%S diet also promoted obesity in the *Δfoxo* mutant, independently of water supplementation, as measured by whole body TAG content (Figure 3F). Furthermore, the TAG levels of *Δfoxo* flies on 5%S ± H_2O were indistinguishable, again uncoupling the obesity and longevity phenotypes. Overall, the *Δfoxo* mutants are hypersensitive to the deleterious effects of a high-sugar diet, even under control conditions of 5%S. Together, these data reveal that flies with dysregulated IIS are more vulnerable to the toxic effects of a high-sucrose diet. These results highlight the importance of considering water-dependent effects of dietary sugar, and that the optimal sugar level will vary according to the genetic context.

Effects of a High-Sugar Diet on Stress Responses and Gut Physiology

The shortened lifespan of flies on a high-sugar diet was assumed to be a consequence of their obesity and insulin resistance. Since this was not the case, we next sought other physiological explanations for the high-sugar-induced pathology. We first tested the response of WT flies to a range of stresses in the context of diet and water status, since survival is often correlated with stress resistance (Gems and Partridge, 2008). Consistent

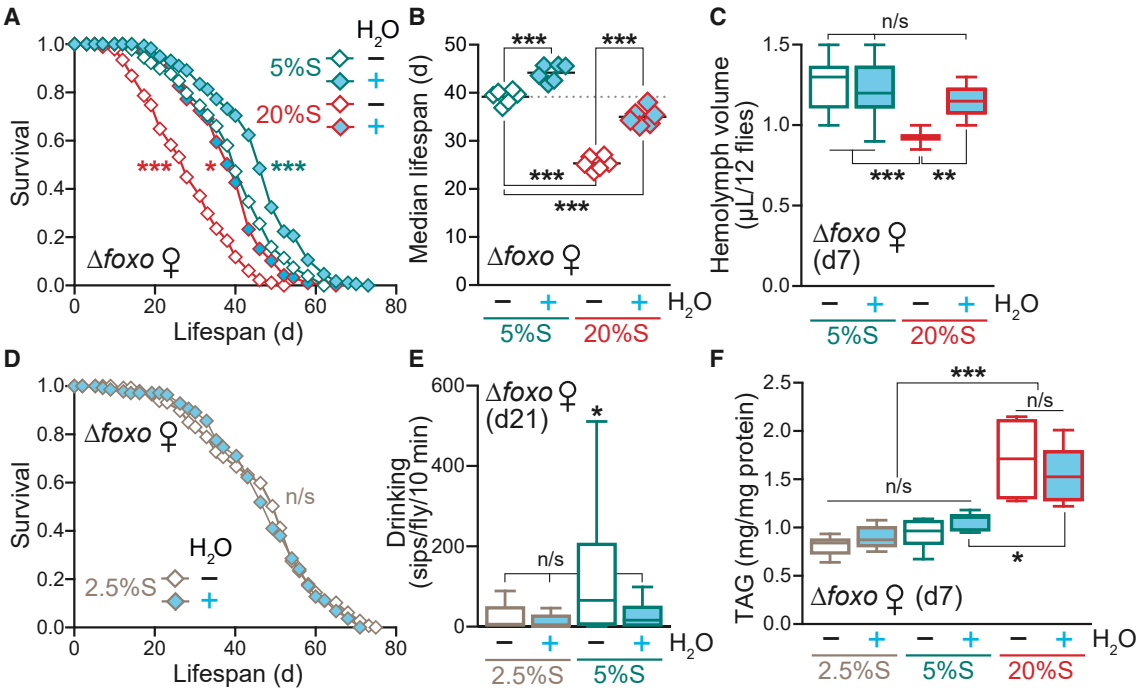


Figure 3. *Δfoxo* Mutants Are Hypersensitive to Dietary Sugar

(A) Lifespan of *Δfoxo* females on 5%S and 20%S ± H_2O (n ~ 195 flies per condition). Statistical analysis was performed by log-rank test (*p < 0.05; ***p < 0.001 against the 5%S – H_2O control). See Table S2 for exact n numbers and p values.

(B) Summary of median survival data for n = 6 independent *Δfoxo* lifespan experiments, analyzed by one-way ANOVA with Tukey correction (***p < 0.001).

(C) Hemolymph volume of *Δfoxo* females pre-treated for 7 days on 5%S or 20%S ± H_2O (n = 12 replicates per condition, each with n = 12 flies per sample). Data are presented as box-and-whisker plots (min-max error bars), analyzed by one-way ANOVA with Tukey correction (n/s, p > 0.05; **p < 0.01; ***p < 0.001).

(D) Lifespan of *Δfoxo* females on 2.5%S ± H_2O (n ~ 150 flies per condition). Statistical analysis was performed by log-rank test (n/s, p > 0.05). See Table S2 for exact n numbers and p values.

(E) Drinking assay of *Δfoxo* females pre-treated for 21 days on 2.5%S, 5%S, or 20%S ± H_2O measured over 10 min by FlyPAD (n = 30 individual flies per condition). Data are presented as box-and-whisker plots (min-max error bars), analyzed by one-way ANOVA with Tukey correction (n/s, p > 0.05; *p < 0.05).

(F) Whole body TAG levels of *Δfoxo* females pre-treated for 7 days on 2.5%S, 5%S, or 20%S ± H_2O (n = 5–6 replicates per condition, each with n = 4 flies per sample). Data are presented as box-and-whisker plots (min-max error bars), analyzed by one-way ANOVA with Tukey correction (n/s, p > 0.05; *p < 0.05; ***p < 0.001).

See also Figure S3.

with their sugar-induced dehydration (Figure 1D), d28 flies on the 20%S – H_2O condition were sensitive to desiccation stress, which was rescued by water pre-treatment (Figure 4A). We also subjected d7 flies pre-treated on 5%S or 20%S food ± H_2O to a subsequent high-salt challenge by transferring to a medium containing 500 mM NaCl (all without further water supplementation), and found that high-sugar feeding significantly sensitized the flies to high-salt stress (Figures 4B and S4A). Water supplementation during the 20%S high-sugar pre-treatment offered partial protection, but unlike lifespan, did not rescue the survival curve back to the 5%S response. This suggests that even though the high-sugar diet is supplemented with water, flies still endured sugar-induced damage that became apparent upon acute high-salt stress. In contrast, there was no difference between all conditions (5%S and 20%S ± H_2O) when flies were exposed to oxidative stress (Figure S4B), confirming that the effect is specific to metabolically induced dehydration stress. Interestingly, flies pre-treated on the 20%S diet were more resistant to starvation stress than 5%S flies, irrespective of water supplementation (Figure S4C), presumably reflecting their increased TAG reserves (Figures 2A and 2B). Therefore, stress responses cannot explain the full water-dependent rescue of WT lifespan on a high-sugar diet.

Since the gut is critical in the context of nutritional physiology (Miguel-Aliaga et al., 2018) and is the first organ exposed to the high-sugar diet, we next explored effects on intestinal function by analyzing the pattern of fly excreta assayed upon feeding the flies blue-dye-containing food (Cognigni et al., 2011; Figure S4D). The 20%S diet caused a pronounced decrease in the total number (Figure 4C) and size (Figure 4D) of deposits, both consistent with a dehydration effect (Cognigni et al., 2011). The 20%S diet also caused an alteration to the morphology of excreta, with an increase in oblong (reproductive oblong deposits [RODs]) versus circular deposits (Figure 4E); again, a reported signature of dehydration (Cognigni et al., 2011), and indeed all three parameters responded to water supplementation (Figures 4C–4E). Furthermore, the presence of a water source increased the lightness of deposits for both the 5%S and 20%S diets (Figure 4F), indicating that the excreta are more dilute. Therefore, the high-sucrose diet is exerting effects on gut physiology associated with water imbalance, which can be modulated by water supplementation.

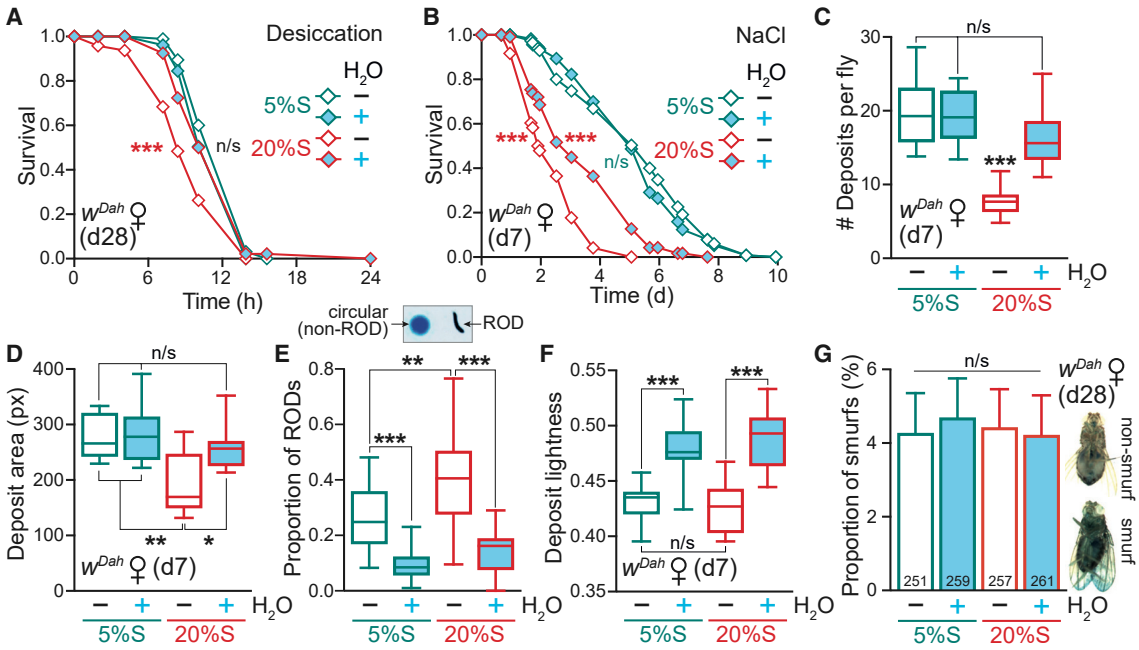


Figure 4. Effects of a High-Sugar Diet on Stress Responses and Gut Physiology

(A and B) Stress response of WT (w^{Dah}) females pre-treated on 5%S or 20%S ± H_2O, then exposed to (A) desiccation at d28 (n ~ 105 flies per condition) and (B) high salt at d7 (500 mM NaCl, n ~ 100–120 flies per condition). Statistical analysis of survival curves was performed by log-rank test (n/s, $p > 0.05$; ***$p < 0.001$). See Table S2 for exact n numbers and p values.

(C–F) Analysis of fly excreta from WT females pre-treated in vials for 7 days on 5%S or 20%S ± H_2O, then transferred to dishes for 24 h (n = 5 flies per plate). Food was supplemented with 2.5% w/v blue dye, while the agar for the water supplementation was undyed (see Figure S4D). Data are presented as box-and-whisker plots (min-max error bars), analyzed by one-way ANOVA with Tukey correction (n/s, $p > 0.05$; *$p < 0.05$; **$p < 0.01$; ***$p < 0.001$). (C) Number of deposits per fly recorded over 24 h (n = 10 plates per condition). (D) Mean area of deposits (n = 10 plates per condition). (E) Proportion of RODs (reproductive oblong deposits) (n = 21–24 plates per condition). (F) Mean lightness of deposits on a 0–1 scale (n = 10 plates per condition).

(G) The proportion of WT females exhibiting a Smurf phenotype at d28. Inset: example image of a non-Smurf fly, where the blue dye is restricted solely to the digestive tract, and a Smurf fly, where gut barrier integrity is compromised and the blue dye disperses throughout the fly body. Data are means + SEM of n = 20 vials per condition, analyzed by one-way ANOVA with Tukey correction (n/s, $p > 0.05$). The total number of flies scored per condition is indicated.

See also Figure S4.

To explore whether gut damage was responsible for the shortened lifespan of flies on a high-sugar diet, we assessed intestinal barrier function, an important parameter of gut health known to deteriorate with age, as determined by the Smurf assay, where flies are fed blue-dye-containing food and screened for dispersal of the dye beyond the digestive tract when gut integrity is compromised (Rera et al., 2012). Flies pre-treated for 28 days on 5%S or 20%S ± H_2O did not display a significant increase in the proportion of Smurfs (Figure 4G), indicating that even close to the onset of death, the barrier function of the gut was still intact in response to the high-sucrose diet. Therefore, although gut physiology was influenced by the high-sugar diet and water supplementation, gut dysfunction does not appear to underlie the lifespan-shortening effect.

A High-Sucrose Diet Is Associated with Tubule Dysfunction from Dysregulation of Purine Catabolism Causing Kidney Stones

In view of the water imbalance, we next assessed the function of the Malpighian tubules, the fly equivalent of the kidney (Figure 5A), which are vital organs for excretion, osmoregulation, and water homeostasis (Dow and Romero, 2010). To investigate the effects of a high-sugar diet on renal physiology, we first examined tubule morphology by light microscopy (Figure S5A). Flies fed the 20%S – H_2O diet exhibited a strongly darkened tubule phenotype, which was fully rescued by water supplementation (Figures 5B and 5C). These dark deposits were intraluminal concretions suggestive of uric acid accumulation (Ghimire et al., 2019). Therefore, we assayed uric acid content biochemically from whole flies (Figure 5D) and dissected tubules (Figure S5B), which was significantly elevated on the 20%S diet (~2- and ~4-fold, respectively) and again fully restored to the 5%S control baseline by water supplementation. In addition to the high-sucrose diet, excess D-glucose or D-fructose also led to the development of tubule stones, which were rescued by water (Figure S5C). We hypothesized that dietary sugars provided precursors for purine biosynthesis fueling the increased levels of uric acid, a waste product derived from purine catabolism (Figure 5E).

To explore the potentially pathogenic role of uric acid accumulation, we treated flies with the purine analog allopurinol (AP), a xanthine oxidase (XO) inhibitor that blocks uric acid production (Bratty et al., 2011; Figure 5E). Supplementation of the 20%S diet with AP (1 mM) completely abolished the elevated uric acid levels in the flies (Figure 5F) and the tubule stones (Figures 5G and 5H). Furthermore, consistent with their hypersensitivity to dietary sugar, aged *Δfoxo* flies developed increased tubule

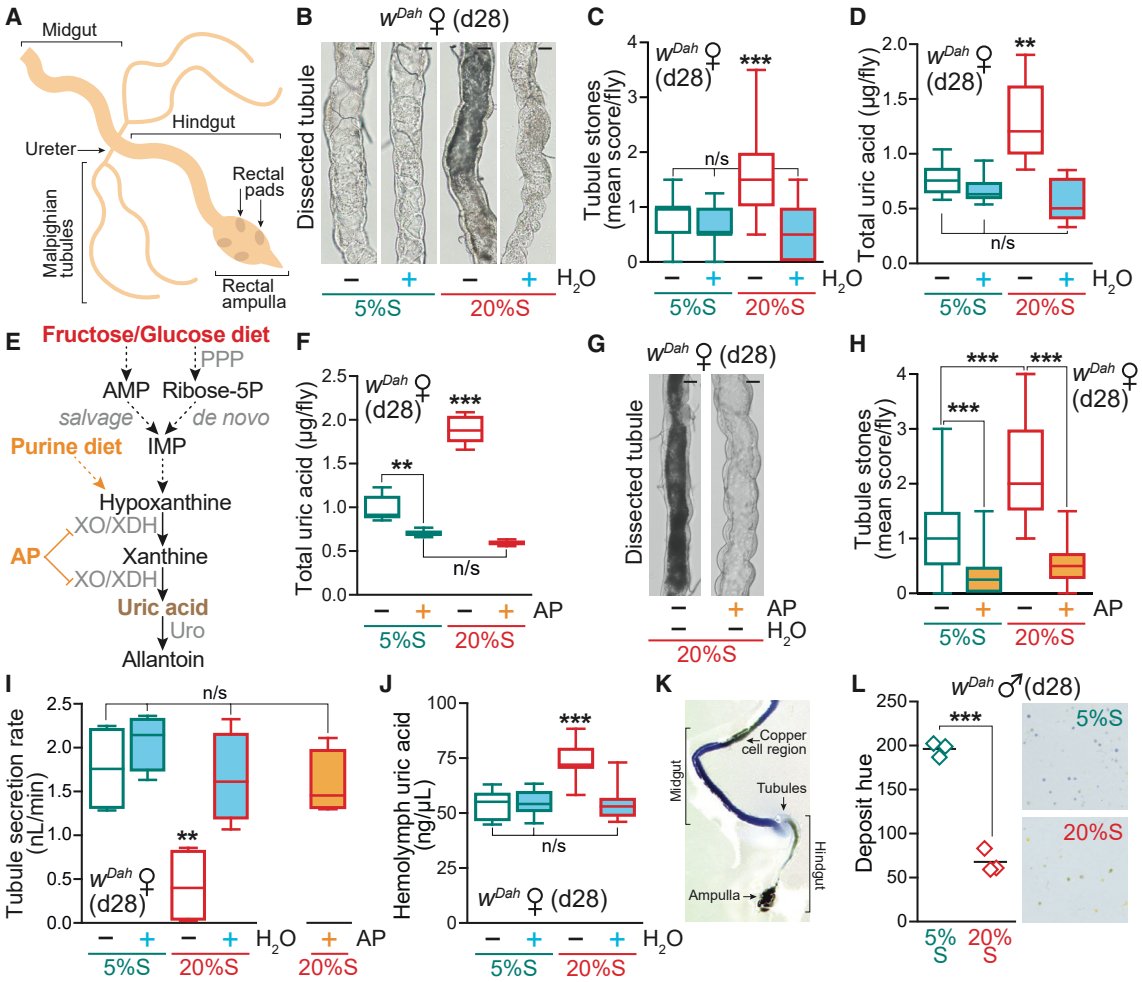


Figure 5. A High-Sugar Diet Induces Uric Acid Deposition and Tubule Dysfunction

(A) Diagram of the *Drosophila* lower digestive tract, terminating in the rectal ampulla. The Malpighian (renal) tubules connect at the junction between the midgut and the hindgut.

(B) Light microscopy images of dissected tubules from WT (w^{Dah}) females fed for 28 days on 5%S or 20%S ± H_2O. Scale bar: 25 µm.

(C) Tubule phenotype scoring of WT females maintained for 28 days on 5%S or 20%S ± H_2O. Data (n = 50 flies per condition) are presented as box-and-whisker plots (min-max error bars), analyzed by Kruskal-Wallis test with Dunn correction (n/s, $p > 0.05$; ***$p < 0.001$). See Figure S5A for the scoring scale.

(D) Uric acid content of whole WT females fed for 28 days on 5%S or 20%S ± H_2O (n = 6 replicates per condition, each with n = 5 flies per sample). Data are presented as box-and-whisker plots (min-max error bars), analyzed by one-way ANOVA with Tukey correction (n/s, $p > 0.05$; **$p < 0.01$).

(E) Biochemical pathway showing how dietary sugars such as D-glucose and D-fructose can lead to enhanced purine metabolism and to the formation of uric acid. Following the action of enzymes such as hexokinase, adenosine monophosphate (AMP) is formed and can be converted to the purine precursor inosine monophosphate (IMP). Alternatively, the purine precursor ribose-5-P is formed via the pentose phosphate pathway (PPP) by *de novo* biosynthesis. The drug allopurinol (AP) prevents uric acid production by inhibiting the enzyme xanthine oxidase (XO)/xanthine dehydrogenase (XDH). Urate oxidase (Uro) catalyzes the degradation of uric acid to allantoin. The enzyme XO/XDH (encoded by *rosy* in *Drosophila*) and Uro are strongly expressed in the tubules (>20-fold and >13,000-fold higher than in the hindgut of females, respectively; Leader et al., 2018).

(F) Uric acid content of whole WT females fed for 28 days on 5%S or 20%S ± AP (1 mM). Box-and-whisker plots (min-max error bars) of n = 5 replicates per condition (each with n = 5 flies per sample), analyzed by one-way ANOVA with Tukey correction (n/s, $p > 0.05$; **$p < 0.01$; ***$p < 0.001$).

(G) Light microscopy images of dissected tubules from WT females fed for 28 days on 20%S ± AP (1 mM). Scale bar: 25 µm.

(H) Tubule phenotype scoring of WT females maintained for 28 days on 5%S or 20%S ± AP (1 mM). Data (n = 50 flies per condition, except n = 25 for 20%S + AP) are presented as box-and-whisker plots (min-max error bars), analyzed by Kruskal-Wallis test with Dunn correction (***$p < 0.001$). See Figure S5A for the scoring scale.

(I) Secretion rates of tubules from WT females pre-treated for 28 days on 5%S or 20%S ± H_2O or ± AP (1 mM). See Figure S5E for a diagram of the secretion assay. Data (n = 4 replicates per condition) are presented as box-and-whisker plots (min-max error bars), analyzed by one-way ANOVA with Tukey correction (n/s, $p > 0.05$; **$p < 0.01$).

(J) Hemolymph uric acid concentration from WT females fed for 28 days on 5%S or 20%S ± H_2O. Data (n = 8 replicates per condition, each with n = 12 flies per sample) are presented as box-and-whisker plots (min-max error bars), analyzed by one-way ANOVA with Tukey correction (n/s, $p > 0.05$; ***$p < 0.001$).

(legend continued on next page)

stones on the 5%S diet (Figure S5D). Therefore, the tubule stone pathology is water-dependent, can be induced by a high-sugar diet, and modulated both pharmacologically and genetically.

To investigate the effects of a high-sugar diet and uric acid deposition on tubule physiology and function, we assayed the secretion rates of dissected WT tubules *ex vivo* (Figure S5E). Consistent with blockage by the intraluminal concretions, flies fed the 20%S diet for 28 days displayed severely compromised tubule secretion rates of ~0.5 nL/min compared to ~1.5-2 nL/min for controls (Figure 5I). Importantly, the impaired tubule secretion on a high-sugar diet was fully rescued by water supplementation, as well as by AP treatment (Figure 5I).

Multiple factors contribute to uric acid stone formation, including uric acid concentration and pH (Moe, 2006). First, we measured circulating uric acid levels in the fly hemolymph in response to a high-sugar diet. The concentration of uric acid was significantly increased at d28 on the 20%S diet, exacerbated by the hemolymph dehydration, and was rescued back to control levels by water supplementation (Figures 5J and S5F). Second, since uric acid crystallization is favored at acidic pH (Moe, 2006), we assessed hemolymph and urine pH in response to a high-sugar diet. Despite the significantly decreased hemolymph volume, we did not detect changes in hemolymph pH at d28 (Figure S5G), suggesting tight homeostatic control. Next, to assess urine pH, we supplemented the fly food with a pH indicator dye (Cognigni et al., 2011). Since in *Drosophila* the renal tubules connect to the digestive tract at the hindgut (see Figure 5A), the deposits produced by the fly are combined urine and feces. Consistent with previous observations (Cognigni et al., 2011), dissection of the digestive tract from dye-fed flies confirmed acidification of the hindgut posterior to the tubules (Figure 5K). Moreover, our excreta analysis revealed pronounced acidification of deposits in response to the 20%S food (Figures 5L and S5H). Therefore, the high-sugar diet results in both elevated uric acid levels and acidified conditions, which promote uric acid stone formation.

Pharmacological Treatments and Dietary Interventions Targeting Purine Metabolism Impact on Lifespan

To gain mechanistic insight and test whether uric acid accumulation upon high-sugar feeding contributed to the shortened survival, we performed lifespan experiments with AP supplementation in the food. Interestingly, a chronic high dose of the XO inhibitor AP (1 mM) shortened lifespan on both control and high-sugar diets (Figure S6A), despite clearing the tubules (Figures 5G and 5H). Upon dissection of AP-treated flies, we observed substantial concretions in the rectal ampulla (Figures 6A, S6B, and S6C), the final anatomical region of the *Drosophila* hindgut (see Figure 5A), with ~80% of control 5%S + AP flies and 100% of high-sugar 20%S + AP flies exhibiting ampulla stones at d28, compared to only <10% for both diets without the drug (Figure 6B). This severe pathology is consistent with the shortened lifespan and has previously been described in honeybees (termed "rectal enteroliths") in the context of colony collapse disorder (vanEngelsdorp et al., 2017) and recently in a *Drosophila* model of kidney disease by RNAi of urate oxidase (Lang et al., 2019). The high-sugar diet (20%S) alone caused a moderate but significant increase in the presence and severity of rectal ampulla stones, which was fully rescued to control levels by water supplementation (Figure 6B). Metabolomics analysis confirmed that the rectal ampulla stones formed on the high-sugar diet (20%S) contained high levels of uric acid, consistent with dysregulation of purine catabolism (Figure S6D; Table S4). Rectal ampulla stones upon AP treatment were composed of xanthine and hypoxanthine, highlighting the accumulation of upstream metabolites in the purine degradation pathway when uric acid formation is blocked (Figures S6D and S6E). The rectal ampulla is involved in pH regulation (Cognigni et al., 2011) and is known to be acidified (Figure 5K), explaining why this region of the digestive tract was particularly susceptible to the formation of stones. Throughout our study, stones were never observed in the midgut (including the acidic copper cell region; see Figure 5K), consistent with flow of stone-precursor metabolites from the tubules into the hindgut.

To overcome this toxicity, we tested a lower AP dose (100 μM) and found that this treatment extended the survival of WT females on a high-sugar diet (20%S ± AP), despite shortening lifespan on control food (5%S ± AP; Figures 6C and S6F). AP supplementation (100 μM) for 7 days did not affect food intake or fecundity on either the 5%S or 20%S diets (Figures S6G and S6H), suggesting that this dose does not have obvious adverse physiological effects in younger flies. Further decreasing the AP concentration to 10 μM had beneficial longevity effects on the high-sugar diet without shortening the survival of flies on the control food 5%S ± AP (Figures S6I and S6J). This partial lifespan rescue by AP indicated that uric acid production contributed to the decreased longevity induced by high-sugar diets. Therefore, to recapitulate the dysregulation of purine catabolism observed on a high-sugar diet, we directly fed flies a high-purine diet. Supplementing our standard 5%S diet with excess purine led to increased levels of uric acid (Figure 6D) and the formation of tubule stones (Figure 6E) to a similar extent as the high-sugar diet, which were both rescued to control levels by water supplementation. Importantly, a high-purine diet significantly shortened lifespan, which was fully rescued by water supplementation (Figures 6F and S6K). Together, these pharmacological and dietary modulations confirmed that dysregulation of purine catabolism as a consequence of high-sugar feeding caused water-dependent uric acid accumulation and concretions underlying decreased lifespan.

Human Metabolomics Analysis Links Dietary Sugar Intake with Renal Function and Circulating Purine Levels

Next, to test whether dietary habits could be linked to circulating purine levels in humans, we analyzed a population cohort of 650

(K) Dissected WT female gut after feeding with the pH indicator dye bromophenol blue (0.5% w/v) showing acidification of the hindgut (posterior to the tubules) and the rectal ampulla. The copper cell region in the midgut, known to be acidified, is also apparent.

(L) Physiological acidification in response to the high-sugar diet. WT males were pre-treated for 28 days on 5%S or 20%S, then incubated in plates with medium containing the pH indicator dye bromocresol purple (0.5% w/v) for 48 h. Mean hue of deposits (n = 3 plates per condition), analyzed by unpaired two-tailed Student's t test (***$p < 0.001$). Inset: scan of a typical plate illustrating the pH-dependent color shift (see Figure S5H).

See also Figure S5.

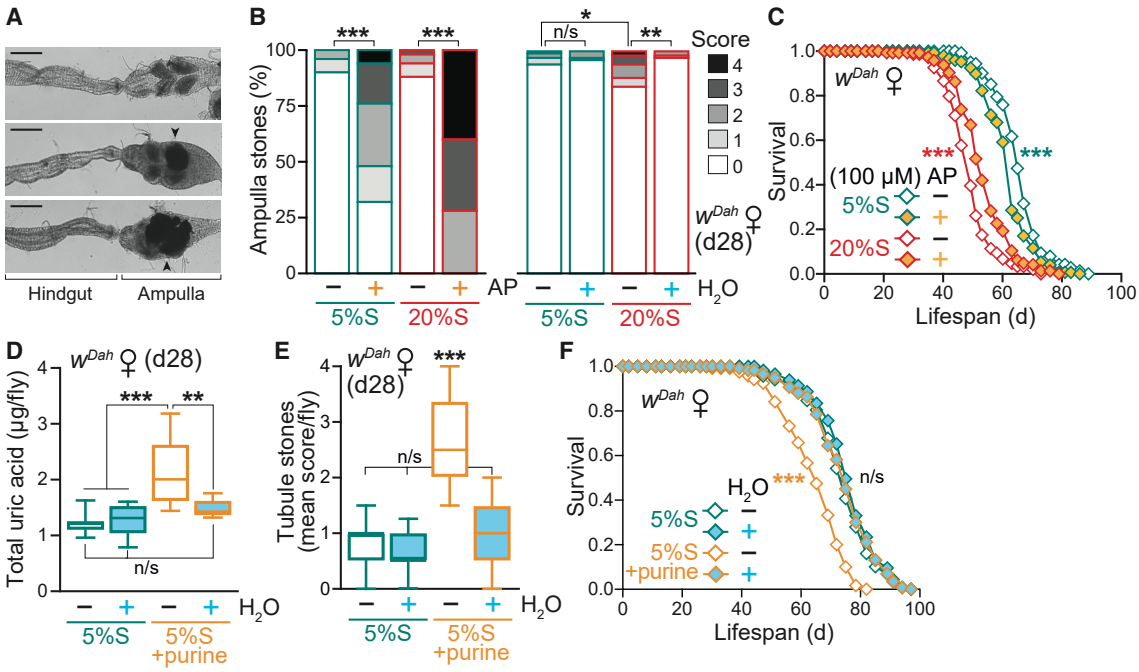


Figure 6. Pharmacological Treatments and Dietary Interventions Targeting Purine Metabolism Impact on Lifespan

(A) Light microscopy images of dissected ampulla: above, a clear ampulla with rectal pads visible; below, examples of stones present in the ampulla. Scale bar: 100 µm.

(B) Rectal ampulla stone phenotype scoring of WT (w^{Dah}) females pre-treated for 28 days on 5%S or 20%S ± AP (1 mM) (n = 50 flies per condition, except n = 25 for 20%S + AP) and 5%S or 20%S ± H_2O (n = 100 flies per condition). Data were analyzed by Kruskal-Wallis test with Dunn correction (n/s, $p > 0.05$; *$p < 0.05$; **$p < 0.01$; ***$p < 0.001$). See Figure S6B for the scoring scale.

(C) Allopurinol treatment (100 µM) extends the survival of WT females on a high-sucrose diet (20%S ± AP), despite shortening lifespan on control food (5%S ± AP) (n ~ 150 flies per condition).

(D) Uric acid content of WT females is elevated after 28 days on a high purine diet (5%S + 10 mM purine), and rescued by water supplementation. Data (n = 8 replicates per condition, each with n = 5 flies per sample) are presented as box-and-whisker plots (min-max error bars), analyzed by one-way ANOVA with Tukey correction (n/s, $p > 0.05$; **$p < 0.01$; ***$p < 0.001$).

(E) Tubule phenotype scoring of females maintained for 28 days on a high-purine diet (5%S + 10 mM purine) ± H_2O. Data (n = 50–60 flies per condition) are presented as box-and-whisker plots (min-max error bars), analyzed by Kruskal-Wallis test with Dunn correction (n/s, $p > 0.05$; ***$p < 0.001$). See Figure S5A for the scoring scale.

(F) A high purine diet (10 mM) shortens lifespan, which is fully rescued by water supplementation (n ~ 120 flies per condition).

Statistical analysis of survival curves (C and F) was performed by log-rank test (n/s, $p > 0.05$; ***$p < 0.001$). See Table S2 for exact n numbers and p values. See also Figure S6.

individuals (Figure 7A). This dataset combines extensive phenotypic information, including clinical parameters (Table S5), with detailed dietary records and comprehensive blood metabolomics (Brandstetter et al., 1999; Koch et al., 2017; Müller et al., 2015). The diet composition was evaluated from food questionnaires for each individual study participant. The estimated glomerular filtration rate (eGFR) determined from creatinine levels in the blood serum (Levey et al., 2006) served as a predictor of renal function and kidney health in our human study subjects. Concentrations of the purines guanosine, xanthosine, inosine, xanthine, hypoxanthine, and uric acid were measured by liquid chromatography-mass spectrometry (LC-MS) from serum samples (Figure S7A).

Using linear modeling, we assessed the direction of interaction between eGFR and each individual circulating purine. Serum levels of guanosine and inosine, corresponding to precursors in the purine metabolic pathway, were negatively associated with kidney function (Figure 7B). Additionally, we found a very strong negative correlation of uric acid serum levels with eGFR in our cohort (Figures 7B and S7B), which is in line with uric acid concentrations as a predictor of chronic kidney disease progression (Bellomo et al., 2010; Johnson et al., 2013a).

Variation of the eGFR was tested against the intake of dietary food groups while controlling for relevant clinical parameters, notably the participant's age and BMI, as well as blood plasma levels of glucose and triglycerides. We found that eGFR was very strongly associated with age, as well as the consumption of sweets, which are rich in sucrose and other sugars (Figure 7C). Thus, the consumption of high-sugar-containing food explains variations in renal function in our human cohort.

To obtain further insight into the association between diet and renal function, we derived the molecular composition of all food items consumed, and observed that sugars, but interestingly, not dietary purines, were associated with eGFR (Figure 7D). Dietary sugar intake by many study participants could mainly be linked to the consumption of sweets and fruits; whereas for some individuals, total dietary sugars were almost exclusively derived from soft drinks or juices (Figure S7C). Milk products, likely due to lactose

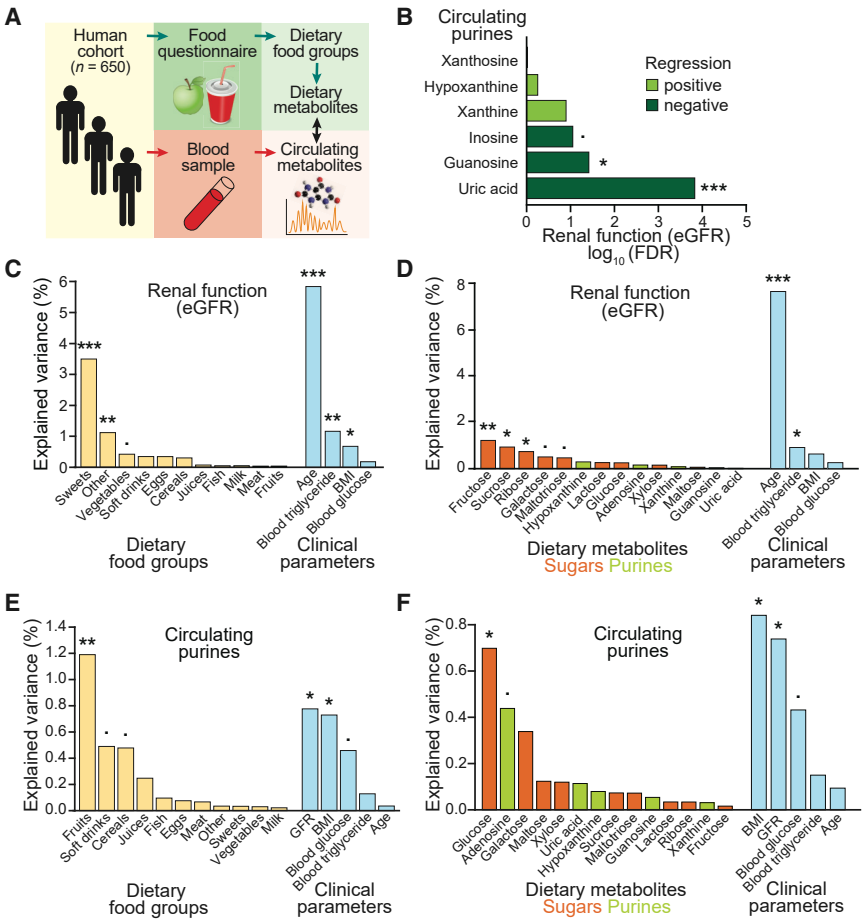


Figure 7. Human Metabolomics Analysis Links Dietary Sugar Intake with Renal Function and Circulating Purine Levels

(A) Scheme of the experimental setup to assess dietary intake and circulating metabolites in a German population cohort (n = 650). Dietary habits and food choices were recorded via the EPIC food frequency questionnaire for the past 12 months on the day of examination and used to impute dietary intake of individual metabolites. Blood was drawn at a single time point, and the serum was subjected to metabolomics by LC-MS to obtain levels of circulating metabolites.

(B) Linear model of eGFR predicting concentrations of each individual circulating purine. Logarithmic FDRs are plotted as bars and color-coded for positive (light green) or negative (dark green) regressions.

(C and D) Explained variance of diet on eGFR via PERMANOVA (·p < 0.1; *p < 0.05; **p < 0.01; ***p < 0.001). Clinical parameters are separated from dietary food groups for visual clarity. (C) Analysis of variance for dietary food groups. The food items contributing significantly from the "other" group were fats and oils (**) and non-alcoholic beverages (*). (D) Analysis of variance for imputed dietary metabolites, color-coded in orange for sugars and green for purines.

(E and F) Explained variance of diet on the levels of circulating purines in the serum via PERMANOVA (·p < 0.1; *p < 0.05; **p < 0.01). Clinical parameters are separated from dietary food groups for visual clarity. Analysis of variance for dietary food groups (E), and for imputed dietary metabolites, color-coded in orange for sugars and green for purines (F).

See also Figure S7.

content, and other food groups contributed only moderately to the total sugar intake of individual diets (Figure S7C).

To further strengthen the link between dietary habits (i.e., sugar consumption) and serum purine levels, we tested the association between circulating purines and dietary food groups while controlling for relevant clinical parameters, including eGFR. Our metabolomics data showed a significant interaction between circulating levels of purines and the consumption of fruits, as well as a marginally significant interaction with soft drinks and cereals (Figure 7E). All these food groups are rich in carbohydrates: soft drinks are expected to be rich in sucrose while cereals mainly contain starch, and fruits are known to have high fructose and glucose content. Surprisingly, circulating purine levels in the serum were not associated with the consumption of purine-rich food groups such as fish and meat (Figure 7E). In order to exclude that dietary intake of these food items was not a general modulator of serum metabolome, we performed a further analysis for circulating fatty acids. We found that levels of circulating fatty acids were most strongly influenced by the consumption of fish and meat (Figures S7D and S7E). Therefore, dietary intake of foods rich in carbohydrates and sugars can strongly predict circulating purine levels, but not fatty acids, in human serum.

In order to identify the specific dietary metabolites within these food groups that most strongly influenced circulating purine levels, we assessed their imputed molecular composition and found that dietary glucose was most strongly associated with circulating purine levels (Figure 7F). As dietary habits can differ between females and males, the previous analysis of the full cohort (n = 650) was repeated after stratification by gender. In female participants (n = 283), the associations did not reach significance thresholds (Figure S7F); however, in males (n = 367), dietary glucose intake was confirmed to be significantly associated with circulating purine levels (Figure S7G). Dietary glucose intake of most study participants could be mainly attributed to the consumption of fruits and sweets; whereas for some individuals, total dietary glucose was almost exclusively derived from soft drinks (Figure S7H). We also detected a strong correlation between dietary intake of glucose and fructose in our cohort (Figure S7I). Furthermore, using analysis of variance (Figures 7E and 7F) and linear modeling (Figure S7J), we found that BMI was significantly correlated with circulating purine levels, and in concordance with a recent study profiling individuals with obesity (Cirulli et al., 2019), especially positively correlated with serum uric acid (Figure S7K). Altogether, from our metabolomics analysis of a human cohort, circulating purine levels were positively correlated to dietary sugar intake, specifically glucose, with the consumption of fruits, sweets, and soft drinks being the most likely contributing food groups. We also found that eGFR was strongly associated with dietary sugars and the

consumption of sweets, as well as negatively correlated with circulating levels of the purines guanosine and uric acid. Therefore, consistent with our findings in *Drosophila*, a high-sugar diet also influences renal function and purine metabolism in humans.

DISCUSSION

Obesity is a major public health concern, with over 650 million adults worldwide estimated as clinically obese (WHO, 2020). Much of this obesity epidemic is attributed to increased consumption of sugary foods and drinks (Lustig et al., 2012). These lifestyle factors have been implicated in decreased human life expectancy, although the impact of obesity on health and survival is complex and not fully understood (Flegal et al., 2013; Hughes, 2013; Ortega et al., 2018). In this study, we show that a high-sugar diet causes a complex pathophysiological response in adult *Drosophila*. High-sugar feeding induced thirst, obesity, hyperglycemia, insulin resistance, and glycation damage—the classical hallmarks of T2D and metabolic disease. Critically, the lifespan-shortening effect of a high-sugar diet was rescued by water supplementation, whereas the metabolic pathologies of obesity and insulin resistance, widely attributed as responsible for the decreased survival, were in fact water independent. Indeed, flies on the high-sugar diet supplemented with water still exhibited all the diabetic-like metabolic defects, yet remarkably had the same survival as healthy controls, showing that obesity and insulin resistance per se do not shorten lifespan. Therefore, our study provides an elegant system to uncouple these aging and disease phenotypes, which is particularly interesting in light of the "fat but fit" paradox (Flegal et al., 2013; Hughes, 2013; Ortega et al., 2018).

We have demonstrated that the lifespan-shortening effects of a high-sugar diet occur via enhanced supply of metabolic precursors for purine biosynthesis, fueling increased purine catabolism. Our finding that *Δfoxo* mutants were hypersensitive to dietary sugar and the formation of tubule stones is consistent with a recent report that FOXO overexpression protects against the formation of uric acid concretions on a high-yeast diet in a fly model of urate oxidase deficiency (Lang et al., 2019). Furthermore, an SNP in human FOXO3 was found to be significantly associated with serum uric acid levels (Lang et al., 2019). Together, these observations highlight the potentially conserved role of the IIS pathway in regulating purine metabolism. From a human population cohort comprising 650 participants for which comprehensive serum metabolomics and detailed dietary records were available, we found that consumption of sugar-rich foods displayed a strong association with circulating purine levels. At the molecular level, the strongest predictor of circulating purine levels was dietary glucose intake. Our observations are supported by an earlier study, which focused only on the consumption of soft drinks and juices, and showed an association with serum uric acid measurements (Choi et al., 2008). Altogether, our population cohort analysis links dietary sugars to circulating purines and supports a shared mechanism between *Drosophila* and humans.

A combination of factors promotes the development of concretions in response to a high-sugar diet: (1) enhanced purine flux, increasing production of stone-precursor metabolites including uric acid, (2) the dehydration state, further concentrating their local levels within the organism, and (3) the acidification of the tubules and digestive tract, biochemically favoring uric acid stone formation (Barr, 1990; Johnson et al., 2018; Moe, 2006). Several human disorders are directly caused by uric acid accumulation, including gout (a form of inflammatory arthritis due to uric acid crystal deposition in the joints) and kidney stones (Barr, 1990; Moe, 2006). T2D is associated with an increased risk for uric acid kidney stones (Daudon et al., 2006), and consistent with the role of low pH in promoting uric acid crystallization, individuals with T2D exhibit urine acidification (pH < 5.5; Bell, 2012). Beyond the specific diseases of gout and kidney stones, elevated serum uric acid (hyperuricemia) has emerged from many clinical studies as a biomarker or risk factor for metabolic disease. Hyperuricemia was found to increase the prevalence of metabolic syndrome (Choi and Ford, 2007; Ford et al., 2007) and to predict the onset of T2D in several prospective studies (Bhole et al., 2010; Johnson et al., 2013b; Kodama et al., 2009; Niskanen et al., 2006). These observations raise the intriguing possibility that asymptomatic hyperuricemia (i.e., elevated serum uric acid without gout or kidney stones) may actually contribute to the progression of metabolic disease and may itself be worthy of therapeutic intervention (Johnson et al., 2013b; Levy and Cheetham, 2015). Hyperuricemia is also associated with cardiovascular disease and is a strong predictor of cardiovascular mortality (Anker et al., 2003; Kanbay et al., 2013; Niskanen et al., 2004; Zuo et al., 2016). Furthermore, hyperuricemia was identified as a predictor of mortality in acute care of hospitalized elderly patients (Breuer et al., 2017) and from several prospective studies as a risk factor for all-cause mortality (Niskanen et al., 2004; Zuo et al., 2016). Overall, this highlights that uric acid is associated with a range of metabolic and physiological disorders and potentially linked to human mortality as suggested by our study.

Here, we show that water imbalance plays an important role in mediating the pathology of both high-sugar and high-purine diets. Water is vital for all living systems, yet its importance is often overlooked in biological studies (Chaplin, 2006). For example, dehydration stress induces innate immunity in *Drosophila* through steroid signaling in the renal tubules (Zheng et al., 2018). Water dysregulation is also relevant in the context of metabolic disease. For instance, thirst is an early symptom of T2D (WHO, 2016), and low water intake is a predictor of hyperglycemia (Roussel et al., 2011). Hydration status is also known to affect kidney function and plasma uric acid levels in humans, and the geographical distribution of kidney stone prevalence is higher in hotter climates associated with dehydration (Chapman et al., 2019; Johnson et al., 2018; Moe, 2006; Sánchez-Lozada et al., 2019). Consistent with our findings in *Drosophila*, human epidemiological studies show positive effects of fluid intake on decreasing the risk of kidney stone formation (Curhan et al., 1998). Uric acid concentrations above ~6–7 mg/dL are prone to crystallization (Barr, 1990), which, interestingly, is equivalent to the ~70 ng/μL detected in the hemolymph of flies fed the high-sugar diet, showing that the levels are surprisingly well controlled and suggesting an evolutionarily conserved biochemical mechanism between distant organisms.

The XO inhibitor AP is widely prescribed to patients for the treatment of conditions associated with uric acid accumulation, including gout and kidney stones (Pacher et al., 2006). In our

study, we adopted a pharmacological approach to prevent uric acid formation by treating flies with AP. Importantly, despite AP treatment successfully clearing the tubules of uric acid stones, the accumulation of upstream metabolites in the purine degradation pathway (Bratty et al., 2011) was itself pathophysiological. Xanthine and hypoxanthine are also biochemically prone to form crystals (Miller et al., 2013), as we observed in the rectal ampulla, which may explain the incomplete rescue of survival upon AP treatment in our experiments. Consistent with our findings, genetic disruption of purine catabolism is detrimental: null mutants for XO, encoded by the *rosy* (*ry*) gene in *Drosophila*, develop xanthine tubule stones (Miller et al., 2013) and are short-lived (Shepherd et al., 1989). Therefore, although AP provided a partial rescue of the high-sugar-induced uric-acid-associated mortality, the blockage of purine catabolism was metabolically disruptive and ultimately detrimental to survival, suggesting a need for novel therapies and approaches, which could be tested for rescue of survival with the *Drosophila* model system.

Overall, our study highlights the purine catabolism pathway as a metabolic mediator of longevity, emphasizing the importance of diet and hydration as factors in promoting uric acid levels. Using *Drosophila* and a human population cohort, we provide a model to explain the pathophysiology of high-sugar diets, independently of obesity and insulin resistance. Our work paves the way for exploring the underappreciated role of both water and uric acid in the context of lifespan and provides a novel approach for discovering therapeutic strategies aimed at reducing high-sugar-induced mortality while maintaining the healthy regulation of purine catabolism.

Limitations of Study

The full relevance of our findings in *Drosophila* to sugar-induced pathophysiology in humans requires further studies in mammalian models. The human dietary information is based on self-reported intake from a food frequency questionnaire, which has inherent bias and refers to an annual average, whereas the serum metabolomics is performed on a single fasted blood sample. Our findings are from an aged cohort in Germany (average 59 years, SD 12.6 years); therefore, the analysis should be expanded to other populations to account for possible genetic and environmental factors. While the human data in our study correlate dietary sugar intake with renal function and serum purine levels, associations with human longevity still need to be explored.

STAR★METHODS

Detailed methods are provided in the online version of this paper and include the following:

- KEY RESOURCES TABLE
- LEAD CONTACT AND MATERIALS AVAILABILITY
- EXPERIMENTAL MODEL AND SUBJECT DETAILS
  - Fly Strains
  - Human Population Cohort
- METHOD DETAILS
  - Fly Media and Agar Tips
  - Fly Husbandry
  - Lifespan and Stress Assays
  - Fecundity Assays
  - Drinking and Feeding Assays
  - Freezing of Fly Samples for Molecular Assays
  - Whole Body Triglyceride Assay
  - Lipid Staining
  - Hemolymph Analysis
  - Fat Body Insulin and Glucose Assays
  - Protein Glycation and Carbonylation Assays
  - Gut Function Assays
  - Tubule and Rectal Ampulla Imaging
  - Uric Acid Assay
  - Tubule Secretion Assay
  - Metabolomics Analysis of Rectal Ampulla Stones
  - Human Blood Analysis and Metabolomics
  - Food Questionnaire and Molecular Diet Composition
  - Analysis of Variance
  - Linear Modeling
- QUANTIFICATION AND STATISTICAL ANALYSIS
  - Fly statistical analysis
  - Human Statistical Analysis
- DATA AND CODE AVAILABILITY

SUPPLEMENTAL INFORMATION

Supplemental Information can be found online at https://doi.org/10.1016/j.cmet.2020.02.016.

ACKNOWLEDGMENTS

Work in the group of H.M.C. is funded by the Medical Research Council, UK (MC-A654-5QB90). E.v.D. was supported by an Erasmus mobility studentship. J.J. was the recipient of a Commonwealth Split-site PhD Scholarship. C.K. acknowledges support by the DFG, Germany (CRC1182 "Metaorganisms" sub-project A1 and EXC2167 "Precision Medicine in Chronic Inflammation" sub-project RTF-VIII). We are grateful to members of the Cochemé lab and our colleagues in the groups of Irene Miguel-Aliaga and Susumu Hirabayashi for helpful discussion and input, especially Dafni Hadjieconomou and Chris Studd. We thank Linda Partridge, Cathy Slack, and the Bloomington Stock Center for fly lines. We acknowledge Paola Cognigni and Matthew Wayland for advice on excreta analysis with TURD software. We thank Filipe Cabreiro, Mike Murphy, Ivana Bjedov, and Jorge Ivan Castillo-Quan for valuable feedback.

AUTHOR CONTRIBUTIONS

H.M.C. conceived the project and supervised the fly work. E.v.D., L.A.G.v.L., E.d.S., J.J., C.L., A.J.V., A. Foley, M.B., and H.M.C. performed and analyzed fly experiments. J.B.M. and H.B.K. performed the fly metabolomics analysis. L.B. and G.M. analyzed the human dietary and metabolomics data, supervised by C.K. W.L., M.L., and A. Franke are responsible for overseeing the human cohort and biobank. H.M.C. wrote the manuscript with input from all authors.

DECLARATION OF INTERESTS

The authors declare no competing interests.

Received: August 19, 2019
Revised: January 29, 2020
Accepted: February 24, 2020
Published: March 19, 2020

REFERENCES

Anker, S.D., Doehner, W., Rauchhaus, M., Sharma, R., Francis, D., Knosalla, C., Davos, C.H., Cicoira, M., Shamim, W., Kemp, M., et al. (2003). Uric acid

and survival in chronic heart failure: validation and application in metabolic, functional, and hemodynamic staging. Circulation *107*, 1991–1997.

Baker, K.D., and Thummel, C.S. (2007). Diabetic larvae and obese flies-emerging studies of metabolism in *Drosophila*. Cell Metab. *6*, 257–266.

Barr, W.G. (1990). Uric Acid. In Clinical Methods: The History, Physical, and Laboratory Examinations, H.K. Walker, W.D. Hall, and J.W. Hurst, eds. (Butterworths), pp. 770–772.

Bass, T.M., Grandison, R.C., Wong, R., Martinez, P., Partridge, L., and Piper, M.D. (2007). Optimization of dietary restriction protocols in *Drosophila*. J. Gerontol. A Biol. Sci. Med. Sci. *62*, 1071–1081.

Bell, D.S. (2012). Beware the low urine pH–the major cause of the increased prevalence of nephrolithiasis in the patient with type 2 diabetes. Diabetes Obes. Metab. *14*, 299–303.

Bellomo, G., Venanzi, S., Verdura, C., Saronio, P., Esposito, A., and Timio, M. (2010). Association of uric acid with change in kidney function in healthy normotensive individuals. Am. J. Kidney Dis. *56*, 264–272.

Benjamini, Y., and Hochberg, Y. (1995). Controlling the False Discovery Rate - a Practical and Powerful Approach to Multiple Testing. Journal of the Royal Statistical Society. Series B *57*, 289–300.

Bhole, V., Choi, J.W., Kim, S.W., de Vera, M., and Choi, H. (2010). Serum uric acid levels and the risk of type 2 diabetes: a prospective study. Am. J. Med. *123*, 957–961.

Brandstetter, B.R., Korfmann, A., Kroke, A., Becker, N., Schulze, M.B., and Boeing, H. (1999). Dietary habits in the German EPIC cohorts: food group intake estimated with the food frequency questionnaire. European Investigation into Cancer and Nutrition. Ann. Nutr. Metab. *43*, 246–257.

Bratty, M.A., Hobani, Y., Dow, J.A.T., and Watson, D.G. (2011). Metabolomic profiling of the effects of allopurinol on *Drosophila melanogaster*. Metabolomics *7*, 542–548.

Breuer, G.S., Schwartz, Y., Freier-Dror, Y., and Nesher, G. (2017). Uric acid level as predictor of mortality in the acute care setting of advanced age population. Eur. J. Intern. Med. *44*, 74–76.

Broughton, S.J., Piper, M.D., Ikeya, T., Bass, T.M., Jacobson, J., Driege, Y., Martinez, P., Hafen, E., Withers, D.J., Leevers, S.J., and Partridge, L. (2005). Longer lifespan, altered metabolism, and stress resistance in *Drosophila* from ablation of cells making insulin-like ligands. Proc. Natl. Acad. Sci. USA *102*, 3105–3110.

Chaplin, M. (2006). Do we underestimate the importance of water in cell biology? Nat. Rev. Mol. Cell Biol. *7*, 861–866.

Chapman, C.L., Johnson, B.D., Sackett, J.R., Parker, M.D., and Schlader, Z.J. (2019). Soft drink consumption during and following exercise in the heat elevates biomarkers of acute kidney injury. Am. J. Physiol. Regul. Integr. Comp. Physiol. *316*, R189–R198.

Chatterjee, S., Khunti, K., and Davies, M.J. (2017). Type 2 diabetes. Lancet *389*, 2239–2251.

Choi, H.K., and Ford, E.S. (2007). Prevalence of the metabolic syndrome in individuals with hyperuricemia. Am. J. Med. *120*, 442–447.

Choi, J.W., Ford, E.S., Gao, X., and Choi, H.K. (2008). Sugar-sweetened soft drinks, diet soft drinks, and serum uric acid level: the Third National Health and Nutrition Examination Survey. Arthritis Rheum. *59*, 109–116.

Cirulli, E.T., Guo, L., Leon Swisher, C., Shah, N., Huang, L., Napier, L.A., Kirkness, E.F., Spector, T.D., Caskey, C.T., Thorens, B., et al. (2019). Profound Perturbation of the Metabolome in Obesity Is Associated with Health Risk. Cell Metab. *29*, 488–500.e2.

Cognigni, P., Bailey, A.P., and Miguel-Aliaga, I. (2011). Enteric neurons and systemic signals couple nutritional and reproductive status with intestinal homeostasis. Cell Metab. *13*, 92–104.

Curhan, G.C., Willett, W.C., Speizer, F.E., and Stampfer, M.J. (1998). Beverage use and risk for kidney stones in women. Ann. Intern. Med. *128*, 534–540.

Daudon, M., Traxer, O., Conort, P., Lacour, B., and Jungers, P. (2006). Type 2 diabetes increases the risk for uric acid stones. J. Am. Soc. Nephrol. *17*, 2026–2033.

DeFronzo, R.A., Ferrannini, E., Groop, L., Henry, R.R., Herman, W.H., Holst, J.J., Hu, F.B., Kahn, C.R., Raz, I., Shulman, G.I., et al. (2015). Type 2 diabetes mellitus. Nat. Rev. Dis. Primers *1*, 15019.

Dow, J.A., and Romero, M.F. (2010). *Drosophila* provides rapid modeling of renal development, function, and disease. Am. J. Physiol. Renal Physiol. *299*, F1237–F1244.

Dow, J.A., Maddrell, S.H., Görtz, A., Skaer, N.J., Brogan, S., and Kaiser, K. (1994). The malpighian tubules of *Drosophila melanogaster*: a novel phenotype for studies of fluid secretion and its control. J. Exp. Biol. *197*, 421–428.

Fanson, B.G., Yap, S., and Taylor, P.W. (2012). Geometry of compensatory feeding and water consumption in *Drosophila melanogaster*. J. Exp. Biol. *215*, 766–773.

Flatt, T. (2011). Survival costs of reproduction in *Drosophila*. Exp. Gerontol. *46*, 369–375.

Flegal, K.M., Kit, B.K., Orpana, H., and Graubard, B.I. (2013). Association of all-cause mortality with overweight and obesity using standard body mass index categories: a systematic review and meta-analysis. JAMA *309*, 71–82.

Ford, E.S., Li, C., Cook, S., and Choi, H.K. (2007). Serum concentrations of uric acid and the metabolic syndrome among US children and adolescents. Circulation *115*, 2526–2532.

Garrido, D., Rubin, T., Poidevin, M., Maroni, B., Le Rouzic, A., Parvy, J.P., and Montagne, J. (2015). Fatty acid synthase cooperates with glyoxalase 1 to protect against sugar toxicity. PLoS Genet. *11*, e1004995.

Gems, D., and Partridge, L. (2008). Stress-response hormesis and aging: "that which does not kill us makes us stronger". Cell Metab. *7*, 200–203.

Ghimire, S., Terhzaz, S., Cabrero, P., Romero, M.F., Davies, S.A., and Dow, J.A.T. (2019). Targeted renal knockdown of Na^+/H^+ exchanger regulatory factor *Sip1* produces uric acid nephrolithiasis in *Drosophila*. Am. J. Physiol. Renal Physiol. *317*, F930–F940.

Ghosh, A.C., and O'Connor, M.B. (2014). Systemic Activin signaling independently regulates sugar homeostasis, cellular metabolism, and pH balance in *Drosophila melanogaster*. Proc. Natl. Acad. Sci. USA *111*, 5729–5734.

Gibbs, A.G., and Markow, T.A. (2001). Effects of age on water balance in *Drosophila* species. Physiol. Biochem. Zool. *74*, 520–530.

Goh, S.Y., and Cooper, M.E. (2008). Clinical review: The role of advanced glycation end products in progression and complications of diabetes. J. Clin. Endocrinol. Metab. *93*, 1143–1152.

Grandison, R.C., Piper, M.D., and Partridge, L. (2009a). Amino-acid imbalance explains extension of lifespan by dietary restriction in *Drosophila*. Nature *462*, 1061–1064.

Grandison, R.C., Wong, R., Bass, T.M., Partridge, L., and Piper, M.D. (2009b). Effect of a standardised dietary restriction protocol on multiple laboratory strains of *Drosophila melanogaster*. PLoS ONE *4*, e4067.

Hughes, V. (2013). The big fat truth. Nature *497*, 428–430.

Ikeya, T., Broughton, S., Alic, N., Grandison, R., and Partridge, L. (2009). The endosymbiont Wolbachia increases insulin/IGF-like signalling in *Drosophila*. Proc. Biol. Sci. *276*, 3799–3807.

Itskov, P.M., Moreira, J.M., Vinnik, E., Lopes, G., Safarik, S., Dickinson, M.H., and Ribeiro, C. (2014). Automated monitoring and quantitative analysis of feeding behaviour in *Drosophila*. Nat. Commun. *5*, 4560.

Ja, W.W., Carvalho, G.B., Mak, E.M., de la Rosa, N.N., Fang, A.Y., Liong, J.C., Brummel, T., and Benzer, S. (2007). Prandiology of *Drosophila* and the CAFE assay. Proc. Natl. Acad. Sci. USA *104*, 8253–8256.

Ja, W.W., Carvalho, G.B., Zid, B.M., Mak, E.M., Brummel, T., and Benzer, S. (2009). Water- and nutrient-dependent effects of dietary restriction on *Drosophila* lifespan. Proc. Natl. Acad. Sci. USA *106*, 18633–18637.

Jacobson, J., Lambert, A.J., Portero-Otín, M., Pamplona, R., Magwere, T., Miwa, S., Driege, Y., Brand, M.D., and Partridge, L. (2010). Biomarkers of aging in *Drosophila*. Aging Cell *9*, 466–477.

Johnson, R.J., Nakagawa, T., Jalal, D., Sánchez-Lozada, L.G., Kang, D.H., and Ritz, E. (2013a). Uric acid and chronic kidney disease: which is chasing which? Nephrol. Dial. Transplant. *28*, 2221–2228.

Johnson, R.J., Nakagawa, T., Sanchez-Lozada, L.G., Shafiu, M., Sundaram, S., Le, M., Ishimoto, T., Sautin, Y.Y., and Lanaspa, M.A. (2013b). Sugar, uric acid, and the etiology of diabetes and obesity. Diabetes *62*, 3307–3315.

Johnson, R.J., Perez-Pozo, S.E., Lillo, J.L., Grases, F., Schold, J.D., Kuwabara, M., Sato, Y., Hernando, A.A., Garcia, G., Jensen, T., et al. (2018). Fructose increases risk for kidney stones: potential role in metabolic syndrome and heat stress. BMC Nephrol. *19*, 315.

Kanbay, M., Segal, M., Afsar, B., Kang, D.H., Rodriguez-Iturbe, B., and Johnson, R.J. (2013). The role of uric acid in the pathogenesis of human cardiovascular disease. Heart *99*, 759–766.

Koch, M., Borggrefe, J., Barbaresko, J., Groth, G., Jacobs, G., Siegert, S., Lieb, W., Müller, M.J., Bosy-Westphal, A., Heller, M., and Nöthlings, U. (2014). Dietary patterns associated with magnetic resonance imaging-determined liver fat content in a general population study. Am. J. Clin. Nutr. *99*, 369–377.

Koch, M., Freitag-Wolf, S., Schlesinger, S., Borggrefe, J., Hov, J.R., Jensen, M.K., Pick, J., Markus, M.R.P., Höpfner, T., Jacobs, G., et al. (2017). Serum metabolomic profiling highlights pathways associated with liver fat content in a general population sample. Eur. J. Clin. Nutr. *71*, 995–1001.

Kodama, S., Saito, K., Yachi, Y., Asumi, M., Sugawara, A., Totsuka, K., Saito, A., and Sone, H. (2009). Association between serum uric acid and development of type 2 diabetes. Diabetes Care *32*, 1737–1742.

Lang, S., Hilsabeck, T.A., Wilson, K.A., Sharma, A., Bose, N., Brackman, D.J., Beck, J.N., Chen, L., Watson, M.A., Killilea, D.W., et al. (2019). A conserved role of the insulin-like signaling pathway in diet-dependent uric acid pathologies in *Drosophila melanogaster*. PLoS Genet. *15*, e1008318.

Leader, D.P., Krause, S.A., Pandit, A., Davies, S.A., and Dow, J.A.T. (2018). FlyAtlas 2: a new version of the *Drosophila melanogaster* expression atlas with RNA-Seq, miRNA-Seq and sex-specific data. Nucleic Acids Res. *46* (D1), D809–D815.

Levey, A.S., Coresh, J., Greene, T., Stevens, L.A., Zhang, Y.L., Hendriksen, S., Kusek, J.W., and Van Lente, F.; Chronic Kidney Disease Epidemiology Collaboration (2006). Using standardized serum creatinine values in the modification of diet in renal disease study equation for estimating glomerular filtration rate. Ann. Intern. Med. *145*, 247–254.

Levy, G., and Cheetham, T.C. (2015). Is It Time to Start Treating Asymptomatic Hyperuricemia? Am. J. Kidney Dis. *66*, 933–935.

Lushchak, O.V., Gospodaryov, D.V., Rovenko, B.M., Yurkevych, I.S., Perkhulyn, N.V., and Lushchak, V.I. (2014). Specific dietary carbohydrates differentially influence the life span and fecundity of *Drosophila melanogaster*. J. Gerontol. A Biol. Sci. Med. Sci. *69*, 3–12.

Lustig, R.H., Schmidt, L.A., and Brindis, C.D. (2012). Public health: The toxic truth about sugar. Nature *482*, 27–29.

Mattila, J., and Hietakangas, V. (2017). Regulation of Carbohydrate Energy Metabolism in *Drosophila melanogaster*. Genetics *207*, 1231–1253.

Miguel-Aliaga, I., Jasper, H., and Lemaitre, B. (2018). Anatomy and Physiology of the Digestive Tract of *Drosophila melanogaster*. Genetics *210*, 357–396.

Miller, J., Chi, T., Kapahi, P., Kahn, A.J., Kim, M.S., Hirata, T., Romero, M.F., Dow, J.A., and Stoller, M.L. (2013). *Drosophila melanogaster* as an emerging translational model of human nephrolithiasis. J. Urol. *190*, 1648–1656.

Moe, O.W. (2006). Kidney stones: pathophysiology and medical management. Lancet *367*, 333–344.

Morris, S.N., Coogan, C., Chamseddin, K., Fernandez-Kim, S.O., Kolli, S., Keller, J.N., and Bauer, J.H. (2012). Development of diet-induced insulin resistance in adult *Drosophila melanogaster*. Biochim. Biophys. Acta *1822*, 1230–1237.

Müller, N., Schulte, D.M., Türk, K., Freitag-Wolf, S., Hampe, J., Zeuner, R., Schröder, J.O., Gouni-Berthold, I., Berthold, H.K., Krone, W., et al. (2015). IL-6 blockade by monoclonal antibodies inhibits apolipoprotein (a) expression and lipoprotein (a) synthesis in humans. J. Lipid Res. *56*, 1034–1042.

Musselman, L.P., Fink, J.L., Narzinski, K., Ramachandran, P.V., Hathiramani, S.S., Cagan, R.L., and Baranski, T.J. (2011). A high-sugar diet produces obesity and insulin resistance in wild-type *Drosophila*. Dis. Model. Mech. *4*, 842–849.

Na, J., Musselman, L.P., Pendse, J., Baranski, T.J., Bodmer, R., Ocorr, K., and Cagan, R. (2013). A *Drosophila* model of high sugar diet-induced cardiomyopathy. PLoS Genet. *9*, e1003175.

Niskanen, L.K., Laaksonen, D.E., Nyyssönen, K., Alfthan, G., Lakka, H.M., Lakka, T.A., and Salonen, J.T. (2004). Uric acid level as a risk factor for cardiovascular and all-cause mortality in middle-aged men: a prospective cohort study. Arch. Intern. Med. *164*, 1546–1551.

Niskanen, L., Laaksonen, D.E., Lindström, J., Eriksson, J.G., Keinänen-Kiukaanniemi, S., Ilanne-Parikka, P., Aunola, S., Hämäläinen, H., Tuomilehto, J., and Uusitupa, M. (2006). Serum uric acid as a harbinger of metabolic outcome in subjects with impaired glucose tolerance: the Finnish Diabetes Prevention Study. Diabetes Care *29*, 709–711.

Ortega, F.B., Ruiz, J.R., Labayen, I., Lavie, C.J., and Blair, S.N. (2018). The Fat but Fit paradox: what we know and don't know about it. Br. J. Sports Med. *52*, 151–153.

Oudes, A.J., Herr, C.M., Olsen, Y., and Fleming, J.E. (1998). Age-dependent accumulation of advanced glycation end-products in adult *Drosophila melanogaster*. Mech. Ageing Dev. *100*, 221–229.

Owusu-Ansah, E., and Perrimon, N. (2014). Modeling metabolic homeostasis and nutrient sensing in *Drosophila*: implications for aging and metabolic diseases. Dis. Model. Mech. *7*, 343–350.

Pacher, P., Nivorozhkin, A., and Szabó, C. (2006). Therapeutic effects of xanthine oxidase inhibitors: renaissance half a century after the discovery of allopurinol. Pharmacol. Rev. *58*, 87–114.

Padmanabha, D., and Baker, K.D. (2014). *Drosophila* gains traction as a repurposed tool to investigate metabolism. Trends Endocrinol. Metab. *25*, 518–527.

Partridge, L., Alic, N., Bjedov, I., and Piper, M.D. (2011). Ageing in *Drosophila*: the role of the insulin/Igf and TOR signalling network. Exp. Gerontol. *46*, 376–381.

Piper, M.D., Wong, R., Grandison, R.C., Bass, T.M., Martinez, P.M., and Partridge, L. (2010). Water-independent effects of dietary restriction in *Drosophila*. Proc. Natl. Acad. Sci. USA *107*, E54–E56, author reply E57.

Pryor, R., Norvaisas, P., Marinos, G., Best, L., Thingholm, L.B., Quintaneiro, L.M., De Haes, W., Esser, D., Waschina, S., Lujan, C., et al. (2019). Host-Microbe-Drug-Nutrient Screen Identifies Bacterial Effectors of Metformin Therapy. Cell *178*, 1299–1312.e29.

Rera, M., Clark, R.I., and Walker, D.W. (2012). Intestinal barrier dysfunction links metabolic and inflammatory markers of aging to death in *Drosophila*. Proc. Natl. Acad. Sci. USA *109*, 21528–21533.

Riera, C.E., Merkwirth, C., De Magalhaes Filho, C.D., and Dillin, A. (2016). Signaling Networks Determining Life Span. Annu. Rev. Biochem. *85*, 35–64.

Roussel, R., Fezeu, L., Bouby, N., Balkau, B., Lantieri, O., Alhenc-Gelas, F., Marre, M., and Bankir, L.; D.E.S.I.R. Study Group (2011). Low water intake and risk for new-onset hyperglycemia. Diabetes Care *34*, 2551–2554.

Rovenko, B.M., Kubrak, O.I., Gospodaryov, D.V., Perkhulyn, N.V., Yurkevych, I.S., Sanz, A., Lushchak, O.V., and Lushchak, V.I. (2015). High sucrose consumption promotes obesity whereas its low consumption induces oxidative stress in *Drosophila melanogaster*. J. Insect Physiol. *79*, 42–54.

Sánchez-Lozada, L.G., Roncal-Jimenez, C.A., García-Arroyo, F.E., Jensen, T., Lanaspa, M.A., and Johnson, R.J. (2019). The perils of rehydrating with soft drinks following heat and exercise. Am. J. Physiol. Regul. Integr. Comp. Physiol. *316*, R187–R188.

Schellinger, J.N., and Rodan, A.R. (2015). Use of the Ramsay Assay to Measure Fluid Secretion and Ion Flux Rates in the *Drosophila melanogaster* Malpighian Tubule. J. Vis. Exp. *105*, 53144.

Schindelin, J., Arganda-Carreras, I., Frise, E., Kaynig, V., Longair, M., Pietzsch, T., Preibisch, S., Rueden, C., Saalfeld, S., Schmid, B., et al. (2012). Fiji: an open-source platform for biological-image analysis. Nat. Methods *9*, 676–682.

Shell, B.C., Schmitt, R.E., Lee, K.M., Johnson, J.C., Chung, B.Y., Pletcher, S.D., and Grotewiel, M. (2018). Measurement of solid food intake in *Drosophila* via consumption-excretion of a dye tracer. Sci. Rep. *8*, 11536.

Shepherd, J.C., Walldorf, U., Hug, P., and Gehring, W.J. (1989). Fruit flies with additional expression of the elongation factor EF-1 alpha live longer. Proc. Natl. Acad. Sci. USA *86*, 7520–7521.

Skorupa, D.A., Dervisefendic, A., Zwiener, J., and Pletcher, S.D. (2008). Dietary composition specifies consumption, obesity, and lifespan in *Drosophila melanogaster*. Aging Cell *7*, 478–490.

Slack, C., Giannakou, M.E., Foley, A., Goss, M., and Partridge, L. (2011). dFOXO-independent effects of reduced insulin-like signaling in *Drosophila*. Aging Cell *10*, 735–748.

Teleman, A.A. (2009). Molecular mechanisms of metabolic regulation by insulin in *Drosophila*. Biochem. J. *425*, 13–26.

Toivonen, J.M., Walker, G.A., Martinez-Diaz, P., Bjedov, I., Driege, Y., Jacobs, H.T., Gems, D., and Partridge, L. (2007). No influence of Indy on lifespan in *Drosophila* after correction for genetic and cytoplasmic background effects. PLoS Genet. *3*, e95.

vanEngelsdorp, D., Traynor, K.S., Andree, M., Lichtenberg, E.M., Chen, Y., Saegerman, C., and Cox-Foster, D.L. (2017). Colony Collapse Disorder (CCD) and bee age impact honey bee pathophysiology. PLoS ONE *12*, e0179535.

Wayland, M.T., Defaye, A., Rocha, J., Jayaram, S.A., Royet, J., Miguel-Aliaga, I., Leulier, F., and Cognigni, P. (2014). Spotting the differences: probing host/microbiota interactions with a dedicated software tool for the analysis of faecal outputs in *Drosophila*. J. Insect Physiol. *69*, 126–135.

WHO (2016). Global Report on Diabetes (World Health Organization).

WHO (2020). "Obesity and Overweight" Factsheet (World Health Organization), https://www.who.int/news-room/fact-sheets/detail/obesity-and-overweight.

Wong, R., Piper, M.D., Wertheim, B., and Partridge, L. (2009). Quantification of food intake in *Drosophila*. PLoS One *4*, e6063.

Zheng, W., Rus, F., Hernandez, A., Kang, P., Goldman, W., Silverman, N., and Tatar, M. (2018). Dehydration triggers ecdysone-mediated recognition-protein priming and elevated anti-bacterial immune responses in *Drosophila* Malpighian tubule renal cells. BMC Biol. *16*, 60.

Zuo, T., Liu, X., Jiang, L., Mao, S., Yin, X., and Guo, L. (2016). Hyperuricemia and coronary heart disease mortality: a meta-analysis of prospective cohort studies. BMC Cardiovasc. Disord. *16*, 207.

STAR★METHODS

KEY RESOURCES TABLE

REAGENT or RESOURCE	SOURCE	IDENTIFIER
Antibodies		
Rabbit polyclonal anti-*Drosophila* phospho-AKT (Ser505), dil: 1/1000	Cell Signaling Technology	Cat# 4054; RRID:AB_331414
Rabbit polyclonal anti-total AKT, dil: 1/1000	Cell Signaling Technology	Cat# 9272; RRID:AB_329827
Mouse monoclonal anti-β-actin, dil: 1/1000	Abcam	Cat# ab8224; RRID:AB_449644
Goat polyclonal anti-AGE (advanced glycated end-products), dil:1/2000	Millipore	Cat# AB9890; RRID:AB_805248
Chemicals, Peptides, and Recombinant Proteins		
Sucrose (granulated sugar)	Tate & Lyle	N/A
Brewer's yeast	MP Biomedicals	Cat# 903312
Agar	Sigma-Aldrich	Cat# A7002
Nipagin (Methyl 4-hydroxybenzoate)	Sigma-Aldrich	Cat# H5501
Propionic acid	Sigma-Aldrich	Cat# P1386
D-Fructose	Sigma-Aldrich	Cat# F0127
D-Glucose	Sigma-Aldrich	Cat# G8270
Allopurinol	Sigma-Aldrich	Cat# A8003
Adenine	Sigma-Aldrich	Cat# A8626
Guanine	Sigma-Aldrich	Cat# G11950
Paraquat	Sigma-Aldrich	Cat# 856177
Brilliant Blue FCF food dye	Town End (Leeds) Plc, UK	https://www.dyes.co.uk/water-soluble-powder-colours.html
Nile Red stain	Thermo Fisher Scientific (Invitrogen)	Cat# N1142
Trehalase	Megazyme	Cat# E-TREH
Insulin	Sigma-Aldrich	Cat# I9278
2-NBDG (2-(*N*-(7-nitrobenz-2-oxa-1,3-diazol-4-yl)amino)-2-deoxyglucose)	Thermo Fisher Scientific (Invitrogen)	Cat# N13195
Mineral oil heavy	Sigma-Aldrich	Cat# 330760
Bromophenol blue	Sigma-Aldrich	Cat# B5525
Bromocresol purple	Sigma-Aldrich	Cat# B5880
Pyranine	Thermo Fisher Scientific (Invitrogen)	Cat# H348
$^{13}C_5$-Hypoxanthine	Cambridge Isotope Laboratories	Cat# CLM-8042
Uric acid	Sigma-Aldrich	Cat# U2625
Allantoin	Sigma-Aldrich	Cat# 05670
Xanthine	Sigma-Aldrich	Cat# X0626
Hypoxanthine	Sigma-Aldrich	Cat# H9377
Critical Commercial Assays		
OxyBlot Protein Detection Kit	Millipore	Cat# S7150
QuantiChrom Uric Acid Assay Kit	BioAssay Systems	Cat# DIUA-250
Deposited Data		
Northern German cohort (metabolome, clinical metadata and nutritional questionnaire)	This study	Available from the PopGen biobank (https://www.uksh.de/p2n/Information+for+Researchers.html)
Experimental Models: Organisms/Strains		
D. melanogaster: *white Dahomey* (w^{Dah})	Linda Partridge (Broughton et al., 2005)	N/A
D. melanogaster: *Dahomey*	Linda Partridge	N/A
D. melanogaster: w^{Dah} *Wolbachia* negative	Linda Partridge (Toivonen et al., 2007)	N/A

(*Continued on next page*)

Continued

REAGENT or RESOURCE	SOURCE	IDENTIFIER
D. melanogaster: w^{1118}	Linda Partridge	N/A
D. melanogaster: ovo^{D1} v^{24}/C(1)DX, y^1 w^1 f^1	Bloomington *Drosophila* Stock Center	RRID:BDSC_1309
D. melanogaster: $foxo^{\Delta 94}$/TM6B, Tb^1	Slack et al., 2011	RRID:BDSC_42220
Software and Algorithms		
TURD (v0.8)	Wayland et al., 2014	http://the-ultimate-reader-of-dung.sourceforge.net
GraphPad Prism 8	GraphPad Software	https://www.graphpad.com/scientific-software/prism/
FIJI (ImageJ v2.0.0)	Schindelin et al., 2012	https://fiji.sc
Image Lab (v5.2.1)	BioRad	https://www.bio-rad.com
Xcalibur software (v4.1)	Thermo Fisher Scientific	https://www.thermofisher.com/
R (v3.6.1)	R Core Team	https://www.r-project.org
Vegan (v2.5-6)	https://cran.r-project.org/package=vegan	N/A
RColorBrewer (v1.1-2)	https://cran.r-project.org/package=RColorBrewer	N/A
Other		
Triglyceride Infinity Reagent	Thermo Fisher Scientific	Cat# TR22421
Glucose Infinity Reagent	Thermo Fisher Scientific	Cat# TR15421
Schneider's *Drosophila* medium	Thermo Fisher Scientific (GIBCO)	Cat# 21720024
Laemmli buffer	BioRad	Cat# 1610737
BCA Protein Assay Kit	Thermo Fisher Scientific (Pierce)	Cat# 23225

LEAD CONTACT AND MATERIALS AVAILABILITY

Further information and requests for resources and reagents should be directed and will be fulfilled by the Lead Contact, Helena Cochemé (helena.cocheme@lms.mrc.ac.uk). This study did not generate new unique reagents.

EXPERIMENTAL MODEL AND SUBJECT DETAILS

Fly Strains

For the majority of experiments, the *white Dahomey* (w^{Dah}) strain of *Drosophila melanogaster* was used as the outbred WT background (Broughton et al., 2005). Additional experiments were performed in the parental *Dahomey* strain, a w^{Dah} strain cured from *Wolbachia* infection (Toivonen et al., 2007), and the isogenic control line w^{1118} (all kindly received from Linda Partridge, UCL). The mutant lines $foxo^{\Delta 94}$ (Slack et al., 2011) and ovo^{D1} (Bloomington, #1309) were backcrossed into the w^{Dah} background for at least 10 generations. Assays were mostly performed on mated females, unless otherwise stated. All experiments were performed at 25°C, 65% humidity on a 12 h light:12 h dark cycle.

Human Population Cohort

We analyzed data from the German population cohort FoCus (Müller et al., 2015), excluding individuals with known diagnosis of inflammatory bowel disease and syndrome, chronic diarrhea, kidney disease, or any type of diabetes. Further stratification was performed based on fasting plasma glucose levels, limited to a maximum of 125 mg/dL, considered as the borderline value between pre-diabetic and diabetic status. We determined the estimated glomerular filtration rate (eGFR) from serum creatinine levels using the formula below (Levey et al., 2006), and excluded participants with eGFR < 60 mL/min per 1.73 m^2 (i.e., mild to moderate loss of kidney function).

$$eGFR\left[\frac{\frac{mL}{min}}{1.73m^2}\right] = 186 \cdot \frac{creatinine\left[\frac{\mu mol}{L}\right]}{88.4}^{-1.154} \cdot age[years]^{-0.203} \cdot sex[female = 0.742; male = 1]$$

We also excluded any individuals on anti-gout medication. Our remaining participant count was n = 650. Besides diagnostic and medication usage information, clinical parameters such as BMI and age were recorded for each participant in the cohort,

summarized in Table S5. The study was approved by the ethical review board of the Medical Faculty of Kiel University (Kiel, Germany). Written informed consent was obtained from all study participants (Koch et al., 2017).

METHOD DETAILS

Fly Media and Agar Tips

Flies were raised on standard sugar-yeast-agar medium (5%S) consisting of: 5% w/v sucrose (granulated sugar, Tate & Lyle), 10% w/v Brewer's yeast (#903312, MP Biomedicals), 1.5% w/v agar (Sigma A7002), supplemented with nipagin (Sigma H5501; 30 mL/L of 10% w/v nipagin in 95% EtOH) and propionic acid (0.3% v/v; Sigma P1386) as preservatives, added once the food had cooled down to < 60°C (Grandison et al., 2009b). For high-sugar food, the sugar content was increased 4-fold to 20% w/v sucrose (20%S). For some experiments, the sugar content was increased 6-fold to 30% w/v sucrose (30%S) or 8-fold to 40% w/v sucrose (40%S). For low-sugar food, the sugar content was deceased to 0%, 1% and 2.5% w/v sucrose (0%S, 1%S and 2.5%S respectively). For selected experiments, the 5%S diet was supplemented with a 15% w/v excess of D-fructose (Sigma F0127) or D-glucose (Sigma G8270). Note that the protein source (yeast) was maintained constant throughout. For drug treatments, the food was supplemented with 10 μM, 100 μM or 1 mM allopurinol (Sigma A8003). For the high-purine diet, the 5%S food was supplemented with 10 mM purine, consisting of 5 mM adenine (Sigma A8626) and 5 mM guanine (Sigma G11950). See Table S1 for all media recipes.

To supply water to the flies, 20 μL filter tips (Starlab) containing 1.5% (w/v) agar were inserted into the food vials. These + H_2O tips were filled to bulging with agar to avoid them drying out (also helped by the lower position of the filter within these 20 μL tips, allowing for a larger volume of agar). As controls, empty 100 μL filter tips (Starlab) were used (the higher position of the filter prevented flies from being stuck in narrower regions of the tip). ~6 mL of food was dispensed into narrow plastic vials (25 × 95 mm; #32-109, FlyStuff, Genesee Scientific). This depth (~2 cm) ensured that the tips were sufficiently secured when inserted into the food and not dislodged during transfer of the flies. Vials were incubated horizontally, with the tip resting at the base (see Figure 1A).

Fly Husbandry

For all experiments, eggs were collected over a < 12 h period to ensure a synchronous population and reared at constant density (~250 eggs per 200 mL bottle) on standard 5%S food (Bass et al., 2007). Eclosing adults of a defined age were kept as a mixed population for ~48 h on standard 5%S to allow maturing and mating, then separated into females and males under mild CO_2 anesthesia, and maintained as separate sexes in vials from then onward. The different diets ± H_2O were initiated at this stage (d2 of adulthood). Flies (typically 15 or 20 flies per vial) were transferred to fresh food every 2-3 days without gassing.

Lifespan and Stress Assays

Lifespan assays were set up as above, with deaths and censors scored every 2-3 days. For desiccation stress, flies were pre-treated on 5%S or 20%S ± H_2O for 28 days, then transferred into empty vials stored inside a container with desiccant. For high salt stress, flies were pre-treated on 5%S or 20%S ± H_2O for 7 days, then transferred onto medium consisting of 500 mM NaCl in 5% w/v sucrose, 1.5% w/v agar. For oxidative stress, flies were pre-treated on 5%S or 20%S ± H_2O for 7 days, then transferred onto 20 mM paraquat (Sigma 856177) in 5%S food. For starvation stress, flies were pre-treated on 5%S or 20%S ± H_2O for 7 days, then transferred onto vials of 1.5% w/v agar. Flies were incubated at 25°C, and deaths were scored several times daily, as appropriate. Typically, a total of n ~100-200 flies were set up per condition for all survival experiments.

Fecundity Assays

Fecundity was assayed as the number of eggs laid per female in each vial after a 24 h period at the indicated age during a lifespan experiment counted under a stereomicroscope (typically, n = 10 vials per condition, each with 15 females per vial). To test the effect of essential amino acid (EAA) supplementation on fecundity, an EAA cocktail was prepared into 1.5% w/v agar tips, and provided with the food. The final EAA concentrations were as follows: Arg, 425 μg/mL; His, 210 μg/mL; Ile, 340 μg/mL; Leu, 475 μg/mL; Lys, 515 μg/mL; Met, 100 μg/mL; Phe, 260 μg/mL; Thr, 365 μg/mL; Trp, 90 μg/mL; Val, 400 μg/mL (Grandison et al., 2009a).

Drinking and Feeding Assays

Drinking was assayed using the automated FlyPAD system (Itskov et al., 2014). Individual flies pre-treated on 5%S or 20%S ± H_2O were transferred without anesthesia into FlyPAD arenas with a source of agar, and the number of sips quantified over time. Alternatively, drinking was assayed by providing flies an agar tip supplemented with 2.5% w/v blue food dye (Brilliant Blue FCF) for ~1.5 h (until the first appearance of blue excreta). Flies were then snap frozen, and the amount of blue dye was quantified spectrophotometrically at 630 nm from clarified homogenates (Wong et al., 2009). Finally, an adaptation of the Capillary Feeder (CAFE) assay (Ja et al., 2007) was used. A 5 μL glass micropipette (ringcaps #9600105, Hirschmann) containing water, supplemented with 0.1 mg/mL blue dye to aid visualization, was inserted at the side of the vial, secured by the cotton plug. The level of the water was marked, and the vials were incubated in a humidified sealed container at 25°C. The volume of water decrease was then recorded after 24 h. Empty vials without flies were also included to control for evaporation.

To assay feeding rates, flies (n ~ 10 vials per condition, each with n = 5 flies) were placed onto observation racks at 25°C, left undisturbed for ~24 h, then the proportion of feeding flies was assayed blinded based on proboscis extension every 2-3 min over 90 min (Wong et al., 2009). Alternatively, feeding was assayed based on the consumption/excretion of dye-containing food as

described (Shell et al., 2018). Media were supplemented with 1% w/v blue food dye and dispensed into plastic caps (#FCS1NA1, MOCAP) that fit wide plastic vials (28.5 × 95 mm; #32-110, FlyStuff, Genesee Scientific). An agar tip was inserted into the food-filled cap for water supplementation. Flies were incubated at 25°C for 24 h, which accounts for any possible circadian effects on feeding, then the food caps and flies were removed, and the insides of the vials were washed with 3 mL H_2O to resuspend all blue-dyed excreta. The absorbance at 630 nm was measured in a plate reader (FLUOstar Omega, BMG Labtech), and the total volume of blue-dyed food excreted per fly over 24 h was calculated as an indicator of overall feeding (Shell et al., 2018).

Freezing of Fly Samples for Molecular Assays

Live flies were rapidly transferred to microtubes pre-chilled on dry ice via a small plastic funnel and snap frozen in liquid nitrogen, then stored at –80°C until required. Flies were always frozen at approximately the same time of day to minimize any circadian variation.

Whole Body Triglyceride Assay

To measure whole body triglyceride (TAG) levels, frozen flies (n = 4 per sample) were homogenized in 0.05% v/v Tween-20. Samples were incubated for 5 min at 70°C, and supernatants assayed using Triglyceride Infinity Reagent (TR22421, Thermo Fisher Scientific) in a 96-well plate, measuring the absorbance at 540 nm in a plate reader (FLUOstar Omega, BMG Labtech) against a glycerol standard curve. Protein content of homogenates was determined using the BCA assay (Pierce #23225) for normalization.

Lipid Staining

For fat body staining, live flies were anesthetized on ice and dissected in ice-cold PBS. The ventral cuticle was cut away from the abdomen using microscissors, and the internal organs and genitalia were removed, leaving the intact abdominal fat body attached to the dorsal cuticle. Samples were fixed in 4% paraformaldehyde on ice for 30 min followed by 3x 10 min washes in PBS. Tissues were then incubated in Nile Red stain (10 μg/mL; Invitrogen N1142), followed by 3x 10 min washes in PBS, and finally mounted onto a slide in VectaShield with DAPI. Images were obtained by confocal microscopy (Leica SP5 II) at excitation/emission 552/636 nm. Brightness was adjusted in Adobe Photoshop to allow visualization of lipid droplet size.

Hemolymph Analysis

To extract hemolymph, live cohorts of 12 flies (n > 6 replicates per condition) were decapitated under mild CO_2 anesthesia using a scalpel blade, and the bodies were placed upside down into pipette tips within a 1.5 mL tube, and gently centrifuged for 15 min at 1,500 x g, 4°C to drain the hemolymph. The volume of extracted hemolymph was recorded using a pipettor. Glucose content was assayed using Glucose Infinity Reagent (TR15421, Thermo Fisher Scientific) in a 96-well plate, measuring the absorbance at 340 nm in a plate reader (FLUOstar Omega, BMG Labtech). To measure trehalose content, 10 mU of trehalase enzyme (#E-TREH, Megazyme) was added to the sample wells to cleave the disaccharide trehalose into two glucose molecules and incubated at 37°C for a minimum of 2 h. Samples were diluted 10-fold into fresh Glucose Infinity Reagent, and the assay repeated to obtain the amount of glucose released from trehalose. For pH analysis, hemolymph was extracted as described above, except that flies were anesthetized and decapitated on ice rather than CO_2. Hemolymph pH was measured using the pH-sensitive dye pyranine (Invitrogen H348) adapted from a published protocol (Ghosh and O'Connor, 2014). 1 μL of pyranine dye (2.4 mM stock in H_2O) was mixed with 1 μL of hemolymph sample, and the absorbance ratio 485/424 nm (corresponding to the protonated and deprotonated peaks of pyranine) was measured using a NanoDrop One (Thermo Fisher). A standard curve was prepared using 1 μL of 50 mM Tris-HCl ranging between pH 6.6 and 7.8, plotted as a second degree polynomial equation.

Fat Body Insulin and Glucose Assays

To assess insulin sensitivity, fat bodies (abdominal carcasses with the ovaries and digestive tract removed, n = 5 per sample) were dissected from live females anesthetized on ice and pooled into 1 mL Schneider's medium (GIBCO 21720024). Samples were incubated for 15 min at 25°C, then treated ± 5 μM insulin (Sigma I9278) for a further 15 min at 25°C. The supernatant was removed and the fat bodies were homogenized into Laemmli buffer (BioRad #1610737) with 5% v/v β-mercaptoethanol. Samples were analyzed by western blotting, probing for phospho-AKT-Ser505 (1:1,000; Cell Signaling #4054) with total AKT (1:1,000; Cell Signaling #9272) and actin (1:1,000; Abcam #ab8224) as controls. Bands were analyzed by densitometry using FIJI software (ImageJ; Schindelin et al., 2012). To measure glucose uptake, dissected adult fat bodies (n = 5 per sample) were incubated in 100 μL Schneider's medium with 200 μM 2-NBDG (2-(*N*-(7-nitrobenz-2-oxa-1,3-diazol-4-yl)amino)-2-deoxyglucose; Invitrogen N13195) ± 5 μM insulin for 15 min at 25°C, protected from light. Samples were washed twice, then homogenized in 120 μL PBS using a pellet pestle and motor. 100 μL of supernatant was loaded in a 96-well plate, and the fluorescence (excitation/emission 485/520 nm) measured in a plate reader (FLUOstar Omega, BMG Labtech) against a 2-NBDG standard curve.

Protein Glycation and Carbonylation Assays

Levels of glycation in whole frozen flies (n = 10 per samples) were assessed by western blotting using an anti-AGE (advanced glycation end-product) antibody (1:2,000; Millipore AB9890), normalized against total protein assessed using the stain-free labeling system (Bio-Rad). Carbonylation was measured using the OxyBlot Protein Detection Kit (Millipore S7150). Whole frozen flies (n = 5 per sample) were homogenized in 100 μL of CelLytic M Cell Lysis Reagent (Sigma C2978) supplemented with 50 mM DTT and protease inhibitor cocktail (complete mini EDTA-free, Roche 11 836 170 001). Protein samples (20 μg, assayed by the Bradford method) were

subjected to OxyBlot derivatization according to the manufacturer's instructions, followed by western blotting. Lanes were analyzed by densitometry using Image Lab software (Bio-Rad).

Gut Function Assays

Intestinal function was determined by analyzing fly excreta (Cognigni et al., 2011). Flies (n = 5 females per plate) pre-treated for 7 days on 5%S or 20%S ± H_2O were transferred without anesthesia to a 6 cm diameter Petri dish containing a $^1/_4$ wedge of the same food type supplemented with 2.5% w/v blue food dye (– H_2O), or a $^1/_8$ wedge of dyed food alongside a $^1/_8$ wedge of undyed 1.5% w/v agar, separated by a strip of cellophane to prevent diffusion (+ H_2O) (see Figure S4D). Flies were incubated in the inverted dishes for 24 h, then the plate lids were scanned (Epson V700 Photo, 1200 dpi), and analyzed by TURD software (version 0.8; Wayland et al., 2014) with the following parameters: block size: 25, offset: 10, brush shape: circle, brush size 3, min size: 35 (max 3,500), circularity threshold: 0.6. For pH analysis of excreta, 5%S and 20%S media were prepared without propionic acid or nipagin, then supplemented with 0.5% w/v bromophenol blue (Sigma B5525) or bromocresol purple (Sigma B5880), and the final pH adjusted to 5.5. Plates were prepared as above and incubated for 48 h at 25°C. Males were used for these experiments to avoid interference from crawling larvae. The TURD software parameters were as above, except the block size was set to 99. Intestinal barrier integrity was assayed by the Smurf assay (Rera et al., 2012). Flies were aged for 28 days on 5%S or 20%S ± H_2O, then transferred onto media supplemented with 2.5% w/v blue food dye. After 24 h, flies were scored for a Smurf phenotype (see Figure 4G inset).

Tubule and Rectal Ampulla Imaging

For imaging of the rectal ampulla and tubules, live flies were anesthetized on ice, dissected in ice-cold PBS onto poly-L-lysine coated slides, and imaged on a Nikon Eclipse 50i microscope with a DXM1200C digital camera. Images were stitched together in Adobe Photoshop CC, using the automated Photomerge function. To quantify the tubule stone phenotype, each of the 4 tubule arms per fly was scored according to the scale in Figure S5A, and averaged to give a mean score per fly (ranging between 0-4).

Uric Acid Assay

Uric acid levels were quantified spectrophotometrically using the QuantiChrom Uric Acid Assay Kit (DIUA-250, BioAssay Systems) according to the manufacturer's instructions. Whole frozen bodies (n = 5 flies per sample) were homogenized in 100 μL of 0.05% v/v Tween-20 using a pellet pestle and motor, while tubules dissected from live flies (n = 6 tubule pairs per sample) were homogenized in 12 μL. Samples and uric acid standards (5 μL) were loaded in a 96-well plate with 200 μL of assay buffer, incubated for 30 min at 30°C, and the absorbance at 590 nm measured in a plate reader (FLUOstar Omega, BMG Labtech). For hemolymph analysis, samples were added directly to the assay buffer.

Tubule Secretion Assay

Tubule secretion rates were measured as described (Dow et al., 1994; Schellinger and Rodan, 2015). Briefly, live flies were anesthetized on ice and the tubules dissected in ice-cold 1:1 *Drosophila* saline:Schneider's medium, then carefully cut at the ureter. One arm of the tubule pair was wrapped around a metal pin secured in a silicone plate, while the other arm was immersed in a bathing drop of 1:1 *Drosophila* saline:Schneider's medium colored with blue food dye for visualization, leaving the ureter exposed under a layer of heavy mineral oil (Sigma 330760). See Figure S5E for a scheme of the experimental setup. Drops secreted from the ureter were removed at 10 min intervals over the course of 1 h using a fine glass rod, and their diameter measured under a microscope. The volume of each drop was calculated (= 4/3 πr^3) to give a secretion rate in nL/min.

Metabolomics Analysis of Rectal Ampulla Stones

Dissected rectal ampulla stones (a combined score of 25 per sample according to the scale in Figure S6B) were dissolved in 100 μL of extraction solvent (20:80 v/v water/methanol) and spiked with 150 ng/mL $^{13}C_5$-hypoxanthine (CLM-8042; Cambridge Isotope Laboratories) as internal standard (IS). Samples (n = 4 per condition) were vortexed (30 s), centrifuged (13,000 x g, 2 min), sonicated using an ultrasonic water bath (15 min) and finally centrifuged again (13,000 x g, 10 min). The supernatant was filtered using spin-filter tubes (PTFE 0.22 μm; Thermo Scientific). Pooled quality controls (QCs) were created for each batch by pooling equal aliquots of each study sample in the batch, in order to assess technical replicate reproducibility.

Liquid chromatography high-resolution mass spectrometry analysis (LC-HRMS) was carried out on a Vanquish Flex Binary UHPLC system (Thermo Scientific) coupled to a benchtop hybrid quadrupole-Orbitrap Q Exactive mass spectrometer (Thermo Scientific). Separation was achieved using an Accucore 150 Amide HILIC column (Thermo Scientific, 150 × 2.1 mm, 2.6 μm) equipped with a guard column (Thermo Scientific, 30 × 2.1 mm, 2.6 μm), both held at a temperature of 40°C and a flow rate of 0.2 mL/min. Mobile phases were 10 mM ammonium acetate (pH 4.60) in 90% (v/v) acetonitrile (solvent A) and 10 mM ammonium acetate (pH 4.60) in 10% (v/v) acetonitrile (solvent B). The gradient elution was performed with a 0%–20% solvent B gradient over 10 min, ramping to 47% B at 12 min, held at this condition for 6 min, and returning to 0% B at 20 min. The column was equilibrated for 10 min, yielding a total run time of 30 min. Ionization was performed in the negative mode using a heated electrospray ionization source, with the following parameters: spray voltage 3.0 KV, heater temperature 330°C, capillary temperature 320°C, S-lens RF level 50, sheath and auxiliary gas flow rate, 35 and 10 units, respectively. The mass accuracy was calibrated prior to sample analysis. Mass spectrometric data were acquired in profile mode using the full scan setting (m/z 70-1050). Automatic gain control (AGC) was set to 1e6 and maximum MS^1 injection time at 250 ms. Metabolomics data acquisition and processing was performed with Xcalibur software (version 4.1). Relative

quantification is reported based on the peak area ratio of the analyte and the IS. For selected compounds (hypoxanthine, xanthine and allopurinol), calibration curves (12.5-250 ng/mL; $R^2 > 0.9974$) were performed to assess their absolute amounts. Details of the compounds quantified by HILIC UPLC-HRMS are listed in Table S4.

Human Blood Analysis and Metabolomics

Blood samples were obtained after an overnight fast and processed for fasting blood glucose and triglyceride levels, as previously detailed (Koch et al., 2014). Untargeted metabolomics profiling by LC-MS/MS analysis was performed at the Helmholtz Zentrum München, Germany, as described (Koch et al., 2017). Briefly, protein was precipitated from 100 μL of blood serum and the metabolites were extracted with 475 μL methanol. Duplicate samples were processed in positive (in 50 μL 0.1% formic acid) and negative (in 50 μL 6.5 mM ammonium bicarbonate, pH 8.0) electrospray ionization mode. Reconstitution solvents were mixed with internal standards as retention reference markers. Metabolite identification was performed by comparison of the recorded LC-MS/MS spectra against the Metabolon library, based on retention index, precursor mass and MS/MS fragmentation patterns (Koch et al., 2017). Detected purines were adenosine, guanosine, xanthosine, inosine, xanthine, hypoxanthine, uric acid (see Figure S7A). Adenosine was excluded from further analysis due to equal values across all study participants in our cohort subset.

Food Questionnaire and Molecular Diet Composition

Dietary information for the past 12 months was obtained from a food frequency questionnaire, previously used in the EPIC cohorts, where food items were divided into 16 main groups and further sub-groups (Brandstetter et al., 1999). For our statistical analysis, we considered vegetables (including potatoes and pulses), milk and dairy products, cereals and products thereof, meat, fish, eggs, and sweets as separate main groups. Fat, sauces, soups, and unclassified foods were combined into a mixed group termed 'other'. Alcoholic and non-alcoholic beverages were also included in this 'other' group, except the sub-groups 'juices' and 'soft drinks', which were considered separately in our analysis.

The metabolic composition of the diet was imputed from the food questionnaire, providing detailed amounts of dietary compounds consumed by each individual participant. Molecular concentrations were estimated based on molecular weights and amounts of each of the 141 consumable food items for each participant (Pryor et al., 2019). Following the *Drosophila* experiments, we focused on dietary sugars and nucleotides of the purine metabolism for statistical testing of metabolites. The dietary purines tested were uric acid, adenosine, deoxyadenosine, guanosine, deoxyguanosine, xanthine and hypoxanthine. The dietary sugars tested were lactose, maltose, sucrose, fructose, galactose, glucose, maltotriose and ribose. Both food groups and dietary metabolites employed in statistical tests were normalized for individual caloric intake and multiplied by the median consumed calories of our study population (8,948.1 kJ).

Analysis of Variance

Permutational multivariate analysis of variance (PERMANOVA; R-package 'vegan' version 2.5-6) testing was performed with the Euclidean inter-sample distances as dependent variable based on eGFR or metabolite serum levels. Independent variables were food groups or dietary metabolites together with clinical parameters. The estimation of explained variance for each term was performed via marginal testing. Probability values were generated by comparing F-distributions of the original data to that of 9999 random sample permutations.

Linear Modeling

Linear regression models were calculated for each measured serum purine as a dependent variable separately (R-package 'stats' R-version 3.6.1). Independent variables were dietary glucose, BMI, eGFR, age and fasting plasma glucose concentrations. Probability values for the terms of interest, BMI, eGFR and dietary glucose, were corrected for multiple testing (Benjamini and Hochberg, 1995) across all six linear models (one for each circulating purine). The slope of the explanatory variables was evaluated, and considered as positively (> 0) or negatively (< 0) correlated. Linear regression analysis for serum uric acid concentrations explained by eGFR (Figure S7B) or BMI (Figure S7K) was calculated without any further independent terms or multiple testing correction.

QUANTIFICATION AND STATISTICAL ANALYSIS

Fly statistical analysis

Survival curves were analyzed by log-rank test. The majority of other experiments were analyzed by one-way ANOVA with Tukey's multiple comparison. Tubule and ampulla scoring was analyzed by Kruskal-Wallis test with Dunn's multiple comparison. Data were plotted and analyzed using GraphPad Prism 8 software. Significance of probability values: n/s, $p > 0.05$; *$p < 0.05$; **$p < 0.01$; ***$p < 0.001$. Sample size is not limiting for *Drosophila* studies, and typically $n \sim 150$ flies were pre-determined and used per condition for survival assays (see Tables S2 and S3 for exact n numbers). For other assays, sample size was determined based on the significance obtained from previous studies with similar experimental setups, or empirically based on the variability of each scored phenotype. Comparable sample sizes were used in each experiment. Experiments were not blinded, except for the feeding assay based on observation of proboscis extension. Experiments were excluded if the positive control failed to work. Control and experimental flies were bred under identical conditions, and were randomized with regard to dietary and/or drug treatment.

Human Statistical Analysis

Data were analyzed in R statistical software using the packages 'vegan' (version 2.5-6) and 'stats' (R-version 3.6.1), and visualized with the package 'RColorBrewer'. Significance of probability values or false discovery rates (FDR): n/s, $p > 0.1$; •$p < 0.1$; *$p < 0.05$; **$p < 0.01$; ***$p < 0.001$.

DATA AND CODE AVAILABILITY

Fly data generated during this study are included in this published article and its supplemental information files. Human cohort data is available upon application from the PopGen biobank (https://www.uksh.de/p2n/Information+for+Researchers.html).

Editorial

Sugar-induced dysregulation of purine metabolism impacts lifespan

Claudia Lennicke, Eliano dos Santos, Helena M. Cochemé

Excess dietary sugar adversely affects human health by promoting the development of metabolic disorders such as obesity and type-2 diabetes (Figure 1). Sugar-rich diets are commonly used to replicate and investigate metabolic diseases in animal models, including the fruit fly *Drosophila melanogaster* [1]. High-sugar diets also shorten survival, which was widely attributed to these diabetic-like metabolic defects. However, our recent work in *Drosophila* reveals that longevity can be uncoupled from obesity and insulin resistance [2].

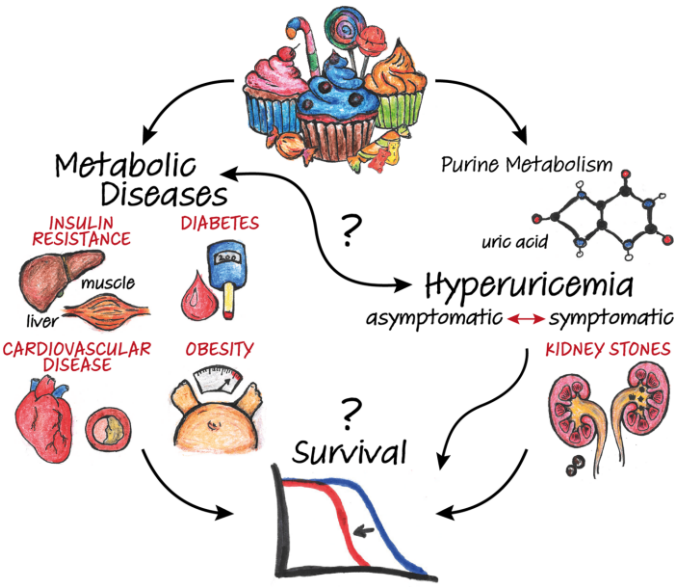


Figure 1. Impact of diet-induced metabolic dysregulation on survival. Excess dietary sugar leads to the dysregulation of carbohydrate and lipid metabolism, resulting in conditions such as obesity, insulin resistance, type-2 diabetes and cardiovascular disease. High-sugar diets also fuel purine catabolism, promoting the accumulation of uric acid as an end-product. Besides causing direct pathologies such as kidney stones, hyperuricemia (i.e. elevated uric acid levels) is associated with metabolic diseases and predictive of their onset. However, the underlying mechanisms and impact on survival are complex and remain to be fully elucidated.

Instead, we show that a chronic high-sugar diet induces water imbalance in the fly, leading to thirst and dehydration, and that their decreased lifespan can be fully rescued by providing an *ad libitum* water source. Importantly, while longevity is restored to control levels, water supplementation does not rescue the metabolic complications typically associated with high-sugar diets, namely the accumulation of triacylglycerides, hyperglycemia, insulin resistance, and glycation damage. This indicates that these metabolic defects are not the limiting factor for fly survival *per se*. As an alternative hypothesis, we propose that the pathophysiology of high-sugar diets is linked to the dysregulation of purine metabolism [3]. Prompted by the water effect, we focused on the fly tubules, which are functionally equivalent to the tubular portion of the mammalian kidney. Just like humans, the fly excretory system can develop lithiasis under dietary challenge [4]. We found that chronic high-sugar feeding fuels the accumulation of uric acid as a breakdown product of purine degradation, and induces the formation of uric acid stones in the fly tubules. Water supplementation can rescue this tubular dysfunction associated with excess dietary sugar, by reversing the dehydration and consequently diluting the concentration of stone-precursor metabolites.

Similarly, supplementing the control diet with excess purines leads to increased systemic levels of uric acid, and recapitulates the tubular pathology and shortened lifespan found on the high-sugar diet, which are also prevented by providing water. This suggests that water imbalance is the key driving factor in determining the longevity of flies under these challenging diets. The usual source of water in insect studies is the food itself, which is typically an agar-set medium containing sugar and yeast. Our results suggest that future studies, particularly those that rely on dietary manipulation to model diseases and those aimed at understanding health through longevity, should consider including a control group provided with *ad libitum* water to exclude a potential contribution of water imbalance in their interventions.

To further explore the importance of uric acid accumulation in stone formation and in determining fly survival independently of water balance, we treated flies on a high-sugar diet with the xanthine oxidase inhibitor allopurinol, a uric acid-lowering drug commonly prescribed in the clinic. Allopurinol prevents the formation of sugar-induced tubule stones and partially rescues the shortened lifespan of flies on a high-sugar diet. However, allopurinol treatment decreases fly survival on the control diet, associated with adverse side-effects

of blocking a major cellular pathway such as purine degradation, and the deleterious accumulation of upstream metabolites. This suggests that allopurinol may not be an adequate pharmacological strategy for preventing diseases and improving survival associated with dysregulation of purine metabolism in a healthy population.

To assess whether dietary sugar intake also impacts purine metabolism in humans, we correlated dietary records with serum metabolomics data from a healthy human cohort of 650 participants. We found that consumption of sugar-rich foods indeed displays a strong association with renal dysfunction and elevated levels of circulating purines. This is consistent with our observations in the fly model, and suggest that dietary sugars may also affect human health via dysregulation of purine metabolism.

Further research is needed to understand whether a sugar-restricted diet may be an effective strategy to prevent uric acid-related diseases, and how purine metabolism modulates health beyond the disorders directly caused by uric acid crystallization, such as urolithiasis or gout, a form of inflammatory arthritis. Interestingly, systemic uric acid levels increase with age, and are linked to the incidence of metabolic disease and survival in humans. In prospective studies, asymptomatic hyperuricemia can predict the onset of conditions such as metabolic syndrome and type-2 diabetes [5, 6], and is a risk factor for cardiovascular and all-cause mortality [7]. Therefore, understanding the pathophysiological links, especially whether these interactions are causal or correlational, will be critical for gaining mechanistic insight into how dysregulation of purine metabolism contributes to disease progression and survival. Overall, these investigations will support the discovery of new translatable targets and preventive strategies for healthier aging.

REFERENCES

1. Musselman LP, Kühnlein RP. J Exp Biol. 2018 (Suppl 1); 221:jeb163881.
   https://doi.org/10.1242/jeb.163881 PMID:29514880
2. van Dam E, et al. Cell Metab. 2020; 31:710–725.e7. https://doi.org/10.1016/j.cmet.2020.02.016 PMID:32197072
3. Johnson RJ, et al. Diabetes. 2013; 62:3307–15. https://doi.org/10.2337/db12-1814 PMID:24065788
4. Lang S, et al. PLoS Genet. 2019; 15:e1008318. https://doi.org/10.1371/journal.pgen.1008318 PMID:31415568
5. Ford ES, et al. Circulation. 2007; 115:2526–32. https://doi.org/10.1161/CIRCULATIONAHA.106.657627 PMID:17470699
6. Bhole V, et al. Am J Med. 2010; 123:957–61. https://doi.org/10.1016/j.amjmed.2010.03.027 PMID:20920699
7. Niskanen LK, et al. Arch Intern Med. 2004; 164:1546–51. https://doi.org/10.1001/archinte.164.14.1546 PMID:15277287

Helena M. Cochemé: MRC London Institute of Medical Sciences, Imperial College London, London W12 8QA, UK

Correspondence: *Helena M. Cochemé*
Email: *helena.cocheme@lms.mrc.ac.uk*

Keywords: *sugar diet, metabolic disease, diabetes, obesity, purine catabolism, uric acid, Drosophila, aging*
Funding: *Work in the Cochemé lab is supported by the Medical Research Council UK (MC-A654-5QB90)*

Copyright: *© 2020Lennicke et al. This is an open access article distributed under the terms of the Creative Commons Attribution License (CC BY 3.0), which permits unrestricted use, distribution, and reproduction in any medium, provided the original author and source are credited*

Received: November 29, 2020
Published: December 27, 2020